Anterior Cruciate Ligament: 3-D Fiber Anatomy, Fluorescence Arthroscopy & Healing

Duy Tan Nguyen

Anterior Cruciate Ligament: 3-D Fiber Anatomy, Fluorescence Arthroscopy & Healing

Duy Tan Nguyen

The research described in this thesis was financially supported by:
Netherlands Organization for Scientific Research
(NWO-Mozaïekbeurs 017.004.076)
National Institutes of Health (NIH #AR39683, NIH #AR41820)
Stichting Annafonds | NOREF
Stichting Marti-Keuning Eckhart

Financial support to attend scientific meetings was received from:
Reumafonds
Stichting Annafonds | NOREF
AUV Spinozafonds

The publication of this thesis was financially supported by:
AMC Graduate School
Annafonds | NOREF
Arthrex, BV
Asian♦American Institute for Research and Education
Biomet
Chipsoft
Össur
Smith&Nephew, CV
Nederlandse Orthopaedische Vereniging
Nederlandse Vereniging voor Traumachirurgie
Nederlandse Vereniging voor Arthroscopie

Layout: Ridderprint BV - www.ridderprint.nl
Printed by: Ridderprint BV - www.ridderprint.nl

ISBN: 978-94-6299-115-6

Anterior Cruciate Ligament: 3-D Fiber Anatomy, Fluorescence Arthroscopy & Healing

ACADEMISCH PROEFSCHRIFT

ter verkrijging van de graad van doctor

aan de Universiteit van Amsterdam

op gezag van de Rector Magnificus

prof. dr. D.C. van den Boom

ten overstaan van een door het College voor Promoties ingestelde commissie,

in het openbaar te verdedigen in de Agnietenkapel

op dinsdag 2 juni 2015, te 14.00 uur

door

Duy Tan Nguyen

geboren te Naarden

PROMOTIECOMMISSIE

Promotores:

prof. dr. C.N. van Dijk	Universiteit van Amsterdam
prof. dr. S.L-Y. Woo	University of Pittsburgh

Copromotor:

dr. ir. L. Blankevoort	Universiteit van Amsterdam

Overige leden:

prof. dr. A. van Kampen	Radboud Universiteit Nijmegen
prof. dr. F. Nollet	Universiteit van Amsterdam
prof. dr. R.J. Oostra	Universiteit van Amsterdam
prof. dr. D.B.F. Saris	Universiteit Utrecht en Universiteit Twente
prof. dr. ir. T.H. Smit	Vrije Universiteit Amsterdam

Faculteit der Geneeskunde

TABLE OF CONTENTS

PREFACE

In this doctoral thesis, I will discuss the results of 2½ years research at the Musculoskeletal Research Center at the University of Pittsburgh and 4 years of research at the department of Orthopedic Surgery at the Academic Medical Center. The research projects are experimental and aim at developing new methods to optimize the surgical treatment of patients with anterior cruciate ligament tears. An injury that can cause pain, instability of the knee joint, and early osteoarthrosis. In the introductory chapter I will formulate the scope and the aims of my thesis.

Chapter 1

Introduction

"It is difficult to say what is impossible, for the dreams of yesterday are the hopes of today, and the realities of tomorrow" – Robert H. Goddard (physicist and rocket engineer (USA, 1882 - 1945))

INTRODUCTION

The musculoskeletal system is built with complexity to provide the human body with mechanical support and stability while at the same time flexibility and motion is permitted. To discuss the function of each element as an isolated entity is to fail to appreciate the close interrelationship of structure and function of this whole system. (1) The skeleton, which forms the framework, has more than 200 bones. Most of them are interconnected by forming a synovial joint. The surface of these bones is covered with cartilage for smooth articulation. The articulating bones are connected by a fibrous joint capsule. Synovial joints which have a larger range of motion have more complex connections and structures. (2) The knee joint, for example has menisci - to increase joint congruency and to absorb shocks - and four knee ligaments that connect the femur to the tibia – the anterior cruciate ligament (ACL), posterior cruciate ligament (PCL), medial collateral ligament (MCL), and lateral collateral ligament (LCL). These ligaments act together with the joint capsule, menisci, articular surfaces of the knee and the muscles to maintain stability as well as to guide the joint through the range of motion. (3-5) The muscles are also called the active stabilizers and the other structures the passive stabilizers. Inherently to balancing between stability and flexibility, joint structures are prone to traumatic injuries and age-related tissue degeneration.

The ACL of the knee is especially susceptible to injury often after twisting the knee during work or sports related activities. (6) As sports participation is increasing worldwide, the incidence of ACL injuries has increased as well. It is estimated that more than 6,000 new ACL tears occur in the Netherlands and more than 200,000 new ACL tears occur annually in the United States - resulting in an estimated annual cost to society on the order of 3 billion dollars. (7, 8) The ACL seldom heals spontaneously. (9-12) For most patients ACL deficiency can lead to multidirectional knee joint instability that can increase the stress levels of the menisci and articular cartilage. These repetitive episodes can cause cumulative damage and wear. This may lead to pain, meniscal tears, early osteoarthrosis and eventually impaired mobility. (5, 13-17) Thus, the main goals of ACL management are to restore normal function, prevent damage to the menisci and cartilage, improve quality of life and minimize the risk of complications. (5, 15-17) Unfortunately, there is currently no such treatment that can realize these goals. Therefore, the ACL remains a major focus in the field of musculoskeletal research.

ANATOMY AND FUNCTION

The ACL spans the knee joint obliquely and inserts distally on the tibia at the anterior part of the intercondylar eminence. The proximal insertion site is at the posterolateral aspect of the intercondylar fossa of the femur. This spatial orientation is important for its function in resisting excessive anterior tibial translation, internal rotation and hy-

perextension. (18, 19) The ACL varies between individuals in shape, length, strength and insertion sites. (20-25) It is predominantly made of highly organized collagen fibers, which provide the ACL with its stiffness and tensile strength. The collagen fibers follow a typical architectural hierarchy with tropocollagen as the basic molecular component and are systematically arranged into microfibrils, subfibrils, fibrils, and fascicles. (6, 26)

The 3-D collagen fiber orientation and fiber length are other important elements for the function of the ACL. Knowledge of the 3-D collagen fiber anatomy can be used as a blueprint to guide the development of new treatments. However, a detailed and objective blueprint of the ACL is still missing. Previous studies are based on anatomical dissection experiments. Some researchers report that the ACL is a single broad continuum of fascicles, with different portions taut throughout the range of motion. (27, 28) Others report that the ACL is divisible into two bundles, namely an anteromedial bundle (AMB) and a posterolateral bundle (PLB). (21, 24, 29) Others defined three functional bundles, namely anteromedial bundle (AMB), a posterolateral bundle (PLB) and an intermediate bundle (IMB). (30-32) Mommersteeg et al., report that there are 6 to10 bundles that define the main fascicle directions within the studied ACL samples. (20) These reports clearly indicate the current controversy regarding the 3-D collagen fiber anatomy and the amount of fiber bundles to be reconstructed during surgery.

BLOOD AND NERVE SUPPLY

The ACL is covered by a synovial layer that contains a network of small penetrating blood vessels that originate predominantly from the middle genicular artery. (33, 34) Additional blood supply comes from the retropatellar fat pad via the inferior medial and lateral geniculate arteries. Though, overall the ACL is relatively hypovascular. The neural supply comes from the posterior articular branches of the tibial nerve, but contains free nerve endings and mechanoreceptors that have a proprioceptive function. (33)

BIOCHEMISTRY

Type I collagen is the major constituent and is primarily responsible for ACL's stiffness and tensile strength. Other collagen types such as type III, V, VI, IX, X, XI, and XII appear in minor amounts. However, they play a significant role in mechanical behavior, collagen fibrillogenesis, and homeostasis. Elastin, another fibrous protein present in the ACL allows the tissue to return to its pre-stretched length following physiological loading. Other constituents include glycoproteins, proteoglycans, and glycosaminoglycans. (6, 35) The predominant cell type within the ACL is the fibroblasts, which

are interspersed between the collagen fibers. They are mainly responsible for the maintenance and production of the constituents that make up the ACL.

BIOMECHANICS

Restraint to excessive anterior translation of the tibia relative to the femur is the primary function of the ACL. (19, 36) Clinically, an ACL deficient knee can be diagnosed by the Lachman test and anterior drawer wherein the tibia is pulled anterior at 30° and 90° degrees flexion, respectively. (37, 38) Excessive anterior movement relative to the intact contralateral knee and loss of a firm end-point indicates an ACL tear. Additionally, the ACL functions as a minor secondary restraint to varus–valgus rotation, and internal-external rotation, particularly during weight bearing conditions. Patients often report a "giving way" of the knee, which is a sensation of the knee slipping away. Clinically this rotational instability symptom can be reproduced with the pivot shift test, which involves applying a combined internal tibial and valgus torque throughout the range of flexion-extension of the knee while providing compression at the same time. (39)

As the major function of the ACL and ligaments is to resist tensile loads, it is of importance that the ACL has the proper biomechanical properties to carry out this function. (36, 40) Uniaxial tensile tests are used to characterize the structural mechanical properties. Generally, a bone–ligament–bone complex is tensile tested; the resulting load-elongation curve exhibits nonlinearity that has an initial nonlinear region called the ''toe region''. During this stage, in which normal joint movements occur, the progressive straightening and stretching of an increasing number of fibers takes place – also called fiber recruitment. Once the majority of the fibers is recruited with an increasing applied load, the curve gradually transitions to a ''linear'' region where the slope of the curve becomes constant. This biphasic behavior allows ligaments and tendons to maintain normal joint laxity in response to low loads - low stiffness toe region - to prevent excessive joint displacement in response to high loads - high stiffness linear region. A continuous increase in loading will eventually cause the ligament to fail. (41, 42) The ACL also exhibit time- and history-dependent viscoelastic properties that reflect complex interactions between the proteoglycan molecules, water, collagen, and other structural components. (40) This behavior is referred to as a stress relaxation. Conversely, there is a time-dependent increasing elongation when a viscoelastic material is subjected to a constant stress. This behavior is called creep. The viscoelastic behavior of the ACL and other ligaments has important physiological and clinical implications. (40, 43) During walking or running, the ligaments undergo cyclic loading; and as a result, cyclic stress relaxation will effectively lower the stress in the ligament substance. This phenomenon may help prevent fatigue failure of ligaments in conditions where repetitive stress causes failure at a much lower load than

required. Similarly, cyclic creep can be used to demonstrate how warm-up exercises and stretching can increase flexibility of a joint, as a constant applied stress during stretching increases the length of the ligaments. (6)

CLINICAL TREATMENTS – HISTORIC PERSPECTIVE

Throughout the centuries many conservative and surgical treatments have been developed to treat the torn ACL. (44, 45) Great progress has been made, though according to a recent meta-analysis only 41% of patients who have been treated with the current surgical gold standard reported their knee as normal. (46) In the early days when the ACL was thought to have little function and in a time when surgery poses high risk for mortality due to the lack of antisepsis, treatment of knee instability was conservative with (hinged) braces. (47) Later certain patients were braced with the aim to provide the circumstances for the torn ends to heal. (10, 11) This conservative treatment, however was only successful in a few patients.

In 1895, dr. Mayo-Robson performed the first surgical ACL repair by stitching the two torn ends to each other with catgut sutures. (48) The patient had a good knee function, though the results of the Mayo-Robson ACL suture repair were unpredictable. Obtaining a reliable suture fixation of the often shredded ACL remnants turned out to be difficult. To overcome this difficulty, dr. Perthes developed a new technique. The distal ligament remnant was pulled against the proximal remnant by suturing the distal remnant with an aluminum-bronze suture to the outer femoral cortical bone. (49) The reported results were "excellent at 1–4 years in three patients". Drs O'Donoghue, MacIntosh and Marshall developed variations on the Perthes technique and reported good clinical results. (50-52) Years later, however, drs Feagin, Sherman and Engebretsen concluded that the suture repairs in their patients had poor long-term results. (53-55) These results combined with the difficulties encountered during suture fixation eventually led to the demise of ACL suture repair. In time, this has led to the common opinion that the ACL does not have an intrinsic healing potential and cannot heal. The introduction of the minimally invasive arthroscopic ACL reconstruction technique may also have contributed to this perception.

Besides the ACL suture repair techniques, surgeons also experimented with open ACL reconstructions to stabilize the knee. Many techniques have been developed based on the existing knowledge, expert opinions, patient outcomes, and technical innovations. Around the 1900, extra-articular reconstructions with silk sutures and tendons grafts were developed to create a restraining band on the lateral side of the knee to reduce the instability. (56) (57-59) The extra-articular reconstructions decreased the lateral rotational instability. However, it did not reliably restrain the anterior translation. In 1913, dr. Wagner proposed to use of fascia lata for the reconstruction of the ACL. (60) Several years later, dr. Hey Groves reported the first anatomical ACL reconstruction

with a tethered fascia lata graft placed at the original insertion sites. (61) Dr. Hey Groves also reported many limitations, i.e. insufficient strength of the transplanted fascia lata, the surgical complexity, extensive open surgical exposure, and the risk of complications. These limitations have led to the use of other grafts such as meniscus, extensor retinaculum, patellar tendon, quadriceps tendon, hamstring tendons, allografts, xenografts, synthetic grafts as well as the development of improved fixation devices and minimally invasive surgical techniques. (62, 63) Thanks to these research efforts and experience, the large variation in surgical techniques could be standardized into a rather satisfactory minimally invasive arthroscopic ACL reconstruction technique with fewer variables as we know it nowadays. (64)

CURRENT CLINICAL TREATMENTS

The main goal of ACL management is to restore normal function, prevent damage to the menisci and cartilage and improve quality of life. (5, 15-17) Currently there are two primary treatment options: structured rehabilitation and ACL reconstruction surgery. Structured rehabilitation aims to reinforce the active knee stabilizers by strengthening the lower limb muscles and increase proprioception in order to cope with or prevent the onset of functional knee instability. ACL reconstruction is performed in patients who have a high demand of their passive and active knee stabilizers such as (professional) athletes and in patients where structured rehabilitation failed. (65)

The current minimally invasive ACL reconstruction technique is arthroscopically assisted. (63) Arthroscopic surgery has many advantages but remains difficult to master primarily due to the suboptimal view between ligament, bone and cartilage when imaged with the current white light endoscopic systems. To overcome these visual limitations, instrumental guides are developed to simplify the graft placement, e.g. transtibial ACL reconstruction. The arthroscopic single bundle transtibial ACL reconstruction technique using autologous hamstrings or 1/3 patellar tendon as a graft has been the gold standard for the past 20 years. The results are relatively satisfactory, but there remains much room for optimization. Already in 2001, researchers have expressed their concern about the accuracy of placing the graft with the transtibial technique and thus its ability to store knee stability. (66, 67) And according to a recent meta-analysis, only 41% of patients have reported their reconstructed knee as normal. (46) Graft misplacement is the most common causes of revision surgery (68-72) and small deviations can result in large changes in knee stability. (73-75) Additionally, harvesting of the autologous hamstrings or 1/3 patellar tendon grafts can cause loss of muscle strength, decreased range of motion and donor site morbidity. (17, 76-82) More recent studies have shown that 70-80% of the patients develop radiographic signs of osteoarthrosis in the ACL reconstructed knee after 10 to 15 years. (79, 83-85)

The development of early osteoarthrosis has been associated to the inability of the transtibial ACL reconstruction to restore normal joint kinematics. (86, 87)

TARGETS FOR OPTIMIZATION

Arthroscopic ACL reconstruction surgery is a technical demanding procedure. Human biology, patient compliance to rehabilitation and graft remodeling has an additional effect on the surgical outcome. Several variables in ACL reconstruction techniques has been and can be optimized such as graft selection, number of bundles, graft placement, graft fixation, graft healing, donor site morbidity, rehabilitation and additional anterolateral ligament reconstruction. (88-91) This thesis focusses on quantifying the anatomy of the ACL, developing a technique to identify the ACL insertions in an ACL-deficient knee and developing a method for end-to-end ACL repair to heal the ruptured ACL.

ACL anatomy

The 3-D collagen fiber orientation and fiber length are important elements for the function of the ACL. Mimicking this anatomy will likely improve the surgical outcome. As above described in the "Anatomy and function" paragraph, there remains controversy whether the ACL consist out of one, two, three or more bundles and whether these bundles need to be reconstructed. To improve the surgical outcome some surgeons started to use two or three bundles to reconstruct the ACL. (92-97) However, due to the divergent data on the amount of ACL bundles, technical difficulty and absence of long-term clinical data there remains controversy regarding this concept. This controversy is illustrated in an editorial "Double Bundle or Double Trouble" in Arthroscopy. Harner and Poehling stated: "It is clear that, as surgeons, we have yet to master the technical aspects of single-bundle ACL reconstruction. Do the theoretical benefits of double-bundle ACLs outweigh the risks of a more technically demanding surgery?". (98) Therefore, more research effort has been placed on quantifying the 3-D collagen fiber anatomy. Additionally, this fundamental knowledge will further our understanding of ACL function and can be used as a blueprint to guide the development of new treatments such as bio-enhanced end-to-end ACL repair.

ACL insertions

Graft placement is one of the most important variables in ACL reconstruction. (66, 68-72, 96, 99, 100) Since 2001, a few studies have criticized the accuracy of placing the femoral bone tunnel with the aid of the guide and the transtibial technique. Arnold et al., reported that the location is 2-4 mm off from the outer margin of the original insertion site. Bebi et al., measured the tunnel location from the center of the original insertion site and reported an error of 9 mm. (66, 67) This non-anatomic placement

is reported in 95% of the ACL reconstructions. (66, 67, 101-103) Five percent is such misplaced that the replacement tendon graft ruptures during the immediate post-reconstruction period. (80, 104) Additionally, 15-20% of the ACL reconstructed knee joints remain instable. (80) Hence, half of the revisions of ACL reconstruction are due to aberrant graft placement. (68-72) For some years a few surgeons have abandoned the transtibial technique and are aiming to place the bone tunnel at its original insertion site during the procedure, the so called "anatomic ACL reconstruction technique". (66, 96, 99, 100) Recently, Abebe et al., showed that the anatomic ACL reconstruction is superior to the transtibial ACL reconstruction technique in restoring the in-vivo knee kinematics. (105) Currently, more and more surgeons are recognizing the importance of the anatomic ACL reconstruction technique. However, accurate localization of the insertion sites is still a challenge. The current anatomic ACL reconstruction technique aims to place the replacement grafts at the native insertion sites by using the traditional "clock face" model or by anatomical landmarks such as the lateral intercondylar ridge, bifurcate ridge, posterior wall, and cartilage edge. (93, 95, 106-108) The features of the lateral intercondylar ridge and bifurcate ridge can vary between individuals. The identification of these features is not always easy and requires much experience. Therefore, research effort has been placed on finding new ways to accurately and per-operatively locate the original insertion sites easily and fast. (109-115)

Bio-enhanced end-to-end ACL repair

Ideally one would like to prevent ACL injury or find a solution at the core of the problem. One strategy is suture repair with subsequent healing of the torn ACL, as attempted in the past. Theoretically, this may restore the function of the ACL, eliminate the need for tendon graft harvest and circumvent other specific issues of ACL reconstruction surgery. Recent studies have found and hypothesized that many factors such as the local environment and intrinsic factors have a profound effect on ACL healing. The fluidal environment and retraction of the ACL ends, immediately after rupture, reduce the chance for healing. Additionally, the movement of the ACL stumps during knee motion and the volume within the joint space may lead to a low probability for direct or indirect contact between the torn ends to allow for contact healing. A stable hematoma would normally bridge the gap and provide a provisional scaffold for reparative cells at the injury site. Yet, the fluidal environment limits the chance for the formation of a hematoma because of the diluting effect of the synovial fluid. (116) Biologically, it is found that the ACL is a hypocellular tissue and that the properties of fibroblasts are different from those derived from other ligaments that do heal. (117) ACL fibroblasts have comparatively low mobility, low proliferation, metabolic activities, and low potential for matrix production. (118-120) All these constraining factors are contri-

buting to the failure of spontaneous healing of the ACL. Furthermore, surgeons have speculated about the failure of healing of the suture repaired ACL. Dr. Feagin stated that his patients (army cadets) could have been too harsh on his ACL repair. Ratford and Amis stated that the poor strength of the suture technique could attribute to the low success rates. (121) During the past decades new basic knowledge of the ACL has been gained, new suture material and suture techniques developed. In addition, recent advances in functional tissue engineering such as growth factors, and bioactive scaffold have shown to enhance ligament healing. (122-124) Especially, bioactive scaffolds such as porcine Small Intestine Submucosa (SIS) have been recently extensively researched. SIS is mainly composed of collagen type I and contains bioactive factors. (125-128) SIS has shown to improve the mechanical and histomorphological properties of the healing of ligaments and tendons. (129-131) These positive effects have been attributed to its ability to act as a provisional scaffold, and the growth and chemotactic factors to promote cell migration into the healing site. In turn these conditions enhance revascularization and tissue repair. All these insights and advances combined with the suboptimal results of ACL reconstruction surgery have led to a renewed interest in suture repair and development of bio-enhanced end-to-end ACL repair techniques.

AIMS

The aims of this thesis are:

1. To develop a near objective methodology to quantify the 3-D collagen fiber anatomy in ligaments
2. To quantify the human ACL collagen fiber anatomy in 3-D
3. To develop a new arthroscopic imaging methodology to per-operatively localize the original insertion sites of the ACL
4. To investigate the effect of the bioscaffold small intestine submucosa (SIS) on the collagen fibrillogenesis in the medial collateral ligament
5. To investigate the effect of cyclic stretch and cell-seeding on the fiber remodeling of SIS
6. To investigate the effect of SIS and a new suture technique on ACL healing in a goat model
7. To investigate whether the human ACL has a healing potential

OUTLINE OF THESIS

One of the current emphases in optimizing ACL reconstructions is closer mimicking the anatomy of the ACL. Previously, many studies have been performed to obtain a blueprint of the ACL's anatomy in order to assist surgical techniques. However, there remains controversy regarding its anatomy due to the discrepancy. The discrepancy

might be due to the manual macroscopic dissection used to divide the ACL into fiber bundles. The aim of **Chapter 2** is to develop a methodology to quantify the 3-D collagen fiber orientation of ligaments, accurately and at a high resolution. **Chapter 3** aims to use the methodology described in chapter 2 to obtain quantitative data on the 3-D collagen fiber anatomy of the ACL. The research question is: how many bundles are present in the human ACL and what should be the amount of bundles to be reconstructed. Another current emphasis in improving the ACL reconstruction is graft placement at the original insertion sites of the torn ACL – the anatomical ACL reconstruction. The aim of **Chapter 4** is to develop a new arthroscopic imaging methodology based on fluorescence of collagen molecules to localize the original insertion sites. The research question is whether this can be done accurate, arthroscopically, and real-time. Another strategy to improve the patient outcome is by healing the torn ACL. The last part of this thesis is aimed at addressing two major constraining factors by using a new suture technique in combination with SIS bioscaffold to heal the ACL. In **Chapter 5** the aim is to evaluate the effect of the small intestine submucosa bioscaffold (SIS) on the collagen fibrillogenesis in the healing medial collateral ligament. **Chapter 6** describes the investigation that aims to improve the efficacy of SIS by remodeling the collagen fibers of SIS. The research question was whether this can be achieved through cell-seeding and cyclic stretch. **Chapter 7** is a pre-translational study and investigates whether the human ACL has a healing potential by histologic analysis of reattached ACL remnants from patients. The aim in **Chapter 8** is to heal the ACL in a goat model and biomechanically evaluate the result. The research question was whether this can be achieved by a new suturing technique and the use of SIS bioscaffold. **Chapter 9** aims to histologically evaluate the healing ACLs. The research question was whether the healing ACL displays typical healing characteristics. The final **Chapter 10** discusses the findings and implications of this thesis and proposes future studies.

REFERENCES

1. Welsh RP. Knee joint structure and function. Clinical orthopaedics and related research. 1980(147):7-14. Epub 1980/03/01.
2. Moore KL, Dalley, A.F. Clinically Oriented Anatomy. 5th ed2005.
3. Grood ES, Noyes FR, Butler DL, Suntay WJ. Ligamentous and capsular restraints preventing straight medial and lateral laxity in intact human cadaver knees. The Journal of bone and joint surgery American volume. 1981;63(8):1257-69. Epub 1981/10/01.
4. Blankevoort L. Passive motion characteristics of the human knee joint: experimental and computer simulations: University of Nijmegen; 1991.
5. Müller W. The knee : form, function, and ligament reconstruction. Berlin ; New York: Springer-Verlag; 1983. xviii, 314 p. p.
6. Woo SLY, Nguyen DT, Liang R, Papas N. Tissue mechanics of ligaments and tendons. 2nd ed. Kumar S, editor. Boca Raton: CRC Press; 2008. xvii, 724 p. p.
7. Mather RC, 3rd, Koenig L, Kocher MS, Dall TM, Gallo P, Scott DJ, Bach BR, Jr., Spindler KP. Societal and economic impact of anterior cruciate ligament tears. The Journal of bone and joint surgery American volume. 2013;95(19):1751-9. Epub 2013/10/04.
8. Brophy RH, Wright RW, Matava MJ. Cost analysis of converting from single-bundle to double-bundle anterior cruciate ligament reconstruction. The American journal of sports medicine. 2009;37(4):683-7. Epub 2009/02/11.
9. Costa-Paz M, Ayerza MA, Tanoira I, Astoul J, Muscolo DL. Spontaneous healing in complete ACL ruptures: a clinical and MRI study. Clinical orthopaedics and related research. 2012;470(4):979-85. Epub 2011/06/07.
10. Fujimoto E, Sumen Y, Ochi M, Ikuta Y. Spontaneous healing of acute anterior cruciate ligament (ACL) injuries - conservative treatment using an extension block soft brace without anterior stabilization. Archives of orthopaedic and trauma surgery. 2002;122(4):212-6. Epub 2002/05/25.
11. Ihara H, Miwa M, Deya K, Torisu K. MRI of anterior cruciate ligament healing. Journal of computer assisted tomography. 1996;20(2):317-21. Epub 1996/03/01.
12. Kurosaka M, Yoshiya S, Mizuno T, Mizuno K. Spontaneous healing of a tear of the anterior cruciate ligament. A report of two cases. The Journal of bone and joint surgery American volume. 1998;80(8):1200-3. Epub 1998/09/08.
13. Noyes FR, Mooar PA, Matthews DS, Butler DL. The symptomatic anterior cruciate-deficient knee. Part I: the long-term functional disability in athletically active individuals. The Journal of bone and joint surgery American volume. 1983;65(2):154-62. Epub 1983/02/01.
14. Fetto JF, Marshall JL. The natural history and diagnosis of anterior cruciate ligament insufficiency. Clinical orthopaedics and related research. 1980(147):29-38. Epub 1980/03/01.
15. Johnson RJ, Beynnon BD, Nichols CE, Renstrom PA. The treatment of injuries of the anterior cruciate ligament. The Journal of bone and joint surgery American volume. 1992;74(1):140-51. Epub 1992/01/01.
16. Jones KG. Reconstruction of the anterior cruciate ligament using the central one-third of the patellar ligament. The Journal of bone and joint surgery American volume. 1970;52(4):838-9. Epub 1970/06/01.
17. Renstrom PA. Eight clinical conundrums relating to anterior cruciate ligament (ACL) injury in sport: recent evidence and a personal reflection. British journal of sports medicine. 2013;47(6):367-72. Epub 2012/09/04.

18. Noyes FR, Grood ES, Butler DL, Malek M. Clinical laxity tests and functional stability of the knee: biomechanical concepts. Clinical orthopaedics and related research. 1980(146):84-9. Epub 1980/01/01.
19. Butler DL, Noyes FR, Grood ES. Ligamentous restraints to anterior-posterior drawer in the human knee. A biomechanical study. The Journal of bone and joint surgery American volume. 1980;62(2):259-70. Epub 1980/03/01.
20. Mommersteeg TJ, Kooloos JG, Blankevoort L, Kauer JM, Huiskes R, Roeling FQ. The fibre bundle anatomy of human cruciate ligaments. Journal of anatomy. 1995;187 (Pt 2):461-71. Epub 1995/10/01.
21. Hara K, Mochizuki T, Sekiya I, Yamaguchi K, Akita K, Muneta T. Anatomy of normal human anterior cruciate ligament attachments evaluated by divided small bundles. The American journal of sports medicine. 2009;37(12):2386-91. Epub 2009/11/27.
22. Sasaki N, Ishibashi Y, Tsuda E, Yamamoto Y, Maeda S, Mizukami H, Toh S, Yagihashi S, Tonosaki Y. The femoral insertion of the anterior cruciate ligament: discrepancy between macroscopic and histological observations. Arthroscopy : the journal of arthroscopic & related surgery : official publication of the Arthroscopy Association of North America and the International Arthroscopy Association. 2012;28(8):1135-46. Epub 2012/03/24.
23. Harner CD, Baek GH, Vogrin TM, Carlin GJ, Kashiwaguchi S, Woo SL. Quantitative analysis of human cruciate ligament insertions. Arthroscopy : the journal of arthroscopic & related surgery : official publication of the Arthroscopy Association of North America and the International Arthroscopy Association. 1999;15(7):741-9. Epub 1999/10/19.
24. Girgis FG, Marshall JL, Monajem A. The cruciate ligaments of the knee joint. Anatomical, functional and experimental analysis. Clinical orthopaedics and related research. 1975(106):216-31. Epub 1975/01/01.
25. Harner CD, Livesay GA, Kashiwaguchi S, Fujie H, Choi NY, Woo SL. Comparative study of the size and shape of human anterior and posterior cruciate ligaments. Journal of orthopaedic research : official publication of the Orthopaedic Research Society. 1995;13(3):429-34. Epub 1995/05/01.
26. Kastelic J, Galeski A, Baer E. The multicomposite structure of tendon. Connective tissue research. 1978;6(1):11-23. Epub 1978/01/01.
27. Odensten M, Gillquist J. Functional anatomy of the anterior cruciate ligament and a rationale for reconstruction. The Journal of bone and joint surgery American volume. 1985;67(2):257-62. Epub 1985/02/01.
28. Fuss FK. Anatomy of the cruciate ligaments and their function in extension and flexion of the human knee joint. The American journal of anatomy. 1989;184(2):165-76. Epub 1989/02/01.
29. Chhabra A, Starman JS, Ferretti M, Vidal AF, Zantop T, Fu FH. Anatomic, radiographic, biomechanical, and kinematic evaluation of the anterior cruciate ligament and its two functional bundles. The Journal of bone and joint surgery American volume. 2006;88 Suppl 4:2-10. Epub 2006/12/05.
30. Norwood LA, Cross MJ. Anterior cruciate ligament: functional anatomy of its bundles in rotatory instabilities. The American journal of sports medicine. 1979;7(1):23-6. Epub 1979/01/01.
31. Amis AA, Dawkins GP. Functional anatomy of the anterior cruciate ligament. Fibre bundle actions related to ligament replacements and injuries. The Journal of bone and joint surgery British volume. 1991;73(2):260-7. Epub 1991/03/01.

32. Otsubo H, Shino K, Suzuki D, Kamiya T, Suzuki T, Watanabe K, Fujimiya M, Iwahashi T, Yamashita T. The arrangement and the attachment areas of three ACL bundles. Knee surgery, sports traumatology, arthroscopy : official journal of the ESSKA. 2012;20(1):127-34. Epub 2011/06/23.
33. Arnoczky SP. Anatomy of the anterior cruciate ligament. Clinical orthopaedics and related research. 1983(172):19-25. Epub 1983/01/01.
34. Scapinelli R. Studies on the vasculature of the human knee joint. Acta anatomica. 1968;70(3):305-31. Epub 1968/01/01.
35. Woo SL, Abramowitch SD, Kilger R, Liang R. Biomechanics of knee ligaments: injury, healing, and repair. Journal of biomechanics. 2006;39(1):1-20. Epub 2005/11/08.
36. Mow VC, Ratcliffe A, Woo SLY. Biomechanics of diarthrodial joints. New York: Springer-Verlag; 1990.
37. Losee RE, Johnson TR, Southwick WO. Anterior subluxation of the lateral tibial plateau. A diagnostic test and operative repair. The Journal of bone and joint surgery American volume. 1978;60(8):1015-30. Epub 1978/12/01.
38. Torg JS, Conrad W, Kalen V. Clinical diagnosis of anterior cruciate ligament instability in the athlete. The American journal of sports medicine. 1976;4(2):84-93. Epub 1976/03/01.
39. Galway HR, MacIntosh DL. The lateral pivot shift: a symptom and sign of anterior cruciate ligament insufficiency. Clinical orthopaedics and related research. 1980(147):45-50. Epub 1980/03/01.
40. Woo SL. Mechanical properties of tendons and ligaments. I. Quasi-static and nonlinear viscoelastic properties. Biorheology. 1982;19(3):385-96. Epub 1982/01/01.
41. Butler DL, Grood ES, Noyes FR, Zernicke RF. Biomechanics of ligaments and tendons. Exercise and sport sciences reviews. 1978;6:125-81. Epub 1978/01/01.
42. Woo SL, Gomez MA, Seguchi Y, Endo CM, Akeson WH. Measurement of mechanical properties of ligament substance from a bone-ligament-bone preparation. Journal of orthopaedic research : official publication of the Orthopaedic Research Society. 1983;1(1):22-9. Epub 1983/01/01.
43. Woo SL, Gomez MA, Akeson WH. The time and history-dependent viscoelastic properties of the canine medical collateral ligament. Journal of biomechanical engineering. 1981;103(4):293-8. Epub 1981/11/01.
44. Paessler H. The History of the Cruciate Ligaments. In: Fu F, Cohen S, editors. Current Concepts in ACL Reconstruction: SLACK Incorporated; 2008.
45. Schindler OS. Surgery for anterior cruciate ligament deficiency: a historical perspective. Knee surgery, sports traumatology, arthroscopy : official journal of the ESSKA. 2012;20(1):5-47. Epub 2011/11/23.
46. Biau DJ, Tournoux C, Katsahian S, Schranz P, Nizard R. ACL reconstruction: a meta-analysis of functional scores. Clinical orthopaedics and related research. 2007;458:180-7. Epub 2007/02/20.
47. Bonnet A. Traite de therapautique des maladies articulaires. 1853.
48. Robson AW. VI. Ruptured Crucial Ligaments and their Repair by Operation. Annals of surgery. 1903;37(5):716-8. Epub 1903/05/01.
49. Perthes G. Uber die Wiederbefestigung des abgerissenen vorderen Kreuzbandes im Kniegelenk. Zentralbl Chir. 1926;53:866-72.
50. O'Donoghue DH. Surgical treatment of fresh injuries to the major ligaments of the knee. The Journal of bone and joint surgery American volume. 1950;32(A:4):721-38. Epub 1950/10/01.
51. MacIntosh DLT, R.J. A follow-up study and eventuation of over-the-top repair of acute tears of the anterior cruciate ligament Journal of Bone and Joint Surgery 1977;59-B(Supp l):505.

52. Marshall JL, Warren RF, Wickiewicz TL, Reider B. The anterior cruciate ligament: a technique of repair and reconstruction. Clinical orthopaedics and related research. 1979(143):97-106. Epub 1979/09/01.
53. Sherman MF, Lieber L, Bonamo JR, Podesta L, Reiter I. The long-term followup of primary anterior cruciate ligament repair. Defining a rationale for augmentation. The American journal of sports medicine. 1991;19(3):243-55. Epub 1991/05/01.
54. Feagin JA, Jr., Curl WW. Isolated tear of the anterior cruciate ligament: 5-year follow-up study. The American journal of sports medicine. 1976;4(3):95-100. Epub 1976/05/01.
55. Engebretsen L, Benum P, Fasting O, Molster A, Strand T. A prospective, randomized study of three surgical techniques for treatment of acute ruptures of the anterior cruciate ligament. The American journal of sports medicine. 1990;18(6):585-90. Epub 1990/11/01.
56. Lange F. Kunstliche Gelenkbander aus Seide. Munch Med Wschr. 1907;52:834-6.
57. Ellison AE. Distal iliotibial-band transfer for anterolateral rotatory instability of the knee. The Journal of bone and joint surgery American volume. 1979;61(3):330-7. Epub 1979/04/01.
58. Matti H. Ersatz des gerissenen vorderen Kreuzbandes durch extraartikulare freie Fascientransplantation. Munch Med Wschr. 1918;17:251-452.
59. Neyret P, Palomo JR, Donell ST, Dejour H. Extra-articular tenodesis for anterior cruciate ligament rupture in amateur skiers. British journal of sports medicine. 1994;28(1):31-4. Epub 1994/03/01.
60. Wagner P. Isolierte Ruptur der Ligamenta Cruciata Universitat Leipzig; 1913.
61. Hey Groves EW. Operation for the repair of crucial ligaments. Lancet. 1917;190:674-5.
62. Eriksson E. Reconstruction of the anterior cruciate ligament. The Orthopedic clinics of North America. 1976;7(1):167-79. Epub 1976/01/01.
63. Watanabe M. [Present status and future of arthroscopy]. Geka chiryo Surgical therapy. 1972;26(1):73-7. Epub 1972/01/01.
64. Saris DBF, Meuffels DE, Diercks RL, Fievez AWFM, Patt TW, Van der Hart CP, Hammacher ER, van der Meer A, Goedhart EA, Lenssen AF. Nederlandse Orthopedische Vereniging Richtlijn Voorste Kruisbandletsels. 2011.
65. Frobell RB, Roos EM, Roos HP, Ranstam J, Lohmander LS. A randomized trial of treatment for acute anterior cruciate ligament tears. The New England journal of medicine. 2010;363(4):331-42. Epub 2010/07/28.
66. Arnold MP, Kooloos J, van Kampen A. Single-incision technique misses the anatomical femoral anterior cruciate ligament insertion: a cadaver study. Knee surgery, sports traumatology, arthroscopy : official journal of the ESSKA. 2001;9(4):194-9. Epub 2001/08/28.
67. Bedi A, Raphael B, Maderazo A, Pavlov H, Williams RJ, 3rd. Transtibial versus anteromedial portal drilling for anterior cruciate ligament reconstruction: a cadaveric study of femoral tunnel length and obliquity. Arthroscopy : the journal of arthroscopic & related surgery : official publication of the Arthroscopy Association of North America and the International Arthroscopy Association. 2010;26(3):342-50. Epub 2010/03/09.
68. Trojani C, Sbihi A, Djian P, Potel JF, Hulet C, Jouve F, Bussiere C, Ehkirch FP, Burdin G, Dubrana F, Beaufils P, Franceschi JP, Chassaing V, Colombet P, Neyret P. Causes for failure of ACL reconstruction and influence of meniscectomies after revision. Knee surgery, sports traumatology, arthroscopy : official journal of the ESSKA. 2011;19(2):196-201. Epub 2010/07/21.
69. Greis PE, Johnson DL, Fu FH. Revision anterior cruciate ligament surgery: causes of graft failure and technical considerations of revision surgery. Clinics in sports medicine. 1993;12(4):839-52. Epub 1993/10/01.

70. Sommer C, Friederich NF, Muller W. Improperly placed anterior cruciate ligament grafts: correlation between radiological parameters and clinical results. Knee surgery, sports traumatology, arthroscopy : official journal of the ESSKA. 2000;8(4):207-13. Epub 2000/09/07.
71. Morgan JA, Dahm D, Levy B, Stuart MJ. Femoral tunnel malposition in ACL revision reconstruction. The journal of knee surgery. 2012;25(5):361-8. Epub 2012/11/15.
72. Rahr-Wagner L, Thillemann TM, Pedersen AB, Lind MC. Increased risk of revision after anteromedial compared with transtibial drilling of the femoral tunnel during primary anterior cruciate ligament reconstruction: results from the Danish Knee Ligament Reconstruction Register. Arthroscopy : the journal of arthroscopic & related surgery : official publication of the Arthroscopy Association of North America and the International Arthroscopy Association. 2013;29(1):98-105. Epub 2013/01/02.
73. Loh JC, Fukuda Y, Tsuda E, Steadman RJ, Fu FH, Woo SL. Knee stability and graft function following anterior cruciate ligament reconstruction: Comparison between 11 o'clock and 10 o'clock femoral tunnel placement. 2002 Richard O'Connor Award paper. Arthroscopy : the journal of arthroscopic & related surgery : official publication of the Arthroscopy Association of North America and the International Arthroscopy Association. 2003;19(3):297-304. Epub 2003/03/11.
74. Howell SM, Taylor MA. Failure of reconstruction of the anterior cruciate ligament due to impingement by the intercondylar roof. The Journal of bone and joint surgery American volume. 1993;75(7):1044-55. Epub 1993/07/01.
75. Markolf KL, Hame S, Hunter DM, Oakes DA, Zoric B, Gause P, Finerman GA. Effects of femoral tunnel placement on knee laxity and forces in an anterior cruciate ligament graft. Journal of orthopaedic research : official publication of the Orthopaedic Research Society. 2002;20(5):1016-24. Epub 2002/10/18.
76. Busam ML, Provencher MT, Bach BR, Jr. Complications of anterior cruciate ligament reconstruction with bone-patellar tendon-bone constructs: care and prevention. The American journal of sports medicine. 2008;36(2):379-94. Epub 2008/01/19.
77. Kartus J, Magnusson L, Stener S, Brandsson S, Eriksson BI, Karlsson J. Complications following arthroscopic anterior cruciate ligament reconstruction. A 2-5-year follow-up of 604 patients with special emphasis on anterior knee pain. Knee surgery, sports traumatology, arthroscopy : official journal of the ESSKA. 1999;7(1):2-8. Epub 1999/02/20.
78. Meyers AB, Haims AH, Menn K, Moukaddam H. Imaging of anterior cruciate ligament repair and its complications. AJR Am J Roentgenol. 2010;194(2):476-84. Epub 2010/01/23.
79. Pinczewski LA, Lyman J, Salmon LJ, Russell VJ, Roe J, Linklater J. A 10-year comparison of anterior cruciate ligament reconstructions with hamstring tendon and patellar tendon autograft: a controlled, prospective trial. The American journal of sports medicine. 2007;35(4):564-74. Epub 2007/01/31.
80. Freedman KB, D'Amato MJ, Nedeff DD, Kaz A, Bach BR, Jr. Arthroscopic anterior cruciate ligament reconstruction: a metaanalysis comparing patellar tendon and hamstring tendon autografts. The American journal of sports medicine. 2003;31(1):2-11. Epub 2003/01/18.
81. Kartus J, Movin T, Karlsson J. Donor-site morbidity and anterior knee problems after anterior cruciate ligament reconstruction using autografts. Arthroscopy : the journal of arthroscopic & related surgery : official publication of the Arthroscopy Association of North America and the International Arthroscopy Association. 2001;17(9):971-80. Epub 2001/11/06.
82. Kamath GV, Redfern JC, Greis PE, Burks RT. Revision anterior cruciate ligament reconstruction. The American journal of sports medicine. 2011;39(1):199-217. Epub 2010/08/17.

83. von Porat A, Roos EM, Roos H. High prevalence of osteoarthritis 14 years after an anterior cruciate ligament tear in male soccer players: a study of radiographic and patient relevant outcomes. Ann Rheum Dis. 2004;63(3):269-73. Epub 2004/02/14.
84. Spindler KP, Parker RD, Andrish JT, Kaeding CC, Wright RW, Marx RG, McCarty EC, Amendola A, Dunn WR, Huston LJ, Harrell FE, Jr. Prognosis and predictors of ACL reconstructions using the MOON cohort: a model for comparative effectiveness studies. Journal of orthopaedic research : official publication of the Orthopaedic Research Society. 2013;31(1):2-9. Epub 2012/08/23.
85. Liden M, Sernert N, Rostgard-Christensen L, Kartus C, Ejerhed L. Osteoarthritic changes after anterior cruciate ligament reconstruction using bone-patellar tendon-bone or hamstring tendon autografts: a retrospective, 7-year radiographic and clinical follow-up study. Arthroscopy : the journal of arthroscopic & related surgery : official publication of the Arthroscopy Association of North America and the International Arthroscopy Association. 2008;24(8):899-908. Epub 2008/07/29.
86. Tashman S, Collon D, Anderson K, Kolowich P, Anderst W. Abnormal rotational knee motion during running after anterior cruciate ligament reconstruction. The American journal of sports medicine. 2004;32(4):975-83. Epub 2004/05/20.
87. Papannagari R, Gill TJ, Defrate LE, Moses JM, Petruska AJ, Li G. In vivo kinematics of the knee after anterior cruciate ligament reconstruction: a clinical and functional evaluation. The American journal of sports medicine. 2006;34(12):2006-12. Epub 2006/08/04.
88. Claes S, Vereecke E, Maes M, Victor J, Verdonk P, Bellemans J. Anatomy of the anterolateral ligament of the knee. Journal of anatomy. 2013;223(4):321-8. Epub 2013/08/03.
89. Beynnon BD, Johnson RJ, Abate JA, Fleming BC, Nichols CE. Treatment of anterior cruciate ligament injuries, part 2. The American journal of sports medicine. 2005;33(11):1751-67. Epub 2005/10/19.
90. Beynnon BD, Johnson RJ, Abate JA, Fleming BC, Nichols CE. Treatment of anterior cruciate ligament injuries, part I. The American journal of sports medicine. 2005;33(10):1579-602. Epub 2005/10/04.
91. van Kampen A, Wymenga AB, van der Heide HJ, Bakens HJ. The effect of different graft tensioning in anterior cruciate ligament reconstruction: a prospective randomized study. Arthroscopy : the journal of arthroscopic & related surgery : official publication of the Arthroscopy Association of North America and the International Arthroscopy Association. 1998;14(8):845-50. Epub 1998/12/16.
92. Mott HW. Semitendinosus anatomic reconstruction for cruciate ligament insufficiency. Clinical orthopaedics and related research. 1983(172):90-2. Epub 1983/01/01.
93. Muneta T, Sekiya I, Yagishita K, Ogiuchi T, Yamamoto H, Shinomiya K. Two-bundle reconstruction of the anterior cruciate ligament using semitendinosus tendon with endobuttons: operative technique and preliminary results. Arthroscopy : the journal of arthroscopic & related surgery : official publication of the Arthroscopy Association of North America and the International Arthroscopy Association. 1999;15(6):618-24. Epub 1999/09/24.
94. Rosenberg T, Graf B. Techniques for ACL reconstruction with Multi-Trac drill guide.: Mansfield, MA: Acufex Microsurgical; 1994.
95. Yasuda K, Kondo E, Ichiyama H, Kitamura N, Tanabe Y, Tohyama H, Minami A. Anatomic reconstruction of the anteromedial and posterolateral bundles of the anterior cruciate ligament using hamstring tendon grafts. Arthroscopy : the journal of arthroscopic & related surgery : official publication of the Arthroscopy Association of North America and the International Arthroscopy Association. 2004;20(10):1015-25. Epub 2004/12/14.

96. Cha PS, Brucker PU, West RV, Zelle BA, Yagi M, Kurosaka M, Fu FH. Arthroscopic double-bundle anterior cruciate ligament reconstruction: an anatomic approach. Arthroscopy : the journal of arthroscopic & related surgery : official publication of the Arthroscopy Association of North America and the International Arthroscopy Association. 2005;21(10):1275. Epub 2005/10/18.
97. Shino K NK, Nakamura N, Mae T, Ohtsubo H, Iwahashi T, Nakagawa S. Anatomic anterior cruciate ligament reconstruction using two double-looped hamstring tendon grafts via twin femoral and triple tibial tunnels. Oper Tech Orthop. 2005;15:130–4.
98. Harner CD, Poehling GG. Double bundle or double trouble? Arthroscopy : the journal of arthroscopic & related surgery : official publication of the Arthroscopy Association of North America and the International Arthroscopy Association. 2004;20(10):1013-4. Epub 2004/12/14.
99. Lopez-Vidriero E, Hugh Johnson D. Evolving concepts in tunnel placement. Sports medicine and arthroscopy review. 2009;17(4):210-6. Epub 2009/11/17.
100. van Eck CF, Gravare-Silbernagel K, Samuelsson K, Musahl V, van Dijk CN, Karlsson J, Irrgang JJ, Fu FH. Evidence to support the interpretation and use of the anatomic anterior cruciate ligament reconstruction checklist. The Journal of bone and joint surgery American volume. 2013;95(20):e1531-9. Epub 2013/10/18.
101. Strauss EJ, Barker JU, McGill K, Cole BJ, Bach BR, Jr., Verma NN. Can anatomic femoral tunnel placement be achieved using a transtibial technique for hamstring anterior cruciate ligament reconstruction? The American journal of sports medicine. 2011;39(6):1263-9. Epub 2011/02/22.
102. Kopf S, Forsythe B, Wong AK, Tashman S, Anderst W, Irrgang JJ, Fu FH. Nonanatomic tunnel position in traditional transtibial single-bundle anterior cruciate ligament reconstruction evaluated by three-dimensional computed tomography. The Journal of bone and joint surgery American volume. 2010;92(6):1427-31. Epub 2010/06/03.
103. Heming JF, Rand J, Steiner ME. Anatomical limitations of transtibial drilling in anterior cruciate ligament reconstruction. The American journal of sports medicine. 2007;35(10):1708-15. Epub 2007/08/01.
104. Wright RW, Magnussen RA, Dunn WR, Spindler KP. Ipsilateral graft and contralateral ACL rupture at five years or more following ACL reconstruction: a systematic review. The Journal of bone and joint surgery American volume. 2011;93(12):1159-65. Epub 2011/07/22.
105. Abebe ES, Utturkar GM, Taylor DC, Spritzer CE, Kim JP, Moorman CT, 3rd, Garrett WE, DeFrate LE. The effects of femoral graft placement on in vivo knee kinematics after anterior cruciate ligament reconstruction. Journal of biomechanics. 2011;44(5):924-9. Epub 2011/01/14.
106. Ziegler CG, Pietrini SD, Westerhaus BD, Anderson CJ, Wijdicks CA, Johansen S, Engebretsen L, LaPrade RF. Arthroscopically pertinent landmarks for tunnel positioning in single-bundle and double-bundle anterior cruciate ligament reconstructions. The American journal of sports medicine. 2011;39(4):743-52. Epub 2010/12/22.
107. Ferretti M, Ekdahl M, Shen W, Fu FH. Osseous landmarks of the femoral attachment of the anterior cruciate ligament: an anatomic study. Arthroscopy : the journal of arthroscopic & related surgery : official publication of the Arthroscopy Association of North America and the International Arthroscopy Association. 2007;23(11):1218-25. Epub 2007/11/08.
108. Farrow LD, Chen MR, Cooperman DR, Victoroff BN, Goodfellow DB. Morphology of the femoral intercondylar notch. The Journal of bone and joint surgery American volume. 2007;89(10):2150-5. Epub 2007/10/03.

109. Larson BJ, Egbert J, Goble EM. Radiation exposure during fluoroarthroscopically assisted anterior cruciate reconstruction. The American journal of sports medicine. 1995;23(4):462-4. Epub 1995/07/01.
110. Moloney G, Araujo P, Rabuck S, Carey R, Rincon G, Zhang X, Harner C. Use of a fluoroscopic overlay to assist arthroscopic anterior cruciate ligament reconstruction. The American journal of sports medicine. 2013;41(8):1794-800. Epub 2013/06/08.
111. Kawakami Y, Hiranaka T, Matsumoto T, Hida Y, Fukui T, Uemoto H, Doita M, Tsuji M, Kurosaka M, Kuroda R. The accuracy of bone tunnel position using fluoroscopic-based navigation system in anterior cruciate ligament reconstruction. Knee surgery, sports traumatology, arthroscopy : official journal of the ESSKA. 2012;20(8):1503-10. Epub 2011/10/25.
112. Klos TV, Habets RJ, Banks AZ, Banks SA, Devilee RJ, Cook FF. Computer assistance in arthroscopic anterior cruciate ligament reconstruction. Clinical orthopaedics and related research. 1998(354):65-9. Epub 1998/10/02.
113. Burkart A, Debski RE, McMahon PJ, Rudy T, Fu FH, Musahl V, van Scyoc A, Woo SL. Precision of ACL tunnel placement using traditional and robotic techniques. Computer aided surgery : official journal of the International Society for Computer Aided Surgery. 2001;6(5):270-8. Epub 2002/03/14.
114. Zaffagnini S, Klos TV, Bignozzi S. Computer-assisted anterior cruciate ligament reconstruction: an evidence-based approach of the first 15 years. Arthroscopy : the journal of arthroscopic & related surgery : official publication of the Arthroscopy Association of North America and the International Arthroscopy Association. 2010;26(4):546-54. Epub 2010/04/07.
115. Dessenne V, Lavallee S, Julliard R, Orti R, Martelli S, Cinquin P. Computer-assisted knee anterior cruciate ligament reconstruction: first clinical tests. Journal of image guided surgery. 1995;1(1):59-64. Epub 1995/01/01.
116. Woo SL, Vogrin TM, Abramowitch SD. Healing and repair of ligament injuries in the knee. The Journal of the American Academy of Orthopaedic Surgeons. 2000;8(6):364-72. Epub 2000/12/05.
117. Hsu SL, Liang R, Woo SL. Functional tissue engineering of ligament healing. Sports Med Arthrosc Rehabil Ther Technol. 2010;2:12. Epub 2010/05/25.
118. Ge Z, Goh JC, Lee EH. Selection of cell source for ligament tissue engineering. Cell Transplant. 2005;14(8):573-83. Epub 2005/12/17.
119. McKean JM, Hsieh AH, Sung KL. Epidermal growth factor differentially affects integrin-mediated adhesion and proliferation of ACL and MCL fibroblasts. Biorheology. 2004;41(2):139-52. Epub 2004/04/20.
120. Nagineni CN, Amiel D, Green MH, Berchuck M, Akeson WH. Characterization of the intrinsic properties of the anterior cruciate and medial collateral ligament cells: an in vitro cell culture study. Journal of orthopaedic research : official publication of the Orthopaedic Research Society. 1992;10(4):465-75. Epub 1992/07/01.
121. Radford WJ, Amis AA, Heatley FW. Immediate strength after suture of a torn anterior cruciate ligament. The Journal of bone and joint surgery British volume. 1994;76(3):480-4. Epub 1994/05/01.
122. Murray MM, Spindler KP, Abreu E, Muller JA, Nedder A, Kelly M, Frino J, Zurakowski D, Valenza M, Snyder BD, Connolly SA. Collagen-platelet rich plasma hydrogel enhances primary repair of the porcine anterior cruciate ligament. Journal of orthopaedic research : official publication of the Orthopaedic Research Society. 2007;25(1):81-91. Epub 2006/10/13.

123. Fisher MB, Liang R, Jung HJ, Kim KE, Zamarra G, Almarza AJ, McMahon PJ, Woo SL. Potential of healing a transected anterior cruciate ligament with genetically modified extracellular matrix bioscaffolds in a goat model. Knee surgery, sports traumatology, arthroscopy : official journal of the ESSKA. 2012;20(7):1357-65. Epub 2011/12/07.
124. Vavken P, Murray MM. Translational Studies in ACL repair. Tissue Eng Part A. 2009. Epub 2009/07/22.
125. Zantop T, Gilbert TW, Yoder MC, Badylak SF. Extracellular matrix scaffolds are repopulated by bone marrow-derived cells in a mouse model of achilles tendon reconstruction. J Orthop Res. 2006;24(6):1299-309. Epub 2006/05/02.
126. Gilbert TW, Stewart-Akers AM, Simmons-Byrd A, Badylak SF. Degradation and remodeling of small intestinal submucosa in canine Achilles tendon repair. The Journal of bone and joint surgery American volume. 2007;89(3):621-30. Epub 2007/03/03.
127. Voytik-Harbin SL, Brightman AO, Kraine MR, Waisner B, Badylak SF. Identification of extractable growth factors from small intestinal submucosa. J Cell Biochem. 1997;67(4):478-91. Epub 1998/01/24.
128. Hodde JP, Record RD, Liang HA, Badylak SF. Vascular endothelial growth factor in porcine-derived extracellular matrix. Endothelium : journal of endothelial cell research. 2001;8(1):11-24. Epub 2001/06/21.
129. Woo SL, Takakura Y, Liang R, Jia F, Moon DK. Treatment with bioscaffold enhances the the fibril morphology and the collagen composition of healing medial collateral ligament in rabbits. Tissue Eng. 2006;12(1):159-66. Epub 2006/02/28.
130. Musahl V, Abramowitch SD, Gilbert TW, Tsuda E, Wang JH, Badylak SF, Woo SL. The use of porcine small intestinal submucosa to enhance the healing of the medial collateral ligament--a functional tissue engineering study in rabbits. Journal of orthopaedic research : official publication of the Orthopaedic Research Society. 2004;22(1):214-20. Epub 2003/12/06.
131. Liang R, Woo SL, Takakura Y, Moon DK, Jia F, Abramowitch SD. Long-term effects of porcine small intestine submucosa on the healing of medial collateral ligament: a functional tissue engineering study. Journal of orthopaedic research : official publication of the Orthopaedic Research Society. 2006;24(4):811-9. Epub 2006/03/04.

Chapter 2

3D Fiber Tractography of the Cruciate Ligaments of the Knee

Martijn van de Giessen, D. Tan Nguyen, Geert J. Streekstra, Lucas J. van Vliet, Cornelis A. Grimbergen, Frans M. Vos, Leendert Blankevoort

Submitted for publication

ABSTRACT

Studying the complex three-dimensional collagen fiber architecture is challenging. The main drawback of most existing techniques is that they distort the ligament geometry during analysis.

In this research we propose to detect the collagen fiber anatomy in the knee by acquiring and processing a 3D volume of imaging data from a cryo-microtome imaging system. The ligament structure is visualized using the autofluorescent properties of collagen and analyzed by estimating the fiber orientations and performing a tractography along the ligaments. Specific image processing algorithms that suppress acquisition artifacts in the cryo-microtome data, while maintaining the fiber structure are presented and validated.

The ligament tractography enabled the visualization of fiber distributions between two connected bones. Tract lengths were found to be 32.0 (6.1) mm, 29.4 (5.4) mm, and 39.5 (4.4) mm on average (standard deviations) for the anterior cruciate ligament (ACL) of the three donors and 35.7 (1.8) mm, 40.1 (2.9) mm, and 39.8 (5.2) for the posterior cruciate ligament (PCL) of the three. Furthermore, connectivity maps between were generated, that showed that adjacent tracts on the femur stayed adjacent for both ACL and PCL.

The detected tracts can serve as a detailed input for biomechanical joint models and used for the optimization of ligament reconstruction procedures, implant designs and tissue engineering.

INTRODUCTION

Human joints play a pivotal role in the movement of the human body. The complex arrangements of bones and load-bearing tissues form mobile, yet stable connections. For example, four major knee ligaments connect the femur and tibia, allowing movement in three dimensions, while limiting excessive movement. Due to the dual function of joints, providing both stability and mobility, joints are frequently injured during work, daily tasks or sports related activities. Injury to ligaments or bone can result in joint instability, abnormal kinematics, pain and eventually osteoarthritis [23]. The development of new treatment methods requires better biomechanical models, which give better, quantitative insight in the complex relation between ligament properties and joint function [40, 8, 27, 19, 17, 26]. Several properties such as the biochemical composition and biomechanical properties of ligaments have been characterized accurately [5, 28, 41, 2, 33]. However, a detailed description of the 3-D collagen fiber architecture is missing, although it is widely recognized that the biomechanical properties and function of load-bearing tissues such as ligaments depend on the collagen fiber orientation. [15, 8, 27, 19].

Previously, Mommersteeg et al. [29] have used a manual digitizing system to obtain the fiber bundle orientation and insertion sites in the knee. The user of this system visually traces selected fiber bundles at a relatively large scale (visible by bare eye), which introduces subjectivity. Other researchers have used three-dimensional representations of ligaments by quantifying the geometry of the bundle volume using magnetic resonance imaging (MRI) or computed tomography (CT) [17, 26]. Unfortunately, the resolution of these imaging modalities is insufficient to visualize and track the fiber architecture.

Using an imaging cryo-microtome [36, 10, 4] it is possible to image a volume containing a complete joint and to measure the orientations and paths of the ligaments in this volume at a resolution on in the order of 50 μm.

In the field of (medical) image processing, estimating orientations of curvilinear structures has been a topic of intensive research. Methods based on steerable filters [13] or on filtering in the Fourier domain [6] can accurately estimate orientations, but the orientation estimates are based on user-defined search directions. Methods that use the Hessian matrix [12] or the structure tensor [24, 38] allow for localized, continuous orientation estimates. Contrary to the Hessian, the structure tensor can suppress noise by smoothing over orientations of parallel structures, such as ligament fiber bundles. The smoothed tensor field permits a tractography of the collagen fibers, similar to those in diffusion tensor imaging (DTI) data of the brain [1, 11] and muscles [14].

In this paper we propose to use cryo-microtome image volumes and a combination of structure tensor orientation estimates and deterministic tracking to quantify

ligament fiber paths, lengths and connectivity. Additionally, new filter techniques are proposed that specifically suppress artifacts in 3D cryo-microtome stacks. The main novelty of this paper is that it presents a pipeline for robust 3D trajectory estimates of collagen fibers in cryo-microtome image volumes.

2 METHODS

Tracts that describe the paths of collagen fibers are obtained by estimating the fiber orientations perpendicular to the intensity gradients in the cryo-microtome image volume. However, strong gradients, that disturb these orientation estimates are present in the imaged volumes, due to two reasons: (I) imperfect imaging conditions such as varying lighting over time and acquisition artifacts specific to the cryo-microtome and (II) the presence of strong edges in the image due to non- ligamentous structures such as cartilage and bone. To increase the robustness of the orientation estimates, the acquired image data is filtered before estimating orientations. In this work, tracts are estimated in the complete image volume. After estimating the orientations and generating tracts through the orientation field, a large number of spurious tracts will be present, e.g. tracts in ligaments or tendons that are not of interest. Valid tracts are selected as tracts that connect two user selected bones.

The complete procedure consists of six steps:

1. Acquire image volume: acquisition of cryo-microtome slices, in which collagen autofluoresces.
2. Annotate bone and cartilage: the annotation of bone and cartilage serves two purposes. First, the annotated areas are used to select tracts that connect bones. Second, the annotations are used to mask out bone and cartilage edges that introduce errors in the ligament orientation estimates.
3. Remove acquisition artifacts: most cryo-microtomes have light sources that vary over time in intensity and it also often occurs that some debris of a previous slice sticks to the surface. These lead to distorting imaging artifacts.
4. Estimate fiber orientations: orientations are estimated in the complete image volume using the structure tensor. Near ligament insertion areas, the orientation is computed using normalized convolution, to prevent mixing between gradients from the collagen structure and the bone edge.
5. Track fiber paths in orientation field: using a deterministic tracking method tracts are estimated in the complete image volume using a dense grid of starting points.
6. Select valid tracts: a subset of the tracts from the previous step is selected such that only tracts connecting user selected bones are preserved.

These steps are schematically shown in Figure 1 and are described in the following subsections.

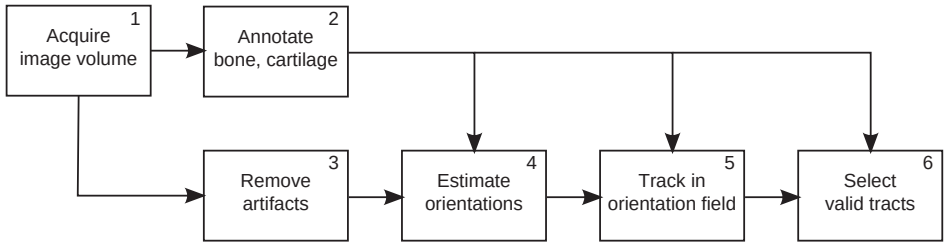

Figure 1: The ligament tracking process as described in Section 2.

2.1 ACQUISITION OF IMAGE VOLUME

2.1.1 Sample preparation

Three fresh-frozen cadaver knees were used from three donors: 53 yr male, 59 yr female, 69 yr male. Radiographs were made to exclude any fractures or severe osteoarthritis within the knees. After thawing, a Lachman and anterior-and posterior drawer test was performed in order to grossly assess if the anterior cruciate ligament (ACL) and posterior cruciate ligament (PCL) in the specimen were intact. Signs of knee joint pathology were absent. The maximum diameter of a sample that can be cut in the imaging cryo-microtome is 10 cm, therefore the femur and tibia were trimmed to a diameter of 9 cm. Further, to facilitate the cutting in the cryomicrotome, the cancellous and a part of the cortical bone of the knee joint were carefully removed. The knees were frozen at -20℃ in extension (53 yr male, 69 yr male), and 90˚ flexion (59 yr female) and embedded in a mixture of 5% carboxy-methylcellulose (CMC) sodium solvent and 4% Indian ink. The complete samples were kept at -20˚C.

2.1.2 Image acquisition

The prepared tissue block for each knee was mounted in a custom built imaging cryo-microtome [36]. Using this device, 50 μm thick slices were cut from the frozen cadaver material (kept at -20˚C) and the surface of the remaining sample was imaged using a Kodak Megaplus 4.2i CCD camera with a 70-180 mm Nikon lens. The in plane pixel size was set to 50 μm×50 μm, giving isotropic voxel sizes. A 300 W Xenon arc-lamp was used as light source. Autofluorescence images were acquired with excitation and emission filters of 480/20 nm and 505/30 nm, respectively (Figure 2a). Each slice was also imaged using reflectance imaging at 480nm (Figure 2b).

2.2 Annotation of bone and cartilage

Cartilage and bone were annotated in the autofluorescence image volume using ITK-SNAP [42]. The annotations were made in 3D using semi-automatic region growing and manual corrections (Figure 2c). Additionally, five cross-sections in each ligament were annotated manually (Figure 2d) by five independent observers to enable evaluation of the tracking accuracy and precision.

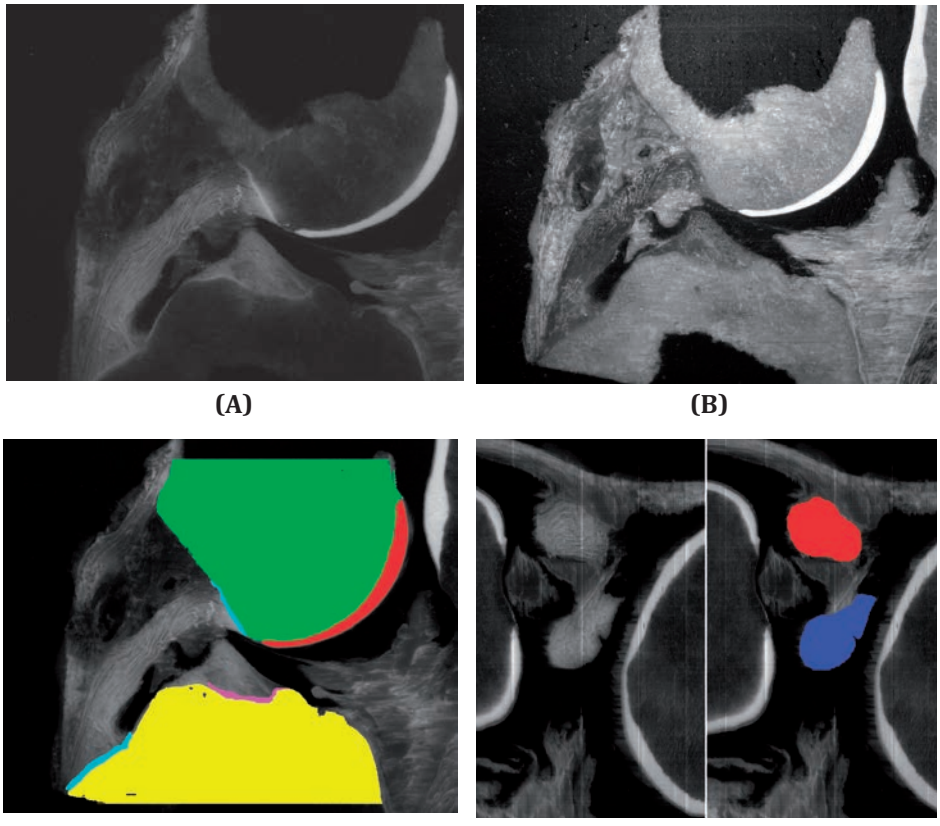

Figure 2: Cryo-microtome slice imaged under (a) autofluorescence and (b) reflectance. (c) Annotated bone and cartilage. (d) Example cross-sectional annotations of ACL and PCL in blue and red, respectively (sagittal view).

2.3 Removal of artifacts

2.3.1 Intensity inhomogeneities

The illumination of the cutting plane of the anatomical sample contained smooth and sharp changes over time that were not uniform over a slice. This was especially the case when a volume was cut in multiple sessions. Besides irreproducible lighting conditions between sessions, the tissue also tended to have varying levels of tissue humidity, a second source of intensity variation. The intensity inhomogeneities were corrected using a simple three step method:

1. Locally estimate the image intensity within each slice by filtering each slice using a 2D Gaussian smoothing filter of scale σi , giving a filtered image volume I_{xy} .

2. Locally estimate the image intensity variation between slices. The local average intensity was given by applying a 3D Gaussian smoothing filter of scale σi to the whole volume, giving a filtered image volume I_{xyz}. The local intensity variation is then given by the voxelwise division $V = I_{xy} / I_{xyz}$.
3. Correct the original image I_0 for the local intensity variations between slices using the voxelwise division $I_i = I_0 / V$.

The parameter σ_i should be chosen large compared to the structure of interest. Note that I_{xyz} can be computed efficiently from I_{xy} using a 1D convolution in the slice direction z due to the separability of Gaussian kernels.

2.3.2 Cutting debris and dark current lines

Cutting debris manifested itself in the image volumes as patches of a different intensity than the surrounding slices that are only present in a single slice (Figure 5). The debris is detected using a one-dimensional median filter of length 3 in the slice direction to obtain an image I_{med}. The difference image $I_d = I_i - I_{med}$ then contains the debris as values in the tails of the intensity distribution. Since a median filter belongs to the group of edge-preserving smoothing filters, we assume that I_d has a Gaussian intensity distribution with mean intensity μ_d and standard deviation σ_d. The probability to find a value $I_d(\mathbf{x})$ is then

$$P(I_d(\mathbf{x})) = \frac{1}{\sqrt{2\pi}\sigma_d} \exp\left(\frac{-\left(I_d(\mathbf{x}) - \mu_d\right)^2}{2\sigma_d^2}\right) \qquad (1)$$

where μ_d is generally close to 0 and large positive or negative values (compared to σ_d) have low probabilities and generally come from cutting debris or other artifacts. We take these probabilities as confidence values c_a for the reliability of a measured intensity.

Bright pixels due to dark current cause lines along the slicing direction (Figure 5). These lines hamper reliable orientation estimates. Although correction using a dark field image reduces these artifacts, not all lines in the slicing direction were removed. These lines are detected in a way that is similar to the cutting debris detection, but this time using the characteristic that in all slices the line tends to have a higher or lower intensity than the surrounding pixels. A sum projection over all slices is made and the locations of brighter/darker lines in the slice directions are detected with a 3 × 3 pixel median filter. Again a difference image is computed and the confidence values c_b are computed analogously to using (1). The map of the confidence values c_b is taken the same for each slice.

The detected debris and dark current lines were removed by filtering the image volume using normalized convolution [25]. For curvi-linear structures normalized convolution has two advantages over a 'normal' linear filtering: (I) For each voxel in the image volume, a confidence value c can be specified that determines the weight of the voxel in the filtering action (c = 1 for linear filtering); (II) higher order interpolation is possible (linear filtering corresponds to a 0 order interpolation), allowing the conservation of texture (and thus oriented structures) in the image [39].

In this work we take compute confidence values for normalized convolution as $c = c_a \cdot c_b$. A small 3D Gaussian kernel with σ_a = 0.9 voxels (45 μm) is used as the filter (applicability function in normalized convolution) that is used to interpolate the unreliable values with a low c. For this small kernel, a second order interpolation is sufficient to preserve the directed structure of the ligaments and minimal smoothing takes place. Further details on how to implement normalized convolution can be found in [39]. The resulting image volume I_c is a slightly blurred version of the original image, but without cutting debris (Figure 5).

2.4 Estimating orientations

Ligaments manifest themselves in the image data as parallel curvi-linear structures (Figure 5). Their intensity is approximately constant along the ligament direction and approximately periodic in directions perpendicular to the parallel curvilinear structures. To estimate the local orientations of the ligaments in the imaged volume, the structure tensor (ST) [24, 38] is computed in the filtered image volume. This tensor estimates orientations and their reliabilities based on the gradient of the image intensity:

$$\mathbf{S} = \overline{\mathbf{g} \cdot \mathbf{g}^T} = \begin{bmatrix} \overline{g_x^2} & \overline{g_x g_y} & \overline{g_x g_z} \\ \overline{g_x g_y} & \overline{g_y^2} & \overline{g_y g_z} \\ \overline{g_x g_z} & \overline{g_y g_z} & \overline{g_z^2} \end{bmatrix} \tag{2}$$

where the bar denotes a local Gaussian tensor smoothing of scale σ_t and $\mathbf{g} = \nabla I_c = [g_x\, g_y\, g_z]^T$ is a gradient vector, computed as the Gaussian intensity derivative [20] at a scale σ_g. The optimal gradient smoothing σ_g is related to the scale of the imaged structure and will be determined experimentally. The tensor smoothing σ_t depends on the size and shape of the texture and can be relatively large, e.g. $\sigma_t \geq 2\sigma_g$. This smoothing is necessary for an unambiguous definition of the six *different* elements of **S** [24]. The eigenvectors $\mathbf{v}i$ (i = 1, 2, 3) and corresponding eigenvalues $\lambda_1 \geq \lambda_2 \geq \lambda_3$ of **S** are measurements of the orientation and the structure of the texture, respectively. The vector $\mathbf{v}_1$ points in the direction of the largest intensity variation, whereas $\mathbf{v}_3$ points in the direction of the smallest intensity variation (Figure 3a), i.e. along the curvi-linear structures.

The reliability of the orientation is measured by the anisotropy

$$a = 1 - \frac{3\lambda_3}{\lambda_1 + \lambda_2 + \lambda_3} = \frac{\lambda_1 + \lambda_2 - 2\lambda_3}{\lambda_1 + \lambda_2 + \lambda_3} \quad (3)$$

which is an intensity invariant measure that varies between 0 (undirected) and 1 (reliable direction) (Figure 3b).

Both the computation of Gaussian derivatives and the tensor smoothing are evaluated on a small image volume. In the vicinity of bone and cartilage surfaces, the image volume includes both edges from the ligament structure as well as (strong) edges of the bone and cartilage, leading to incorrect orientation estimates. Therefore, in this work the structure tensors **S** are estimated using a first-order normalized convolution, with confidences set to 0 in annotated bone and cartilage regions.

2.5 Ligament tractography

The tractography method employed in this research is a deterministic tracking similar to tracking developed for diffusion tensor imaging (DTI) [1]. This method starts tracts at user-defined locations and integrates along the vectors that are oriented along the ligament structures using an Euler integration with step size *s*. For curvi-linear structures like ligaments, the intensity variation is minimal in the direction of the structure and the integration takes place in the direction of eigenvector $\mathbf{v}_3$. In this work tracts are started on all points of a 3D rectangular grid in the both the direction of $\mathbf{v}_3$ and $-\mathbf{v}_3$ at each grid point. The tracking stops when the image border is reached or when one of three user-defined stopping criteria is met:

1. The angle α between the orientations of two subsequent steps is higher than a user-defined threshold α_{max} . A large change in orientation between two consecutive steps indicates two crossing structures.
2. The anisotropy value a after the next step is lower than a user-defined threshold a_{min} . A low anisotropy indicates an unreliable orientation estimate.
3. A user-defined maximum number of n_{max} steps is exceeded. This stops tracts that wind around umbilic points such as “circular” objects.

To ensure that ligaments stop at the annotated bones and cartilage, the anisotropy a at these regions is set to 0 (Figure 3c).

2.6 Selecting valid tracts

Although the lengths of the tracts can be adjusted using the three user-defined stopping criteria it is likely that a number of tracts do not connect to the bone surfaces that the tracked ligament connects. For example, tracts stop early at (small) regions of low anisotropy and tracts that have their starting points outside the ligament of interest do not stop at either of the bones. Tracts that actually describe the orientation of collagen fibers within the ligament of interest are detected by only selecting the tracts that have their end points on a different bone surface.

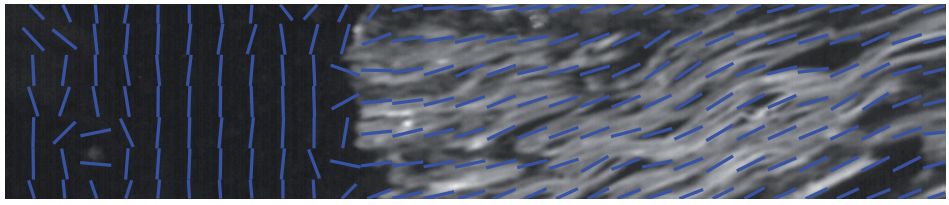

(A)

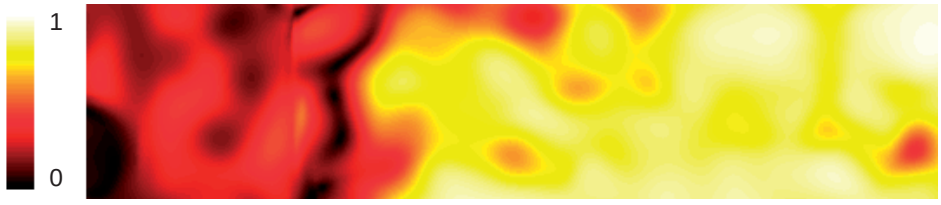

(B)

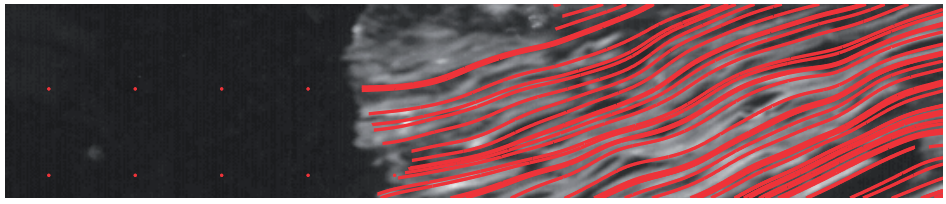

(C)

Figure 3: Illustration of tracking in 2D: (a) Orientation estimates (sparsely sampled in visualization), (b) anisotropy estimates a, a is close to 1 within the ligament and close to 0 outside, (c) tracts in regions with anisotropy higher than 0.5. Dots outside the ligament are starting points within low anisotropy regions, with zero-length tracts. Tracts appear smoother than the underlying image due tensor smoothing with σ_t .

2.7 Parameters

The most important parameters that influence the tracking are listed below.

Orientation estimate The scale parameters for the structure tensor σ_g , σ_t depend on the period p (Section 2.4). In experiments we test which σ_g and σ_t are optimal for the data at hand.

Tracking The step size s is chosen to be 0.5 voxel, which equals 25 µm in our data, giving a sub-voxel accuracy. The maximum number of iterations n_{max} is fixed at 10,000 (= 25 cm), much larger than the ligament lengths in our data. The stopping criteria of maximum angle between steps $\alpha_{max} = \pi/4$ and minimum anisotropy $a_{min} = 0.1$. These settings impose almost no limits on the tracking results. In this work this is possible because the annotated insertion areas are used for stopping the tractography at bone/cartilage surfaces and selecting valid tracts.

3 VALIDATION

3.1 Comparison of ligament autofluorescence to histology

To validate if the intensity variations in the image data correspond to the collagen fibers in the ligaments, a histological experiment was performed. A human ACL was prepared for cryo-microtome imaging and Masson's trichrome staining. The ACL was harvested from a fresh frozen cadaver knee and was embedded in Tissue-Tek O.C.T. compound (Sakura Finetek). The ACL was cut with a cryostat into sagittal sections of 50μm and collected on slides. The slides were first imaged with the cryo-microtome. Subsequently, the same slides were fixed in 4% formalin and stained with Masson's trichrome according to standard procedures, where collagen was stained in blue. The cryo-microtome and histological images were registered using an affine registration to allow a direct visual and quantitative comparison. The registration used mutual information as similarity criterion to cope with the differences in intensities between the two imaging modalities.

3.2 Removal of artifacts

For one knee (69 yr male) the ligament fiber orientations were estimated before and after the removal of artifacts with $\sigma_g = 50\ \mu$m and $\sigma_t = 150\ \mu$m. Subsequently tracking was performed between annotated ligament cross-sections. The accuracy of the ligament tracts was evaluated as the overlap between annotated cross-sectional regions and the regions covered by tracts passing through the regions. In this comparison, each tract is assumed to have a 1 voxel diameter. The Dice coefficent D [9] is used as a measure for comparison between two sets of voxels A (intersecting tracts) and B (annotations), defined as

$$D = \frac{2\,|A \cap B|}{|A| + |B|} \tag{4}$$

where $|\cdot|$ denotes the number of annotated voxels.

3.3 Optimal orientation estimation parameters

For each knee and each cruciate ligament, the insertion regions as well as the cross- sectional areas on five equally spaced slices approximately perpendicular to the main ligament orientation were annotated by hand. These slices serve as ground truth ligament locations. Optimal values for σ_g and σ_t were determined by computing structure tensors within an annotated volume using all combinations of $\sigma_g \in \{0.8, 1.4, 2.0, 2.6\}$ and $\sigma_t \in \{2.0, 4.0, 6.0, \ldots, 16.0\}$. Trackings were performed from each annotated slice. Tracking parameters were set to allow any tract, i.e. $\alpha_{max} = 90^\circ$, $a_{min} = 0$, $n_{max} = 10^6$. The accuracy of the ligament tracts is evaluated as the overlap between the annotated cross-sectional and insertion regions and the tracts passing through these regions. In this comparison each tract is assumed to have a single voxel diameter and Dice's coefficient (4) is used as a measure for comparison between two sets of voxels A (tracts) and B (annotations).

3.4 Anatomical validation

The validity of the tracts as a measure for ligament fiber geometry was investigated by deriving parameters that characterize the ligaments and the connectivity between femur and tibia.

3.4.1 Anatomical parameters

The lengths of the tracts within the anterior and posterior cruciate ligaments were measured to describe the distribution of fiber lengths within each of the ligaments. The length of each tract was determined by counting the number of steps taken in the Euler integration and multiplying these by the step lengths (25 μm). Lengths from ligaments which stopped early due to weakly directed image data (low anisotropy) close to the bone were corrected by extrapolation to the annotated bone surface along the tract direction.

3.4.2 Connectivity

The two endpoints of a tract describe which areas of femur and tibia are connected. This connectivity was visualized by assigning the same color to each endpoint of a tract, where endpoints on the femur that are close together have a similar color. The colors of the tract endpoints were mapped to the segmented bone surfaces to facilitate interpretation.

4 RESULTS

4.1 Comparison of autofluorescencing ligament to histology

Autofluorescence (Figure 4a) and Masson's trichrome staining (Figure 4b) showed visibly similar patterns on a human ACL slice, with clear fiber-like structures. Autofluorescence and inverse staining intensities within the ligaments (i.e. after masking out the background, Figure (4c)) correlated with a Pearson correlation coefficient of 0.67. This correlation can be considered high, given the fact that a linear relationship between intensities in 4a and 4b is not to be expected due to the different acquisition methods.

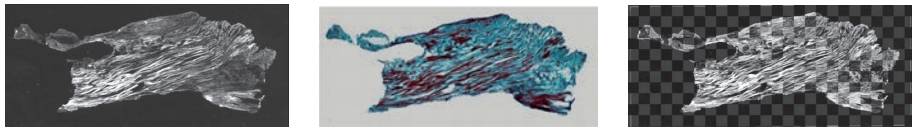

(A) **(B)** **(C)**

Figure 4: Comparison between (a) an autofluorescence acquisition (cryo- microtome) and (b) a Masson's trichrome staining of the same tissue slice of a human ACL. (c) Checkerboard overlay of the autofluorescene acquisition (a) and the intensity inverse of the histological staining (b) after affine registration. The correspondence between autofluorescing fibers and the trichrome staining (both bright) is clear from the continuous fibers at the checkerboard edges.

4.2 Removal of artifacts

Visual inspection showed an almost complete removal of artifacts in the estimated orientation maps after removal using normalized convolution (Figure 5) in all three knees. Without artifact removal orientation estimates were distorted at locations far from the actual artifacts. After correction, the orientation estimates did not contain clear distortions. Quantitatively, the agreement between manual annotations and tract bundle intersections improved considerably after the artifacts are removed (Table 1). Especially for longer tracking distances the increased robustness of the tracking became clear. For example for the tracts that connect the annotated slices that are furthest apart (4 interleaved slices), the mean Dice coefficient increased from 0.17 to 0.58. The first and last slices were on average (averaged over three knees and ACL and PCL) 11.0 mm apart, or 220 image slices. The decrease in D_u for longer tracking distances is for a large part due to tracts that halt due to large bending angles or because tracts leave the ligament. These are both caused by artifacts. After removal of these artifacts, D_c still shows a decrease for larger tracking distances. This decrease can mainly be attributed to intensity differences between adjacent collagen fibers. The gradients resulting from these variations in intensity induce a clustering of tracts near high intensity fibers. Although the tracking does not stop, the tracts are not homogeneously distributed over the ligament cross-sections anymore.

Table 1

Annotated slices	D_u	D_c
0	0.93 (0.07)	0.95 (0.03)
1	0.55 (0.13)	0.76 (0.09)
2	0.37 (0.12)	0.70 (0.11)
3	0.25 (0.11)	0.61 (0.12)
4	0.17 (0.09)	0.58 (0.12)

Agreement between manual annotations and areas covered by tracts in one knee (69 years, male). The agreement before and after artifact removal is described by Dice coefficients *Du* and *Dc* for uncorrected and corrected image volumes, re- spectively. Spacing between annotated slices varied slightly between knees and was in the order of 2.7 mm. Standard deviations are between parentheses.

4.3 Optimal orientation stimation parameters

Tract cross-sections and manual annotations displayed the best agreement (i.e. the highest Dice coefficients) for low σ_g and high σ_t (Figures 6a and 6b). In all three knee volumes, for higher values than σ_t of approximately 500 μm, only slight improvement takes place. For fibers with a high curvature and for high values of σ_t , tracts tended to 'escape' the real bundle. Therefore we set σ_t to 500 μm and σ_g to 40 μm. For smaller values of σ_g , the resulting gradient filter will produce a bias of the estimated orientation.

4.4 Anatomical validation

ACL and PCL tractographies were obtained for all three knees (Figure 7) with σ_g = 40 μm, σ_t = 500 μm, $ami\ n$ = 0.5 and $\alpha m\ a\ x$ = 45 $^\circ$. Tract lengths and connectivity were determined based on these tracts. In one sample (Figure 7b) only few tracts were found that connected femur and tibia. In this knee collagen fluorescence was very bright in the PCL, leading to regions where the acquisition was overexposed and no orientation could be estimated.

Mean tract lengths in the ACL for each of the three donors were (standard deviations between parenthesis): 32.0 (6.1) mm, 29.4 (5.4) mm, and 39.5 (4.4) mm. For the PCL, mean tract lengths were 35.7 (1.8) mm, 40.1 (2.9) mm, and 39.8 (5.2). Tracts in the ACL showed a broader distribution in length than PCL tracts (Figure 8). Tracts with lengths of about 20 mm in the ACL were incorrectly detected tracts between femur and tibia. In the PCL of one of the donors additional fibers between femur and tibia were detected that are not part of the PCL (Figure 7c, left most part of PCL). These were due to a meniscus fragment that apparently had come loose during sample preparation.

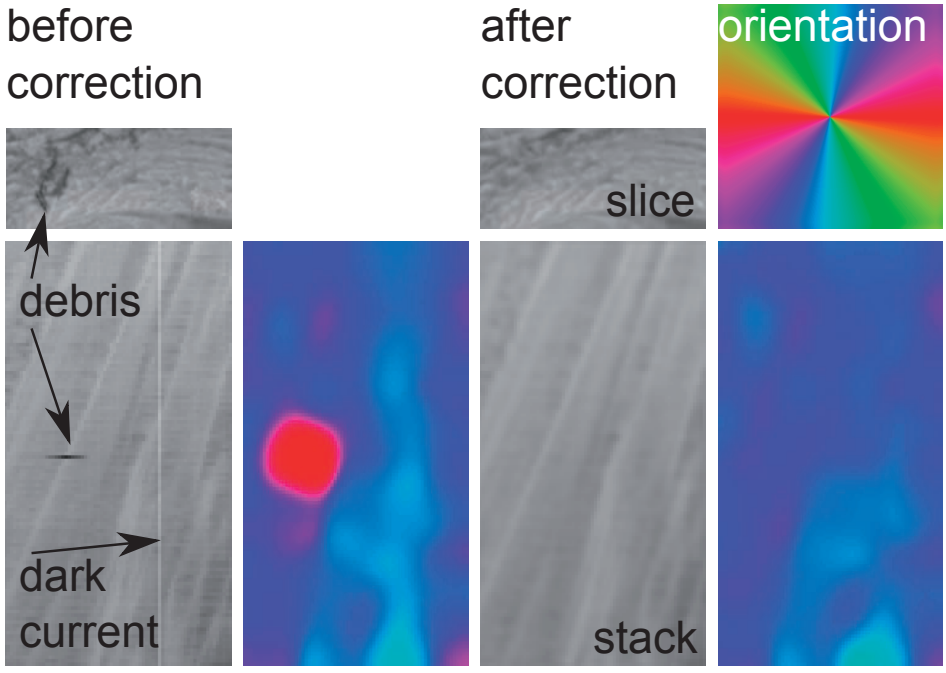

Figure 5:

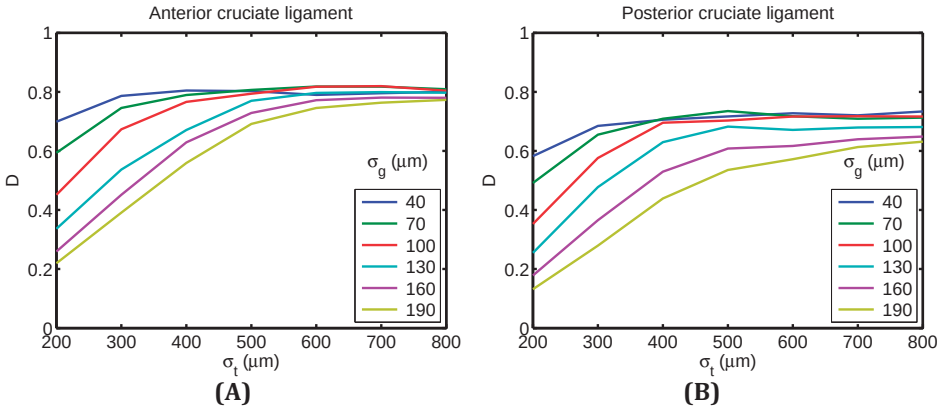

Figure 6: Agreement between annotated (a) anterior and (b) posterior ligament cross-sections and tracts for one of three knees (69 years, male), expressed as Dice coefficients D as a function of the tensor sigma σ_t . Each line corresponds to a gradient sigma σ_g , expressed in μm. The presented Dice coefficients are based on tracts between the annotations closest to the bones , i.e. covering the longest ligament length

Connectivity between femur and tibia for both ACL and PCL was studied by location dependent color-coding of each fiber tract and coloring their respective tibial and femoral insertion site with the same color (Figure 9). In the resulting connectivity maps fiber tracts that were neighbors at the tibial insertion site in general remained neighbors at the femoral site (Figure 9). Exceptions were incorrectly found connections in the first donor (Figure 8a), where the light blue area on the tibia has a (falsely) corresponding area where the femoral condyles are connected (Figure 9a). The light-blue area on the femur in the second donor (Figure 9c) is hidden by the cartilage layer close to the green area. At this location cartilage and insertion area were difficult to discern, leading to tracts finishing in the region annotated as cartilage. Connectivity maps were consistent between the three donors, apart from the size of the insertion areas. Although these area variations are also visible in the original data, the insertion site of the second donor (Figures 9c and 9d) were underestimated due to missed tracts as a result of the previously mentioned overexposure. This is also apparent from the low tract count in Figure 8b.

5 DISCUSSION

In this study a new method to quantify and visualize collagen fiber geometry in 3D was proposed and validated. By imaging collagen autofluorescence in a cryo-microtome, the fiber structure of anterior and posterior cruciate ligaments in the knee were made visible. By estimating the orientations of the ligament fibers using the structure tensors and performing a tractography through these tensor fields, we were able to obtain reconstructions of the 3-D collagen fiber tracts and were able perform analyses

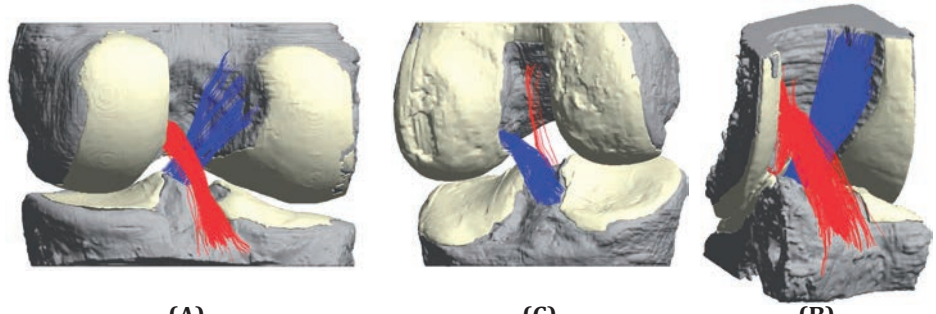

(A) **(C)** **(B)**

Figure 7: Visualization of tracts of ACL (blue) and PCL (red) between femur and tibia for all three knees: (a) 53 years, male, (b) 59 years, female, (c) 69 years, male. The PCL in (b) only has few tracts connecting femur and tibia due to regions with over-exposure where orientation could not be estimated. The bone (grey) and cartilage (off-white) are manually segmented surfaces.

on this data. Apart from visualizing the ligament geometry, statistics on tract lengths and connectivity maps were given as examples of applicability.

The feasibility of collagen autofluorescence imaging for fiber anatomy was validated through dual imaging of the same anatomical slice under autofluorescence and Masson's trichrome staining. The custom image processing algorithms for acquisition artifact suppression, for fiber orientation estimation were all written in MATLAB (The Mathworks, Natick, MA, USA) using the DipLib toolbox (www.diplib.org) and validated by comparing estimated connectivity to ground truth annotations. The meaning of the estimated tracts was studied by computing tract lengths and connectivity maps between insertion areas of both anterior cruciate ligaments and posterior cruciate ligaments.

Obtaining objective and detailed information of the anatomy of the ACL is fundamental for understanding its function as well as for developing effective treatments. Furthermore, the tracts can directly serve as input with unprecedented detail for biomechanical models aimed at studying the joint function. Currently, there is still debate regarding the 3D collagen fiber anatomy of the ACL and its surgical reconstruction. We think that the added value of the proposed method lies in the preservation of the 3D geometry. In previous studies, where researchers manually dissected the ACL and illustrated the fiber orientation with essentially 2D anatomical drawings and photographs, the full 3D geometry was inherently lost [16, 18, 22, 30, 31, 7]. To a lesser extent this holds for manual digitizing systems, where fiber bundles are traced in 3D, but surrounding structures such as bone and cartilage are lost [29]. Most importantly, due to the automated tracking and the preservation of the 3D image volume, the method that we propose is much less user-dependent than the aforementioned dissection methods.

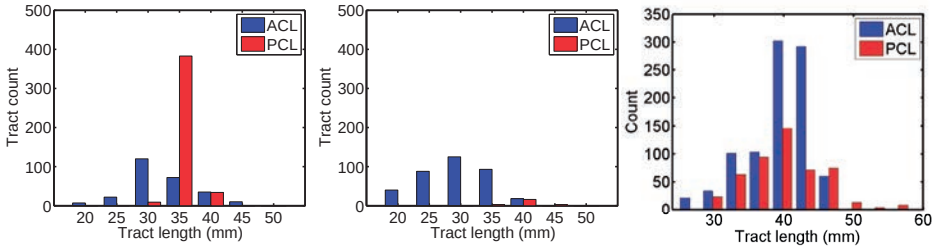

Figure 8: Histogram of tract lengths within ACL and PCL in all three donors: (a) 53 years, male, (b) 59 years, female, (c) 69 years, male. The ACL tract lengths of 20 mm and lower were incorrectly detected connections between femur and tibia. The tract lengths on the horizontal axis denote the bin centers.

Although providing insight into the geometry of the ligament structures, one should be careful in interpreting the tracts that describe the ligaments. Most importantly, the tracts only follow the directions of the fibers. They are, however not the fibers themselves: Figure 3c clearly illustrates this, where multiple tracts follow the same bright structure. The presented image processing methods are therefore not fit to determine the fiber density within a ligament. For such applications, one may prefer imaging modalities with a higher resolution such as scanning electron microscopy (SEM), transmission electron microscopy (TEM), confocal microscopy, 3-D histology, and small angle light scattering [35, 32, 21, 34]. These are, however, limiting the imaged volume.

Generating the fiber tracts is very sensitive to artifacts in the data. Although many of these artifacts can be filtered out (Section 2.3), deterministic tracking cannot progress through (image) regions without structure, e.g. homogeneous bright regions due to overexposure. Probabilistic fiber tracking methods that take these kind of uncertainties into account, e.g. [43], might be a solution. Application, however, is not straightforward due to a different type of tensors (structure tensors vs. diffusion tensors), inhomogeneous cryo-microtome data (along tracts) and very large data volumes.

The most important limitation of our method lies in the destructive nature of the acquisition method. The usage of our method is therefore usable for modeling and *ex-vivo* anatomical studies, but cannot be translated directly to a clinical application. Future developments may enable 3D fiber bundle geometry imaging using MRI [37, 3], but the current resolution of MRI is insufficient to visualize the detailed fiber architecture of the ACL and PCL.

Although this work focuses on studying cruciate ligaments, many other fibrous structures may be studied in a similar fashion. Obvious applications are anatomical data of other ligaments and collagenous load bearing tissues such as menisci and the intervertebral discs. Other structures of interest are heart valves. Such research may increase our understanding of the function and pathophysiology of these structures

by incorporating the anatomical data in biomechanical models. The fiber anatomy can also be a blueprint to guide the development of new treatments and scaffold design.

In conclusion, we have shown the feasibility of obtaining objective and detailed information on the 3D geometry and connectivity of ligaments in the knee. We propose this method as an objective alternative to the characterization of ligamentous tissue by (macroscopic) dissection methods. Our presented integrated pipeline of cryo-microtome imaging, image processing and visualization enables accurate ligament characterization while preserving joint geometry.

ACKNOWLEDGEMENTS

The authors acknowledge the assistance of dr. Jeroen P. van den Wijngaard and dr. Pepijn van Horssen with the acquisition of the cryo-microtome images.

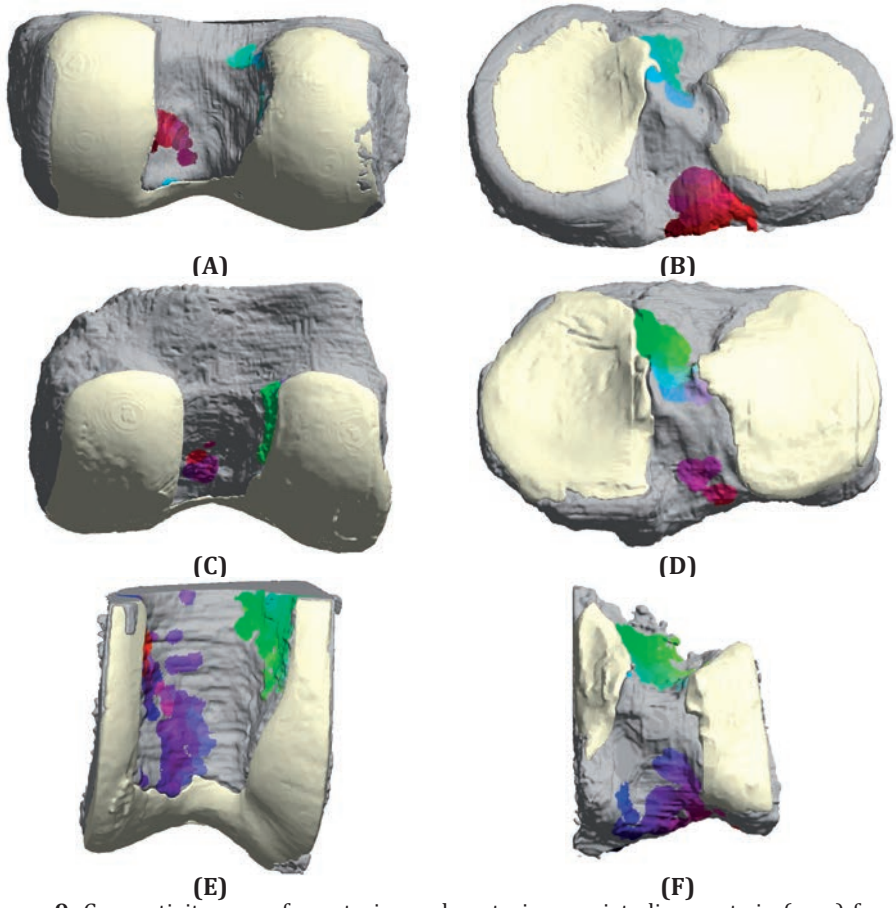

Figure 9: Connectivity maps for anterior and posterior cruciate ligaments in (a,c,e) femur and (b,d,f) tibia for three donors. Corresponding colors denote connected insertions.

REFERENCES

1. P. J. Basser, S. Pajevic, C. Pierpaoli, J. Duda, and A. Aldroubi. In vivo fiber tractography using DT-MRI data. *Magn Reson Med*, 44(4):625–32, 2000.
2. R. A. Berger, T. Imeada, L. Berglund, and K. N. An. Constraint and material properties of the subregions of the scapholunate interosseous ligament. *J Hand Surg Am*, 24(5):953–62, 1999.
3. M. J. Breitenseher and M. E. Mayerhoefer. Oblique MR imaging of the anterior cruciate ligament based on three-dimensional orientation. *J Magn Reson Imaging*, 26(3):794–8, 2007.
4. G. A. Buijze, N. A. Dvinskikh, S. D. Strackee, G. J. Streekstra, and L. Blankevoort. Osseous and ligamentous scaphoid anatomy: Part ii. evaluation of ligament morphology using three-dimensional anatomical imaging. *J Hand Surg Am*, 36(12):1936–1943, Dec 2011.
5. D. L. Butler, F. R. Noyes, and E. S. Grood. Ligamentous restraints to anteriorposterior drawer in the human knee. A biomechanical study. *J Bone Joint Surg Am*, 62(2):259–70, 1980.
6. S. Chaudhuri, H. Nguyen, R. M. Rangayyan, S. Walsh, and C. B. Frank. A Fourier domain directional filtering method for analysis of collagen alignment in ligaments. *IEEE Trans Biomed Eng*, 34(7):509–18, 1987.
7. A. Chhabra, J. S. Starman, M. Ferretti, A. F. Vidal, T. Zantop, and F. H. Fu. Anatomic, radiographic, biomechanical, and kinematic evaluation of the anterior cruciate ligament and its two functional bundles. *J Bone Joint Surg Am*, 88 Suppl 4:2–10, 2006.
8. W. J. T. Daniel. Three-dimensional orthotropic viscoelastic finite element model of a human ligament. *Comput Method Biomech Biomed Eng*, 4(3):265 – 279, 2001.
9. L. R. Dice. Measures of the amount of ecologic association between species. *Ecology*, 26(3):297–302, 1945.
10. N. A. Dvinskikh, L. Blankevoort, M. Foumani, J A E. Spaan, and G. J. Streekstra. Quantitative detection of cartilage surfaces and ligament geometry of the wrist using an imaging cryomicrotome system. *J Biomech*, 43(5):1007–1010, 2010.
11. P. T. Fletcher, R. Tao, W. K. Jeong, and R. T. Whitaker. A volumetric approach to quantifying region-to-region white matter connectivity in diffusion tensor MRI. In *Information Processing in Medical Imaging - Lecture Notes in Computer Science*, volume 4584, pages 346–58, 2007.
12. A. F. Frangi, W. J. Niessen, R. M. Hoogeveen, T. van Walsum, and M. A. Viergever. Model-based quantitation of 3-d magnetic resonance angiographic images. *IEEE Trans Med Imaging*, 18(10):946–56, 1999.
13. W. T. Freeman and E. H. Adelson. The design and use of steerable filters. *IEEE Trans Patt Anal Mach Int*, 13(9):891–906, 1991.
14. M. Froeling, A. J. Nederveen, K. Nicolay, and G. J. Strijkers. Dti of human skeletal muscle: the effects of diffusion encoding parameters, signal-to-noise ratio and t2 on tensor indices and fiber tracts. *NMR Biomed*, 26(11):1339–1352, Nov 2013.
15. Y. C. Fung. *Biomechanics: Mechanical properties of living tissues*. Springer- Verlag, Berlin, 1993.
16. F. K. Fuss. Anatomy of the cruciate ligaments and their function in extension and flexion of the human knee joint. *Am J Anat*, 184(2):165–76, 1989.
17. J. C. Gardiner and J. A. Weiss. Subject-specific finite element analysis of the human medial collateral ligament during valgus knee loading. *J Orthop Res*, 21(6):1098–106, 2003.
18. F. G. Girgis, J. L. Marshall, and A. Monajem. The cruciate ligaments of the knee joint. anatomical, functional and experimental analysis. *Clin Orthop Relat Res*, (106):216–31, 1975.

19. M. K. Gislason, D. H. Nash, A. Nicol, A. Kanellopoulos, M. Bransby-Zachary, T. Hems, B. Condon, and B. Stansfield. A three-dimensional finite element model of maximal grip loading in the human wrist. *Proc Inst Mech Eng H*, 223(7):849–61, 2009.
20. R.C. Gonzalez and R.E. Woods. *Digital Image Processing*. Pearson/Prentice Hall, 3rd edition, 2008.
21. P. T. Hadjicostas, P. N. Soucacos, N. Koleganova, G. Krohmer, and I. Berger. Comparative and morphological analysis of commonly used autografts for anterior cruciate ligament reconstruction with the native ACL: an electron, microscopic and morphologic study. *Knee Surg Sports Traumatol Arthrosc*, 16(12):1099–107, 2008.
22. K. Hara, T. Mochizuki, I. Sekiya, K. Yamaguchi, K. Akita, and T. Muneta. Anatomy of normal human anterior cruciate ligament attachments evaluated by divided small bundles. *Am J Sports Med*, 37(12):2386–91, 2009.
23. P. Kannus and M. Jarvinen. Conservatively treated tears of the anterior cruciate ligament. long-term results. *J Bone Joint Surg Am*, 69(7):1007–12, 1987. +++
24. H. Knutsson. Representing local structure using tensors. In *Proceeding of the 6th Scandinavian Conference on Image Analysis*, pages 244–251, Oulu, Finland, 1989.
25. H. Knutsson and C. F. Westin. Normalized and differential convolution. In *Computer Vision and Pattern Recognition, 1993. Proceedings CVPR '93., 1993 IEEE Computer Society Conference on*, pages 515–523, 1993.
26. G. Li, J. Gil, A. Kanamori, and S. L. Woo. A validated three-dimensional computational model of a human knee joint. *J Biomech Eng*, 121(6):657–62, 1999.
27. G. Limbert, M. Taylor, and J. Middleton. Three-dimensional finite element modelling of the human ACL: simulation of passive knee flexion with a stressed and stress-free ACL. *J Biomech*, 37(11):1723–31, 2004.
28. K. L. Markolf, J. S. Mensch, and H. C. Amstutz. Stiffness and laxity of the knee– the contributions of the supporting structures. a quantitative in vitro study. *J Bone Joint Surg Am*, 58(5):583–94, 1976.
29. T. J. Mommersteeg, J. G. Kooloos, L. Blankevoort, J. M. Kauer, R. Huiskes, and F. Q. Roeling. The fibre bundle anatomy of human cruciate ligaments. *J Anat*, 187 (Pt 2):461–71, 1995.
30. L. A. Norwood and M. J. Cross. Anterior cruciate ligament: functional anatomy of its bundles in rotatory instabilities. *Am J Sports Med*, 7(1):23–6, 1979.
31. M. Odensten and J. Gillquist. Functional anatomy of the anterior cruciate ligament and a rationale for reconstruction. *J Bone Joint Surg Am*, 67(2):257–62, 1985.
32. P. P. Provenzano, C. Hurschler, and Jr. Vanderby, R. Microstructural morphology in the transition region between scar and intact residual segments of a healing rat medial collateral ligament. *Connect Tissue Res*, 42(2):123–33, 2001.
33. M. J. Ritt, R. A. Berger, A. T. Bishop, and K. N. An. The capitohamate ligaments. a comparison of biomechanical properties. *J Hand Surg Br*, 21(4):451–4, 1996.
34. M. P. Rubbens, A. Driessen-Mol, R. A. Boerboom, M. M. Koppert, H. C. van Assen, B. M. TerHaar Romeny, F. P. Baaijens, and C. V. Bouten. Quantification of the temporal evolution of collagen orientation in mechanically conditioned engineered cardiovascular tissues. *Ann Biomed Eng*, 37(7):1263–72, 2009.
35. M. S. Sacks, D. B. Smith, and E. D. Hiester. A small angle light scattering device for planar connective tissue microstructural analysis. *AnnBiomed Eng*, 25(4):678–89, 1997.
36. J. A. Spaan, R. ter Wee, J. W. van Teeffelen, G. Streekstra, M. Siebes, C. Kolyva, H. Vink, D. S. Fokkema, and E. VanBavel. Visualisation of intramural coronary vasculature by an imaging

cryomicrotome suggests compartmentalisation of myocardial perfusion areas. *Med Biol Eng Comput*, 43(4):431–5, 2005.

37. H. Steckel, G. Vadala, D. Davis, and F. H. Fu. 2D and 3D 3-tesla magnetic resonance imaging of the double bundle structure in anterior cruciate ligament anatomy. *Knee Surg Sports Traumatol Arthrosc*, 14(11):1151–8, 2006.
38. G. M. P. van Kempen, N. van den Brink, L. J. van Vliet, M. van Ginkel, P. W. Verbeek, and H. Blonk. The application of a local dimensionality estimator to the analysis of 3D microscopic network structures. In *Proc. 11th Scandinavian Conference on Image Analysis*, pages 447–455, Kangerlussuaq, Greenland, 1999.
39. C. van Wijk, R. Truyen, R.E. van Gelder, L.J. van Vliet, and F.M. Vos. On normalized convolution to measure curvature features for automatic polyp detection. In Christian Barillot, David R. Haynor, and Pierre Hellier, editors, *Medical Image Computing and Computer-Assisted Intervention - MICCAI 2004*, volume 3216 of *Lecture Notes in Computer Science*, pages 200–208. Springer Berlin Heidelberg, 2004.
40. J. A. Weiss, J. C. Gardiner, B. J. Ellis, T. J. Lujan, and N. S. Phatak. Three- dimensional finite element modeling of ligaments: technical aspects. *Med Eng Phys*, 27(10):845–61, 2005.
41. S. L. Woo, M. A. Gomez, and W. H. Akeson. The time and history-dependent viscoelastic properties of the canine medical collateral ligament. *J Biomech Eng*, 103(4):293–8, 1981.
42. P. A. Yushkevich, J. Piven, H. C. Hazlett, R. G. Smith, S. Ho, J. C. Gee, and G. Gerig. User-guided 3d active contour segmentation of anatomical structures: significantly improved efficiency and reliability. *Neuroimage*, 31(3):1116–28, 2006.
43. F. Zhang, E. R. Hancock, C. Goodlett, and G. Gerig. Probabilistic white matter fiber tracking using particle filtering and von Mises-Fisher sampling. *Med Image Anal*, 13(1):5–18, 2009.

Chapter 3

Analysis of the 3-D Collagen Fiber Anatomy of the Human Anterior Cruciate Ligament: a Preliminary Investigation

D. Tan Nguyen, Martijn van de Giessen, Jeroen P. van den Wijngaard,
Pepijn van Horssen, Jos A. Spaan, Geert J. Streekstra,
C. Niek van Dijk, Leendert Blankevoort

Submitted for publication

ABSTRACT

The aim of this study is to assess the applicability of autofluorescent fiber tracking (AFT) to obtain quantitative data on the 3-D collagen fiber anatomy of the human ACL. Based on the majority of the literature, the hypothesis is that the ACL has at least two anatomically distinct fiber bundles with different fiber orientations. AFT combines an imaging cryomicrotome for serial sectioning, collagen autofluorescence, image acquisition and fiber tracking software to reconstruct the fiber tracts in three dimensions and to analyze the fiber tract orientation, lengths of the fiber tracts and connectivity map of the ACLs. In this pilot study, three fresh-frozen human knees were processed, two in extension and one in flexion.

All fiber tracts of the ACL in extension are running parallel from the femoral insertion towards the tibial insertion. A twist of fiber tracts is observed with the knee in flexion. However, the twist is not caused by anatomically distinct fiber bundles as the length maps reveal a clear pattern of gradual length change across the insertion sites with short fibers posterolateral and gradually longer fibers towards anteromedial direction. In addition, the connectivity maps confirm that neighboring fiber tracts remain neighbors.

In conclusion, this pilot study demonstrates that autofluorescent fiber tracking is able to quantify the 3-D fiber anatomy of the ACL and shows that the 3-D fiber anatomy of the three specimens is a single broad continuum of collagen fibers with short fibers posterolateral and gradually longer fibers towards anteromedial.

INTRODUCTION

The anterior cruciate ligament (ACL) is frequently ruptured, often after twisting the knee joint. The surgical treatment in chronically instable knees is a reconstruction of the ruptured ACL with either a single- or double-bundle tendon graft. [14] Previously, many studies were performed to obtain a blueprint of the ACL's anatomy in order to better understand its function and to develop surgical techniques that closely reconstruct the native ACL. It was recognized that the ACL has a complex collagen fiber anatomy. Some authors report that the ACL is a single broad continuum of fascicles, with different portions taut throughout the range of motion, [12,5] while other authors report that the ACL consists of anatomically distinct bundles, namely an anteromedial bundle (AM) and a posterolateral bundle (PL). [6,7,4] The ACL is also divided into three functional bundles, namely anteromedial bundle (AM), a posterolateral bundle (PL) and an intermediate bundle (IM). [11,1,13] Mommersteeg et al., conducted an anatomical study for the purpose of modeling the knee joint. [9] They reported that 6 to10 bundles can define the main fascicle directions within the studied ACL samples. Although the number of fiber bundles was arbitrary and not the same for all ACL's in the experiments. The femur and the tibia were connected in a consistent way by these bundles. From these reports it is clear that there is still disagreement regarding the 3-D collagen fiber anatomy. As a result, the number of fiber bundles to be reconstructed and the number of tendon grafts to be used in order to closely reconstruct the native ACL remains a subject of debate. [16]

The difference in the reported ACL anatomy may be explained by the definition and methodology used. All previously referenced studies report in their methods section that the division of the ACL into two or more macroscopically separate bundles was principally based on methods that can vary in the interpretation: visual inspection, palpation, translation and/or rotation of the joint and manual dissection. The aim of this pilot study is to evaluate *a more objective* method to acquire quantitative data on the three-dimensional collagen fiber anatomy of the anterior cruciate ligament by automatic data acquisition at a high resolution and 3-D reconstruction of the fiber tracts. The quantitative data includes: fiber tract orientation, lengths of the fiber tracts, connectivity maps and morphology of the insertion sites. Based on previous anatomical studies, it is hypothesized that the human ACL has at least two anatomically distinct fiber bundles with different fiber orientations and different lengths. The specific purpose of the pilot study is to assess the applicability of the method to address this hypothesis.

MATERIALS AND METHODS

A novel and validated method, autofluorescent fiber tracking (AFT) was developed for the purpose of quantifying the collagen fiber anatomy in 3-D of the ACL. [van de Gies-

sen et al., submitted] The AFT combines an imaging cryomicrotome for automated serial sectioning, the autofluorescence property of collagen, image acquisition, and fiber tracking software to reconstruct the fiber tracts in 3-D.

Autofluorescent property of collagen

Collagen molecules are autofluorescent and upon excitation emit green light (peak wavelength at ~505nm) after excitation by illumination in blue (wavelength ~480nm). By taking advantage of this autofluorescent property, collagen molecules which are the main constituents of the fibers of the ACL can be visualized accurately at a high resolution without the need for staining.

Imaging Cryomicrotome

The current imaging cryomicrotome system was originally developed for the purpose of organ imaging with (fluorescent) probes. [15,3,17,10] The particular system as developed by Spaan et al. [15] consists of an automated cryomicrotome, lighting system for fluorescence excitation and a 8 bits CCD camera with a minimal resolution of 2000 x 2000 pixels (Figure 1). The automated microtome removes 50µm thick sections from the frozen tissue block containing the ACL and embedding material. After each cut, the surface of the remaining tissue block is illuminated with a 300 W Xenon lamp or power-LED at appropriate spectral properties, in our case 480/20 nm. The fluorescent signal returning from the tissue block surface is subsequently captured for this study at 505/30 nm (Figure 1). The stack of resulting images was used to form a 3-D reconstruction of the fluorescence signal from the complete knee joint, including the ligaments and other collagenous structures. The images of the cryomicrotome are stored as 3-D arrays of 8bit gray scale values representing the spatial fluorescence intensity distribution. The voxel size of the 3-D reconstruction is 50 µm x 50 µm x 50 µm.

Fiber Tractography

Within the image volume, each ligament is visible as a bundle of almost-parallel bright linear structures. The local orientation of the collagen fibers can be detected by the smallest change in intensity along the fiber direction. Based on this notion and to be robust to noise in the images, the fiber orientations in the cryomicrotome volume are estimated at each voxel using a so-called structure tensor. [18] This tensor is a 3x3 matrix that does not only contain the local orientation of the fiber bundle, but also an estimate of the reliability of the orientation estimate. After reconstructing the fiber orientations at the level of the voxels within the 3-D data set, similar to fiber tractography in diffusion tensor imaging of the brain [2], a tractographical analysis of the collagen fibers was performed. Cartilage and bone were annotated in the autofluo-

rescence image volume using ITK-SNAP (V2.4, PICSL, University of Pennsylvania, PA, USA). [19] The annotations were made in 3-D using semi-automatic region growing and manual corrections. For a detailed description of the orientation estimation and tractography methods, see Giessen et al. (submitted).

Data interpretation

Fiber tractography yields numerous fiber tracts that makes interpretation complex due to the overlap when illustrated in a figure. Additionally, the decision whether a certain population of fiber tracts forms a distinct anatomical bundle remains subjective due to the manual separation. To enable a more objective assessment, a connectivity map of the fiber tracts was created. By color-coding each fiber tract and coloring their respective tibial and femoral insertion site with the same color as the tract, an analysis can be performed that indicates whether there are distinct anatomical fiber bundles present. Fiber tracts that are neighbors at the tibial insertion site which remain neighbors at the femoral site are parallel orientated fiber tracts and can thus be considered to belong to the same anatomical fiber bundle. Populations of fiber tracts that do not remain neighbors can be considered to belong to different distinct anatomical fiber bundles. Additionally, the length of each fiber tract can be calculated and color-coded on the insertion site. This length map can also provide insight where certain fiber tracts are located, i.e. a continuum of fiber tracts will be depicted as an area map with a gradual change in fiber tract length

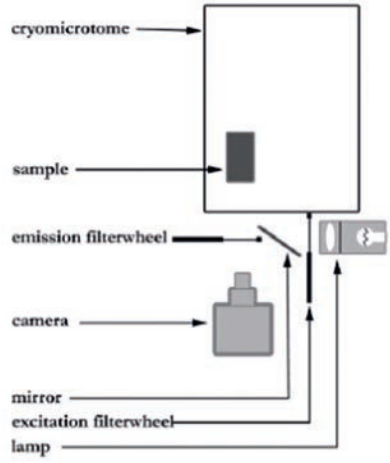

Figure 1. A simplified schematic set-up of the fluorescent imaging cryomicrotome. In the microtome a slice is cut from the tissue sample. The CCD camera acquires fluorescent images of the sample surface. The process of cutting and imaging is repeated to obtain a three-dimensional image of the sample.

TISSUE PROCESSING

Three fresh-frozen cadaveric knees were used (53 yr male right [ACL1], 59 yr female left [ACL2], and 69 yr right male [ACL3]). Radiographs were made to exclude any fractures or severe osteoarthritis within the knees. After thawing, a Lachman and anterior- and posterior drawer test were performed in order to grossly assess if the ACL and the PCL in the specimen was intact. Signs of knee gross joint pathology were absent. The maximum diameter of a sample that can be cut in the imaging cryomicrotome is approximately 10 cm, the knees were therefore trimmed to a diameter of 9 cm. Further, to ease the cutting, the cancellous bone and a part of the cortical bone of the knee joint were carefully removed. The knees were embedded in 5% carboxy-methylcellulose sodium solvent with 4% Indian ink (CMC). After embedding and refreezing the whole intact knee joint (two knees frozen in extension (ACL1 and ACL3) and one in flexion (ACL2), the tissue block was mounted in the imaging cryomicrotome and cut at -20˚C. In flexion the posterolateral ACL fibers will be more taut, whereas the anteromedial fibers more in extension. For the purpose of a shorter time in the cryomicrotome, knee ACL3 was trimmed further into a femur-ACL-tibia complex, while maintaining the extension with external fixators during embedding and freezing.

RESULTS

The fluorescent signals mainly originate from the collagen fibers. Cross-sections of collagen fibers constituting ligaments, menisci, cartilage and bone can be clearly distinguished (Figure 2A, B).

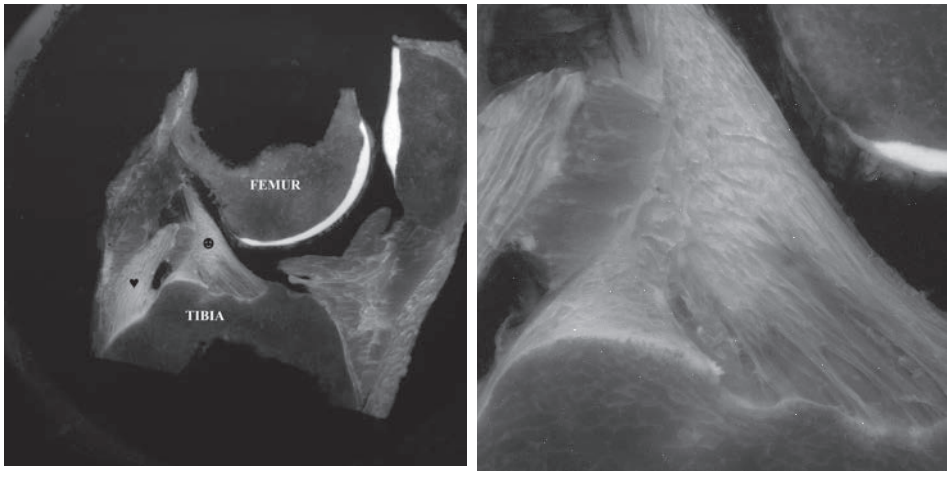

(A) **(B)**

Figure 2 (A.) Cryo-microtome image of a mid-sagittal section knee joint, ♥ indicates the posterior cruciate ligament, ☻ indicates the anterior cruciate ligament as a line pattern. (B) Magnification of figure 2A of the ACL.

Fiber tracts

The fiber tracts of the two knees that are sectioned in extension follow parallel trajectories (Figure 3A and 3E). Rotating the 3-D fiber tract reconstruction around the x, y-, z-axis does not show fiber tracts bundles with different orientations. In contrast to the knee that is sectioned in 90 degrees of flexion, where fiber tracts can be observed twisting around each other (Figure 3C). This twisting is observed more clearly with the visualization of 10% of the total fibers tract (Figure 3D).

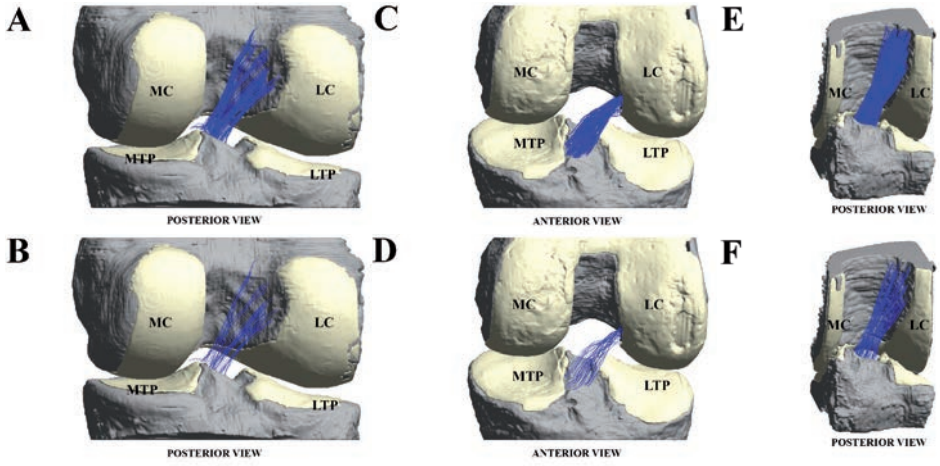

Figure 3. Figure 3A and 3C shows the fiber tracts of ACL1 and ACL3 with the knee in extension and the view from posterior. All fiber tracts are depicted as blue lines running parallel from the femoral insertion towards the tibial insertion. To increase visibility of the fiber tracts in the 2-D figures, 10% of the fiber tracts of ACL 1 and ACL3 are visualized (Figure 3B, 3F). The fibers are still running parallel. Figure 3C depicts the fiber tracts of ACL2 with the knee in 90 degrees of flexion and the view from anterior. A twist can be noted which is more clearly seen in figure 3D in which 10% of the fiber tracts are shown.

Length maps

At the tibial insertion there is a gradual change in fiber tract length: the fiber tracts shorten from anteromedially to posterolaterally (Figure 4B, D, F). At the femoral insertion, the fiber tracts increases in length from the posterior border of the residents' ridge with cartilage margin to the posterior part of the notch roof (Figure 4A, C, E). Note the dark blue spot in figure 4C & D. This does not represent the ACL fiber tract, upon second inspection of the cryomicrotome images this dark blue spot originates from a dense fibrous synovial membrane running from the tibia to the femur.

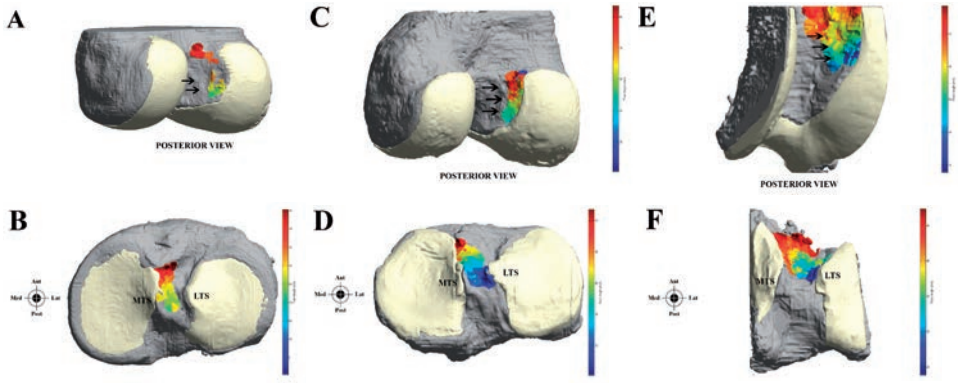

Figure 4. The fiber tract lengths of ACL1 (A, B), ACL2 (C, D) and ACL3 (E, F), respectively, plotted at the femoral and tibial insertion sites. Note that the longer fiber tracts are located anteromedial at the tibial insertion site and at the posterior part of the notch roof at the femoral insertion site. While the shorter fiber tract length is are located at the lateral tibial spine and at the posterior border of the residents' ridge with cartilage margin to the posterior part of the notch roof. This pattern holds for all three ACL's. The arrows indicate the resident's ridge. Also note that in figure 4C and 4D, a dark blue spot can be observed which does not represent the ACL fiber tracts, but a dense fibrous synovial membrane. MTS: Medial tibial spine, LTS: Lateral tibial spine.

Connectivity maps

The evaluation whether the fiber tracts within the ACL are anatomical distinct fiber tract bundles can be further assessed by color-coding each fiber tract and coloring their respective tibial and femoral insertion site with the same color as the tract resulting in a connectivity map. In all three knees, the fiber tracts that are neighbors at the tibial insertion site remain neighbors at the femoral site (Figure 5). This confirms that the ACL is a continuous band of collagen fiber tracts.

Relating fiber tracts to arthroscopically visible landmarks

The fiber tracts with the shortest length start anterior to and bordering at the arthroscopically visible lateral tibial spine (figure 4B, D, F). The femoral insertions of these fiber tracts are located just posterior of the resident's ridge at the cartilage margin (figure 4A, C, E). The longest fiber tracts can be found by moving diagonally from the lateral tibial spine toward the anteromedial aspect of the tibia. The femoral insertion site of these fiber tracts are located diagonally from the start point of the short fiber tracts (just behind the resident's ridge and cartilage margin) and inserting just up to but not at the roof of the notch.

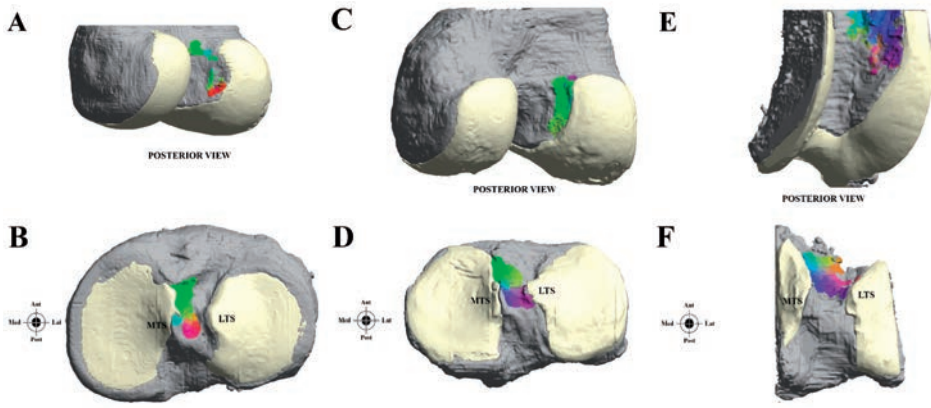

Figure 5. The connectivity maps of ACL1 (A, B), ACL2 (C, D) and ACL3 (E, F), respectively, plotted at the femoral and tibial insertion sites. Note that the color pattern at the insertion sites remains nearly the same. Also note that in figure 5C and 5D, the purple spot does not represent the ACL fiber tract, but a dense fibrous synovial membrane.

DISCUSSION

In this pilot study a novel and validated method was utilized to quantify the collagen fiber architecture of the human ACL in 3-D. The combination of the imaging cryomicrotome, using the fluorescence of collagen, and fiber tracking software provided more objective anatomical data without the need for manual dissection or staining. The imaging cryomicrotome facilitated automated serial sectioning for accurate data collection at a high-resolution. Though, inherent to the automated processing of the high-resolution images, subtle fiber structures such as the synovial membrane can be interpreted as ACL collagen fiber tracts, as illustrated in sample ACL2. The fiber tracking software reconstructed the 3-D collagen fiber tracts, length and connectivity maps. Despite the limited sample size, it was possible to answer basic questions within the samples. Contrary to the hypothesis, the results of this study show that the human ACL from the three cadaveric knees is a single continuous construct of collagen fibers. The twist of the fiber tracts in flexion is not present for the knee in extension. Moreover, no distinct separation between the fibers or bundles can be objectified with the connectivity maps. Differences between the three specimens are noticeable. Grossly, neighboring fiber tracts at one insertion site remain neighbors at the other insertion site. The length maps reveal a clear pattern of gradual length change across the ligament which can be used as a design criterion for ACL reconstruction techniques. Starting from the posterolateral tibial insertion site, the length of the fiber tracts are short while traveling towards anteromedial they progressively increase in length. This length pattern is also present at the femoral insertion site, at the cartilage border of

the medial wall of the lateral condyle, the fibers that attaches there are short while they progressively increase posterocranially up to but not at the roof of the notch.

The results confirm an anatomical dissection study performed by Fuss [5], who reported that the ACL is a single continuous band of collagen fibers with a gradual change in fiber length. Others authors who defined the ACL in anatomical distinct fibers also reports that the PL bundle is shorter in length than the AM bundle. [6,7,4] While the findings in the current study and of Fuss's study agree with other studies concerning the length, the conclusion regarding the amount of bundles is different. Most probably this discrepancy is a matter of definition and interpretation of what an anatomical distinct band or bundle is. Several authors have shown that as the knee flexes, the distance between the proximal and distal insertion sites of the posterolateral fibers decreases. [6,8] This change results in a crease within the ACL as the anteromedial fibers remain tensioned while the posterolateral fibers loosen. Flexing and rotating the knee and removal of the menisci during dissection may further accentuate the crease and the appearance of an anatomically distinct bundle.

The limitation of the current study is that it contains only three specimens and the older age of the specimens. Due to the exploratory nature of this study, it was not possible to generalize the findings. A follow-up study with a larger sample size would be helpful to further support and generalize the conclusions. Further recommendations include: performing an arthrotomy to remove synovial membranes cords and other fibrous cords within the joint, these fibrous cords can give "false-positive" fiber tracts, see ACL2. Also, more care should be given when trimming the bone, in sample ACL3 the cut was too close to the femoral insertion site. Nevertheless, the autofluorescent fiber tracking (AFT) methodology is novel, validated and useful to quantify the 3-D collagen fiber orientation of the ACL. The AFT methodology may also be a useful tool to obtain the fiber architecture of other collagenous structures such as menisci, the intervertebral disc, heart valves, etc. As the knowledge of the detailed fiber anatomy and combined with previous functional studies of the load bearing structures may increase our understanding of the function and pathophysiology of these structures. Additionally, surgical techniques, including bio-enhanced end-to-end ACL healing may be improved.

In conclusion, this study demonstrates that autofluorescent fiber tracking is able to quantify the 3-D fiber anatomy of the ACL and shows that the 3-D fiber anatomy of the three specimens is a single broad continuum of collagen fibers with short fibers posterolateral and gradually longer fibers towards anteromedial.

ACKNOWLEDGEMENTS

The authors acknowledge the financial support of the Netherlands Organization for Scientific Research (NWO).

REFERENCES

1. Amis AA, Dawkins GP (1991) Functional anatomy of the anterior cruciate ligament. Fibre bundle actions related to ligament replacements and injuries. The Journal of bone and joint surgery British volume 73 (2):260-267
2. Basser PJ, Pajevic S, Pierpaoli C, Duda J, Aldroubi A (2000) In vivo fiber tractography using DT-MRI data. Magnetic resonance in medicine : official journal of the Society of Magnetic Resonance in Medicine / Society of Magnetic Resonance in Medicine 44 (4):625-632
3. Bernard SL, Ewen JR, Barlow CH, Kelly JJ, McKinney S, Frazer DA, Glenny RW (2000) High spatial resolution measurements of organ blood flow in small laboratory animals. American journal of physiology Heart and circulatory physiology 279 (5):H2043-2052
4. Chhabra A, Starman JS, Ferretti M, Vidal AF, Zantop T, Fu FH (2006) Anatomic, radiographic, biomechanical, and kinematic evaluation of the anterior cruciate ligament and its two functional bundles. The Journal of bone and joint surgery American volume 88 Suppl 4:2-10. doi:10.2106/JBJS.F.00616
5. Fuss FK (1989) Anatomy of the cruciate ligaments and their function in extension and flexion of the human knee joint. The American journal of anatomy 184 (2):165-176. doi:10.1002/aja.1001840208
6. Girgis FG, Marshall JL, Monajem A (1975) The cruciate ligaments of the knee joint. Anatomical, functional and experimental analysis. Clinical orthopaedics and related research (106):216-231
7. Hara K, Mochizuki T, Sekiya I, Yamaguchi K, Akita K, Muneta T (2009) Anatomy of normal human anterior cruciate ligament attachments evaluated by divided small bundles. The American journal of sports medicine 37 (12):2386-2391. doi:10.1177/0363546509340404
8. Inderster A, Benedetto KP, Künzel KH, Gaber O, Balyk RA (1993) Fiber orientation of anterior cruciate ligament: An experimental morphological and functional study, part I. Clinical Anatomy 6 (1):26-32
9. Mommersteeg TJ, Kooloos JG, Blankevoort L, Kauer JM, Huiskes R, Roeling FQ (1995) The fibre bundle anatomy of human cruciate ligaments. Journal of anatomy 187 (Pt 2):461-471
10. Nakaya N, Chung BH, Patsch JR, Taunton OD (1977) Synthesis and release of low density lipoproteins by the isolated perfused pig liver. The Journal of biological chemistry 252 (21):7530-7533
11. Norwood LA, Cross MJ (1979) Anterior cruciate ligament: functional anatomy of its bundles in rotatory instabilities. The American journal of sports medicine 7 (1):23-26
12. Odensten M, Gillquist J (1985) Functional anatomy of the anterior cruciate ligament and a rationale for reconstruction. The Journal of bone and joint surgery American volume 67 (2):257-262
13. Otsubo H, Shino K, Suzuki D, Kamiya T, Suzuki T, Watanabe K, Fujimiya M, Iwahashi T, Yamashita T (2012) The arrangement and the attachment areas of three ACL bundles. Knee surgery, sports traumatology, arthroscopy : official journal of the ESSKA 20 (1):127-134. doi:10.1007/s00167-011-1576-z
14. Renstrom PA (2013) Eight clinical conundrums relating to anterior cruciate ligament (ACL) injury in sport: recent evidence and a personal reflection. British journal of sports medicine 47 (6):367-372. doi:10.1136/bjsports-2012-091623
15. Spaan JA, ter Wee R, van Teeffelen JW, Streekstra G, Siebes M, Kolyva C, Vink H, Fokkema DS, VanBavel E (2005) Visualisation of intramural coronary vasculature by an imaging cryomi-

crotome suggests compartmentalisation of myocardial perfusion areas. Medical & biological engineering & computing 43 (4):431-435

16. Tiamklang T, Sumanont S, Foocharoen T, Laopaiboon M (2012) Double-bundle versus single-bundle reconstruction for anterior cruciate ligament rupture in adults. The Cochrane database of systematic reviews 11:CD008413. doi:10.1002/14651858.CD008413.pub2
17. van den Wijngaard JP, Schwarz JC, van Horssen P, van Lier MG, Dobbe JG, Spaan JA, Siebes M (2013) 3D Imaging of vascular networks for biophysical modeling of perfusion distribution within the heart. Journal of biomechanics 46 (2):229-239. doi:10.1016/j.jbiomech.2012.11.027
18. van Kempen G, van den Brink N, van Vliet L, van Ginkel M, Verbeek P, Blonk H The application of a Local Dimensionality Estimator to the analysis of 3-D microscopic network structures. In: 11th Scandinavian Conference on Image Analysis, 1999, June 7-11 1999. pp 447-455
19. Yushkevich PA, Piven J, Hazlett HC, Smith RG, Ho S, Gee JC, Gerig G (2006) User-guided 3D active contour segmentation of anatomical structures: significantly improved efficiency and reliability. NeuroImage 31 (3):1116-1128. doi:10.1016/j.neuroimage.2006.01.015

Chapter 4

Fluorescence Imaging for Improved Visualization of Joint Structures during Arthroscopic Surgery

D. Tan Nguyen, Pepijn van Horssen, Hans Derriks,
Martijn van de Giessen, Ton van Leeuwen

Submitted for publication

ABSTRACT

Arthroscopic knee surgery has many advantages over open surgery. However, the visualization of the surgical field with the current white light endoscopic systems suffers from poor contrast between femoral insertion site and its surroundings. We hypothesize that joint structures display different autofluorescent spectral responses (ASRs) and that these differences can be used to improve the contrast during intra-operative visualization. Based on this hypothesis we report the development of a Fluorescence Arthroscope (FA).

The feasibility of autofluorescence imaging of the femoral insertion site was validated on bovine and human knees. Accuracy was evaluated with manual annotations in visible light and spectral unmixed autofluorescence acquisitions.

The results showed that the joint structures have different ASRs. Spectral unmixing enabled separation of the ASRs and improved contrast between the joint structures. The agreement between visible light and autofluorescence ligament insertions had a mean Dice coefficient of 0.84 and the mean Dice coefficient of the interobserver variability for visible light imaging was 0.85.

In conclusion, we have shown that the femoral insertion site can be accurately visualized with autofluorescence imaging combined with spectral unmixing. The FA demonstrates the feasibility of real-time and subject-specific visualization of the femoral insertion site.

INTRODUCTION

Many joint surgeries are nowadays performed arthroscopically. This minimally invasive approach has resulted in a reduction of post-operative complications, faster recovery and improved patient outcome compared to open surgery (*1-4*). Accordingly, numerous arthroscopic procedures for small and large joints have been developed. Currently, more than 4 million arthroscopic procedures in the knee joint are performed worldwide per annum and is increasing (*5*). Despite its advantages, arthroscopic joint surgery is challenging due to the restricted working space, hand-eye coordination, lack of palpation and visual limitations. The visual limitations are related to the standard white light endoscopic systems and include: small viewing angle and poor contrast between the collagenous joint structures (as they all appear off-white). Additionally, injury or degeneration of the joint structures further hampers the contrast and visualization. Thus, improved contrast between the joint structures will be of great value as clear visual feedback is paramount for effective and safe arthroscopic surgery.

Recent advances in optical imaging demonstrated the importance of fluorescence imaging in the field of urology, gastroenterology and abdominal surgery (*6, 7*). Researchers were able to visualize precancerous tissues, tumors and metastasis in real-time and with high contrast by using exogenous fluorescent markers against the targeted structures. This approach facilitated more complete tumor resection and even resection of (pre-)malignant tissues that otherwise were not detected with the standard white-light endoscopy. Similarly, the autofluorescence of tissue can be utilized to enhance the visibility of tissues with low contrast under regular visible light reflectance imaging. Collagen is such an autofluorescent tissue component which can emit blue/green light after excitation with violet/blue light. The fluorescent imaging of collagen may be advantageous for orthopedic surgeons and rheumatologists as collagen is the main constituent of the joint structures such as ligaments, bone and cartilage.

Arthroscopic anterior cruciate ligament (ACL) reconstruction is one of the most performed surgical procedures by the orthopedic surgeon. The location of the bone tunnels is a crucial factor for the success of the reconstruction surgery and the bone tunnel should be placed at the original insertion site of the ruptured ACL (*8, 9*). Hence, graft misplacement is the most common causes of revision surgery (*10-14*) and small deviations can result in large changes in knee stability (*15-17*). Before the introduction of the arthroscopic surgery, the surgeon could easily distinguish the insertion sites from the surrounding bone and cartilage due to the wide-open field of view with open surgery. With the introduction of the arthroscope, the localization of the insertion site became more challenging due to the aforementioned technical limitations. Our research question was whether the femoral insertion site can be accurately visualized with fluorescence imaging either with or without image post-processing techniques

such as spectral unmixing. Since joint structures differ in biochemical composition, and specifically in collagen content and collagen distribution, we hypothesize that the spectral response between these tissues differs and thus the femoral insertion site can be visualized separately based on the difference in the spectral response. In this study we investigated three different approaches to visualize the ACL insertion site, each one more directed to a practical implementation of a clinical imaging setup. First, we explore the possibility to maximize the contrast of the ACL with its surroundings by choice of optimal excitation and emission wavelengths such that a unique ACL insertion site image is obtained. Secondly, we apply a post-processing strategy where a fixed excitation wavelength is used for illumination with spectral unmixing performed on two different emission images obtained consecutively. And third, a real-time approach is shown which utilizes the spectral unmixing principal on separate color channels of RGB images with a fixed excitation wavelength. The optimal set of imaging parameters was determined to develop a pre-clinical prototype of the Fluorescence Arthroscope (FA) to improve the contrast between joint structures during arthroscopy, particularly between the insertion site with respect to bone and cartilage. The boundary conditions of the FA we imposed were accuracy, real-time, robust, and compatible with the current white light endoscopic systems. We evaluated our approach on cadaveric bovine and cadaveric human knees.

MATERIALS & METHODS

Spectral responses of bovine and human ACL insertion sites, bone and cartilage

Fresh bovine cadaveric knees (n=10) from a local abattoir (Van Kooten B.V., Montfoort, NL) were prepared for the excitation and emission scans. The knees were all dissected until the ACL were exposed. The ACL was removed with an arthroscopic scissor punch (Arthrex, Naples, USA), mimicking the clinical situation, and leaving a short remnant (2 mm) on the lateral wall of the intercondylar notch. The bovine samples were placed in a light blocking box on a height adjustable table. The optic fiber of the fluorospectrometer (Perkin-Elmer, LS55, Rodgau, Germany) was consecutively aimed at the femoral insertion of the ACL, its bony surroundings on the lateral condyle and the cartilage of the lateral femoral condyle. A 5 mm thick reference was placed between the sample and the optical fiber probe and subsequently the z-axis table was adjusted until the distance between the sample and the probe was 5 mm. Excitation-emission maps of the samples were obtained by scanning the excitation wavelength, starting at 280 nm and ending at 480 nm in steps of 10 nm, while detecting the emission light from 300-800 nm. The excitation and emission slits used during the experiment were both 2.5 nm. During all the experiments dehydration of the samples was prevented by moistening them with 0.9% NaCl solution. Fresh-frozen human cadaveric knees (n=3) were thawed and cut into three small samples (5mm x 5mm x 8mm) each containing

only the insertion site, bony surrounding and cartilage and placed consecutively in the cuvette holder of the fluorospectrometer. Again, excitation emission maps were obtained (excitation wavelength from 200 nm to 490 nm in 10 nm steps and an emission range of 200-700 nm). After obtaining the excitation and emission spectra, an optimal combination of excitation and emission wavelengths to visualize the insertion site was determined by calculating the difference in intensity and difference between emission peaks.

ACL insertion site imaging based on spectral unmixing

Tissue autofluorescence spectra tend to be wide and strongly overlapping (*18*). Therefore, obtaining a set of excitation and emission wavelengths that can directly separate tissues visually is not possible in general. However, using wavelength dependent ratios between tissue specific spectra, imaged tissues can be separated. This method, called spectral unmixing, requires at least as many images as the number of structures to be separated (*19*). We used a straightforward two component linear spectral unmixing technique, with the components identified as ACL insertion site and surrounding tissue composed primarily of bone. They have to be extracted only once from fluorescent images by manually measuring the ratio of intensity of the ACL and bone for both image A and B. These factors can then be used to do spectral unmixing for all other datasets obtained with that particular imaging setup. The excitation wavelength is chosen such that a maximum difference between the ratio of the components exists in the emission images, as this provides the conditions for maximal contrast between ACL and it surroundings (*19*).

Validation of spectral unmixing in bovine knees

The spectral unmixing was tested on open knees such that the accuracy of fluorescence imaging of the ACL insertion site could be evaluated by comparing the annotations of the femoral insertion site made in images acquired in white light of open dissected knees (mimicking the open surgery/ pre-arthroscopy period) with the annotations acquired with fluorescence imaging from the same knees. The lateral condyle of 10 bovine knees was imaged with a hyperspectral imaging setup. Each sample was illuminated with five power-LEDs, with the optimal excitation wavelength derived from the fluorospectrometer measurements (Roithner lasertechnik, Vienna, Austria). Spectra were acquired by a hyperspectral camera equipped with a liquid crystal tunable filter (Varispec, PerkinElmer, Massachusetts, USA) and a digital camera (PCO.Pixelfly, Kelheim, Germany). The spectral sweep ranged from 400nm to 720nm with 2nm steps and a spectral resolution of 7nm. Spectra for ligament and bone were determined from annotations in one knee and measuring the intensity within the annotation for the full spectral range. Based on these spectra, two optimal emission images were selected

with the largest difference in intensity ratio between ACL and its surroundings. Spectral unmixing was applied and the resulting visualization of ligament and bone were false colored in red and green, respectively. White light images were approximated by taking the average intensity of the images from: 470-500nm for the blue channel, 510-560nm for the green channel and 600-700nm for the red channel. Three independent observers (M.F., T.N., and H.T.) drew contours of the femoral insertion site in the visible light and the spectrally unmixed images. The areas contained in these annotations were compared per observer between the unmixed and white light images. Again, as the femoral insertion site in an open knee is easily distinguished from the surrounding, the contour of the femoral insertion site in visible light is considered as the gold standard. The annotation accuracy was quantified by calculating Dice coefficient of the overlap between these annotations as $D = 2(A \cup B)/(A+B)$, where $A \cup B$ is the number of overlapping pixels in the segmented insertion sites and A+B is the total number of pixel in both insertion sites. D=1 corresponds to a complete agreement and D=0 signifies no agreement at all. The interobserver variability was evaluated for the annotations in unmixed and white light images separately, also by computing Dice coefficients, where consensus annotations were obtained by majority voting over the observers.

Real-time spectral unmixing with prototype of Fluorescence Arthroscope

Real-time imaging is a necessity for a clinical implementation, which requires simultaneous acquisition of the channels that capture the emitted light. The collagen autofluorescence spectrum spans the blue, red and green channel or regular white light endoscopy RGB cameras and consumer RGB cameras, allowing for the rapid building of a prototype. A real-time FA was assembled which consisted of: 1) an external Light-Emitting-Diodes 390±5nm light source [OSA OPTO LIGHT, Berlin, Germany] to excite the collagen, 2) a 1.3 MPixel digital camera Webcam Pro WB-6250X (Trust, Dordrecht, The Netherlands), 3) a 430nm long pass filter to reflected excitation light, 4) a laptop, 5) custom image processing software written in Labview (Austin, Texas, USA). The real-time video stream was processed using a real-time spectral unmixing of the red and green channels. Real-time video captures were made of the insertion sites in dissected bovine knees (n=5) (see supplementary material).

Feasibility in human knees: ex vivo Fluorescence Arthroscopy

The FA was incorporated into a commercially available endoscopy system (Smith & Nephew C.V., Hoofddorp, NL) and a fluorescence arthroscopy was performed in fresh-frozen human knees (n=2). The factors for spectral unmixing for ligament insertion and bone needed to be derived that were specific to this setup composed of the commercially endoscopic system. Spectra were calibrated from one human knee

acquisition and used for unmixing the remaining knees. The video stream from the commercially available endoscopy system does not permit real-time separation of the RGB channels for unmixing, therefore the color video was saved and post-processed. Lateral and medial portals were made *lege artis*. The knee was irrigated with NaCl 0,9% (Baxter, Deerfield, USA) and routinely inspected with the arthroscope on the white light modus. The ACL was then shaved with a shaver blade (Dyonics, 4.5mm Synovator), leaving a small remnant of the ACL of approximately 2mm on the lateral femoral wall. The LED probe was then introduced to the knee joint and the FA was turned on.

Statistical test

An unpaired Student's t-test was used for statistical analysis of the Dice's coefficients. A probability of $p<0.05$ was considered statistically significant.

RESULTS

Spectral response of the bovine ACL insertion site, bone and cartilage

Typical 3D excitation-emission maps of the three tissues within one bovine knee depict differences in intensity and shape (Figure 1). Results throughout the study will be presented in arbitrary units (arb. units) and will be denoted in the figures as intensity values normalized to the peak value. For the insertion site (n=10 bovine knees), the mean peak autofluorescence intensity was found at the emission wavelength 390 nm and at the corresponding excitation wavelength 330 nm. The autofluorescence intensity from the surrounding bone was measured at the same emission and excitation wavelength as the insertion site. The peak autofluorescence intensity from the surrounding cartilage was higher than the insertion site, and found at the emission wavelength 390 nm and the corresponding excitation wavelength 330 nm. The difference in intensity between the insertion and bone was 111 arb. units (interquartile range 54.6-180.1 arb. units). The difference in intensity between the insertion and the cartilage was -179.4 arb. units (interquartile range -150.2 - -220.7 arb. units).

The largest difference between the emission peaks of the insertion and the bone was 25 nm (interquartile range 20.25 - 33 nm) and found at an excitation wavelength of 280 nm. At this excitation wavelength the distance between the peaks of the insertion and the cartilage at the excitation was 8 nm (interquartile range -1.25 - 13.63 nm). For the insertion and the cartilage tissue, the largest difference was 44.5 nm (interquartile range 38.63 - 48.38 nm) and found at an excitation wavelength of 360 nm. At this excitation wavelength the distance between the peaks of the insertion and the bone was 3.5 nm (interquartile range -4.36 - -8.75 nm).

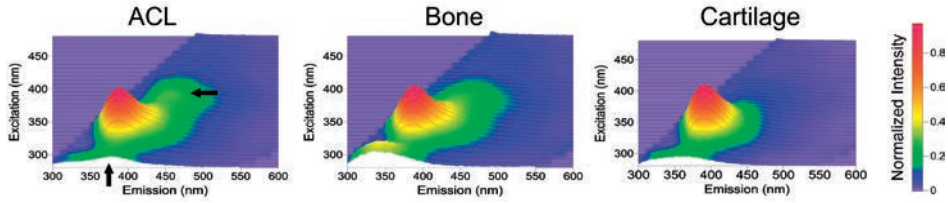

Figure 1. Typical 3D excitation-emission maps normalized to the peak intensity of insertion site (ACL), bone and cartilage from one bovine knee. Note the differences in autofluorescent response between the separate components indicated by arrows.

Spectral response of human ACL insertion site, bone and cartilage

Spectroscopy of human insertion site, bone and cartilage was performed to assess its spectral response (n=3). Spectral responses between the human tissue and bovine tissue were similar, which allowed a similar imaging and unmixing strategy to be used for both sample types, (Figure 2).

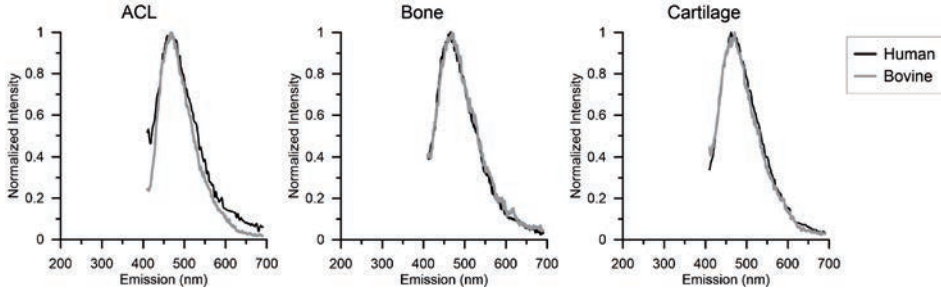

Figure 2: Emission spectra at 390 nm excitation of bone, ACL, and cartilage for the bovine (gray) and human (black) samples superimposed to display the resemblance in fluorescent response.

ACL insertion site imaging based on spectral unmixing

The measurements with the fluorospectrometer were used to find the most optimal method to enhance the contrast between the tissues as described in the previous paragraph. It followed from these measurements that direct excitation with 280 nm can be used to obtain the largest difference in emission peak. Excitation with 330-340 nm can be used to obtain the largest intensity difference between the tissues. Because both approaches are technically not practicable, as elaborated in the discussion, we decided to focus on the small but distinctive difference in emission spectra above 525 nm between the insertion site and its surroundings for a fixed excitation wavelength of 390±20 nm (Figure 3).

Such difference can be utilized to obtain a unique ACL insertion site image with spectral unmixing and displayed in pseudocolors. Typical contrasting results of the knee after spectral unmixing with an excitation of 390±20 nm are shown in figure

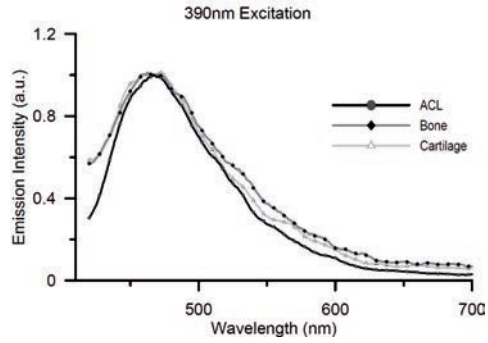

Figure 3. Normalized excitation-emission curves of ACL, Bone and Cartilage. Note that the curve between ACL and Bone deviates around 525nm.

4B. The femoral insertion site is shown in bright red while the bony and cartilage surrounding seen in a contrasting green.

Validation of spectral unmixing in bovine knees

The accuracy of the spectral unmixing in discerning the femoral ACL insertion site from the background was assessed by three independent observers who draw the contour of the femoral insertion site in the images (n=10). These contours were then compared to the segmented images from the spectral unmixing routine by creating binary images of the ACL insertion site. The Dice coefficient for observer 1, 2 and 3 between the unmixed and the white light images was 0.809, 0.831 and 0.874 respectively (table 1).

The observers preferred annotating in the unmixed autofluorescence images. The Dice coefficient for interobserver variability for the white light images for observer

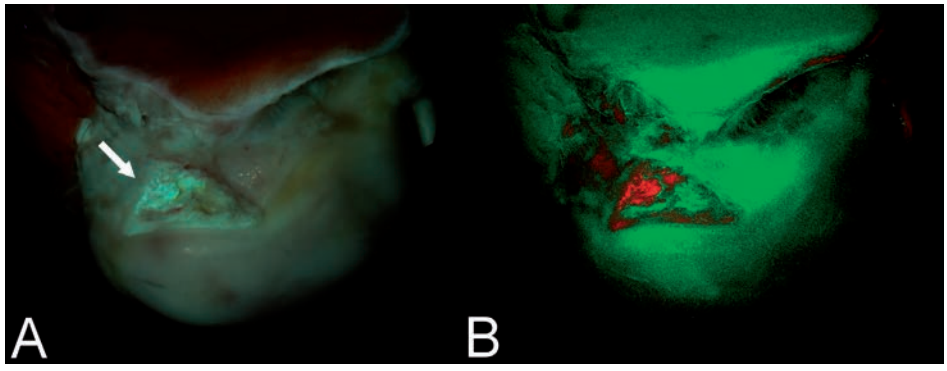

Figure 4) A: Bovine lateral femoral condyle in grayscale. ACL is indicated by arrow. It has to be noted that the insertion site can be easily seen in this macroscopic and sagittal section, however this is difficult when viewed arthroscopically. B: False color image of the same bovine lateral femoral condyle with femoral insertion site. Notice how the other ligaments are also enhanced by the method.

Table 1. Dice coefficient spectral unmixed vs white light

Knee	Observer 1	Observer 2	Observer 3
1	0.878	0.915	0.900
2	0.875	0.899	0.860
3	0.834	0.722	0.760
4	0.737	0.813	0.727
5	0.892	0.831	0.938
6	0.673	0.761	0.911
7	0.721	0.725	0.887
8	0.888	0.903	0.941
9	0.754	0.872	0.913
10	0.836	0.868	0.906
mean	0.809±0.08	0.831±0,07	0.874±007

1, 2 and 3 was 0.844, 0.865, and 0.836 respectively (table 2). The Dice coefficient for interobserver variability for the unmixed images for observer 1, 2 and 3 was 0.796, 0.853, and 0.832 respectively (table 3). The Dice coefficients of the white light images vs unmixed images and the white light interobserver Dice were not statistically different (p=0.57). The same holds for white light images vs unmixed images and the unmixed interobserver Dice (p=0.56) and the white light images interobserver vs unmixed images interobserver Dice (p=0.20).

Table 2. Dice coefficient Interobserver variability white light

Knee	Observer 1	Observer 2	Observer 3
1	0.867	0.905	0.900
2	0.858	0.872	0.864
3	0.859	0.848	0.810
4	0.872	0.892	0.865
5	0.889	0.890	0.864
6	0.744	0.796	0.694
7	0.713	0.789	0.747
8	0.880	0.890	0.847
9	0.871	0.890	0.869
10	0.882	0.882	0.896
Mean	0,844±0.06	0,865±0.04	0.836±0.06

Real-time spectral unmixing images and video with prototype of Fluorescence Arthroscope

The knees were excited with 390±20 nm and the fluorescent video was captured and processed real time (figure 5 and see supplementary material). The video shows a sharp bordered femoral insertion site in bright red with a contrasting background in green. The clear image quality remained during the imaging and no decrease of the autofluorescence (photo bleaching) and image quality was noted.

Table 3. Dice coefficient Interobserver variability spectral unmixed

Knee	Observer 1	Observer 2	Observer 3
1	0.913	0.914	0.921
2	0.842	0.892	0.870
3	0.699	0.793	0.805
4	0.670	0.776	0.733
5	0.904	0.926	0.903
6	0.864	0.901	0.863
7	0.778	0.809	0.799
8	0.809	0.865	0.816
9	0.734	0.810	0.784
10	0.743	0.843	0.827
Mean	0.796±0.08	0.853±0.05	0.832±0.05

Proof of concept: ex vivo human Fluorescence Arthroscopy

The next step was to adapt the FA prototype for inclusion in a commercial available endoscopic system to visualize the insertion site as in the clinic. The view through an arthroscope of a cadaveric human insertion site was consecutively shown in white light mode, fluorescence mode and spectral unmixed mode, (figures 6A, 6B, and 6C). From all these modes, the spectral unmix mode clearly shows the most optimal contrast between the insertion site and its background. The structure on the left of the ACL that have is same color and intensity is the posterior cruciate ligament.

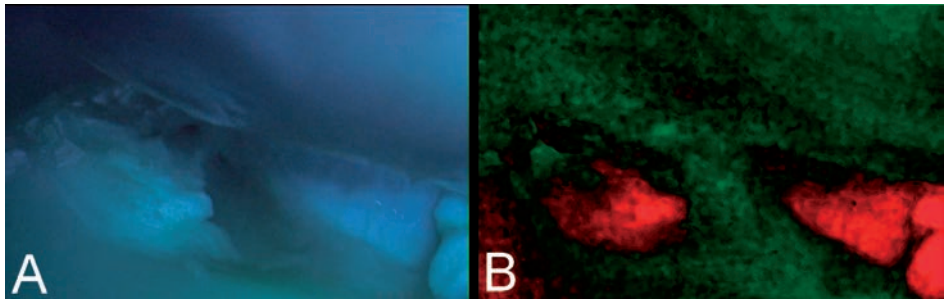

Figure 5. Inferior view of femoral condyles in bovine knee. Figure 4A: color image of the fluorescent response as directly captured by the digital camera. Notice the subtle differences between the ACL site (bluish/greenish) and its surroundings. Figure 4B: Real-time unmixed result of the color image left, with red the ACL and part of PCL and in green the background composed of the cartilage and bone. Fibrocartilaged notch (typical for bovine knees) also reveals in red.

DISCUSSION

In this study, we have shown that the spectral response between the insertion site, surrounding bone and cartilage differs. Due to this difference and with the aid of fluorescence imaging combined with spectral unmixing, the femoral insertion site could

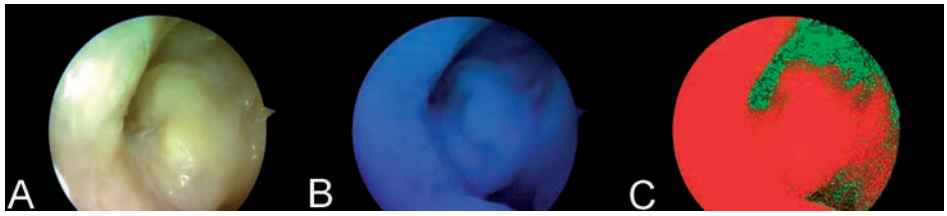

Figure 6. Arthroscopic view of a cadaveric human femoral insertion site. Consecutively shown in white light mode (A), fluorescence mode (B), and spectral unmixed mode (C)

be visualized in contrasting pseudo-colors. The accuracy of localization of the femoral insertion site with fluorescence imaging is high and comparable to localization of the femoral insertion site during open surgery (the gold standard). As a proof of concept, we have developed a prototype of the Fluorescence Arthroscope which was successfully tested in an *ex vivo* setting, including the 30˚ degrees arthroscope. The FA demonstrated to be robust and easily integrated into a current commercial white light endoscopic system. Additional improvements and *in vivo* studies are needed prior to clinical use. Excitation with 330-340 nm yields the largest intensity difference between the tissues. However, using excitation wavelengths of 330-340 nm turned out to be technically not feasible. 330 nm falls within the UV range and may be harmful with prolonged exposure. Additionally, current commercially available 330-340 nm power LEDs do not generate enough output to excite the tissues. Excitation with 280 nm to obtain the largest difference in emission peak was for the same reasons not feasible. Excitation with a longer and safe wavelength (390nm) showed autofluorescence of the insertion site, surrounding bone and cartilage. Though the relative intensity of the insertion site was not enough to clearly discern it from the background by eye. Also, using a filter to block the autofluorescence of the background was not to be effective to enhance the contrast between these tissues. Spectral unmixing with excitation at 390nm and emission based on 520nm and 620 images did enable accurate and subject specific visualization of the native femoral insertion site.

A limitation of our study is that the FA has not yet been tested in patients. The questions whether the femoral remnant is still present after rupture and whether the used excitation wavelength is safe, are legitimate. Literature has reported that the femoral remnant is still present in 98% of the patients and is collagenous (*20, 21*). Hence, orthopedic surgeons routinely use a shaver to remove the femoral and tibial remnant. Future studies need to assess photo toxicity of excitation wavelengths in violet (390 nm-405 nm) to the tissues within the joints. Though, previous applications within the urology gastro-enterology and abdominal surgery have shown that the illumination with fluorescence excitation wavelengths in violet (390 nm-405 nm) is safe and harmless (*22*). Additionally, excitation will be short in duration (seconds). The use of fresh bovine knees and fresh-frozen cadaveric human knees has demonstrated its

robustness. Therefore, we have the belief that the native insertion site will be visible in patients. Another concern was that the image quality of the cadaveric bovine knee had a better SNR than the cadaveric human knees. A reason for this difference can be explained by the difference in freshness and storage of the samples. The bovine knees were fresh and never frozen while the human knees were frozen and stored for at least a year. Literature has shown that the autofluoresence of collageneous tissue decreases with tissue freshness and with freezing-thaw cycles (*23*).

In 2001, researchers have reported their concern about the accuracy of placing the graft with the transtibial technique and thus its ability to restore knee stability (*24, 25*). According to a recent meta-analysis, only 41% of patients have reported their reconstructed knee as normal (*26*). Due to these suboptimal results, there is a paradigm shift ongoing from the "transtibial" towards the "anatomic" ACL reconstruction technique (*8, 9, 27, 28*). The "anatomic" ACL reconstruction aims to place the graft at the native insertion sites by relying on arthroscopically visualizing anatomical landmarks such as the posterior wall, cartilage edge, the lateral intercondylar ridge, and bifurcate ridge to locate the native insertion sites (*9, 27-31*). This method, though is time consuming and demanding due to the visual limitations with the current white light endoscopic systems, careful dissection, biological variability, and additional visual impairment in the injured and degenerated joint. Hence, the "transtibial" technique was introduced to circumvent these difficulties. Several aides for arthroscopic visualization have been proposed to assist anatomic ACL reconstructions, including intraoperative fluoroscopic (*32-35*) and computer-aided navigation systems (*36-38*). The use of these systems, however are often criticized for being expensive, time consuming, and ionizing hazards (*39, 40*). The FA, however does not have these drawbacks. Additional advantages of the FA include: real time, tissue specific, subject specific imaging, as well as easy, fast and low cost.

The FA system was developed to image autofluorescence of collagen and injury- or degeneration related spectral variations due to changes in collagen content or distribution. Apart from imaging the ACL, examples in which the use of the FA can be valuable include, but are not limited to: posterior cruciate ligament reconstruction, partial meniscectomy, (preventive) meniscal repair, glenoid repair, labrum repair. Also, bony lesions causing impingement (subacromial, hip or ankle) and bone tumors may be visualized. Furthermore, degeneration of other musculoskeletal tissues can be easily detected. Thus the FA can be also used diagnostically.

In conclusion, we have shown that the femoral insertion site can be accurately visualized with fluorescence imaging combined with spectral unmixing. The prototype of the FA demonstrates the capability to real-time and subject specific visualize the femoral insertion site. Furthermore, the FA system may facilitate arthroscopic pro-

cedures in other joints and may be used as a diagnostic tool during a fluorescence arthroscopy.

ACKNOWLEDGEMENTS

The authors gratefully acknowledge the assistance of Mahyar Foumani MD,

Tam Nguyen, MD and Hung Tran, MS with the validation experiment. The authors also thank Saskia Lambrechts, PhD for the use of the fluorospectrometer. The financial support from the Annafund | NOREF and the Mozaïek PhD training grant of the Netherlands Organization for Scientific Research (NWO) are gratefully acknowledged.

DISCLOSURES

Patent is pending. The arthroscopic system was lent from Smith & Nephew C.V. (Hoofddorp, the Netherlands) without any monetary compensation and without any condition.

REFERENCES

1. M. Watanabe, [Present status and future of arthroscopy]. *Geka chiryo. Surgical therapy* **26**, 73 (Jan, 1972).
2. M. D. Miller, B. J. Cole. (Saunders,, Philadelphia, Pa., 2004), pp. 1 online resource (xxiv, 862 p.).
3. M. Strobel, *Manual of arthroscopic surgery*. (Springer, Berlin ; New York, 2002), pp. xiv, 1090 p.
4. G. R. Scuderi, A. J. Tria, SpringerLink (Online service). (Springer Science+Business Media, LLC, New York, NY, 2010), pp. xix, 694 p.
5. D. Solomon. (2008).
6. Q. T. Nguyen, R. Y. Tsien, Fluorescence-guided surgery with live molecular navigation--a new cutting edge. *Nature reviews. Cancer* **13**, 653 (Sep, 2013).
7. A. L. Vahrmeijer, M. Hutteman, J. R. van der Vorst, C. J. van de Velde, J. V. Frangioni, Image-guided cancer surgery using near-infrared fluorescence. *Nature reviews. Clinical oncology* **10**, 507 (Sep, 2013).
8. O. Chechik *et al.*, An international survey on anterior cruciate ligament reconstruction practices. *International orthopaedics* **37**, 201 (Feb, 2013).
9. C. F. van Eck, B. P. Lesniak, V. M. Schreiber, F. H. Fu, Anatomic single- and double-bundle anterior cruciate ligament reconstruction flowchart. *Arthroscopy : the journal of arthroscopic & related surgery : official publication of the Arthroscopy Association of North America and the International Arthroscopy Association* **26**, 258 (Feb, 2010).
10. C. Trojani *et al.*, Causes for failure of ACL reconstruction and influence of meniscectomies after revision. *Knee surgery, sports traumatology, arthroscopy : official journal of the ESSKA* **19**, 196 (Feb, 2011).
11. P. E. Greis, D. L. Johnson, F. H. Fu, Revision anterior cruciate ligament surgery: causes of graft failure and technical considerations of revision surgery. *Clinics in sports medicine* **12**, 839 (Oct, 1993).
12. C. Sommer, N. F. Friederich, W. Muller, Improperly placed anterior cruciate ligament grafts: correlation between radiological parameters and clinical results. *Knee surgery, sports traumatology, arthroscopy : official journal of the ESSKA* **8**, 207 (2000).
13. J. A. Morgan, D. Dahm, B. Levy, M. J. Stuart, Femoral tunnel malposition in ACL revision reconstruction. *The journal of knee surgery* **25**, 361 (Nov, 2012).
14. L. Rahr-Wagner, T. M. Thillemann, A. B. Pedersen, M. C. Lind, Increased risk of revision after anteromedial compared with transtibial drilling of the femoral tunnel during primary anterior cruciate ligament reconstruction: results from the Danish Knee Ligament Reconstruction Register. *Arthroscopy : the journal of arthroscopic & related surgery : official publication of the Arthroscopy Association of North America and the International Arthroscopy Association* **29**, 98 (Jan, 2013).
15. J. C. Loh *et al.*, Knee stability and graft function following anterior cruciate ligament reconstruction: Comparison between 11 o'clock and 10 o'clock femoral tunnel placement. 2002 Richard O'Connor Award paper. *Arthroscopy : the journal of arthroscopic & related surgery : official publication of the Arthroscopy Association of North America and the International Arthroscopy Association* **19**, 297 (Mar, 2003).
16. S. M. Howell, M. A. Taylor, Failure of reconstruction of the anterior cruciate ligament due to impingement by the intercondylar roof. *The Journal of bone and joint surgery. American volume* **75**, 1044 (Jul, 1993).

17. K. L. Markolf *et al.*, Effects of femoral tunnel placement on knee laxity and forces in an anterior cruciate ligament graft. *Journal of orthopaedic research : official publication of the Orthopaedic Research Society* **20**, 1016 (Sep, 2002).
18. G. A. Wagnieres, W. M. Star, B. C. Wilson, In vivo fluorescence spectroscopy and imaging for oncological applications. *Photochemistry and photobiology* **68**, 603 (Nov, 1998).
19. N. Keshava, J. F. Mustard, Spectral unmixing. *Signal Processing Magazine, IEEE* **19**, 44 (2002).
20. J. Wittstein, M. Kaseta, R. Sullivan, W. E. Garrett, Incidence of the remnant femoral attachment of the ruptured ACL. *Clinical orthopaedics and related research* **467**, 2691 (Oct, 2009).
21. I. K. Lo, G. H. de Maat, J. W. Valk, C. B. Frank, The gross morphology of torn human anterior cruciate ligaments in unstable knees. *Arthroscopy : the journal of arthroscopic & related surgery : official publication of the Arthroscopy Association of North America and the International Arthroscopy Association* **15**, 301 (Apr, 1999).
22. J. Schmidbauer *et al.*, Improved detection of urothelial carcinoma in situ with hexaminolevulinate fluorescence cystoscopy. *The Journal of urology* **171**, 135 (Jan, 2004).
23. G. M. Palmer, C. L. Marshek, K. M. Vrotsos, N. Ramanujam, Optimal methods for fluorescence and diffuse reflectance measurements of tissue biopsy samples. *Lasers in surgery and medicine* **30**, 191 (2002).
24. M. P. Arnold, J. Kooloos, A. van Kampen, Single-incision technique misses the anatomical femoral anterior cruciate ligament insertion: a cadaver study. *Knee surgery, sports traumatology, arthroscopy : official journal of the ESSKA* **9**, 194 (Jul, 2001).
25. A. Bedi, B. Raphael, A. Maderazo, H. Pavlov, R. J. Williams, 3rd, Transtibial versus anteromedial portal drilling for anterior cruciate ligament reconstruction: a cadaveric study of femoral tunnel length and obliquity. *Arthroscopy : the journal of arthroscopic & related surgery : official publication of the Arthroscopy Association of North America and the International Arthroscopy Association* **26**, 342 (Mar, 2010).
26. D. J. Biau, C. Tournoux, S. Katsahian, P. Schranz, R. Nizard, ACL reconstruction: a meta-analysis of functional scores. *Clinical orthopaedics and related research* **458**, 180 (May, 2007).
27. K. Yasuda *et al.*, Anatomic reconstruction of the anteromedial and posterolateral bundles of the anterior cruciate ligament using hamstring tendon grafts. *Arthroscopy : the journal of arthroscopic & related surgery : official publication of the Arthroscopy Association of North America and the International Arthroscopy Association* **20**, 1015 (Dec, 2004).
28. T. Mae *et al.*, Anatomic double-bundle anterior cruciate ligament reconstruction using hamstring tendons with minimally required initial tension. *Arthroscopy : the journal of arthroscopic & related surgery : official publication of the Arthroscopy Association of North America and the International Arthroscopy Association* **26**, 1289 (Oct, 2010).
29. C. G. Ziegler *et al.*, Arthroscopically pertinent landmarks for tunnel positioning in single-bundle and double-bundle anterior cruciate ligament reconstructions. *The American journal of sports medicine* **39**, 743 (Apr, 2011).
30. M. Ferretti, M. Ekdahl, W. Shen, F. H. Fu, Osseous landmarks of the femoral attachment of the anterior cruciate ligament: an anatomic study. *Arthroscopy : the journal of arthroscopic & related surgery : official publication of the Arthroscopy Association of North America and the International Arthroscopy Association* **23**, 1218 (Nov, 2007).
31. L. D. Farrow, M. R. Chen, D. R. Cooperman, B. N. Victoroff, D. B. Goodfellow, Morphology of the femoral intercondylar notch. *The Journal of bone and joint surgery. American volume* **89**, 2150 (Oct, 2007).

32. B. J. Larson, J. Egbert, E. M. Goble, Radiation exposure during fluoroarthroscopically assisted anterior cruciate reconstruction. *The American journal of sports medicine* **23**, 462 (Jul-Aug, 1995).
33. G. Moloney *et al.*, Use of a fluoroscopic overlay to assist arthroscopic anterior cruciate ligament reconstruction. *The American journal of sports medicine* **41**, 1794 (Aug, 2013).
34. Y. Kawakami *et al.*, The accuracy of bone tunnel position using fluoroscopic-based navigation system in anterior cruciate ligament reconstruction. *Knee surgery, sports traumatology, arthroscopy : official journal of the ESSKA* **20**, 1503 (Aug, 2012).
35. T. V. Klos *et al.*, Computer assistance in arthroscopic anterior cruciate ligament reconstruction. *Clinical orthopaedics and related research*, 65 (Sep, 1998).
36. S. Zaffagnini, T. V. Klos, S. Bignozzi, Computer-assisted anterior cruciate ligament reconstruction: an evidence-based approach of the first 15 years. *Arthroscopy : the journal of arthroscopic & related surgery : official publication of the Arthroscopy Association of North America and the International Arthroscopy Association* **26**, 546 (Apr, 2010).
37. A. Burkart *et al.*, Precision of ACL tunnel placement using traditional and robotic techniques. *Computer aided surgery : official journal of the International Society for Computer Aided Surgery* **6**, 270 (2001).
38. V. Dessenne *et al.*, Computer-assisted knee anterior cruciate ligament reconstruction: first clinical tests. *Journal of image guided surgery* **1**, 59 (1995).
39. G. Rivkin, M. Liebergall, Challenges of technology integration and computer-assisted surgery. *The Journal of bone and joint surgery. American volume* **91 Suppl 1**, 13 (Feb, 2009).
40. P. Kasten *et al.*, What is the role of intra-operative fluoroscopic measurements to determine tibial tunnel placement in anatomical anterior cruciate ligament reconstruction? *Knee surgery, sports traumatology, arthroscopy : official journal of the ESSKA* **18**, 1169 (Sep, 2010).

Chapter 5

Effects of a Bioscaffold on Collagen Fibrillogenesis in Healing Medial Collateral Ligament in Rabbits

Rui Liang, Savio L-Y. Woo, D. Tan Nguyen, Ping-Cheng Liu, Alejandro Almarza

Journal of Orthopaedic Research, 2008 Aug;26(8):1098-104

ABSTRACT

Bioscaffolds have been successfully used to improve the healing of ligaments and tendons. In a rabbit model, the application of porcine small intestine submucosa (SIS) to the healing medial collateral ligament (MCL) resulted in improved mechanical properties with the formation of larger collagen fibrils. Thus, the objective of the study was to find out whether the SIS bioscaffold could improve the gene expressions of fibrillogenesis-related molecules, specifically, collagen types I, III, V and small leucine-rich proteoglycans including decorin, biglycan, lumican and fibromodulin, as well as collagen fibril morphology and organization, in the healing rabbit MCL at an early time point (6 weeks post-injury). Twenty skeletally mature rabbits were equally divided into two groups. In the SIS-treated group, a 6mm gap was surgically created and a layer of SIS was sutured to cover the gap while the gap was left open in the non-treated group. At 6 weeks post-injury, Masson's trichrome staining showed that the SIS-treated group had more regularly aligned collagen fibers and cells. Transmission electron microscopy revealed that the SIS-treated group had larger collagen fibrils with a diameter distribution from 24 to 120nm while the non-treated group had only small collagen fibrils (range from 26 to 87nm, $p<0.05$). Finally, the quantitative real-time PCR showed that the mRNAs of collagen type V, decorin, biglycan and lumican in the SIS-treated group were 41%, 58%, 51% and 43% lower than those in the non-treated group, respectively ($p<0.05$). Such significant reduction in the gene expressions are closely related to the improved morphological characteristics, which are known to be coupled with better mechanical properties, as previously reported in longer term studies.

INTRODUCTION

The medial collateral ligament (MCL) in the knee has been the most-used model for ligament and tendon healing studies because it can heal spontaneously and is frequently injured in sports and work related activities. Although its structural properties are restored post-injury without surgical intervention [1-4], the quality of the healing tissue remains abnormal for more than one year [5-7]. The collagen fibers in the healed MCL are relatively disorganized and the fibril diameters are homogeneously small when compared to the bimodal distribution of both large and small collagen fibrils in the normal MCL [8-11].

In the literature, a group of fibrillogenesis-related molecules, specifically collagen type III, collagen type V, and the small leucine-rich proteoglycans (SLRPs) including decorin, biglycan, lumican and fibromodulin, have been found to play important roles in the formation, organization and regulation of collagen fibrils [12-21]. In the healing ligament, the gene expressions and/or protein levels of these collagen subtypes and SLRPs were found to be up-regulated and concomitantly, the collagen fibrils were uniformly small [22-25].

With new tissue engineering approaches, the morphological, mechanical and biochemical properties of healing ligaments and tendons could be improved by means of the application of a biologically derived scaffold, namely the porcine small intestine submucosa (SIS) [9, 10, 26-29]. This scaffold is mainly composed of collagen type I and contains a small amount of growth factors and chemotactic factors that can promote cell migration into the healing site to enhance revascularization and tissue repair [30]. Previous studies from our research center used a single layer of SIS sutured to cover a 6 mm gap created in the rabbit MCL and found that the SIS treatment could induce the formation of larger collagen fibrils at both 12 weeks and 26 weeks post-injury. Concomitantly, the mechanical properties of the healing MCL were also significantly improved [9, 10, 26]. However, the earlier effects of SIS on the collagen fibrillogenesis in the healing ligaments remain to be elucidated. It invokes the research question of whether the SIS could improve the process of fibrillogenesis at an early stage of ligament healing in terms of morphology and the gene expressions of the fibrillogenesis-related molecules. Thus, the objective of this study was to determine the gene expressions of collagen type III, and collagen type V and SLRPs, and the morphology of collagen fibrils in the healing ligament following SIS treatment at 6 weeks post-injury. We hypothesized that the SIS could down-regulate the higher levels of the gene expressions of collagen type III, collagen type V, biglycan, lumican in the healing MCL, which would lead to the genesis of collagen fibrils with larger diameter and better organization. To test this hypothesis, the collagen organization, collagen fibril diameter and distribution, and the gene expressions of the fibrillogenesis-related molecules of the healing tissue were examined and compared with the methods of

Masson's trichrome staining, transmission electron microscopy (TEM) and quantitative real time PCR (Q-PCR).

MATERIALS AND METHODS

Twenty skeletally mature female New Zealand White rabbits (11-12 month old, body mass 5.2 ± 0.6 kg), obtained from Myrtle Rabbitries (Thompson Station, TN), were used for this study. Surgery and maintenance of the animals followed an established study protocol approved by the University of Pittsburgh's Institutional Animal Care and Use Committee.

A 6 mm segment of ligament centered at the joint line was surgically removed from the MCL of the right hind limb [9]. The MCLs of the left hind limb were only undermined but not injured, serving as a sham-operated control. In 10 animals serving as the SIS-treated group, a single strip of SIS, approximately 10 mm x 5 mm x 0.2 mm (Cook® Biotech Inc., Bloomington, IN), was sutured with one stitch on each of the four corners to cover the gap (abluminal side of SIS facing down) using non-absorbable 6-0 black silk sutures (Ethicon, Inc., Somerville, NJ). For the remaining 10 animals serving as the non-treated group, the gap injury was left open with sutures placed as markers in the same pattern as the SIS-treated group. The wound was irrigated with 0.9% saline solution and the fascia and skin were closed sequentially. All rabbits were allowed unrestricted activity in their cages (7 square feet) within one day after surgery. At 6 weeks after surgery, all animals were euthanized with an overdose of sodium pentobarbital (Euthanyl, MTC Pharmaceutical, Cambridge, Ontario, Canada). Four rabbits (2 in each group) were used for Masson's trichrome staining to examine the collagen fiber morphology. The other 16 rabbits (8 in each group) were used for gene expression analysis by means of Q-PCR. Among these 16 rabbits, a piece of tissue approximately 1mm x 1mm x 4mm was taken from the center of the healing tissue from 8 rabbits (4 in each group), which were randomly chosen, for the purpose of TEM examination.

For Masson's trichrome staining, the tissue was immediately embedded in the O.C.T. compound, frozen in liquid nitrogen, and stored at -80°C. The tissue blocks then underwent serial cryosections of 8μm thickness. Slides were fixed in Bouin's fixation overnight at room temperature and stained sequentially in Weigert's Iron Hematoxylin solution, Biebrich Scarlet-Acid Fuchsin, and Aniline Blue solution according to the manufacturer's instruction (SIGMA). The nuclei were stained in black, cytoplasm in red and collagen in blue. The slides were observed under a Nikon light microscope. Pictures were taken with a range of magnification from low grade (40x) to high grade (200x), from which the pictures with higher magnitudes (200x) obtained from the healing areas were shown in the results. TEM was done according to the previously published method [9, 10]. Briefly, tissue specimens were fixed in Karnovsky's fixative,

post-fixed in a solution containing 1% OsO4 buffered with PBS (pH 7.4) and dehydrated in EtOH (50%, 70%, 80%, 90%, and 100%). The tissue was infiltrated in a series of mixtures of LR White embedding resin (Electron Microscopy Sciences, Fort Washington, PA) and propylene oxide (PO), placed in gelatin capsules, and polymerized for 48 hours at 60°C. The embedded specimens were then thin sectioned transversely to obtain cross sectional view of the collagen fibrils and stained with 1% uranyl acetate and Reynolds lead citrate. The sections were viewed on a Hitachi H-7100 TEM (Hitachi High Technologies America, Inc., Pleasanton, CA) operating at 75kV. Digital images were obtained using an AMT Advantage 10 CCD Camera System (Advanced Microscopy Techniques Corporation, Danvers, MA) and NIH Image software. The images taken at a magnification of x 70,000 were used to measure the collagen fibril diameter, while those having artifacts and oblique or longitudinal fibrils were not used for analysis [5]. The minimum diameters of collagen fibrils in each image were measured by a SimplePCI analysis computer software (Compix Inc., Cranberry Township, PA). A 21,574 lines/cm calibration grid image at a magnification of x 70,000 was utilized in conjunction with the program's calibration function to convert all measurements from pixels to nanometers. For each group, at least 500 collagen fibrils from each sample in the sham group and at least 1000 collagen fibrils from each sample in the non-treated and SIS-treated group were measured (totally n=6500 for the sham-operated group, n=9161 for the non-treated group, and n=8133 for the SIS-treated group). The results were expressed in a histogram format. The average collagen fibril diameters for each group were calculated by averaging the mean values of fibril diameter for each specimen in the group, respectively.

For the Q-PCR, the total RNA was extracted with the Trizol method, following the manufacturer's instructions. Briefly, the harvested tissue was snap frozen in liquid nitrogen, pulverized in a freezer molar and homogenized in 1ml Trizol reagent (Invitrogen, Carlsbad, CA) using a tissue homogenizer (Biospec Products, Bartlesville, OK). Chloroform was added, and the samples were centrifuged. The RNA was precipitated from the upper aqueous phase with isopropanol and washed with 75% alcohol. Following the Trizol isolation, the total RNA was cleaned using an RNeasy cleaning kit (Qiagen, Chatsworth, CA). The concentration of the total RNA was determined in a spectrophotometer at the reading of 260 nm. The 260/280 ratio ≥ 1.8 was used to control the RNA purity. Following RNA extraction, 1μg of total RNA, isolated from each of the tissue samples, was reverse transcribed to cDNA by using the Superscript™ First-Strand Synthesis System for RT-PCR (Invitrogen, Carlsbad, CA), following the manufacturer's instruction. Rabbit-specific primers were used for glyceraldehyde-3-phosphate dehydrogenase (GAPDH), collagen type I (COL1A2), collagen type III (COL3A1), collagen type V (COL5A1), decorin, biglycan, lumican, and fibromodulin (Table 1). The primers were synthesized by IDT (Integrated DNA Technologies, Inc.,

Table 1. Sequence of primers used in quantitative polymerase chain reactions (QPCR)

Gene	Primer sequence (sense/antisense)	Expected PCR product size (bp)	Source
COL1A2	5'-CCTGGCACCCCAGGTCCTCA-3'	227	Cooper, et al [34]
	5'-TCGCTCCCAGGGTTGCCATC-3'		
COL3A1	5'-TTATAAACCAACCTCTTCCT-3'	255	S83371
	5'-TATTATAGCACCATTGAGAC-3'		
COL5A1	5'-ATGAGGAGATGTCCCACGAC-3'	171	AF451331
	5'-CGAATTTCTGTGTGGCTTCA-3'		
Decorin	5'-TGTGGACAATGGTTCTCTGG-3'	419	S76584
	5'-CCACATTGCAGTTAGGTTCC-3'		
Biglycan	5'-GATGGCCTGAAGCTCAA-3'	406	AF020290
	5'-GGTTGTTGAAGAGGCTG-3'		
Lumican	5'-CATCCCTGATGAGTATTTCAAGC-3'	124	AF020292
	5'-ATCCAGCTCAACCAGAGATGATA-3'		
Fibromodulin	5'-CAACGAGATCCAGGAGGTG-3'	255	Guehring, et al [35]
	5'-CTGCTGGAGTTGAAGGTGT-3'		
Glyceraldehyde-3-phosphate dehydrogenase	5'-TCGGCATTGTGGAGGGGCTC-3'	177	Cooper, et al [34]
	5'-TCCCGTTCAGCTCGGGGATG-3'		

bp = length of promer product in base pair; source = Genbank accession number or journal article reference

Coralville, IA). Prior to being used in the experiment, all primers were tested by conventional polymerase chain reaction (PCR). The PCR products were verified on 2% agarose gels with ethidium bromide. Specifically, the PCR products from the primers for COL5A1 designed in our research center were further verified by DNA sequencing.

To quantify mRNA levels of the genes, Q-PCR was performed with a Lightcycler, in which SYBR Green fluorescent dye, incorporated in double-strand DNA, can be detected. A total of 20 μL of reaction included 16 μL of SYBR Green mix, 2 μL of primer mix, and 2 μL of cDNA. PCR was run for 40 cycles, with denaturation at 95°C for 15min, annealing at 58°C (GAPDH, COL1A2), 52°C (COL3A1, COL3A1, decorin, lumican, fibromodulin) and 50°C (biglycan), respectively, for 2 minutes; and extension at 72°C for 2 minutes. The measurement was repeated 3 times. Each PCR product was verified according to fragment size on agarose gels. For each individual gene, the PCR efficiency was decided by standard curves derived from dilutions of cDNA in a range from 1 to 10^{-6} by 10-fold serial dilution prior to amplification of the samples. Efficiency above 90% was accepted as a good PCR condition. Quantification is done relative to the mRNA level of GAPDH by subtracting the cycle threshold (Ct) of the GAPDH from the Ct of the gene of interest. The resulting difference in cycle number (ΔCt) is the

exponent of the base 2 (due to the doubling function of PCR), representing the fold difference of template for these two genes [31].

The Kolmogorov-Smirnov test was used to compare the distributions of collagen fibril diameters between the groups. One-factor analysis-of-variance method (ANOVA) and Bonferroni multiple comparison tests were used to compare the mean value of collagen fibril diameter and Q-PCR data for different gene expressions between the non-treated, SIS-treated, and sham operated groups. The results were expressed as mean ± standard deviation. All values of $p < 0.05$ were accepted as statistically significant. Statistical analysis was performed using SPSS statistical software (version 12.0, SPSS, Chicago, IL).

RESULTS

Gross inspection showed that the appearance of the sham-operated ligaments was white and shiny as normal and loosely covered by the overlying fascia (Figure 1A). For the non-treated group at 6 weeks post injury, the healing ligaments were yellowish

with obvious adhesion to surrounding tissues, and sharp dissection was needed in order to remove the ligaments from the fascia. In 5 out of the 10 specimens, the gaps between the remaining ligament tissue on the femoral and tibial sides were not completely filled with the healing tissue (Figure 1B). In comparison, the healing ligaments from the SIS treated group were also yellowish but with clear ligament border and were easily dissected from the fascia (Figure 1C). The SIS bioscaffold was no longer visible. The gap was filled with healing tissue and joined at both ends with the remaining ligament tissue from the femoral and tibial insertions.

Following Masson's trichrome staining, the MCL from the sham-operated group showed regularly aligned and compact collagen fibers that were stained in blue (Figure 2A).

The cytoplasm of the cells (stained in red) and the nuclei (stained in black), were spindle-shaped and aligned along the collagen fibers. Whereas, for the healing ligaments from the non-treated group, the extracellular matrix had faint staining without dense collagen fibers and was highly disorganized with no obvious orientation (Figure 2B). The cells also appeared to be mostly rounded and oriented irregularly without specific direction. After SIS-treatment, the collagen fibers in the healing ligament appeared more oriented in the longitudinal direction (Figure 2C). Furthermore, there were an abundant number of cells in the SIS-treated MCL and many of these cells were spindle-shaped and oriented along the collagen fibers. In both non-treated and SIS-treated groups, a group of cells with black nuclei and round red cytoplasm that appeared differently from the fibroblasts could be observed. The SIS-treated group seemed to have more of these cells. The identities and sources of these cells remained to be clarified in future studies.

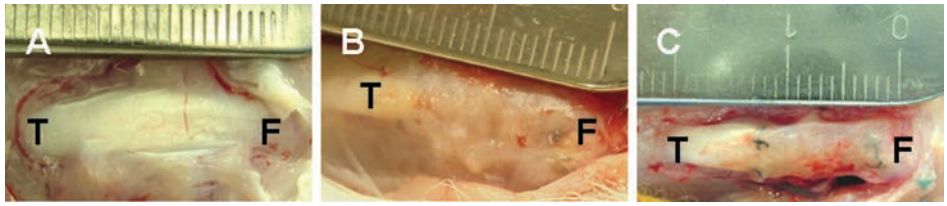

Figure 1. The appearance of the MCL at 6 weeks post-injury under gross inspection from **A**. Shamoperated group; **B**. Non-treated group; **C**. SIS-treated group. F = Femur insertion site, T = Tibia insertion site.

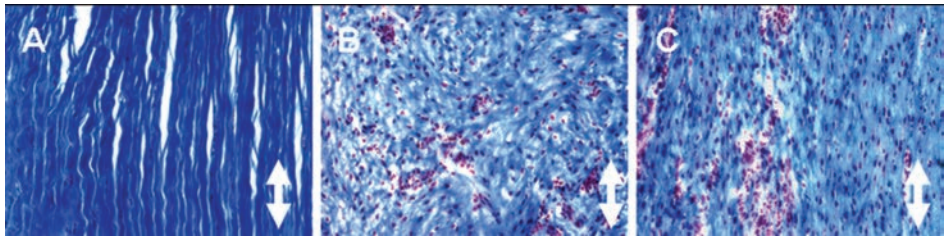

Figure 2. Masson's Trichome staining of the MCL at 6 weeks post-injury from **A**. Sham-operated group; **B**. Non-treated group; **C**. SIS-treated group. Magnified at 200 x under light microscopy. The double-headed arrows indicate the longitudinal axis of the ligament.

The collagen fibrils examined by TEM revealed that the morphology of the collagen fibrils in the sham group had a typical heterogeneous appearance of large and small collagen fibrils (Figure 3(A)-A). In contrast, the non-treated group had uniformly small collagen fibrils (Figure 3(A)-B). In the SIS-treated group, however, some larger collagen fibrils could be found around the fibroblasts in all 4 specimens (Figure 3(A)-C). The diameters for the collagen fibrils in the sham group ranged from 23 to 276 nm, whereas those in the non-treated group were limited from 26 to 87 nm (Figure 3(B)). The diameters of the collagen fibrils in the SIS-treated group spread over a larger range from 24 to 120 nm, which was significantly different from those for the non-treated group ($p < 0.05$). The peak of the distribution histogram for the SIS-treated group was shifted further to the right when compared with that for the non-treated group. The SIS-treated group had an average collagen fibril diameter of 55 ± 5 nm that was 12% larger than that in the non-treated group (48 ± 3 nm, $p < 0.05$), while those in both groups were smaller than that in the sham group (103 ± 34 nm, $p < 0.05$).

The gene expressions of collagen types I, III and V as measured with the quantitative real-time PCR (Figure 4(A)) showed that their mRNA levels in the healing ligaments from the non-treated group were significantly elevated when compared with those in the sham-operated group (117%, 233% and 112%, respectively, $p < 0.05$). After SIS treatment, the mRNA levels of collagen type I and III in the healing ligament were still significantly higher than those for the sham-operated group (63% and 218%

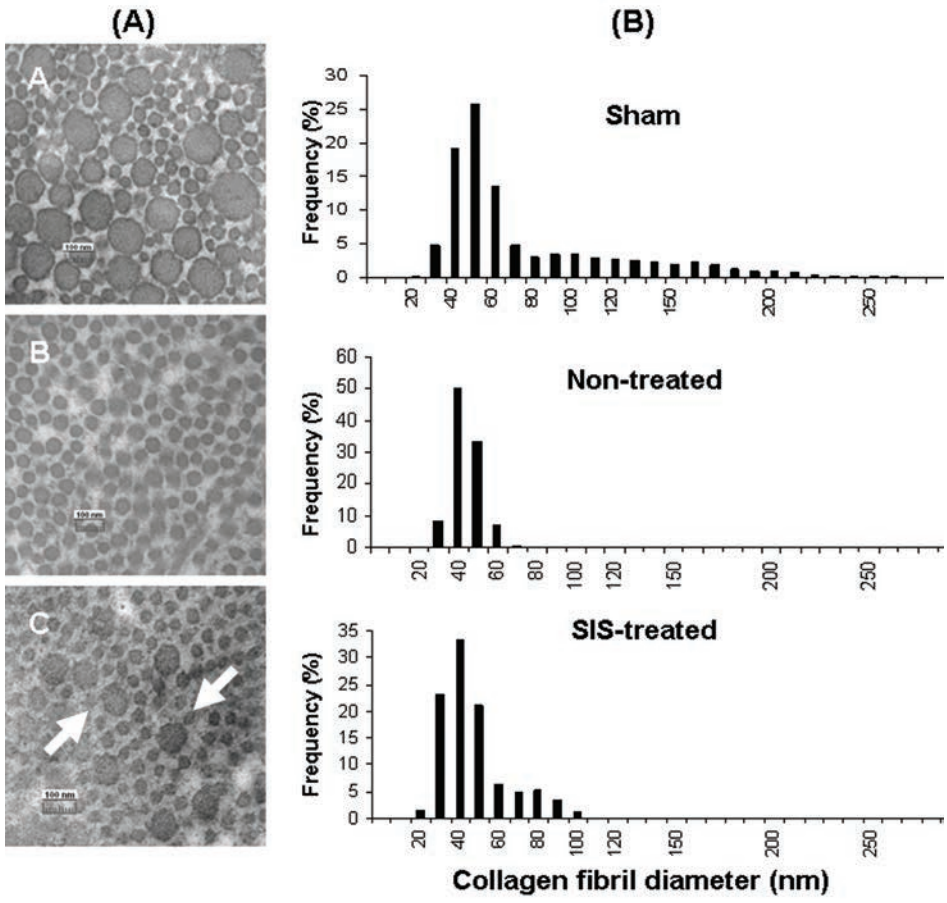

Figure 3. (A). Transmission electron microscopy images (70,000 x) of collagen fibrils in MCLs from **A**. Sham-operated group; **B**. Non-treated group; **C**. SIS-treated group, at 6 weeks post-injury. The arrows indicate the larger collagen fibrils appeared in the SIStreated group. (B). Histogram describing the collagen fibril distributions in MCLs from sham-operated group (n = 8), non-treated group (n = 4) and SIS-treated group (n = 4) at 6 weeks post-injury.

over sham values, respectively, $p < 0.05$) and did not show significant changes from those for the non-treated group ($p = 0.09$ for collagen type I and $p = 0.11$ for collagen type III). However, the mRNA for collagen type V in the SIS-treated group was down-regulated to a level that was not significantly different from that in the sham-operated group ($p = 0.23$) but 41% lower than that in the non-treated group ($p < 0.05$). The gene expressions of the SLRP molecules (Figure 4(B)) showed that the mRNA levels of biglycan and lumican in the non-treated group were 93% and 114% higher ($p < 0.05$), while those for the decorin and fibromodulin were 60% and 66% lower than those in the sham-operated group, respectively ($p < 0.05$). After SIS treatment, the mRNA levels of biglycan and lumican in the healing ligaments were down-regulated

to levels that were not significantly different from those in the sham-operated group ($p = 0.73$ for biglycan and $p = 0.77$ for lumican), but 51% and 43% lower than those in the non-treated group, respectively ($p < 0.05$). Interestingly, the mRNA of decorin in the SIS-treated group was brought down to a level that was 83% lower than that for the sham group ($p < 0.05$) and 58% lower than that in the non-treated group ($p < 0.05$). The mRNA of fibromodulin in the SIS-treated group was 60% lower than that in the sham group ($p < 0.05$) and did not show significant difference from that in the non-treated group ($p = 0.81$).

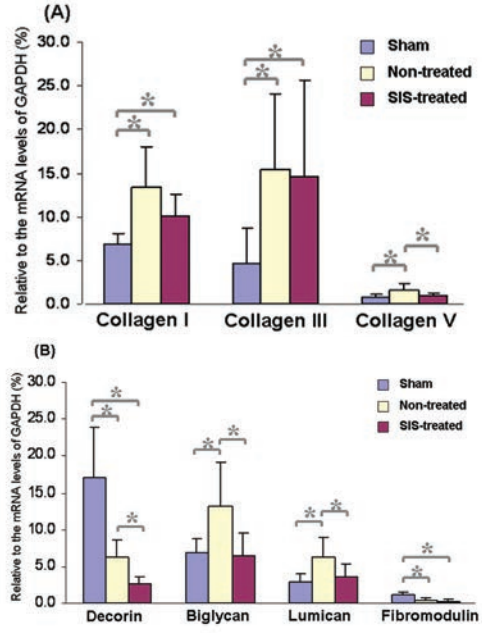

Figure 4. Results of the quantitative real time PCR for (A) The gene expressions of collagen types I, III and V; (B) The gene expressions of small leucine-rich proteoglycan molecules including decorin, biglycan, lumican and fibromodulin in the sham-operated (n = 16), non-treated (n = 8), and SIS-treated groups (n = 8) at 6 weeks post-injury. * indicates $p < 0.05$. The error bars represent standard deviations.

DISCUSSION

The study demonstrated that with the application of SIS bioscaffold to a 6 mm gap injury of the MCL in rabbit, the collagen fibrillogenesis in the healing ligament could be improved as the collagen fibers were more organized along the longitudinal axis of the ligament with larger collagen fibrils (up to 120nm), and concomitantly the gene expressions of fibrillogenesis-related molecules, specifically collagen type V, decorin, biglycan and lumican were down-regulated. These results were in sharp contrast to

the disorganization of collagen fibers, homogenously small collagen fibrils and higher levels of the gene expression of those molecules in the healing MCLs from the non-treated group. The early morphological and molecular improvements brought by the application of SIS scaffold may serve as the basis for the enhanced mechanical properties of the healing ligament in the long term, i.e. at 12 and 26 weeks post injury [9, 10].

The distributions of collagen fibril diameters in the sham-operated and non-treated group were similar to the literature [8, 10]. Compared to that in the non-treated group, the healing ligament in the SIS-treated group had a wider range of fibril diameter distribution and there were larger collagen fibrils up to 120nm in diameter. Literature has demonstrated that the healing rabbit MCL contained a homogeneous population of small collagen fibrils. It was not until 104 weeks post-injury when the larger collagen fibrils could be found [8]. Thus, our data suggest that SIS-treatment could have accelerated the process of MCL healing. This suggestion is further supported by the down-regulation of the gene expression of collagen type V at the early time point. Previous work has shown that the level of collagen type V remained elevated in the healing ligament even after 2 years [23]. With the treatment of SIS, a decrease in the collagen type V/I ratio was concomitantly observed with increased mechanical properties at later time points [9, 10].

In this study, we have further examined additional factors that affect collagen fibrillogenesis in the healing ligament, i.e. the SLRP molecules including decorin, biglycan, lumican and fibromodulin. Previous investigations, both *in vitro* and *in vivo* [12-18, 21] have shown that the SLRPs played important roles in regulating collagen fibril diameter, distribution and orientation by combining with or directly incorporating into the fibrils. It was found that higher levels of decorin, biglycan and lumican relative to collagen type I would cause the collagen fibrils to remain small *in vitro* [14, 17, 20]. Further, in gene knockout studies of these molecules, larger collagen fibrils formed albeit they appeared to be disorganized and fragile[13, 16, 32]. These findings suggested that these molecules are regulated homeostatically at appropriate levels in order to have the normal size distribution and organization of collagen fibrils, which are suited for their load bearing functions in ligaments and tendons. In this study, the gene expressions of these molecules in the non-treated ligament were similar to those in the literature [24]. However, following SIS- treatment, the mRNA levels of biglycan and lumican were down-regulated closer to those for the sham group, and concurrently, larger collagen fibrils were formed with an improved organization of the extracellular matrix. The implication of the lower gene expression of decorin in the healing ligament from the non-treated group than that in the sham-operated group remains to be elucidated. Others have documented that decreasing the level of decorin by anti-sense oligonucleotides could result in larger collagen fibrils and improved mechanical properties in rabbit healing MCL [33]. Therefore, the down-regulation of

the gene expression of decorin in the healing ligaments from SIS-treated group may have also contributed to the formation of larger collagen fibrils.

One limitation of this study is that the animal MCL gap-injury model is not the same as a rupture injury that is commonly seen in clinic. However, for the purpose of investigating the mechanisms of the application of SIS bioscaffold on fibrillogenesis, this model of injury is highly reproducible. Furthermore, since our results were based on the mRNA levels of the fibrillogenesis-related molecules, which do not necessarily reflect the protein levels, further studies regarding the changes of these molecules at the protein level will be necessary.

It should be acknowledged that the animal studies have a lot of limitations, which could not represent the clinical situation on many aspects such as injury type, post-operative rehabilitation and so on. However, the positive results in the study still suggest that the approach of using a bioscaffold to accelerate and improve the healing of injured ligaments is promising. In combination with appropriate post-operative rehabilitation protocols, the clinical outcomes of the patients could be better.

The improved collagen fibrillogenesis in the healing rabbit MCL with SIS treatment at an early time point could serve as a mechanistic basis for the clinical application of this tissue engineering approach in the treatment of injured ligaments and tendons, also a basis for future studies that will focus on how the healing cells sense the signals of the bioscaffold and react accordingly to improve the quality of the healing tissue.

ACKNOWLEDGEMENT

This project described was supported by NIH Grant AR41820. The authors thank Dr. Hiles of Cook Biotech, Inc. for supplying the SIS, Mr. Joe Suhan for his technical assistance in TEM, Dr. Chin-Yi Chuo for helping with the surgery, Miss Rayna Nolla for her assistance in analyzing the TEM data, and Dr. Changfu Wu for helping with the statistical analysis.

REFERENCES

1. Ballmer, P.M. and R.P. Jakob, *The non operative treatment of isolated complete tears of the medial collateral ligament of the knee. A prospective study.* Arch Orthop Trauma Surg, 1988. **107**(5): p. 273-6.
2. Gomez, M.A., et al., *Medical collateral ligament healing subsequent to different treatment regimens.* J Appl Physiol, 1989. **66**(1): p. 245-52.
3. Inoue, M., et al., *Effects of surgical treatment and immobilization on the healing of the medial collateral ligament: a long-term multidisciplinary study.* Connect Tissue Res, 1990. **25**(1): p. 13-26.
4. Reider, B., *Medial collateral ligament injuries in athletes.* Sports Med, 1996. **21**(2): p. 147-56.
5. Frank, C., et al., *Medial collateral ligament healing. A multidisciplinary assessment in rabbits.* Am J Sports Med, 1983. **11**(6): p. 379-89.
6. Weiss, J.A., et al., *Evaluation of a new injury model to study medial collateral ligament healing: primary repair versus nonoperative treatment.* J Orthop Res, 1991. **9**(4): p. 516-28.
7. Woo, S.L., et al., *Medial collateral knee ligament healing. Combined medial collateral and anterior cruciate ligament injuries studied in rabbits.* Acta Orthop Scand, 1997. **68**(2): p. 142-8.
8. Frank, C., D. McDonald, and N. Shrive, *Collagen fibril diameters in the rabbit medial collateral ligament scar: a longer term assessment.* Connect Tissue Res, 1997. **36**(3): p. 261-9.
9. Liang, R., et al., *Long-term effects of porcine small intestine submucosa on the healing of medial collateral ligament: a functional tissue engineering study.* J Orthop Res, 2006. **24**(4): p. 811-9.
10. Woo, S.L., et al., *Treatment with bioscaffold enhances the the fibril morphology and the collagen composition of healing medial collateral ligament in rabbits.* Tissue Eng, 2006. **12**(1): p. 159-66.
11. Frank, C., et al., *Collagen fibril diameters in the healing adult rabbit medial collateral ligament.* Connect Tissue Res, 1992. **27**(4): p. 251-63.
12. Liu, X., et al., *Type III collagen is crucial for collagen I fibrillogenesis and for normal cardiovascular development.* Proc Natl Acad Sci U S A, 1997. **94**(5): p. 1852-6.
13. Danielson, K.G., et al., *Targeted disruption of decorin leads to abnormal collagen fibril morphology and skin fragility.* J Cell Biol, 1997. **136**(3): p. 729-43.
14. Hakkinen, L., et al., *A role for decorin in the structural organization of periodontal ligament.* Lab Invest, 2000. **80**(12): p. 1869-80.
15. Iozzo, R.V., *The family of the small leucine-rich proteoglycans: key regulators of matrix assembly and cellular growth.* Crit Rev Biochem Mol Biol, 1997. **32**(2): p. 141-74.
16. Corsi, A., et al., *Phenotypic effects of biglycan deficiency are linked to collagen fibril abnormalities, are synergized by decorin deficiency, and mimic Ehlers-Danlos-like changes in bone and other connective tissues.* J Bone Miner Res, 2002. **17**(7): p. 1180-9.
17. Rada, J.A., P.K. Cornuet, and J.R. Hassell, *Regulation of corneal collagen fibrillogenesis in vitro by corneal proteoglycan (lumican and decorin) core proteins.* Exp Eye Res, 1993. **56**(6): p. 635-48.
18. Vogel, K.G. and J.A. Trotter, *The effect of proteoglycans on the morphology of collagen fibrils formed in vitro.* Coll Relat Res, 1987. **7**(2): p. 105-14.
19. Birk, D.E. and R. Mayne, *Localization of collagen types I, III and V during tendon development. Changes in collagen types I and III are correlated with changes in fibril diameter.* Eur J Cell Biol, 1997. **72**(4): p. 352-61.
20. Birk, D.E., et al., *Collagen fibrillogenesis in vitro: interaction of types I and V collagen regulates fibril diameter.* J Cell Sci, 1990. **95 (Pt 4)**: p. 649-57.

21. Svensson, L., et al., *Fibromodulin-null mice have abnormal collagen fibrils, tissue organization, and altered lumican deposition in tendon.* J Biol Chem, 1999. **274**(14): p. 9636-47.
22. Lo, I.K., et al., *Comparison of mRNA levels for matrix molecules in normal and disrupted human anterior cruciate ligaments using reverse transcription-polymerase chain reaction.* J Orthop Res, 1998. **16**(4): p. 421-8.
23. Niyibizi, C., et al., *Type V collagen is increased during rabbit medial collateral ligament healing.* Knee Surg Sports Traumatol Arthrosc, 2000. **8**(5): p. 281-5.
24. Boykiw, R., et al., *Altered levels of extracellular matrix molecule mRNA in healing rabbit ligaments.* Matrix Biol, 1998. **17**(5): p. 371-8.
25. Plaas, A.H., et al., *Proteoglycan metabolism during repair of the ruptured medial collateral ligament in skeletally mature rabbits.* Arch Biochem Biophys, 2000. **374**(1): p. 35-41.
26. Musahl, V., et al., *The use of porcine small intestinal submucosa to enhance the healing of the medial collateral ligament--a functional tissue engineering study in rabbits.* J Orthop Res, 2004. **22**(1): p. 214-20.
27. Badylak, S.F., et al., *The use of xenogeneic small intestinal submucosa as a biomaterial for Achilles tendon repair in a dog model.* J Biomed Mater Res, 1995. **29**(8): p. 977-85.
28. Dejardin, L.M., S.P. Arnoczky, and R.B. Clarke, *Use of small intestinal submucosal implants for regeneration of large fascial defects: an experimental study in dogs.* J Biomed Mater Res, 1999. **46**(2): p. 203-11.
29. Dejardin, L.M., et al., *Tissue-engineered rotator cuff tendon using porcine small intestine submucosa. Histologic and mechanical evaluation in dogs.* Am J Sports Med, 2001. **29**(2): p. 175-84.
30. Badylak, S., et al., *Naturally occurring extracellular matrix as a scaffold for musculoskeletal repair.* Clin Orthop Relat Res, 1999(367 Suppl): p. S333-43.
31. Ginzinger, D.G., *Gene quantification using real-time quantitative PCR: an emerging technology hits the mainstream.* Exp Hematol, 2002. **30**(6): p. 503-12.
32. Jepsen, K.J., et al., *A syndrome of joint laxity and impaired tendon integrity in lumican- and fibromodulin-deficient mice.* J Biol Chem, 2002. **277**(38): p. 35532-40.
33. Nakamura, N., et al., *Decorin antisense gene therapy improves functional healing of early rabbit ligament scar with enhanced collagen fibrillogenesis in vivo.* J Orthop Res, 2000. **18**(4): p. 517-23.
34. Cooper, J.A., Jr., et al., *Evaluation of the anterior cruciate ligament, medial collateral ligament, achilles tendon and patellar tendon as cell sources for tissue-engineered ligament.* Biomaterials, 2006. **27**(13): p. 2747-54.
35. Guehring, T., et al., *Stimulation of gene expression and loss of anular architecture caused by experimental disc degeneration--an in vivo animal study.* Spine, 2005. **30**(22): p. 2510-5.

Chapter 6

Effects of Cell Seeding and Cyclic Stretch on the Fiber Remodeling in an Extracellular Matrix–Derived Bioscaffold

D. Tan Nguyen, Rui Liang, Savio L-Y. Woo, Shawn D. Burton, Changfu Wu, Alejandro Almarza, Michael S. Sacks, Steven Abramowitch

Tissue Engineering Part A. 2009 Apr;15(4):957-63

ABSTRACT

The porcine small intestine submucosa, an extracellular matrix derived bioscaffold (ECM-SIS), has been successfully used to enhance the healing of ligaments and tendons. Since the collagen fibers of ECM-SIS have an orientation of ±30^{o}, its application in improving the healing of the parallel-fibered ligament and tendon may not be optimal. Therefore, the objective of this study was to improve the collagen fiber alignment of ECM-SIS in-vitro with fibroblast-seeding and mechanical cyclic stretch. The hypothesis was that with the synergistic action of seeded cells and mechanical stimuli, the collagen fibers in the ECM-SIS would be remodeled to be more aligned, making it a better bioscaffold with enhanced conductive effects on the healing cells through the effects of "contact guidance". Three experimental groups were established: Group I (n=14), the ECM-SIS were seeded with fibroblasts & cyclically stretched; Group II (n=13), the ECM-SIS were seeded with fibroblasts but no cyclic stretch was applied; and Group III (n=8), the ECM-SIS were cyclically stretched but no fibroblasts were seeded. After 5 days' experiments, the scaffolds from all the three groups (n=9 for Group I; n=8 for Group II and III) were processed for the quantification of the collagen fiber orientation with a small angle light scattering (SALS) system. For Group I and II that contained seeded cells, the cell morphology and orientation, and newly produced collagen fibrils were examined with confocal fluorescent microscopy (n=3/group) and transmission electronic microscopy (TEM) (n=2/group). The results revealed that the collagen fiber orientation in Group I was more aligned closer to the stretching direction when compared to the other two groups. The mean angle improved from 25.3° before treatment to 7.1° degrees after treatment ($p<0.05$), and the associated dispersion of angles was also reduced (18.5° vs. 37.4°, $p<0.05$). In contrast, Groups II and III demonstrated minimal changes. The cells in Group I were more aligned in the direction of stretch than those in Group II. Newly produced collagen fibrils could be observed along the cells in both Groups I and II. This study demonstrated that a combination of fibroblast-seeding and cyclic stretch could remodel the fiber orientation of the ECM-SIS bioscaffold. The better aligned ECM-SIS has the prospect of eliciting improved effects on enhancing the healing of ligaments and tendons.

INTRODUCTION

Ligaments and tendons are soft connective tissues composed of closely packed, parallel aligned collagen fiber bundles which connect bone to bone and muscle to bone, respectively. The alignment of the collagen fibers to the direction of tensile loading makes ligaments and tendons suitable to resist high stresses and strains. [1, 2] In healing ligaments and tendons, however, it has been shown that the newly synthesized extracellular matrix (ECM) is not organized and well-aligned, which could be correlated to their inferior stiffness and strength. [1, 3, 4] Therefore, if the newly synthesized collagen fibers could be aligned from the initial healing process, the mechanical properties of healing ligaments and tendons could be potentially improved.

An approach to achieve this goal is to use an aligned scaffold, which can elicit such effects through a phenomenon called "contact guidance", in which the cells align along the topographical cues of their substratum and subsequently produce new matrix in a similar orientation.[5] At the same time, the biological properties of the scaffold such as cell biocompatibility, biodegradability and bioactive function etc. need to be considered for its in vivo application. Recently, an extracellular matrix (ECM) bioscaffold derived from the porcine small intestine submucosa (SIS), has been successfully used to improve the healing of ligaments and tendons.[3, 6, 7] Its positive effects on the healing have been attributed to its unique natural ECM ultrastructure and biological properties (i.e. it is mainly composed of collagen type I and contains bioactive factors like growth factors and various cytokines). However, it has been noticed that it has only relatively aligned collagen fibers in which two distinct fiber populations oriented at ~±30° with respect to the longitudinal axis of the intestine.[8-10] Therefore, in order to improve the conductive effect of this ECM scaffold to guide the healing cells be more aligned and to produce aligned matrices in the healing ligament and tendon, the objective of this study was to remodel and improve the collagen fiber alignment of the ECM-SIS in-vitro by employing a combination of fibroblast-seeding and cyclic stretch. We hypothesized that with the synergistic action of seeded cells and mechanical stimuli, the collagen fibers in the bioscaffold would be remodeled to be more aligned, making it a better scaffold with enhanced conductive effects on the healing cells through the effects of "contact guidance".

To test this hypothesis, we seeded fibroblasts derived from the rabbit medial collateral ligament (MCL) on SIS scaffolds and mechanically stimulated them with cyclic uniaxial stretch. The collagen fiber orientation of SIS was quantified by a small angle light scattering (SALS) system, while the cell morphology, orientation and the presence of newly produced collagen were visualized by confocal fluorescent microscopy and transmission electron microscopy (TEM), respectively.

MATERIALS & METHODS

Thirty-five SIS scaffolds (Cook BioTech, Indianapolis, USA) were rehydrated in Dulbecco's Modified Eagle Medium (DMEM, Invitrogen, Carlsbad, CA) and cut into dog-bone shaped specimens (clamp to clamp length was 2cm with a width of 1cm). The long axis of the specimen corresponded with the longitudinal axis of the small intestine, which has been shown to be the preferred direction of collagen fiber alignment. [10] The scaffolds (n=35) were randomly divided into the following experimental groups: Group I: Cell-Seeded & Cyclically Stretched (n=14); Group II: Cell-Seeded & Non-stretched (n=13) and Group III: Non-seeded & Cyclically Stretched (n=8).

For the groups that were seeded with cells (Group I and II), fibroblasts derived from female skeletally mature New Zealand White rabbit MCL were used. Briefly, the midsubstance of MCL was dissected, rinsed with Hank's buffered salt solution (HBSS, Invitrogen, Carlsbad, CA, USA), cut into small pieces in aseptic conditions, and then placed into a Petri dish with 6 ml of DMEM (Sigma-Aldrich, St. Louis, MO) supplemented with 10% fetal bovine serum (FBS; Invitrogen, Carlsbad, CA, USA) and 1% penicillin/streptomycin (P/S; Invitrogen) for explant culture, for which standard cell culture conditions (37°C, humidified and 5% CO_2) were used. The culture medium was replaced every 2 days. [11] The cells were passaged after reaching 80-90% confluence. To seed cells, the dog-boned ECM-SIS scaffold was fixed on the bottom of a custom-made silicone dish of the same dimension by using a solid block at each clamping end. Each bioscaffold was seeded with passage 2 fibroblasts at a density of 3 x 10^5cells/cm^2. [12] After seeding on the scaffolds, the fibroblasts were allowed 24 hours to attach. The cell-seeded scaffolds were then transferred to the individual stations of a custom-designed Cyclic Stretching Tissue Culture (CSTC) system, where they were allowed to acclimate in culture medium. After 24-36 hours, the scaffolds in Group I were subjected to cyclic stretch while those in Group II were not stretched but kept in the same condition as Group I. For Group III in which no fibroblasts were seeded, the scaffolds were stretched directly after immersed in the culture medium for the same hours as the other two groups. The CSTC system was specifically developed in our research center for the purpose of studying the remodeling of extracellular matrix scaffolds. This system is capable of independently applying precise cyclic displacement waveforms to each specimen. [12] The CSTC system (Figure 1) consists of 3 independent stretching chambers which can apply precise displacement profiles while measuring the load in each scaffold.

The samples were mounted on custom-made clamps and immersed in culture medium supplemented with 50μg/ml ascorbic acid. Immediately before cyclic stretch, all samples were pre-loaded with 0.05N to establish a standardized starting point, and then subjected to a cyclic stretching regimen of 2 hrs, allowed to rest 2 hrs, stretched another 2 hrs, and finally rested for 18 hrs. This stretching pattern was repeated for 5

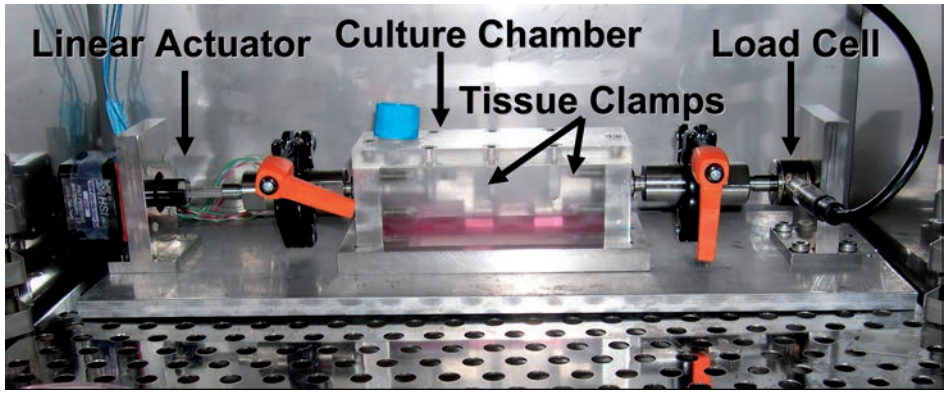

Figure 1. Cyclic Stretching Tissue Culture (CSTC) system

consecutive days. The elongation and frequency were set at 10% and 0.5 Hz, respectively. The culture medium was changed every two days.

A small angle light scattering (SALS) system was used to quantify the collagen fiber orientation of the ECM-SIS before and after experimentation (Group 1: n=9; Group 2: n=8; Group 3: n=8). This technique uses the spatial intensity distribution of the scattered light pattern resulting from the sum of the structural information of the tissue in the path of a laser beam [13]. The SALS device passes a 4-mW unpolarized helium-neon laser beam through the tissue, which was chosen because its wavelength (632.8 nm) is within an order of magnitude of the collagen fiber diameter. For dense fibrous tissues, it has been shown that they do not exhibit measurable multiple scattering effects. Thus, the distribution of light intensity is a representation of the sum of the structural information throughout the thickness of a tissue at the point of the laser beam (about 260 μm in diameter). For each ECM-SIS specimen, a total of 1000 points at the midsubstance (about 0.8 x 1.25 cm) were scanned before and after experimentation using the SALS system. The collagen fiber orientation at each point was expressed as the angle with respect to the longitudinal axis of the ECM-SIS. The average of these 1000 angles represented the mean collagen fiber orientation of each ECM-SIS specimen. The mean angle as well as the associated angular dispersion (represented by the circular standard deviation of the angles) of each experimental group before and after experimentation were compared statistically to evaluate the effect of seeding and/or stretch.

It should be noted that the collagen fiber orientations obtained fall into the category of circular data, for which conventional methods of calculating arithmetic mean and performing inferential analysis do not apply. Thus, statistical methods for circular data were employed in the present study. Specifically, a second-order analysis for circular data was conducted for the mean angle of collagen fiber orientation, as the mean angle of each group was the mean of the mean angle of each specimen. [14] In addition, a

Watson-Williams test was performed on the angular dispersion. The significance level was set at 0.05.

Another parameter called the orientation index (OI) reflecting the fiber organization was also calculated. The OI represents the angle containing 50% of the fibers at one scan point. Thus, a highly organized collagen fiber network at the point of laser beam intersection will have a lower OI while randomly oriented fibers will have larger values. The OI distribution was portrayed on a schematic graph with a color scale ranging from purple (low OI, high fiber organization) to blue (high OI, low fiber organization).

To evaluate cell morphology and orientation, and to determine the presence of newly produced collagen, scaffolds from Group I and Group II were processed for confocal fluorescent microscopy (n=3/group) and TEM (n=2/group) after 5 day's experimentation, respectively. For confocal fluorescent microscopy, the ECM-SIS were fixed in 4% paraformaldehyde and cell membranes were permeabilized with 0.1% Triton X-100 for 10 minutes. The specimens were then incubated with Rhodamine phalloidin (Molecular Probes, Eugene, OR, USA) for 1h and then with Sytox Green (Molecular Probes, Eugene, OR, USA) for 15 min at room temperature to stain actin filaments and the nuclei, respectively. The specimens were then viewed under a Bioptechs Confocal System featuring an Olympus IX70 inverted microscope. Images from at least 4 randomly chosen regions in each specimen were captured and recorded in LaserSharp software via a Radiance liquid light acquisition system.

For TEM, the ECM-SIS were fixed for at least 1 h in Karnovsky's fixative. The specimens were washed with 3 changes of 0.1M sodium cacodylate buffer pH 7.4 and post-fixed for 1h in a solution containing 1% OsO4 buffered with 0.1M sodium cacodylate (pH 7.4). After washed in 3 changes of dH2O and dehydrated in EtOH (50%, 70%, 80%, 90%, and 3 changes of 100%), the specimens was infiltrated overnight in a 1:2 mixture of Epon-Araldite embedding resin (Electron Microscopy Sciences, Fort Washington, PA) and propylene oxide (PO) for 24 h, followed by a 1:1 mixture of resin and PO for 24h, and finally a 2:1 mixture of resin and PO overnight. The following day the 2:1 mixture was removed and replaced with 100% Epon-Araldite. The specimens were infiltrated for an additional 8h, placed in flat embedding molds, and polymerized for 48 h at 60°C. The embedded specimens were thin sectioned (0.1μm) using a Reichert-Jung Ultracut E (Leica Microsystems AG, Wetzlar, Germany) and a DDK diamond knife (Delaware Diamond Knives, Wilmington, DE). Thin sections were stained with 1% uranyl acetate and Reynolds lead citrate and viewed on a Hitachi H-7100 TEM (Hitachi High Technologies America, Pleasanton, CA) operating at 50 kV. Digital images were obtained from at least 4 randomly chosen regions by using an AMT Advantage 10 CCD Camera System (Advanced Microscopy Techniques, Danvers, MA) and NIH Image software at both 20,000 x and 70,000 x magnification.

RESULTS

Grossly, there were no tears or failures of the scaffolds during or following the cyclic stretching. The quantitative data from SALS showed that the initial fiber orientation of all ECM-SIS scaffolds in the three groups was not significantly different (Table 1, $p>0.05$), in which Group I had a mean angle of 25.3° with an angular dispersion of 37.4°; Group II had a mean angle of 26.1° with an angular dispersion of 30.1°; and Group III had a mean angle of 8.9° with an angular dispersion of 12.8°. The average mean angle of all the scaffolds in the three groups before experiments, which represented the inherent collagen fiber orientation of the ECM-SIS, was 25.2 ± 13.5°. After 5 days of stretch, the fiber orientation of the scaffolds in Group I was significantly improved when compared to those in the other two groups. The mean angle of the fibers was decreased from initial 25.3° to 7.4° after stretch ($p<0.05$), which indicated that in Group I the orientation of fibers of the scaffolds had become closer to the stretching direction. In addition, the angular dispersion decreased from the initial 37.4° to 18.5° ($p<0.05$), indicating that the variance of the angles had become smaller (Table 1).

In contrast, for the scaffolds in Group II, the mean angle of the fiber orientation and the angular dispersion did not shown significant improvement after experiments (mean angle: 20.5° vs. 26.1°, $p>0.05$; angular dispersion: 24.8° vs. 30.1°, $p>0.05$). Similarly, the two parameters of fiber orientation for the scaffolds in Group III did not show significant changes after experiments as well (mean angle: 10.2° vs. 8.9°, $p>0.05$; angular dispersion: 10.2° vs. 12.8°, $p>0.05$).

The fiber organization as reflected by the orientation index (OI) was also improved for the scaffolds in Group I when compared to those in the other two groups (Figure 2). From the scanning images, it could be observed that the collagen fibers of the scaffolds in Group I were more organized as indicated by the large area of the red to purple coloration (low OI), as compared to the images before experiments, which showed yellow to blue coloration (high OI) (Figure 2A).

Comparatively, the scaffolds in Group II and III did not show the predominant change after stretching or seeding (Figure 2B, 2C). For these two groups, colors on the schematic scanning images from before and after the experimentation did not show

Table 1. The effects of cell seeding and cyclic stretching on the orientation of collagen fibers in the ECM bioscaffold as quantified by SALS. (* indicate significant difference before and after stretching).

Groups	Mean angle		Angular dispersion	
	Before	After	Before	After
I (Seeded & Cyclically Stretched)	25.3°	7.1° *	37.4°	18.5° *
II (Seeded & non-stretched)	26.1°	20.5°	30.1°	24.8°
III (Non-seeded & Cyclically Stretched)	8.9°	10.2°	12.8°	10.2°

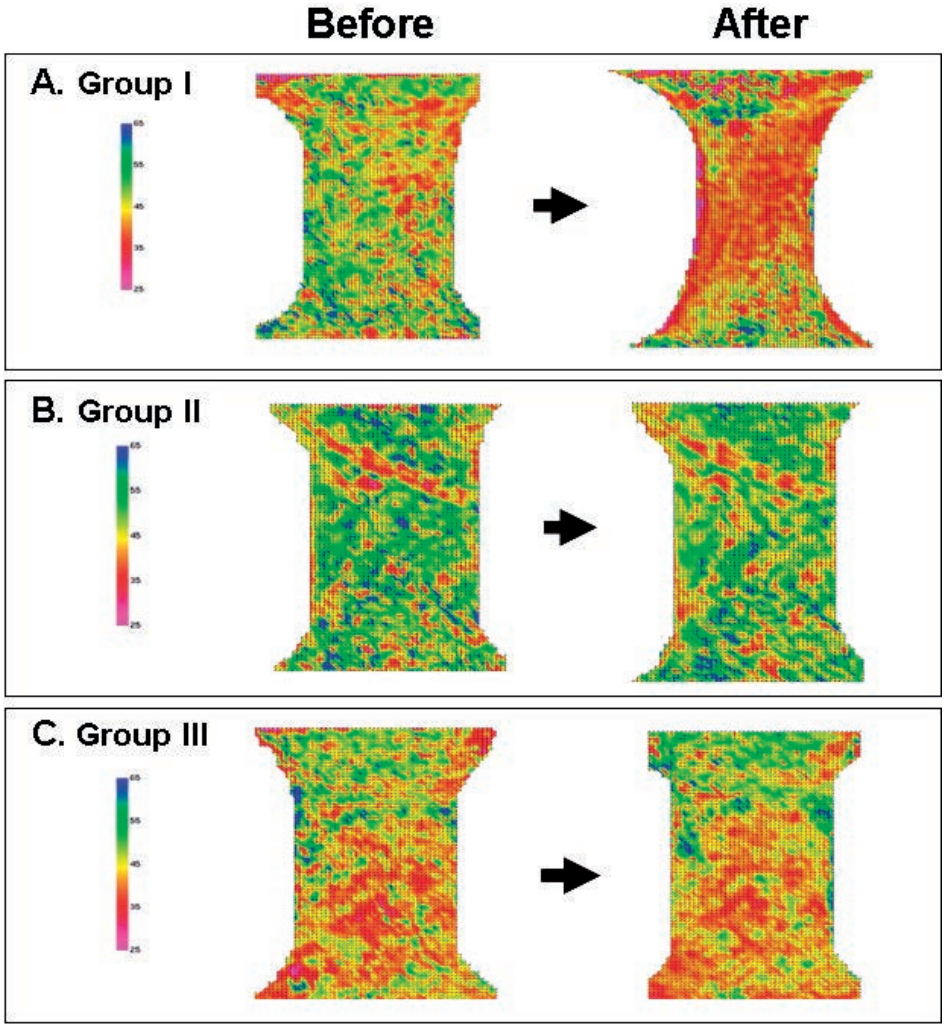

Figure 2. Schematic scanning images of SALS for ECM-SIS before and after cell-seeding and / or cyclic stretching. Representative samples shown. (A). Group I; (B). Group II; (C). Group III.

much change, indicating that the organization of the fibers at individual points were not improved (Figure 2B, 2C).

With the confocal fluorescent microscopy, the cell morphology and orientation could be observed in the two cell-seeded groups (Figure 3).

The fibroblasts in Group I became aligned along the stretching direction after cyclic stretch while those in Group II without stretch remained unoriented. As shown in Figure 3, both the green-colored nuclei and the red-colored intracellular actin filaments were more aligned along the stretching direction in Group I. Comparatively, the major-

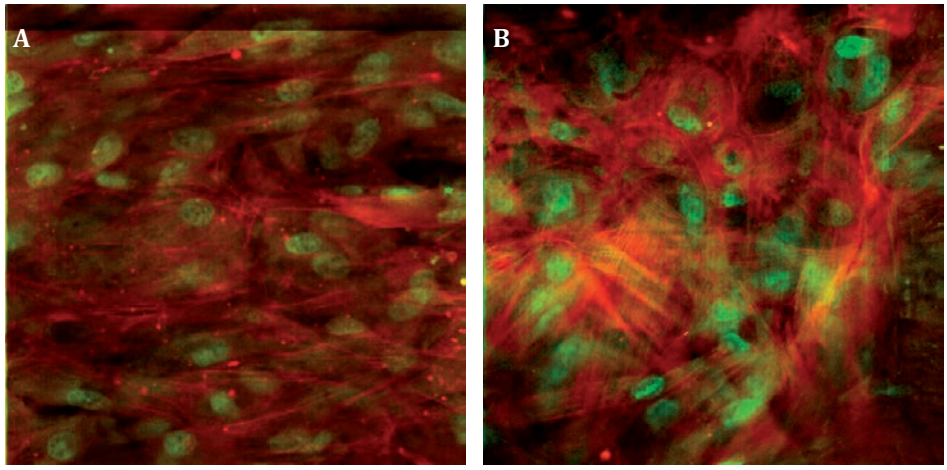

Figure 3. Fluorescent staining of the cells seeded on the SIS observed under confocal microscope. (A). Group I; Arrow indicates the stretching direction. (B). Group II. Actin fibers were stained in red and nuclei were stained in green.

ity of the nuclei and actin filament in Group II did not have any noticeable preferred orientation.

In addition, TEM revealed that in both cell-seeded groups (Group I and II), some fibroblasts had migrated into the scaffolds (Figure 4A), and those that remained on the surface of the SIS appeared flat and stacked, forming cell layers, as shown in Figure 4B and 4C. Newly produced collagen fibrils that appeared as collagen fibrils with much smaller diameter than those of the scaffold could also be observed between the fibroblasts (Figure 4B and 4C).

DISCUSSION

This study showed that a combination of fibroblast-seeding and cyclic uniaxial stretching could effectively improve the collagen fiber alignment in the ECM-SIS bioscaffold towards the axis of the applied stretch, while mechanical stretching or cell-seeding alone was not sufficient to affect the ultrastructure of the scaffold. These findings support our hypothesis and suggest that the dynamic cell-matrix interaction under mechanical stimuli was necessary to stimulate the cells to remodel the matrix fibers to align along the stretching direction.[15]

Our data emphasized the importance of the synergistic actions of cells and mechanical stimuli in the process of matrix remodeling. Studies have shown that cells have the responses to avoid axial surface strain.[5, 16-18] When cells were embedded in fibrous substrate, the cells tended to align along the fibers in the stretching direction (stress shielding) and remodel the matrix rapidly by up-regulating MMPs.[15, 19-21] Our results are in congruency with those in these studies as we observed that the fibro-

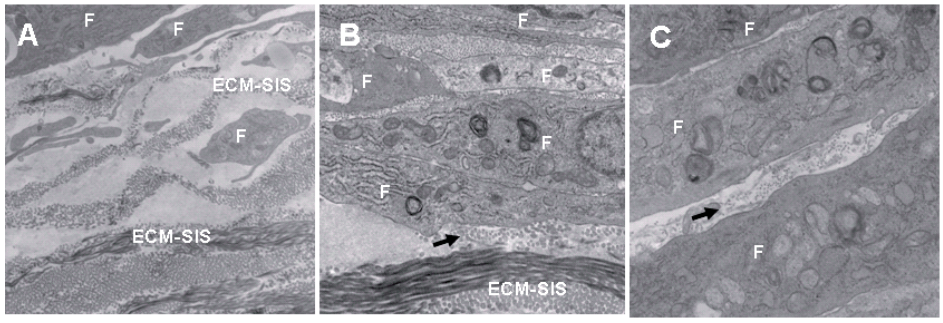

Figure 4. Transmission electron microscopy of SIS after cell-seeding. (A). Fibroblasts migrated into the scaffold. Magnification at 10,000. (B) Newly produced collagen in Group I as indicated by the arrow. Note the cells were stacked on the scaffold. (C). Newly produced collagen in Group II as indicated by the arrow. Note the cells were stacked. Magnification at 70,000 for B and C. F indicates fibroblast.

blasts seeded on the ECM-SIS bioscaffolds became aligned in the direction they were stretched. Moreover, it was documented that cell orientation determined the alignment of the cell-produced collagenous fibers.[22, 23] Therefore, a possible mechanism for our findings is that under mechanical stimuli, the seeded fibroblasts tended to align in the stretching direction, broke down the collagen fibers that were not in the same orientation in the scaffold and simultaneously produced new fibers that aligned to the stretching direction, by which the fibers in the scaffold became more aligned and more organized. The possible alterations of the levels of MMPs, which are considered as an indication for the matrix remodeling, will be investigated in our subsequent studies.

In the study, the collagen fiber orientation in the ECM-SIS scaffolds prior to experimentation was found to be 25.2 ± 13.5 ^{o} as measured by SALS, which is similar to the published results from previous studies.[10] With cell-seeding and cyclic stretch, the orientation and organization of the collagen fibers in the scaffold were significantly improved, as confirmed by both quantitative and morphological fiber orientation results. This improvement in the fiber architecture in the ECM-SIS bioscaffold has an important implication in its application in repairing injured ligaments and tendons in that the remodeled bioscaffold possesses further topographic advantages in addition to its unique biological properties, which would increase its existing repairing capability through the effects of "contact guidance".

The phenomenon of "contact guidance" has been documented in previous studies using various substrates such as microgrooved substrates, orientated collagen fibrils and fibronectin fibers.[21, 24, 25] It was found that cellular behavior such as movement and arrangement can be affected by the topographical morphology of their substratum. Furthermore, it was also shown that fibroblasts that were aligned through contact guidance were also producing aligned collagen.[22, 23] These findings support our

study to create a bioactive and aligned scaffold to meet the special needs in repairing injured ligaments and tendons, which have a unique structure of parallel-aligned collagen fibers to sustain load in normal status. The remodeled ECM-SIS bioscaffold could provide a better contact guidance for the healing cells in the injured ligaments and tendons, thus improve the alignment of the healing cells and consequently the alignment of the newly formed collagen fibers. Finally biomechanical properties of the healing ligaments and tendons could be improved better.

A limitation of this study is that only one frequency and magnitude of the cyclic stretching and stretching duration were chosen to remodel the scaffold. Thus, it is necessary to expand this treatment regimen in order to get more optimal values. Nevertheless, the chosen regimen was able to successfully remodel an ECM-scaffold following cell-seeding and cyclic stretching.

This study provides the basis for in-vitro modification of SIS scaffold for the enhancement of its application in-vivo to improve the healing of ligaments and tendons. Furthermore, the use of SALS provides a novel method to detect changes or improvements in the ultrastructure of ECM-bioscaffolds. In the future, the stretching regimen will be optimized and the in-vivo effects of the remodeled SIS scaffold will be tested.

ACKNOWLEDGEMENTS

The authors wish to express their gratitude to the technical assistance of Kira Lathrop, David Merryman, Dr. Tom Gilbert and Cook Biotech for supplying the ECM-SIS, and the financial support of NIH #AR39683 and the Dutch Anna Fund is gratefully acknowledged.

REFERENCES

1. Frank, C., Woo, S.L., Amiel, D., Harwood, F., Gomez, M., and Akeson, W. Medial collateral ligament healing. A multidisciplinary assessment in rabbits. Am J Sports Med. 11, 379-389, 1983.
2. Woo, S.L., Gomez, M.A., Sites, T.J., Newton, P.O., Orlando, C.A., and Akeson, W.H. The biomechanical and morphological changes in the medial collateral ligament of the rabbit after immobilization and remobilization. J Bone Joint Surg Am. 69, 1200-1211, 1987.
3. Liang, R., Woo, S.L., Takakura, Y., Moon, D.K., Jia, F., and Abramowitch, S.D. Long-term effects of porcine small intestine submucosa on the healing of medial collateral ligament: a functional tissue engineering study. J Orthop Res. 24, 811-819, 2006.
4. Niyibizi, C., Kavalkovich, K., Yamaji, T., and Woo, S.L. Type V collagen is increased during rabbit medial collateral ligament healing. Knee Surg Sports Traumatol Arthrosc. 8, 281-285, 2000.
5. Wang, J.H., and Grood, E.S. The strain magnitude and contact guidance determine orientation response of fibroblasts to cyclic substrate strains. Connect Tissue Res. 41, 29-36, 2000.
6. Musahl, V., Abramowitch, S.D., Gilbert, T.W., Tsuda, E., Wang, J.H., Badylak, S.F., and Woo, S.L. The use of porcine small intestinal submucosa to enhance the healing of the medial collateral ligament--a functional tissue engineering study in rabbits. J Orthop Res. 22, 214-220, 2004.
7. Woo, S.L.-Y., Takakura, Y., Liang, R., Jia, F., and Moon, D.K. Treatment with bioscaffold enhances the the fibril morphology and the collagen composition of healing medial collateral ligament in rabbits. Tissue Eng. 12, 159-166, 2006.
8. Hodde, J.P., Record, R.D., Liang, H.A., and Badylak, S.F. Vascular endothelial growth factor in porcine-derived extracellular matrix. Endothelium. 8, 11-24, 2001.
9. Voytik-Harbin, S.L., Brightman, A.O., Kraine, M.R., Waisner, B., and Badylak, S.F. Identification of extractable growth factors from small intestinal submucosa. J Cell Biochem. 67, 478-491, 1997.
10. Sacks, M.S., and Gloeckner, D.C. Quantification of the fiber architecture and biaxial mechanical behavior of porcine intestinal submucosa. J Biomed Mater Res. 46, 1-10, 1999.
11. Ross, S.M., Joshi, R., and Frank, C.B. Establishment and comparison of fibroblast cell lines from the medial collateral and anterior cruciate ligaments of the rabbit. In Vitro Cell Dev Biol. 26, 579-584, 1990.
12. Gilbert, T.W., Stewart-Akers, A.M., Sydeski, J., Nguyen, T.D., Badylak, S.F., and Woo, S.L. Gene expression by fibroblasts seeded on small intestinal submucosa and subjected to cyclic stretching. Tissue Eng. 13, 1313-1323, 2007.
13. Sacks, M.S., Smith, D.B., and Hiester, E.D. A small angle light scattering device for planar connective tissue microstructural analysis. Ann Biomed Eng. 25, 678-689, 1997.
14. Zar, J.H.: Biostatistical Analysis, 4th ed: Prentice Hall, 1998
15. Prajapati, R.T., Chavally-Mis, B., Herbage, D., Eastwood, M., and Brown, R.A. Mechanical loading regulates protease production by fibroblasts in three-dimensional collagen substrates. Wound Repair Regen. 8, 226-237, 2000.
16. Neidlinger-Wilke, C., Grood, E., Claes, L., and Brand, R. Fibroblast orientation to stretch begins within three hours. J Orthop Res. 20, 953-956, 2002.
17. Buckley, M.J., Banes, A.J., Levin, L.G., Sumpio, B.E., Sato, M., Jordan, R., Gilbert, J., Link, G.W., and Tran Son Tay, R. Osteoblasts increase their rate of division and align in response to cyclic, mechanical tension in vitro. Bone Miner. 4, 225-236, 1988.
18. Dartsch, P.C., and Hammerle, H. Orientation response of arterial smooth muscle cells to mechanical stimulation. Eur J Cell Biol. 41, 339-346, 1986.

19. Huang, D., Chang, T.R., Aggarwal, A., Lee, R.C., and Ehrlich, H.P. Mechanisms and dynamics of mechanical strengthening in ligament-equivalent fibroblast-populated collagen matrices. Ann Biomed Eng. 21, 289-305, 1993.
20. Eastwood, M., Mudera, V.C., McGrouther, D.A., and Brown, R.A. Effect of precise mechanical loading on fibroblast populated collagen lattices: morphological changes. Cell Motil Cytoskeleton. 40, 13-21, 1998.
21. Mudera, V.C., Pleass, R., Eastwood, M., Tarnuzzer, R., Schultz, G., Khaw, P., McGrouther, D.A., and Brown, R.A. Molecular responses of human dermal fibroblasts to dual cues: contact guidance and mechanical load. Cell Motil Cytoskeleton. 45, 1-9, 2000.
22. Wang, J.H., Jia, F., Gilbert, T.W., and Woo, S.L. Cell orientation determines the alignment of cell-produced collagenous matrix. J Biomech. 36, 97-102, 2003.
23. den Braber, E.T., de Ruijter, J.E., Ginsel, L.A., von Recum, A.F., and Jansen, J.A. Orientation of ECM protein deposition, fibroblast cytoskeleton, and attachment complex components on silicone microgrooved surfaces. J Biomed Mater Res. 40, 291-300, 1998.
24. Ejim, O.S., Blunn, G.W., and Brown, R.A. Production of artificial-orientated mats and strands from plasma fibronectin: a morphological study. Biomaterials. 14, 743-748, 1993.
25. Guido, S., and Tranquillo, R.T. A methodology for the systematic and quantitative study of cell contact guidance in oriented collagen gels. Correlation of fibroblast orientation and gel birefringence. J Cell Sci. 105 (Pt 2), 317-331, 1993.

Chapter 7

Intrinsic Healing Response of the Human Anterior Cruciate Ligament: an Histological Study of Reattached ACL Remnants

D. Tan Nguyen, Tamara H. Ramwadhdoebe, Cor van der Hart, Leendert Blankevoort, Paul-Peter Tak, C. Niek van Dijk

Journal of Orthopaedic Research, 2014 Feb;32(2):296-301

ABSTRACT

A reattachment of the tibial remnant of the torn anterior cruciate ligament (ACL) to the posterior cruciate ligament is sometimes observed during surgery and apparently implies that the human ACL does have a healing response. The aim of this study was to investigate whether this reattachment tissue has similar histological characteristics of a healing response as the medial collateral ligament (MCL), which can heal spontaneously. Standard histology and immunostaining of α-smooth muscle actin and collagen type 3 was performed.

The results shows that the reattached tissue has typical characteristics of a healing response: the reattached ACL remnant could not be released by forceful traction; microscopy showed that the collagen fibers of the reattached tissue were disorganized with no preferred direction; increased neovascularization; the presence of lipid vacuoles; the mean number of cells within the biopsy tissue was 631 ± 269 cells per mm^2; and 68% ± 20 was expressing α-SMA; semi-quantitative analysis of collagen type 3 expression showed that collagen type 3 had an high expression with an average score of 3.

In conclusion, this study shows that the human proximal 1/3 ACL has an intrinsic healing response with typical histological characteristics similar to the MCL.

INTRODUCTION

The anterior cruciate ligament (ACL) is a collagenous tissue within the knee joint that spans from the tibia to the femur. The ACL prevents excessive anterior translation and internal rotation of the tibia with respect to the femur. (*1*) A complete tear of the ACL may lead to knee joint instability and early osteoarthrosis. (*2*) The current surgical treatment in persistent instable knees is a reconstruction of the ruptured ACL with autologous hamstring or patellar tendon grafts. The results are generally good, though there remains room for further optimization. (*3-5*) In the early days, surgeons tried to heal the ruptured ACL by suturing the ends together with multiple U-loops. The results, however were unpredictable and the long-term results were not satisfactory. (*6-8*) The poor results of multiple U-loops suture repair have been attributed to the poor healing potential of the ACL and the harsh intra-articular environment. (*9, 10*) This in time, and despite the few reports documenting spontaneous healing of the ruptured ACL (*11, 12*), has led to the common opinion that the ACL does not have a healing potential. However, recently, three research groups including ours have demonstrated in an animal model that the transected ACL can heal by bio-enhanced suture repair. (*13-15*) The following question was whether the human ACL has healing potential. During ACL reconstruction surgeries, it was interesting to observe that the tibial remnant of the ruptured ACL was sometimes attached to the surrounding tissues, for example to the posterior cruciate ligament (PCL) or the intercondylar notch. This reattachment phenomenon apparently implies that the ACL does have a healing potential even without any suturing. This phenomenon was previously described. (*16-18*) Lo et al. conducted a prospective observational study and reported that reattachments of the torn ACL occurred in 74 of the 101 patients. (*16*) New attachments of the ACL to the PCL were found in 67 of the patients. They concluded that some kind of healing processes occurs in many torn ACLs. The current research question was whether there are other typical characteristics of the healing potential besides the physical attachment.

Unlike the ACL, extra-articular ligaments such as the medial collateral ligament (MCL) heal spontaneously and from previous MCL studies, it is known that the healing response in the MCL proceeds through three overlapping dynamic phases. The inflammatory phase is triggered by tissue and capillary damage, which leads to the formation of a blood clot and functions as a provisional matrix. The inflammatory phase is followed by a proliferative phase, in which active angiogenesis creates new capillaries and fibroblasts differentiate into myofibroblasts. The healing phase — healing (or scar) tissue formation — involves gradual remodeling of the granulation tissue, voids and a decrease of myofibroblasts. Collagen type 3, the main component of granulation tissue, is gradually replaced by collagen type 1. The remodeling phase in which these matrix elements are rearranged or removed can take months to years. (*19-21*) Sum-

marizing, the typical histological characteristics of this ligament healing response are: disorganized collagen fiber orientation, increased neovascularization, voids (e.g. lipid vacuoles), increased number of myofibroblasts and elevated content of collagen type 3. The hypothesis is that these typical histological characteristics are also present in the reattached ACL tissue. In order to test our hypothesis, reattached ACL tissue was collected and investigated by standard histology and immunohistochemistry to assess the collagen fiber orientation, the extracellular matrix, presence of capillaries, voids, the number of myofibroblasts and the presence of collagen type 3. The purpose of the present study was to further characterize the end stage of this process.

METHODS

All patients who were scheduled for an ACL reconstruction were included in this study. None of the patients wore a brace after the initial trauma nor prior to surgery. For histology purpose, the inclusion was ended when 5 patients with reattachments of the tibial remnants to the PCL were identified and the tissue collected. Approval from the Institutional Review Board was waived since the ACL tissue would normally be removed as 'waste' material. Informed consent for the use of the anonymized material was obtained from each patient. During the arthroscopy, the gross morphology of the ACL was described. The length of the tibial remnant was estimated from the recorded arthroscopic videos by using the tip of the probe as a reference. Reattachment was defined by a visibly reattached tibial remnant to the PCL either anteriorly, posteriorly, or both and the sustainment of the reattachment after a forceful pull with the hooked probe. The interface between the ACL remnant and PCL was identified by scissor punching and shaving the debris tissue around the attachment. During the dissection the ACL was regularly hooked and pulled to identify the interface. Once identified one biopsy of each interface was collected by carefully scissor punching within the ACL and between the interface and PCL. The biopsy measuring approximately 7 mm x 5 mm x 5 mm was embedded in TissueTek, directly frozen, and stored in -80˚C until further processing.

Histology

Five-micrometer thick sections were cut in a cryostat microtome and mounted on glass slides (Star Frost adhesive slides, Knittelgläser, Germany), and stored at -80˚C until staining was performed. Standard Haematoxylin & Eosin was performed to grossly evaluate cell morphology and the extracellular matrix. Lendrum Masson's trichrome stainings were performed to evaluate cell morphology, extracellular matrix and collagen fiber orientation. In brief, the sections were stained sequentially in celestine blue, haematoxylin, ponceau de xylidine and tartrazine. The collagen was stained in

yellow, the cytoplasm in red and the nuclei in blue. The slides were observed under a light microscope (Leica) and pictures were taken at 200X and 400X magnification.

Immunohistochemical staining

An AEC (3-Amino-9-ethylcarbazole) labeling immunohistochemical methodology was used with the following antibodies: monoclonal mouse anti-human alpha-smooth muscle actin (α-SMA) antibody (Sigma-Aldrich, St. Louis, MO) as a marker for myofibroblasts and monoclonal mouse anti-human collagen type 3 antibody (Abcam, Cambridge, UK) to identify collagen type 3. Briefly, the sections were fixed in 100% acetone for 10 min at room temperature and washed with PBS, three times for 5 minutes. Endogenous peroxidase activity was blocked using peroxidase 3% for 30 minutes at room temperature. The sections were rinsed once in PBS and 10% normal goat serum, 1% BSA in PBS was applied for 1 hour at room temperature as a blocking agent. The monoclonal α-SMA antibody in 5% normal goat serum, 1% BSA in PBS (5 μg/ml) was applied and incubated overnight at 4°C on a shaker. Collagen type 3 was stained with monoclonal mouse collagen type 3 antibody in 5% normal goat serum, 1% BSA in PBS (0.5 μg/ml). Subsequently the sections were washed in PBS three times for 5 minutes each. The secondary antibody, a rabbit anti-mouse immunoglobulin (IgG) horseradish conjugate (Abcam, Cambridge, UK), was applied to the sections 1 μg/ml for 60 minutes at room temperature. After a final rinse with PBS, HRP activity was visualized as a brown-red color by incubation with AEC (Sigma-Aldrich). Sections were counterstained with Mayer's haematoxylin and mounted in Kaiser's glycerol gelatin (Merck). Appropriate isotype controls were assessed in all experimental series. Positive controls for α-SMA and collagen type 3 were human artery and human skin, respectively.

Digital Image Analysis

Quantification of α-SMA expressing cells in the reattached tissue was performed with digital image analysis (DIA), as previously described. (*22*) In brief, for each acquisition session the microscope, camera, and computer were calibrated according to a standardized procedure, settings were recorded and stored and used for the entire session. After immunohistochemical staining, three representative regions of 1.45 x 1.45 mm in each section were identified at low power (without capillaries, fat voids and artifacts) and separated in 18 consecutive high power fields (HPF). The18 HPF images were analyzed by computer-assisted image analysis using a Syndia algorithm on a Qwin-based analysis system (Leica, Cambridge, UK). The software identified positive cells by combining two masks where areas of a nucleus surrounded by a red-brown staining were identified as positive cells, and isolated blue (nuclei without staining) or red were ignored. Positive staining of α-smooth muscle actin was expressed as

number of positive cells/mm^2. Two sections per sample stained for collagen type 3 (n=10) were semi-quantitatively analyzed by DTN and MdB with a standard binocular light microscope (Olympus) at 200x magnification. The expression of collagen type 3 was scored on a 5-point scale (range 0–4), as previously described. (*23*) A score of 0 represented no expression, while a score of 4 represented abundant expression of collagen type 3 within the reattached tissue. Differences between observers were resolved by consensus.

RESULTS

The patients' characteristics, injury mechanism, grade of instability, time to surgery and MRI results are listed in table 1. Preoperative MRI's were made in two patients and were made at 6 and 10 weeks post-injury respectively. The MRI's show that the ACL reattachment to the PCL is already present at these time points (Figure 1A and 1B).

Table 1. Patient characteristics and MRI results

Patient	Age	Sex	Activity & Injury mechanism	Grade of instability	Time to surgery	MRI
# 1	17	F	Korfball / rotation trauma	Lachman 2+, pivot shift 2+	30 weeks	10 wks post-injury: complete proximal 1/3 tear with reattachment to PCL
# 2	30	M	Soccer / rotation trauma	Lachman 2+, pivot shift 2+	45 weeks	Not made
# 3	40	F	Kickboxing / valgus rotation trauma	Lachman 3+, pivot shift 2+	105 weeks	Not made
# 4	27	M	Soccer / rotation trauma	Lachman 2+, pivot shift 2+	17 weeks	Not made
# 5	41	M	Field hockey / rotation trauma	Lachman 2+, pivot shift 2+	64 weeks	6 wks post-injury: complete proximal 1/3 tear with reattachment to PCL

Gross appearances

In 5 of the 9 consecutive ACL reconstructions, reattachments of the tibial remnant of the ruptured ACL to the PCL could be observed (figure 2). The reattached ACL remnant was long and the median length was approximately 3,5 cm (range: 3-3,5 cm). The reattachment could not be released by forceful pulling on the tibial ACL remnant with a hooked probe.

It was interesting to observe that in all reattached remnants the proximal part attaching to the PCL was covered by fatty tissue (figure 2). In two patients, ferritin deposition within the capsule was noted indicating a previous haemarthros. In the 4 patients without a reattachment, the tibial ACL remnant was relatively short.

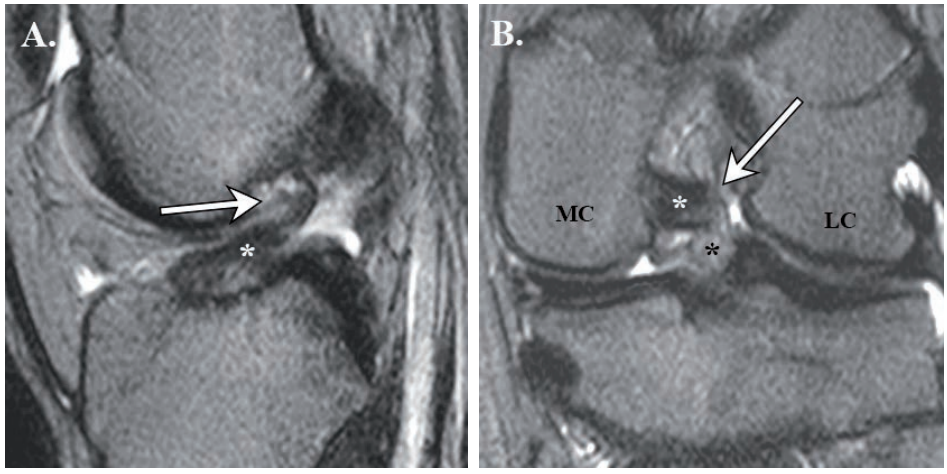

Figure 1. MRI of reattached ACL. (A) Sagital plane of knee joint. Tibial ACL remnant indicated by white asterisk (femoral PCL not visible on this slice). ACL reattachment indicated by arrow. (B) Coronal plane of the same knee. Tibial ACL remnant indicated by black asterisk and PCL indicated by white asterisk. MC is medial condyle and LC is lateral condyle. ACL reattachment indicated by arrow.

Histology

Microscopy showed that the collagen fibers in all 5 reattached tissue biopsies were disorganized with no preferred orientation (figure 3). Every tissue biopsy showed areas of neovascularization and lipid vacuoles (figure 3). The cell nuclei tended to be more round with inhomogeneous staining of the haematoxylin, suggesting that the cells were metabolically more active. In addition, nucleoli could be observed in several nuclei. (figure 4 and 5B). The mean number of cells in the tissue biopsies was 631 (± 269 s.d.) cells per mm^2; and 68% (± 20% s.d.) was expressing α-smooth muscle actin (Table 2).

Semi-quantitative analysis of collagen type 3 expression within the reattached tissue showed that collagen type 3 had an high expression (figure 6) with an average score of 3 (range 1-4).

DISCUSSION

This study addressed the question whether the human ACL has a healing potential as demonstrated indirectly by investigating spontaneously reattached tibial ACL remnants. The results confirm and extend the conclusion of Lo et al. (*16*) , that the human ACL indeed has a healing potential. Our results not only demonstrate the healing potential based on gross morphological characteristics but additionally show the typical histological characteristics that are seen in the healing process in the MCL. The reattached ACL tissues have (1) a firm attachment to the PCL, (2) disorganized colla-

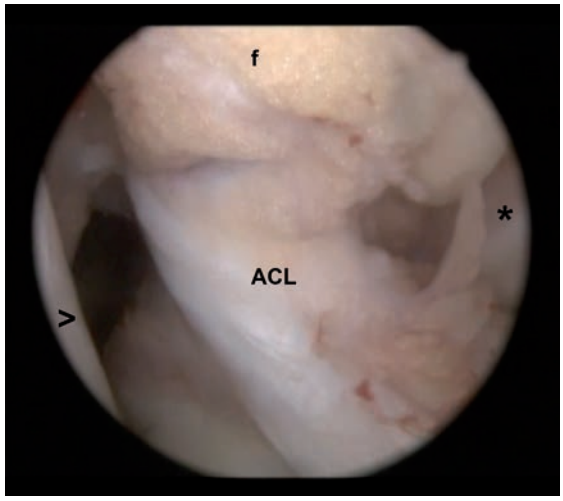

Figure 2. Arthroscopic view of the tibial ACL remnant reattached to the PCL. The triangle indicates the area on the medial wall of the lateral condyle where normally the ACL inserts on the femur. The asterisk indicates the medial condyle. Note the proximal fatty tissue (f) covering the reattachment.

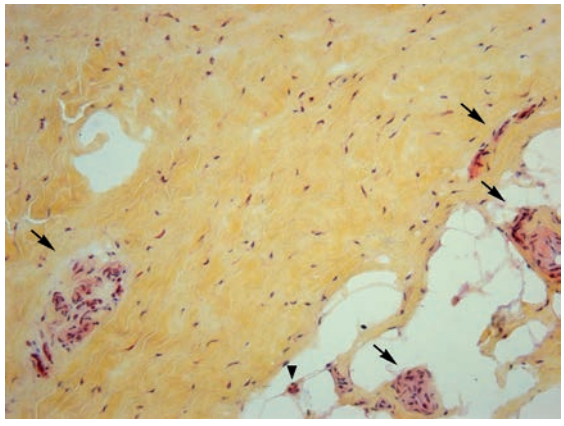

Fig. 3. Example of Lendrum Masson Trichrome staining. The collagen fibers (stained in yellow) are disorganized. Arrows indicate capillaries. The arrowhead indicates an adipocyte. Also note the presence of fat vacuoles, right bottom side. (x200)

Table 2. Total cell count and myofibroblast cell count in the samples of reattached ACL tissue

	Reattached ACL tissue (n=5)
Number of cells per mm^2 Mean ± SD	631 ± 269
Number of myofibroblast per mm^2 Mean ± SD	473 ± 313
Percent myofibroblast of total cell count (%) Mean ± SD	68 ± 20

gen fibers, (3) increased neovascularization, (4) fat voids, (5) abundance of myofibroblasts and (6) high content of collagen type 3. These characteristics are typical for a spontaneous healing process like in the MCL. (*19-21, 24*) It can thus be concluded that the human ACL has an intrinsic healing response. Since only relatively long (±3,5 cm)

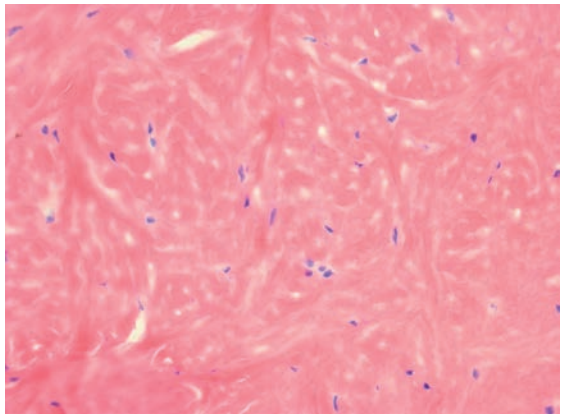

Fig. 4. Example of H&E staining shows the scattered cells within the disorganized extracellular matrix. (x400)

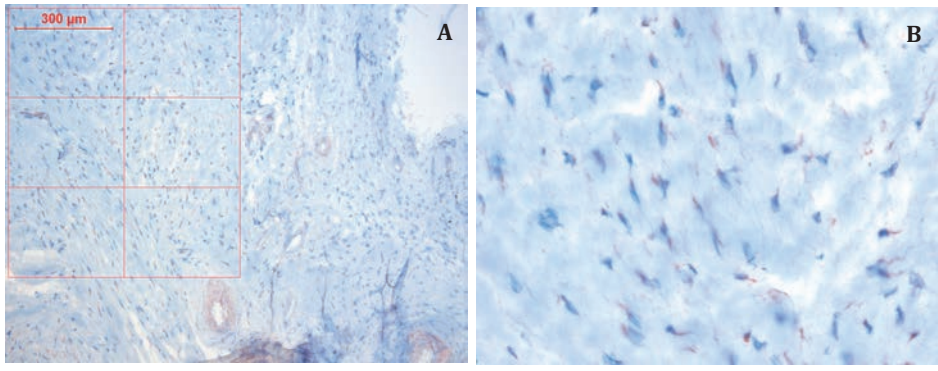

Fig. 5A. Example of a digital image analysis of α-smooth muscle actin expressing cells. (A) Low magnification and (B) high magnification of the reattached ACL tissue showing blue stained nuclei and integrated staining of blue stained nuclei and red-brown stained nuclei, identifying α-smooth muscle actin expressing cells. (x100)
Figure 5B. Note the inhomogeneous staining of the haematoxylin and the presence of nucleoli. (x400)

tibial remnants were reattached, contact between the ACL and its surrounding tissue may be a prerequisite for a healing response to occur. This study shows that fibroblasts within the reattached ACL tissue express a high level of α-SMA, which is a specific marker for myofibroblasts. It is known that myofibroblasts play an important role in normal wound repair by facilitating wound closure through transmitting contractile forces to the early granulation tissue. (*20, 25*) They modulate the behavior of other cells in the healing response by cell-cell interactions as well as via the secretion of cytokines, growth factors, chemokines, inflammatory mediators and matrix molecules and proteins that are important in growth, differentiation and wound repair, such as collagen types 1, 3, 4, 8, glycoproteins, proteoglycans and matrix modifying proteins. (*26*) Several studies have shown that cyclic stretching or mechanical tension during

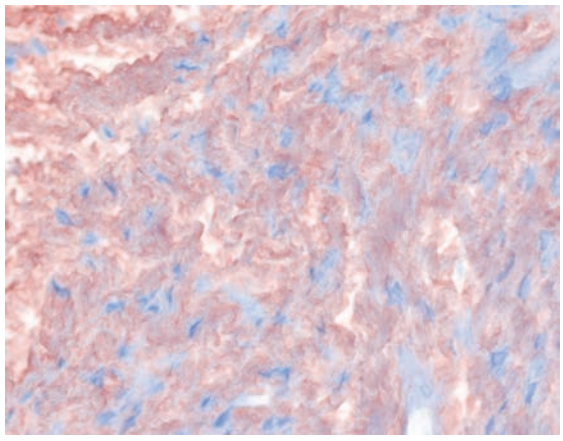

Fig. 6. Example of collagen type 3 staining. High magnification shows the identification of red-brown staining of collagen type 3. (x400)

healing upregulate α-smooth muscle actin within fibroblasts resulting in an increase of myofibroblasts. (*27*) The finding that 68% of fibroblasts are myofibroblasts suggests a relative high percentage compared to the MCL studies of Faryniarz et al., and Menetrey et al. in rabbits (*20, 21*). Faryniarz et al., found approximately 10% myofibroblasts in the healing rabbit MCL. Menetrey et al. performed a study to elucidate the difference between the healing response of the MCL and ACL and created a mop-end MCL injury and a partial ACL injury in rabbits. They reported up to 15.2% myofibroblasts within the healing MCL and less than 1.5% myofibroblasts in the partially injured ACL. The high number of myofibroblast might be explained by the fact that prior to harvesting the reattached ACL tissue is experiencing intermittent stretching at the reattachment site with the PCL during walking causing the increase of number of myofibroblasts. Also, the differences between these studies and ours are obviously the study model, i.e. (1) rabbit vs human, (2) MCL vs ACL but moreover (3) a partial ACL injury with no healing tissue vs. complete rupture with reattachment tissue.

Collagen type 3 was observed at high levels in the reattached ACL tissue. Several researchers have postulated that collagen type 3 is important for remodeling, growth and healing. (*1, 28*) Robins et al., showed that the early appearance of type 3 collagen after skin injury is associated with an early increase in collagen synthesis and postulated that collagen type 3 may function in providing initial wound structure and support for subsequent healing events. (*29*) It has been reported that collagen type 3 is essential for normal type 1 collagen fibrillogenesis. (*30*)

A limitation of our study is that a direct comparison with the contralateral normal ACL tissue was not feasible due to ethical concerns. Also with the given material it was not feasible to determine which factors were responsible for the torn ACL to heal to the PCL. It was interesting to note that within 6-10 weeks reattachments could be observed on the MRI. Biopsies including normal PCL tissue around this time could provide more clues. It appears that the length of the distal ACL remnant has to be

relatively long enough (± 3,5cm) to be attached to the PCL. This was the case in five of the nine consecutive ACL reconstructions. In the remaining four knees the tibial ACL remnant was either too short to attach to the PCL or had resorbed to a short remnant. The contact between the ACL and its surrounding tissue may facilitate the formation of a stable hematoma and a provisional scaffold allowing the first phase of healing to take place. While the tibial remnant had healed to the PCL, the knees remained clinically instable requiring a reconstruction. Crain et al., explained this instability by the fact that the PCL loosens with anterior translation thus the reattachment is effectively not limiting anterior translation. (*18*) Additionally they stated that for any biomechanical function the ACL fibers has to cross the joint and attach to the femur. The number of reattached tibial ACL remnants in our study was five out of nine cases. Crain et al., and Lo et al. observed 18 reattachments out of 48 cases and 67 reattachments out of 101 cases, respectively (*16, 18*) In contrast, Murray et al., and Wittstein et al. reported that in all cases that the tibial ACL remnant was resorbed and a reattachment of the ACL remnants was not present in any of the cases. (*9, 31*) This difference in the incidence of reattachments may be explained by the difference in injury mechanism between the patients, which could result in a difference in tibial ACL remnant length and in turn in the chance to reattach.

In conclusion, this study shows that the human proximal 1/3 ACL has an intrinsic healing response with typical characteristics similar to the MCL that can heal spontaneously. Combined with the recent findings of ACL healing in animal models there is sufficient support to warrant future translational studies to develop and evaluate the bio-enhanced suture repair of torn ACL in humans.

ACKNOWLEDGEMENTS

The authors are grateful for the technical assistance of Maarten de Boer with the immunohistochemistry experiments. The study was sponsored by Mozaïek PhD training grant 017.004.076 from the Netherlands Organization for Scientific Research (NWO) and the Marti-Keuning Eckhart foundation.

REFERENCES

1. S. L. Woo, S. D. Abramowitch, R. Kilger, R. Liang, Biomechanics of knee ligaments: injury, healing, and repair. *Journal of biomechanics* **39**, 1 (2006).
2. P. Kannus, M. Jarvinen, Conservatively treated tears of the anterior cruciate ligament. Long-term results. *The Journal of bone and joint surgery. American volume* **69**, 1007 (Sep, 1987).
3. J. O. Drogset *et al.*, Autologous patellar tendon and quadrupled hamstring grafts in anterior cruciate ligament reconstruction: a prospective randomized multicenter review of different fixation methods. *Knee surgery, sports traumatology, arthroscopy : official journal of the ESSKA* **18**, 1085 (Aug, 2010).
4. J. Kartus *et al.*, Complications following arthroscopic anterior cruciate ligament reconstruction. A 2-5-year follow-up of 604 patients with special emphasis on anterior knee pain. *Knee surgery, sports traumatology, arthroscopy : official journal of the ESSKA* **7**, 2 (1999).
5. S. Li *et al.*, A systematic review of randomized controlled clinical trials comparing hamstring autografts versus bone-patellar tendon-bone autografts for the reconstruction of the anterior cruciate ligament. *Archives of orthopaedic and trauma surgery* **132**, 1287 (Sep, 2012).
6. N. Kaplan, T. L. Wickiewicz, R. F. Warren, Primary surgical treatment of anterior cruciate ligament ruptures. A long-term follow-up study. *Am J Sports Med* **18**, 354 (Jul-Aug, 1990).
7. M. F. Sherman, L. Lieber, J. R. Bonamo, L. Podesta, I. Reiter, The long-term followup of primary anterior cruciate ligament repair. Defining a rationale for augmentation. *Am J Sports Med* **19**, 243 (May-Jun, 1991).
8. D. H. O'Donoghue *et al.*, Repair and reconstruction of the anterior cruciate ligament in dogs. Factors influencing long-term results. *The Journal of bone and joint surgery. American volume* **53**, 710 (Jun, 1971).
9. M. M. Murray, S. D. Martin, T. L. Martin, M. Spector, Histological changes in the human anterior cruciate ligament after rupture. *The Journal of bone and joint surgery. American volume* **82-A**, 1387 (Oct, 2000).
10. C. N. Nagineni, D. Amiel, M. H. Green, M. Berchuck, W. H. Akeson, Characterization of the intrinsic properties of the anterior cruciate and medial collateral ligament cells: an in vitro cell culture study. *J Orthop Res* **10**, 465 (Jul, 1992).
11. M. Costa-Paz, M. A. Ayerza, I. Tanoira, J. Astoul, D. L. Muscolo, Spontaneous healing in complete ACL ruptures: a clinical and MRI study. *Clinical orthopaedics and related research* **470**, 979 (Apr, 2012).
12. H. Ihara, M. Miwa, K. Deya, K. Torisu, MRI of anterior cruciate ligament healing. *Journal of computer assisted tomography* **20**, 317 (Mar-Apr, 1996).
13. M. B. Fisher *et al.*, Potential of healing a transected anterior cruciate ligament with genetically modified extracellular matrix bioscaffolds in a goat model. *Knee surgery, sports traumatology, arthroscopy : official journal of the ESSKA* **20**, 1357 (Jul, 2012).
14. M. M. Murray *et al.*, Collagen-platelet rich plasma hydrogel enhances primary repair of the porcine anterior cruciate ligament. *J Orthop Res* **25**, 81 (Jan, 2007).
15. D. T. Nguyen *et al.*, Healing of the Goat Anterior Cruciate Ligament After a New Suture Repair Technique and Bioscaffold Treatment. *Tissue engineering. Part A*, (Jul 10, 2013).
16. I. K. Lo, G. H. de Maat, J. W. Valk, C. B. Frank, The gross morphology of torn human anterior cruciate ligaments in unstable knees. *Arthroscopy : the journal of arthroscopic & related surgery : official publication of the Arthroscopy Association of North America and the International Arthroscopy Association* **15**, 301 (Apr, 1999).

17. T. N. Vahey, D. R. Broome, K. J. Kayes, K. D. Shelbourne, Acute and chronic tears of the anterior cruciate ligament: differential features at MR imaging. *Radiology* **181**, 251 (Oct, 1991).
18. E. H. Crain, D. C. Fithian, E. W. Paxton, W. F. Luetzow, Variation in anterior cruciate ligament scar pattern: does the scar pattern affect anterior laxity in anterior cruciate ligament-deficient knees? *Arthroscopy : the journal of arthroscopic & related surgery : official publication of the Arthroscopy Association of North America and the International Arthroscopy Association* **21**, 19 (Jan, 2005).
19. C. Frank *et al.*, Medial collateral ligament healing. A multidisciplinary assessment in rabbits. *Am J Sports Med* **11**, 379 (Nov-Dec, 1983).
20. D. A. Faryniarz, C. Chaponnier, G. Gabbiani, I. V. Yannas, M. Spector, Myofibroblasts in the healing lapine medial collateral ligament: possible mechanisms of contraction. *J Orthop Res* **14**, 228 (Mar, 1996).
21. J. Menetrey *et al.*, alpha-Smooth muscle actin and TGF-beta receptor I expression in the healing rabbit medial collateral and anterior cruciate ligaments. *Injury* **42**, 735 (Aug, 2011).
22. P. O. van der Hall, M. C. Kraan, P. P. Tak, Quantitative image analysis of synovial tissue. *Methods in molecular medicine* **135**, 121 (2007).
23. P. P. Tak *et al.*, Expression of adhesion molecules in early rheumatoid synovial tissue. *Clinical immunology and immunopathology* **77**, 236 (Dec, 1995).
24. D. Amiel, C. B. Frank, F. L. Harwood, W. H. Akeson, J. B. Kleiner, Collagen alteration in medial collateral ligament healing in a rabbit model. *Connective tissue research* **16**, 357 (1987).
25. G. Serini, G. Gabbiani, Mechanisms of myofibroblast activity and phenotypic modulation. *Experimental cell research* **250**, 273 (Aug 1, 1999).
26. D. W. Powell *et al.*, Myofibroblasts. I. Paracrine cells important in health and disease. *The American journal of physiology* **277**, C1 (Jul, 1999).
27. B. Hinz, D. Mastrangelo, C. E. Iselin, C. Chaponnier, G. Gabbiani, Mechanical tension controls granulation tissue contractile activity and myofibroblast differentiation. *The American journal of pathology* **159**, 1009 (Sep, 2001).
28. E. H. Epstein, Jr., (Alpha1(3))3 human skin collagen. Release by pepsin digestion and preponderance in fetal life. *The Journal of biological chemistry* **249**, 3225 (May 25, 1974).
29. S. P. Robins *et al.*, Increased skin collagen extractability and proportions of collagen type III are not normalized after 6 months healing of human excisional wounds. *The Journal of investigative dermatology* **121**, 267 (Aug, 2003).
30. X. Liu, H. Wu, M. Byrne, S. Krane, R. Jaenisch, Type III collagen is crucial for collagen I fibrillogenesis and for normal cardiovascular development. *Proceedings of the National Academy of Sciences of the United States of America* **94**, 1852 (Mar 4, 1997).
31. J. Wittstein, M. Kaseta, R. Sullivan, W. E. Garrett, Incidence of the remnant femoral attachment of the ruptured ACL. *Clinical orthopaedics and related research* **467**, 2691 (Oct, 2009).

Chapter 8

Healing of the Goat Anterior Cruciate Ligament after a New Suture Repair Technique and Bioscaffold Treatment

D. Tan Nguyen, Jurre Geel, Martin Schulze, Michael J. Raschke, Savio L-Y. Woo, C. Niek van Dijk, Leendert Blankevoort

Tissue Eng Part A. 2013 Oct;19(19-20)

ABSTRACT

Primary suture repair of the ACL has been used clinically in an attempt to heal the ruptured ACL. The results, however were not satisfactory which in retrospect can be attributed to the used suturing technique and the suboptimal healing conditions. These constraining conditions can be improved by introducing a new suturing technique and by using small intestine submucosa (SIS) as a bioscaffold. It is hypothesized that the suturing technique will keep the torn ends together and that SIS will enhance and promote the healing of the ACL.

The goat was used as the study model. In the Suture group, the left ACL was transected and suture repaired with a new locking suture repair technique (n=5) allowing approximation and fixation under tension. The Suture-SIS group underwent the same procedure with the addition of SIS (n=5). The right ACL served as control. After 12 weeks of healing, anterior-posterior translation and in-situ force of the healing ACL were measured, followed by the measurement of the cross-sectional area and structural stiffness. Routine histology was performed on tissue samples.

Gross morphology showed that the healing ACL was continuous with collagenous tissue in both groups. The cross-sectional area of the Suture and the Suture-SIS group was 35% and 50% of the intact control, respectively. The anterior-posterior translations at different flexion angles were statistically not different between the Suture group and the Suture-SIS group. Only the in-situ force at 30° in the Suture-SIS group was higher than in the Suture group. Tensile tests showed that the stiffness for the Suture group was not different from the Suture-SIS group (31.1±8.1 N/mm vs. 41.9±18.0 N/mm ($p>0.05$)). Histology showed longitudinally aligned collagen fibers from origo to insertion. More fibroblasts were present in in the healing tissue than in the control intact tissue. The study demonstrated the proof of concept of ACL repair in a goat model with a new suture technique and SIS. The mechanical outcome is not worse than previously reported for ACL reconstruction.

In conclusion, the approach of using a new suture technique, with or without a bioscaffold to heal the ACL is promising.

INTRODUCTION

The anterior cruciate ligament (ACL) plays an important role in stabilizing the knee joint. It has a complex collagen fiber architecture which makes it well suited to guide the knee joint and prevent excessive translations and rotations during functional activities. However, during daily living and sports activities the forces on the ACL occasionally exceed its limit, leading to a rupture. Previously, ACL ruptures were suture repaired like the medial collateral ligament (MCL) and Achilles' tendon ruptures. In contrast to the MCL and Achilles' tendon which can heal relatively well without surgical intervention, the ACL seldom heals spontaneously. The reported success rates after suture repair of the ACL varied between 0% and 60%. (*1-3*) Due to this inconsistent outcome, suture repair was abandoned in favor of ACL reconstruction with tendon grafts. In retrospect, these low success rates could be attributed to the previously used suture techniques. (*4*)

The current ACL reconstruction with tendon grafts is a rather successful procedure. However, there are drawbacks related to ACL reconstruction surgeries. (*5-7*) Recent studies have also shown that 70-80% of the patients develop radiographic signs of osteoarthritis (OA) in the ACL reconstructed knee after 10 to 15 years. (*8, 9*) Therefore, clinicians and researchers are aiming to improve the current treatment for ACL ruptures. (*10*) This quest is likewise stimulated by the gained basic knowledge of the ACL and the recent advances in functional tissue engineering. Previous studies have found and hypothesized that many factors such as the local environment and biological characteristics of the ACL have a profound effect on ACL healing. The fluidal environment and retraction of the ACL ends, immediately after rupture, limit the chance for healing. (*11*) Additionally, it can be imagined that by the movement of the ACL stumps during knee motion and the volume within the joint space lead to a low probability for direct or indirect contact to allow for contact healing between the torn ends. The fluidal environment also limits the chance for the formation of a hematoma because of the diluting effect of the synovial fluid. (*12*) A stable hematoma would normally bridge the gap and provide a provisional scaffold for reparative cells at the injury site. Biologically, it is also found that the ACL is a hypocellular tissue and that the properties of fibroblasts are different from those derived from other ligaments that do heal. (*13*) ACL fibroblasts have comparatively low mobility, low proliferation and metabolic activities as well as a low potential for matrix production. (*14-16*) All these constraining factors are contributing to the failure of spontaneous functional healing of the ACL. This study is aimed at addressing two major constraining factors by using a new suture technique in combination with a bioscaffold. The first objective is to apply a new suture technique that has a higher tensile and pull-out strength then previously used suture techniques such as the grasping U-loops or multiple depth suture. It is hypothesized that the new suture technique will approximate and keep the ACL torn

ends together and thus will lead to healing. The second objective is to evaluate the effect of porcine derived small intestinal submucosa (SIS) bioscaffold (Cook Biotech Inc., West Lafayette, IN, USA) as an initiator and enhancer on the healing of the ACL. SIS is mainly composed of collagen type 1 and contains endogenous growth factors such as FGF and TGF-β and other chemoattractants. (*17-19*) Several studies have shown that SIS can provide a collagenous matrix to promote cell migration into the healing site to enhance revascularization and repair. (*20-24*) It is hypothesized that SIS will enhance and promote the healing of the ACL. Instead of using the SIS as a load bearing ten-layered bioscaffold, like in the rotator cuff repair, only a single layer of SIS was used to recruit sufficient healing cells to the hypocellular ACL. To test these hypotheses we used 10 goats and evaluated the effects of the sutures and SIS application on the healing of the ACL in terms of its contribution to the knee laxity, ACL stiffness, in-situ ACL forces and histologic appearance.

METHODS

Locking suture technique

The suture technique used in this study is a modification based on the Becker locking suture. Due to its locking configuration, the suture tightens around the collagen fibers when tensile forces are applied, thus providing approximation under tension, greater ultimate tensile strength and resistance to gapping. (*25, 26*) The suture configuration resembled three X's and for ease it was designated as triple X analogous to multiple U-loops (figure 1). Absorbable Vicryl 2-0 (Ethicon, Inc., USA) was used as suture material. The needle was modified to a smaller needle (±8 mm in length and 1/2 circle form) with round-nose pliers and a side cutter in order to accustom the narrow notch and the small ACL. To anatomically approximate the ACL's torn ends we used eight sutures according to the triple X. The sutures were placed on the four corners of the distal part of the ACL stump: anteromedial, anterolateral, posteromedial and posterolateral. The same was done for the proximal part of the ACL stump. Subsequently, the ACL stumps were approximated by knotting each suture to its opposite counterpart.

Animal model

Ten skeletally mature female Dutch milk goats (body weight: 78.0 kg ± 9.5) were used in this study. Surgery and maintenance of the animals followed the study protocol approved by the institutional Animal Ethics Committee at the University of Amsterdam.

All surgical procedures were performed by one surgeon (DTN) using sterile conditions under general endotracheal isoflurane anesthesia. In the left knee, a medial parapatellar incision was made to expose the ACL. The ACL was hooked and transected in its midsubstance with a No 11 scalpel. The transection was made with three consecutive cuts, which resulted in a total transection with frayed edges, mimicking a

clinical mop-end tear. Because of the visco-elastic nature of the tissue, the tissue will retract over time after cutting. This did not appear to affect the suturing in our goat model because the time was short. The transverse meniscal ligament was partially incised to expose the whole tibial ACL attachment. In the Suture repair group (N=5), the suture repair was performed using absorbable Vicryl 2-0 sutures, according to the technique described above. Subsequently, the medial patellofemoral ligament was repaired and the joint capsule, fascia, subcutaneous tissue, and skin were closed as separate layers. In the Suture-SIS group (N=4), the same procedures were performed as in the Suture group with the addition of SIS (Cook Biotech Inc., West Lafayette, IN, USA). The material was used from the package as supplied. No additional treatment was required prior to use. Six small pieces of SIS (2 mm x 2 mm x 200 μm) were placed within the midsubstance of the injury site. These six pieces would be too small to act as a spacer. The rationale behind placing these small pieces of SIS was that these pieces would act as a "wick wire" to recruit cells to the injury site. A hydrated sheet of SIS (5 cm x 2,5 cm x 200 μm) was wrapped around the injury site and affixed with Vicryl 6-0 to the ACL. The ACL in the right hind limb was unoperated in both groups and served as internal intact control.

Buprenex 0.01 mg/kg IM once and a Fentanyl patch transdermal were given for postoperative analgesia. Post-operatively, the animals were not immobilized and were allowed free cage activity, food and water ad libitum. After 4 weeks the goats were transferred to a pasture. At twelve weeks post-surgery, all animals were euthanized with an overdose of sodium pentobarbital. Both hind limbs were disarticulated at the hip joint, wrapped in saline-soaked plaid, sealed in double plastic bags, and immediately stored at -20 C until testing.

Robotic testing

To examine the effects of suture repair of the ACL with the application of SIS on knee laxity and in situ forces, all knees were tested using a robotic universal force-moment sensor (UFS) testing system. (*27, 28*) The robotic manipulator (KR 125, KUKA Robots, Augsburg, Germany) is capable of achieving position control in 6 degrees of freedom (DOF) of motion. The UFS (FTI Theta 1500-240, Schunk, Lauffen, Germany) can measure three orthogonal forces and three orthogonal moments. The robotic/UFS testing system was used in a force-control mode via the force feedback from the UFS to the robot. For human and goat cadaveric knees, this system has been used successfully to apply external loads to the joint at preselected angles of knee flexion, while the kinematics of the remaining 5 DOF (medial-lateral, proximal-distal, anterior posterior (A-P) translations, internal-external and varus-valgus rotations) joint motions are determined by minimizing the constraint forces and moments measured by the UFS. By repeating these positions with a high level of accuracy after removing all soft-

tissue except the ACL, the in situ forces in the ACL can be determined. (*29, 30*) Prior to biomechanical testing, each specimen was thawed for 20 h at room temperature. The specimens were kept moist with 0.9% saline during dissection and biomechanical testing. The femur and tibia were cut at 15 cm from the joint line, the surrounding skin and muscles were removed leaving the capsule intact. Before potting the bones with polyurethane (VossChemie, Belgium) within thick walled aluminum cylinders, nails were inserted into two predrilled holes to secure the potting. The femoral cylinder was rigidly fixed relative to the base of the robotic manipulator and the tibial cylinder was mounted to the end-actuator of the robot distal to the UFS. The center of the knee (defined as the midpoint between the femoral insertions of the MCL and LCL) was measured relative to the UFS coordinate system. To identify the neutral flexion motion path, the joint was moved in 1° increments from full extension to 90° of flexion, while the positions with minimized forces and moments within the joint, were recorded. These positions served as the reference locations for the remainder of the protocol. The robotic-UFS testing system was then operated in force-control mode. An anterior and posterior tibial load of 67 N was applied to determine the anterior and posterior laxity at 30°, 60° and 90°. The flexion angle of 30° corresponds to extension in the human knee. Subsequently, to determine the in-situ force in the healing ACL, all soft tissue structures in and around the knee except the ACL were dissected. The articulating surfaces of the femoral condyles were also removed to prevent possible bone-to-bone contact. The recorded kinematics was repeated by the robotic manipulator and the UFS directly recorded the in situ force that was in the ACL since it is the only structure attaching the femur to the tibia.

Uniaxial tensile testing

The specimen was removed from the robotic/UFS testing system and was further prepared for uniaxial tensile testing to determine the stiffness of the ACL after healing. The cross-sectional area of the ACL was measured by means of a mechanical area micrometer (*31, 32*) The protocol followed was similar to that of Lyon et al., whereby the joint was positioned in such fashion that the ACL was along the direction of loading. (*33*) For this, each specimen was mounted in custom-made clamps that enabled the orientation of the ACL to be adjusted and aligned. The specimen was tested on a uniaxial tensile testing machine (Zwick/Roell Z005, Zwick, Germany). After a preload of 2 N, the gauge length reference position of the Zwick's crosshead was reset to 0 mm. Each femur-ACL-tibia complex (FATC) underwent preconditioning by cyclical elongation between 0 and 1 mm for 10 cycles at 20 mm/min. Thereafter, the ACL was loaded to 5N and elongated from 0 to 2 mm. The load-elongation curves of each complex were recorded and the linear stiffness was calculated from the linear section of the

load-elongation curves. By loading the FATC before subfailure (from 0 to 2 mm) the ACL could be kept intact for histologic evaluation while obtaining the stiffness values.

Histology

The whole ACL was removed from the FATC by cutting the whole ACL from its tibial and femoral bone insertion. Subsequently the ACL was embedded in O.C.T. compound (Sakura Finetek, Japan), frozen, and stored at -80°C. The tissue blocks were cut with a cryostat into sections of 5μm. The sections were stained with Masson's trichrome. The sections were fixed in and stained sequentially in Weigert's Iron Hematoxylin solution, Biebrich Scarlet-Acid Fucshin, and Aniline Blue solution according to the manufacturer's instructions (Sigma, St. Louis, MO). The collagen was stained in blue, the cytoplasm in red and the nuclei in black. The slides were observed under a Nikon light microscope and pictures were taken with a low magnification (10X) to show the whole ACL and with a higher magnification (200X) obtained from the midsubstance to show the healing areas.

Statistical tests

An unpaired Student t-test was used for statistical analysis. A probability of $p < 0.05$ was considered statistically significant.

RESULTS

Gross observations

One suture repair in the Suture-SIS group failed per-operatively due to knot slippage while testing the suture repair by passive flexion and extension of the knee. This specimen was excluded from follow-up and analysis (N=4). The approved protocol did not allow the replacement of this goat. All animals were weight bearing on both hind limbs within a few hours after surgery. Within an hour, recovering goats were challenged for new herd hierarchy through head butting while standing on their hind limbs. This was concerning since head butting and standing on their hind limb may put unnecessary load to the suture repair. Normal food intake was resumed within 24h. Normal gait, as determined by visual inspection, was observed in all animals within 2 weeks after surgery.

Robotic testing

The anterior-posterior translation of the tibia with 67N anterior and posterior force at 30°, 60° and 90° was not different between the Suture and Suture-SIS groups, ($p=0.92$, $p=0.24$, $p=0.14$) but considerably higher than in the Control knees (Table 1).

The in situ forces of the healing ACLs in response to a 67N anterior tibial load was not different between the Suture and Suture-SIS groups at 60° and 90° flexion,

Table 1. Anterior-posterior translation of the joint and in-situ forces in response to 67N anterior posterior load at 30°, 60° and 90° flexion, (mean ± SD),**statistical difference between Suture and Suture & SIS (unpaired t-test, p<0.05)

	A. Anterior-Posterior Tibial Translation (mm)		
	30°	60°	90°
I. Suture	12.4 ± 3.2	11.3 ± 1.7	6.4 ± 1.3
II. Suture-SIS	12.2 ± 3.9	13.3 ± 2.9	8.2 ± 1.8
III. Control	2.8 ± 0.7*	3.2 ± 0.8*	2.2 ± 0.8*
	B. In Situ Forces (N)		
	30°	60°	90°
I. Suture	21.5 ± 17.5	4.1 ± 1.6	5.3 ± 0.6
II. Suture-SIS	45.9 ± 11.3 **	11.3 ± 6.9	4.8 ± 0.7
III. Control	61.2 ± 4.4*	54.9 ± 6.5*	46.2 ± 10.1*

*For all parameters the differences between Suture and Control and between Suture-SIS and Control were statistically significant (paired t-test, p<0.05)

(p=0.06, p=0.26) and lower than Control (Table 1). The in-situ force at 30° in Suture-SIS group was about double the ACL force in the Suture group and neared the forces of the control ACL (Table 1), p<0.05).

Visual inspection

The menisci and cartilage showed no evidence of tears or degeneration. The Vicryl 2-0 sutures were fully resorbed and gross inspection revealed healing tissue formation in all knees. In the Suture group, the healing ACL was a continuous band of collagenous tissue with its attachment to the tibia and femur (figure 2B). In Suture-SIS group, the healing ACL was more opaque and had more visible fiber bundles (figure 2C).

Another interesting observation was that the geometry of the tibial insertion of the healing ACL's in both experimental groups was different from that of the normal ACL. The brackets in figure 2 indicate the area of the normal tibial ACL insertion site which spans over the eminentia intercondylaris. In the healing ACL's it was observed that a part of the anteromedial fiber bundles were missing.

The cross-sectional areas of the healing ACL´s were about half to one third of the control ACL´s (Table 2). This partly accounted for the lower structural stiffness of the healing ACL´s. The ratio of structural stiffnesses over cross-sectional area of the healing ACL´s was 38% and 51% of that of the control ACL´s for the Sutured and Sutured-SIS, respectively (Table 2). There were no statistically significant differences between the Suture and Suture-SIS groups as regard to the cross-sectional area, stiffness and, the ratio stiffness over cross-sectional area (Table 2).

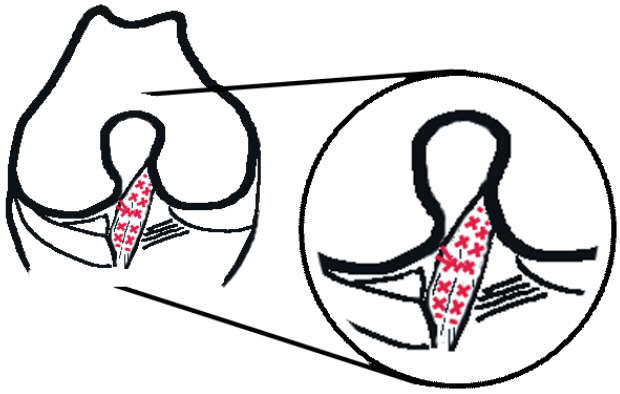

Figure 1. Sutured ACL according to customized Becker-suture-technique (triple X), red denotes suture threads

Table 2. Cross-sectional area, stiffness and stiffness/cross-sectional area of the specimens.

	I. Suture	II. Suture-SIS	III. Control
Cross-sectional area (mm^2)	7.6 ± 4.0	10.8 ± 7.4	21.7 ± 6.1
Stiffness (N/mm)	31.1 ± 8.1	41.9 ± 18.0	179.5 ± 32.7
Stiffness/Cross-sectional area (N/mm^3)	3.6 ± 0.5	4.9 ± 2.1	9.6 ± 4.7

Histology

The Masson's trichrome staining showed that the collagen fibers (stained in blue) of the normal ACL's, were compact, regularly aligned and had a clear crimp pattern (Figure 3A,D). The fibroblasts (stained in red) were ovoid/spindle-shaped and aligned along the collagen fibers (Figure 3D). The overview pictures from the ACL's in the Suture group and the Suture-SIS group showed that the ACL's healed or were at least in a process of healing and were continuous from the distal part to the proximal part (Figure 3B,C). The original transection site could no longer be recognized and the tissue had remodeled over the entire length of the ligament. The tissue was hypercellular (Figure 3E,F). The healing ACL's from the sutured group, had aligned collagen fibers but were less compact and had no discernible crimp pattern (Figure 3B), that was also not found with polarized light (not shown in the figure). The fibroblasts appeared long and spindle shaped (Figure 3E). With SIS, the collagen fibers in the healing ACL's were also aligned and oriented in the longitudinal direction and the fiber arrangement appeared to be more compact (Figure 3C). The fibroblasts were also spindle-shaped and oriented along the collagen fibers (Figure 3F). Interestingly, when comparing the morphology of the fibroblast, it can be observed that the cells in the Suture- and Suture-SIS samples are more elongated while those in the control sample are more ovoid-shaped. In addition, there were also more fibroblasts in the healing ACL's than in the control ACL's.

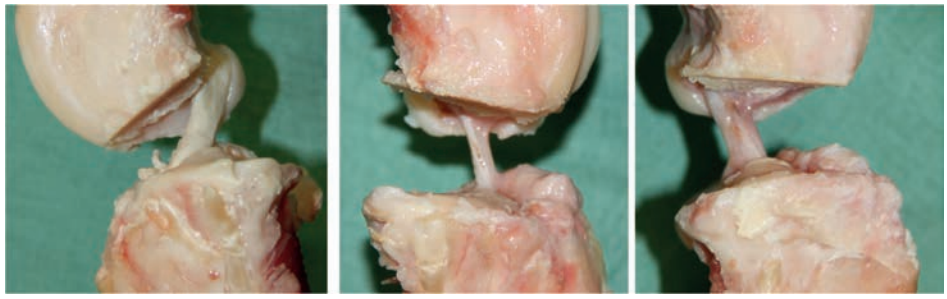

Figure 2. A) Medial side view of a normal ACL. B) A healing ACL after suture repair only. C) A healing ACL after suture repair and SIS. Brackets indicate area of normal insertion site. It can be seen that the treated ACL's do not cover the whole area of normal insertion site.

DISCUSSION

The study demonstrated that suturing the transected ACL with the new suture repair technique and an absorbable suture resulted in healing of the ACL in all goats. The reason for the failure in one goat was purely technical. If the suturing is successful at the time of surgery, than the tissue would be healing. The ACL was continuous with collagenous healing tissue with a cross-sectional area that was 35% of the intact control. In terms of knee stability, the AP translation was 4.4 times higher and the stiffness was 17% compared to the intact control. In the Suture-SIS group, the ACL was also continuous with collagenous healing tissue with a cross-sectional area that was 50% of the intact control. The AP translation was not different from the Suture group and the Suture-SIS group. The stiffness was 23% compared to the intact control. When normalizing the stiffness to its cross-sectional area, thereby taking the amount of tissue into account, the normalized stiffness of the healing ACL´s was about half of the control ACL´s. Histologic evaluation confirmed that the healing tissue in the ACL's was indeed collagenous and consisted of continuous and aligned collagen fibers. It can be concluded that the new suture technique was able to provide contact between the ligament ends for healing. Contact is a requirement for healing of the intra-articular situated ACL. This conclusion is also further supported by several animal studies which have shown that transected ACLs do not heal but are rather resorbed. (*12, 34*) Previously, Zantop et al., have shown in the Achilles tendon model that the SIS is repopulated by bone marrow derived cells for the regeneration process. Adding SIS to the suture repair could have recruited more reparative cells to the ACL injury site by its chemoattractant properties, leading to more mature collagen fibers and an in situ force that is closer to the intact ACL at 30°. This, however, is not sufficient to claim a positive effect of the SIS on the mechanical outcome of the repair. That the in-situ force was not closer to the intact ACL at 60˚ and 90˚ degrees flexion might be due to the fact that a part of the anteromedial (AM) bundles of both experimental groups was missing and therefore could not be recruited. This absence was reflected in the

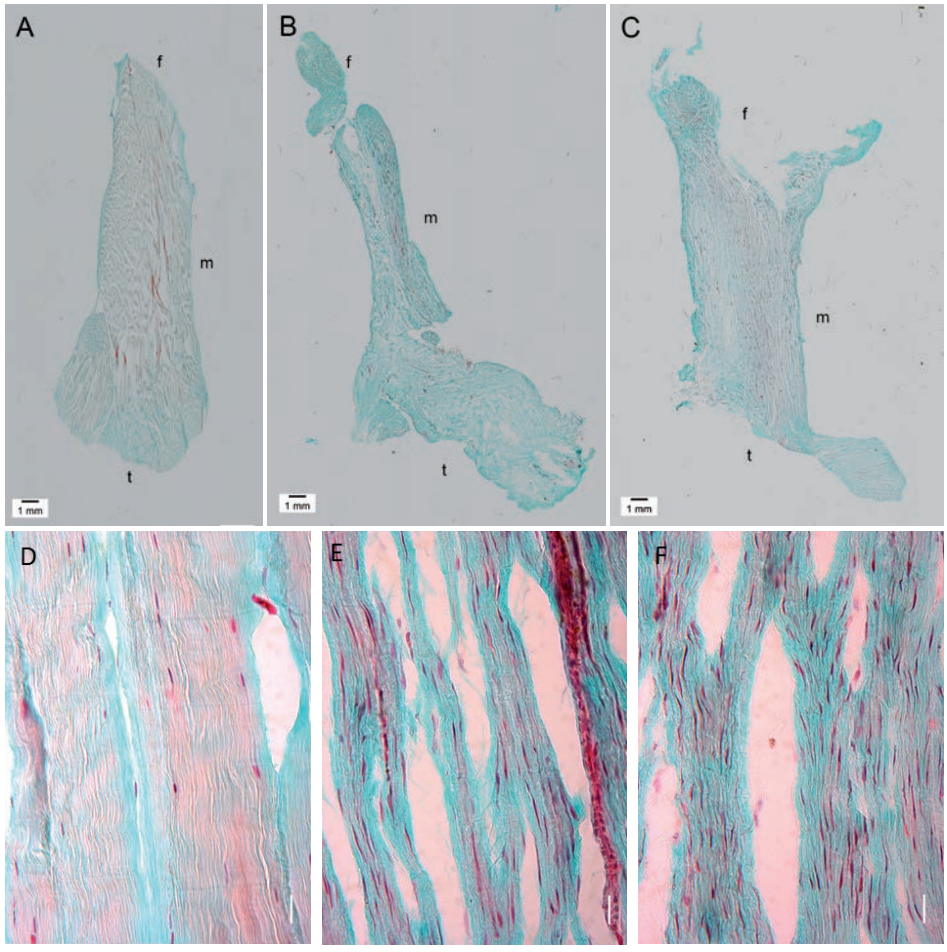

Figure 3. Histologic sections of a normal ACL (A,D), sutured ACL (B,E) and sutured ACL with SIS (C,F). The sections are stained with Masson's trichrome; the collagen fibers are stained in blue, the fibroblasts are stained in red and the nuclei in black; m denotes midsubstance, f denotes femoral insertion site and t denotes tibial insertion site. The transection site could not be recognized and the tissue was remodeled over the entire length of the ACL. Note that the tissue is hypercellular in both the sutured and suture-SIS ACL and that the fibroblasts are more spindle shaped than the intact ACL.

smaller cross-sectional area and could in turn also explain the lower stiffness and higher values for the anterior tibial translation (ATT). A recent study by Tischer et al., showed that transection of AM bundle of an intact goat ACL lead to a 88% increase in the ATT. (*35*) A possible explanation for the absence of the AM bundles might be the high forces during the post-operative rehabilitation period. The goats were not immobilized and unexpectedly the goats were head butting within hours after the operation. In following days and weeks they resumed their normal gait which also included

hyperextension and hyperflexion when lying down. These movements could have led to repetitive and excessive forces on the sutures and could have led to suboptimal healing during the initial healing phase. If overloading actually occurs and the ACL-suture construct is too weak then goats should be rehabilitated such that excessive loads on the ACL can be prevented, especially during the initial healing phase, by e.g. (short-term) casting with a limited range of flexion and extension.

Compared to recent research that focused on suture repair of the ACL in combination with platelet-rich plasma (PRP) delivery and scaffolds, (*36-39*) the results in the current study are not far off in terms of the functional outcomes. The total AP translation of the repaired ACL was 290% to 440% of the intact control under 67N anterior and posterior tibial load (AP load). Fisher et al., found a 302% increase with the same AP load and Fleming, Murray et al., found a 350% increase in anterior tibial translation with a 35N anterior tibial load. (*40, 41*) In terms of stiffnesses of the healing ACL, these were respectively 23% in our study, 42% for Fisher et al., and 25% for Fleming, Murray et al. Besides similarities there are also differences between these studies. For example, the other studies used a mechanical augmentation, where the current study was relying only on the locking suture technique with absorbable sutures. The laxity and stiffness data are comparable to those for an ACL reconstruction with a bone-patellar tendon-bone graft in goats in terms of the AP laxity and stiffness at 6 weeks post-surgery. The result of ACL healing for the AP laxity was 13.3 ± 2.9mm, where Abramowitch et al. reported 17.2 ± 3.5mm, and Spindler et al. reported 19,0 ± 4.5mm. The stiffness of the healing ACL was 41.9 ± 18 N/mm, which compared well with the reported 41.3 ± 26.1 N/mm and 22 ± 14 N/mm of Abramowitch et al. and Spindler et al., respectively. (*29, 42*). These ACL reconstruction studies evaluated the outcome at 6 weeks instead of 12 week. However, Zantop et al. showed that the outcome of the ACL reconstruction in goats at 12 weeks was not significantly different from 6 weeks. (*43*) This supports the conclusion that the outcome with respect to AP laxity and ligament stiffness is not worse nor better than the ACL reconstruction in the goat. The study is of an exploratory nature, demonstrating the proof of concept of ACL repair in a goat model. No failure testing was performed because the study was aimed at the functional outcome, in terms of stiffness and laxity; thus not aimed at the strength of the construct. With this, the repaired ACL´s could be preserved for histologic evaluation. The power of the study was low to draw definitive conclusions on the beneficial effects of the SIS scaffold. Still, the finding that the ACL has a healing potential and that the mechanical outcome is not worse than the previously reported outcomes of ACL reconstruction in the goat by using a tendon graft is exciting. This study needs to be followed-up by more extensive animal studies, addressing the questions that are raised and by the development of arthroscopic tools that are required for suturing the torn ACL in humans. Furthermore, an evaluation should be conducted

of the type of ACL ruptures and the characteristics to decide which ruptures can be considered as good candidates for primary repair. Also the timing of the surgery and the postoperative rehabilitation protocol are to be determined. Hence, there are many challenges ahead on the road to primary repair as the alternative to reconstruction with a tendon. This study is one of the first steps on that road.

In conclusion, the positive results in the study suggest that the approach of using the new suture technique, with or without a bioscaffold to heal the ACL is promising.

ACKNOWLEDGEMENT

The authors are grateful for the technical assistance of Maarten van den Berg, Mahyar Foumani, Mikel Reilingh and Sietske Dellbrügge. The study was sponsored by Mozaïek PhD-training grant 017.004.076 from the Netherlands Organization for Scientific Research (NWO).

AUTHOR DISCLOSURE STATEMENT

The SIS material was provided by Cook Biotech Inc., West Lafayette, IN, USA, under a Material Use Agreement, without any monetary compensation and without any condition. None of the authors had any relation with any other third parties, commercial or otherwise, that has interest in the study or could have influenced the study.

REFERENCES

1. M. F. Sherman, L. Lieber, J. R. Bonamo, L. Podesta, I. Reiter, The long-term followup of primary anterior cruciate ligament repair. Defining a rationale for augmentation. *The American journal of sports medicine* **19**, 243 (May-Jun, 1991).
2. J. A. Feagin, Jr., W. W. Curl, Isolated tear of the anterior cruciate ligament: 5-year follow-up study. *The American journal of sports medicine* **4**, 95 (May-Jun, 1976).
3. N. Kaplan, T. L. Wickiewicz, R. F. Warren, Primary surgical treatment of anterior cruciate ligament ruptures. A long-term follow-up study. *The American journal of sports medicine* **18**, 354 (Jul-Aug, 1990).
4. W. J. Radford, A. A. Amis, F. W. Heatley, Immediate strength after suture of a torn anterior cruciate ligament. *The Journal of bone and joint surgery. British volume* **76**, 480 (May, 1994).
5. J. Kartus *et al.*, Complications following arthroscopic anterior cruciate ligament reconstruction. A 2-5-year follow-up of 604 patients with special emphasis on anterior knee pain. *Knee surgery, sports traumatology, arthroscopy : official journal of the ESSKA* **7**, 2 (1999).
6. A. B. Meyers, A. H. Haims, K. Menn, H. Moukaddam, Imaging of anterior cruciate ligament repair and its complications. *AJR Am J Roentgenol* **194**, 476 (Feb, 2010).
7. M. L. Busam, M. T. Provencher, B. R. Bach, Jr., Complications of anterior cruciate ligament reconstruction with bone-patellar tendon-bone constructs: care and prevention. *The American journal of sports medicine* **36**, 379 (Feb, 2008).
8. A. von Porat, E. M. Roos, H. Roos, High prevalence of osteoarthritis 14 years after an anterior cruciate ligament tear in male soccer players: a study of radiographic and patient relevant outcomes. *Ann Rheum Dis* **63**, 269 (Mar, 2004).
9. L. A. Pinczewski *et al.*, A 10-year comparison of anterior cruciate ligament reconstructions with hamstring tendon and patellar tendon autograft: a controlled, prospective trial. *The American journal of sports medicine* **35**, 564 (Apr, 2007).
10. B. D. Beynnon, R. J. Johnson, J. A. Abate, B. C. Fleming, C. E. Nichols, Treatment of anterior cruciate ligament injuries, part 2. *The American journal of sports medicine* **33**, 1751 (Nov, 2005).
11. S. L. Woo, S. D. Abramowitch, R. Kilger, R. Liang, Biomechanics of knee ligaments: injury, healing, and repair. *Journal of biomechanics* **39**, 1 (2006).
12. M. M. Murray, S. D. Martin, T. L. Martin, M. Spector, Histological changes in the human anterior cruciate ligament after rupture. *The Journal of bone and joint surgery. American volume* **82-A**, 1387 (Oct, 2000).
13. S. L. Hsu, R. Liang, S. L. Woo, Functional tissue engineering of ligament healing. *Sports Med Arthrosc Rehabil Ther Technol* **2**, 12 (2010).
14. C. N. Nagineni, D. Amiel, M. H. Green, M. Berchuck, W. H. Akeson, Characterization of the intrinsic properties of the anterior cruciate and medial collateral ligament cells: an in vitro cell culture study. *Journal of orthopaedic research : official publication of the Orthopaedic Research Society* **10**, 465 (Jul, 1992).
15. J. M. McKean, A. H. Hsieh, K. L. Sung, Epidermal growth factor differentially affects integrin-mediated adhesion and proliferation of ACL and MCL fibroblasts. *Biorheology* **41**, 139 (2004).
16. Z. Ge, J. C. Goh, E. H. Lee, Selection of cell source for ligament tissue engineering. *Cell Transplant* **14**, 573 (2005).
17. J. P. Hodde, D. M. Ernst, M. C. Hiles, An investigation of the long-term bioactivity of endogenous growth factor in OASIS Wound Matrix. *Journal of wound care* **14**, 23 (Jan, 2005).

18. S. L. Voytik-Harbin, A. O. Brightman, M. R. Kraine, B. Waisner, S. F. Badylak, Identification of extractable growth factors from small intestinal submucosa. *J Cell Biochem* **67**, 478 (Dec 15, 1997).
19. R. Liang, M. Fisher, G. Yang, C. Hall, S. L. Woo, Alpha1,3-galactosyltransferase knockout does not alter the properties of porcine extracellular matrix bioscaffolds. *Acta biomaterialia* **7**, 1719 (Apr, 2011).
20. T. Zantop, T. W. Gilbert, M. C. Yoder, S. F. Badylak, Extracellular matrix scaffolds are repopulated by bone marrow-derived cells in a mouse model of achilles tendon reconstruction. *J Orthop Res* **24**, 1299 (Jun, 2006).
21. R. Liang *et al.*, Long-term effects of porcine small intestine submucosa on the healing of medial collateral ligament: a functional tissue engineering study. *Journal of orthopaedic research : official publication of the Orthopaedic Research Society* **24**, 811 (Apr, 2006).
22. R. Liang, S. L. Woo, T. D. Nguyen, P. C. Liu, A. Almarza, Effects of a bioscaffold on collagen fibrillogenesis in healing medial collateral ligament in rabbits. *Journal of orthopaedic research : official publication of the Orthopaedic Research Society* **26**, 1098 (Aug, 2008).
23. R. H. Raeder, S. F. Badylak, C. Sheehan, B. Kallakury, D. W. Metzger, Natural anti-galactose alpha1,3 galactose antibodies delay, but do not prevent the acceptance of extracellular matrix xenografts. *Transplant immunology* **10**, 15 (Jun, 2002).
24. T. W. Gilbert, A. M. Stewart-Akers, A. Simmons-Byrd, S. F. Badylak, Degradation and remodeling of small intestinal submucosa in canine Achilles tendon repair. *The Journal of bone and joint surgery. American volume* **89**, 621 (Mar, 2007).
25. H. Hatanaka, J. Zhang, P. R. Manske, An in vivo study of locking and grasping techniques using a passive mobilization protocol in experimental animals. *J Hand Surg Am* **25**, 260 (Mar, 2000).
26. H. Becker, M. Davidoff, Eliminating the gap in flexor tendon surgery. A new method of suture. *The Hand* **9**, 306 (Oct, 1977).
27. S. L. Woo, R. E. Debski, E. K. Wong, M. Yagi, D. Tarinelli, Use of robotic technology for diathrodial joint research. *J Sci Med Sport* **2**, 283 (Dec, 1999).
28. H. Fujie, G. A. Livesay, S. L. Woo, S. Kashiwaguchi, G. Blomstrom, The use of a universal force-moment sensor to determine in-situ forces in ligaments: a new methodology. *Journal of biomechanical engineering* **117**, 1 (Feb, 1995).
29. S. D. Abramowitch, C. D. Papageorgiou, J. D. Withrow, T. W. Gilbert, S. L. Woo, The effect of initial graft tension on the biomechanical properties of a healing ACL replacement graft: a study in goats. *Journal of orthopaedic research : official publication of the Orthopaedic Research Society* **21**, 708 (Jul, 2003).
30. M. Sakane *et al.*, In situ forces in the anterior cruciate ligament and its bundles in response to anterior tibial loads. *Journal of orthopaedic research : official publication of the Orthopaedic Research Society* **15**, 285 (Mar, 1997).
31. D. G. Ellis, Cross-sectional area measurements for tendon specimens: a comparison of several methods. *Journal of biomechanics* **2**, 175 (May, 1969).
32. F. R. Noyes, E. S. Grood, The strength of the anterior cruciate ligament in humans and Rhesus monkeys. *The Journal of bone and joint surgery. American volume* **58**, 1074 (Dec, 1976).
33. R. M. Lyon, S. L. Woo, J. M. Hollis, J. P. Marcin, E. B. Lee, A new device to measure the structural properties of the femur-anterior cruciate ligament-tibia complex. *Journal of biomechanical engineering* **111**, 350 (Nov, 1989).

34. M. Richter *et al.*, Acutely repaired proximal anterior cruciate ligament ruptures in sheep - by augmentation improved stability and reduction of cartilage damage. *J Mater Sci Mater Med* **8**, 855 (Dec, 1997).
35. T. Tischer *et al.*, Biomechanics of the goat three bundle anterior cruciate ligament. *Knee surgery, sports traumatology, arthroscopy : official journal of the ESSKA* **17**, 935 (Aug, 2009).
36. B. C. Fleming, K. P. Spindler, M. P. Palmer, E. M. Magarian, M. M. Murray, Collagen-platelet composites improve the biomechanical properties of healing anterior cruciate ligament grafts in a porcine model. *The American journal of sports medicine* **37**, 1554 (Aug, 2009).
37. P. Vavken, M. M. Murray, Translational Studies in ACL repair. *Tissue Eng Part A*, (Jul 21, 2009).
38. M. M. Murray *et al.*, Enhanced histologic repair in a central wound in the anterior cruciate ligament with a collagen-platelet-rich plasma scaffold. *Journal of orthopaedic research : official publication of the Orthopaedic Research Society* **25**, 1007 (Aug, 2007).
39. M. M. Murray *et al.*, Collagen-platelet rich plasma hydrogel enhances primary repair of the porcine anterior cruciate ligament. *Journal of orthopaedic research : official publication of the Orthopaedic Research Society* **25**, 81 (Jan, 2007).
40. B. C. Fleming, E. M. Magarian, S. L. Harrison, D. J. Paller, M. M. Murray, Collagen scaffold supplementation does not improve the functional properties of the repaired anterior cruciate ligament. *Journal of orthopaedic research : official publication of the Orthopaedic Research Society* **28**, 703 (Jun, 2010).
41. M. B. Fisher *et al.*, Potential of healing a transected anterior cruciate ligament with genetically modified extracellular matrix bioscaffolds in a goat model. *Knee Surg Sports Traumatol Arthrosc*, (Dec 6, 2011).
42. K. P. Spindler, M. M. Murray, J. L. Carey, D. Zurakowski, B. C. Fleming, The use of platelets to affect functional healing of an anterior cruciate ligament (ACL) autograft in a caprine ACL reconstruction model. *Journal of orthopaedic research : official publication of the Orthopaedic Research Society* **27**, 631 (May, 2009).
43. T. Zantop *et al.*, Effect of tunnel-graft length on the biomechanics of anterior cruciate ligament-reconstructed knees: intra-articular study in a goat model. *The American journal of sports medicine* **36**, 2158 (Nov, 2008).

Chapter 9

Histological Characteristics of Ligament Healing after Bio-enhanced repair of the Transected Goat ACL

D. Tan Nguyen, Sietske Dellbrügge, Paul Peter Tak, Savio L-Y. Woo,
Leendert Blankevoort, C. Niek van Dijk

Accepted for publication in Journal of Experimental Orthopaedics

ABSTRACT

Recently, healing of a ruptured anterior cruciate ligament (ACL) is reconsidered. In a previous study, we have shown that the transected anterior cruciate ligament (ACL) can heal after treatment with the triple X locking suture alone or combined with small intestine submucosa (SIS). The first research question of this study was whether the healing ACLs in both groups show histological characteristics that are typical for ligament healing. Secondly, did the combined treatment with SIS lead to improved histological healing, in terms of the morphology of the fibrous synovial layer, the extracellular matrix (ECM), collagen fiber orientation, cellularity, ratio of myofibroblasts, and collagen type 3 staining. The hypothesis was that SIS enhances the healing by the scaffolding effect, endogenous growth factors, and chemoattractants.

In the Suture group, the left ACL was transected and sutured with the triple X locking suture repair technique. In the Suture-SIS group, the left ACL underwent the same procedure with the addition of SIS. The right ACL served as internal control. Standard histology and immunostaining of α-smooth muscle actin (SMA) and collagen type 3 were used.

Microscopy showed that the fibrous synovial layer around the ACL was reestablished in both groups. The collagen fibers in the Suture-SIS group stained denser, were more compactly arranged, and the ECM contained fewer voids and fat vacuoles. Neovasculature running between the collagen fibers was observed in both experimental groups. Collagen type 3 stained less in the Suture-SIS group. The cellularity in the Suture group, Suture-SIS group and Control was 1265±1034 per mm^2, 954±378 per mm^2, 254 ± 92, respectively; 49%, 26% and 20% of the cells stain positive for α-SMA, respectively. In conclusion, the healing ACL in both treated groups showed histological characteristics which are comparable to the spontaneously healing medial collateral ligament and showed that the ACL has a similar intrinsic healing response. Though, no definitive conclusions on the beneficial effects of the SIS scaffold on the healing process can be made.

INTRODUCTION

The anterior cruciate ligament (ACL) of the knee joint is frequently ruptured and may often require reconstruction with autologous tendon grafts to treat chronic knee instability. (1, 2) The clinical and functional outcome of ACL reconstruction is generally satisfactory, allowing the majority of the patient population to return to work and a part to return to pre-injury level sports activity. However, ACL reconstruction does not fully restore the function of the intact ACL. Additionally, there are several drawbacks. (3-5) Though, it is commonly believed that the ACL does not have a healing response and cannot heal, some researchers are re-exploring methods to repair the ACL in the acute phase. (6-10) In a previous study, our research group reported that the treatment of the transected ACL with a new suture repair technique in combination with the small intestinal submucosa (SIS) bioscaffold lead to healing in a goat model. (9) The ACLs in both experimental groups were healing and continuous. Biomechanical testing showed that the repaired ACLs contributed to the knee function. (9) The total AP translation of the repaired ACL was 290% to 440% of the intact control under 67N anterior and posterior tibial load (AP load). The normalized stiffness of the healing ACLs was about half of the control ACLs. The ACLs were retained for this study with the aim to histologically investigate whether the healing ACL has histologically characteristics as the healing medial collateral ligament (MCL). The comparison with the MCL was made as the MCL is regarded as the knee ligament that has a healing response and that can heal spontaneously. As such, the first research question of this study was whether the ACLs treated with the triple X suture alone or combined with small intestine submucosa (SIS) resemble the histological healing characteristics as observed in the healing MCL. Secondly, does the combined treatment with SIS leads to improved histological healing characteristics, in terms of the morphology of the fibrous synovial layer, the extracellular matrix (ECM), collagen fiber orientation, cellularity, ratio of myofibroblasts over total cell count, and collagen type 3 staining. These parameters provide a general evaluation of the healing process in ligaments. Myofibroblasts have shown to play an important role in the healing and remodeling of MCL, with an initial increase in density after injury and steadily normalization during the remodeling phase. Myofibroblasts have also been shown in the injured but non-healing ACL, though the density remained low (<1.5%). (11) SIS bioscaffold is mainly composed of collagen type 1 and contains endogenous growth factors such as fibroblast growth factors (FGF) and TGF-β, as well as other chemoattractants which enhances the healing. (12-14) Several studies have shown that SIS can act as a provisional scaffold to promote cell migration and to enhance revascularization and repair. (15-19) It was thus hypothesized that SIS enhances the healing of the ACL and that the SIS-treated ACL is closer to the normal ACL histologically, i.e. compacter ECM, less voids, more cells, less myofibroblasts and less collagen type 3 staining.

MATERIALS & METHODS

The goat ACLs from the Suture group (n=4), Suture-SIS group (n=4), and their respective intact control group (n=8) were retained from a previous study. (9) Initially, there were five samples in the Suture group; however due to an embedding error and consequently cutting errors one sample was lost for histological analysis. For a detailed description of the animal protocol and surgery, which was approved by the institutional Animal Ethics Committee at the University of Amsterdam, see Nguyen et al., (9) Briefly, in the left goat knee, a medial parapatellar incision was made to expose the ACL. The ACL was hooked and transected in its midsubstance. In the Suture repair group, the suture repair was performed using absorbable Vicryl 2-0 sutures, using a previously described triple X locking suture technique. Due to its locking configuration, the suture tightens around the collagen fibers when tensile forces are applied, thus providing approximation under tension, greater ultimate tensile strength, and resistance to gapping. (20, 21) Subsequently, the medial arthrotomy was closed in separate layers. In the Suture-SIS group, the same procedures were performed as in the Suture group with the addition of porcine derived SIS (Cook Biotech Inc., West Lafayette, IN, USA). Six small pieces of SIS (2 mm x 2 mm x 200 μm) were loosely placed within the midsubstance of the injury site. A hydrated sheet of SIS (5 cm x 2,5 cm x 200 μm) was wrapped around the injury site and affixed with Vicryl 6-0 to the ACL. The ACL in the right hind limb was unoperated in both groups and served as internal intact control. Postoperatively, the animals were allowed full weight bearing immediately after the operation without any external bracing of the operated limb. Free cage activity and later a pasture, food and water was *ad libitum*. At twelve weeks post-surgery, all animals were euthanized and the hind limbs were immediately stored at -20°C until biomechanical testing. The ACLs were kept intact during biomechanical testing and were not tested to failure. The whole ACL was removed from the femur-ACL-tibia complex by cutting the whole ACL from its tibial and femoral bone insertion. The whole ACL was embedded in Tissue-Tek O.C.T. compound (Sakura Finetek, Japan), frozen, and stored at -80°C.

Histology

Five-micrometer thick sections were cut in a cryostat microtome and mounted on glass slides (Star Frost adhesive slides, Knittelgläser, Germany), and stored at -80˚C until staining. The cryosections was made by SD and number coded. The staining and analyses were done by DTN and MdB. Standard Haematoxylin & Eosin (H&E) was performed to grossly evaluate the fibrous synovial membrane, the ECM, and cell morphology. Lendrum Masson's trichrome staining was performed to specifically stain the collagen and to evaluate the collagen fiber orientation. The sections were stained sequentially in celestine blue, haematoxiline, Ponceau de Xylidine and tartrazine. The

collagen was stained in yellow, the cytoplasm in red and the nuclei in blue. The slides were observed under a light microscope and pictures were taken from the midsubstance at the healing areas with a low magnification (10X) to show the whole ACL and with higher magnifications (100X, 200X and 400X).

Immunohistochemical staining

An AEC (3-Amino-9-ethylcarbazole) labeling immunohistochemical methodology was used with the following antibodies: goat monoclonal mouse anti-human alpha-smooth muscle actin (α-SMA) antibody (Sigma-Aldrich, St. Louis, MO) as a marker for myofibroblasts and monoclonal mouse anti-human collagen type 3 antibody (Abcam, Cambridge, UK) to identify collagen type 3. Briefly, the sections were fixed in 100% acetone for 10 min at room temperature and washed with phosphate-buffered saline (PBS), three times for 5 minutes. Endogenous peroxidase activity was blocked using peroxidase 3% for 30 minutes at room temperature. The sections were rinsed once in PBS and 10% normal goat serum, 1% Bovine Serum Albumin (BSA) in PBS was applied for 1 hour at room temperature as a blocking agent. The monoclonal α-SMA antibody in 5% normal goat serum, 1% BSA in PBS (5 μg/ml) was applied and incubated overnight at 4°C on a shaker. Collagen type 3 was stained with monoclonal mouse collagen type 3 antibody in 5% normal goat serum, 1% BSA in PBS (0.5 μg/ml). Subsequently the sections were washed in PBS three times for 5 minutes each. The secondary antibody, a rabbit anti-mouse immunoglobulin (IgG) horseradish conjugate (HRP) (Abcam, Cambridge, UK), was applied to the sections 1 μg/ml for 60 minutes at room temperature. After a final rinse with PBS, HRP activity was visualized as a brown-red color by incubation with AEC (Sigma-Aldrich). Sections were counterstained with Mayer's haematoxylin and mounted in Kaiser's glycerol gelatin (Merck). Appropriate isotype controls were assessed in all experimental series. Positive controls for α-SMA and collagen type 3 were goat artery vessels and goat skin, respectively.

Digital Image Analysis

Quantification of α-SMA expressing cells in the healing tissue was performed with digital image analysis (DIA), as previously described. (22) In brief, for each acquisition session the microscope, camera, and computer were calibrated according to a standardized procedure. Settings are recorded and stored and used for the entire session. After immunohistochemical staining, three representative regions of 1.45 x 1.45 mm in each section are identified at low power magnification (without capillaries, fat voids and artifacts) and separated in 18 consecutive high power fields (HPF). The18 HPF images are analyzed by computer-assisted image analysis using a Syndia algorithm on a Qwin-based analysis system (Leica, Cambridge, UK). (23) The software identified positive cells by combining two masks where areas of a nucleus surrounded

by a red-brown staining are identified as positive cells, and isolated blue (nuclei without staining) or red are ignored. Positive staining of α-smooth muscle actin was expressed as number of positive cells/mm^2.

Two sections per sample stained for collagen type 3 (n=16) are semi-quantitatively analyzed by DTN and MdB with a standard binocular light microscope (Olympus) at 200X magnification. The expression of collagen type 3 was scored on a 5-point scale (range 0–4), as previously described. (24) A score of 0 represented no expression, while a score of 4 represented abundant expression of collagen type 3 within the healing tissue. Differences between the two observers are resolved by consensus.

Statistical test

A paired or unpaired Student's t-test was used for statistical analysis, where appropriate. A probability of $p<0.05$ was considered statistically significant.

RESULTS

Gross morphology

The ACLs in both experimental groups are healing and continuous. The transection site cannot be recognized. The Vicryl sutures and SIS are fully resorbed. In the Suture-SIS group, the ACL appears more opaque and denser than the Suture group (figure 1). The cross-sectional areas of the healed ACLs in the Suture group and Suture-SIS group as reported previously are 35% and 50% of the intact control. (9)

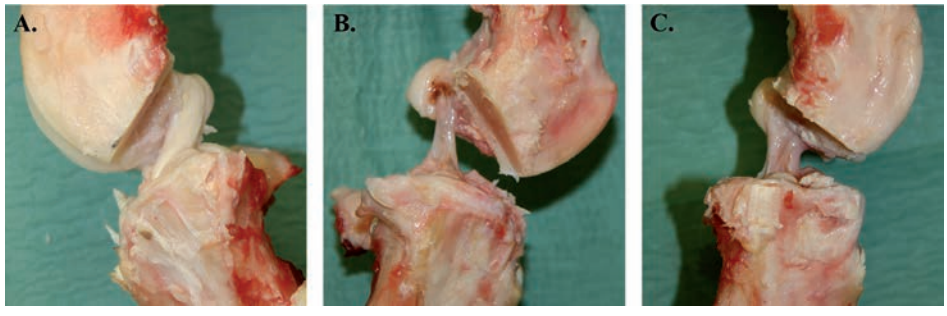

Figure 1. A) Medial side view of a normal ACL. B) A healing ACL after suture repair only. C) A healing ACL after suture repair and SIS.

Fibrous synovial layer

Microscopy shows that the surface of the ACL in both the two experimental groups and the intact control ACLs were covered by a layer of cells and formed the fibrous synovial layer (figure 2). The sub-intimal synovial layer can be observed along the whole length of the ACL without any disruption.

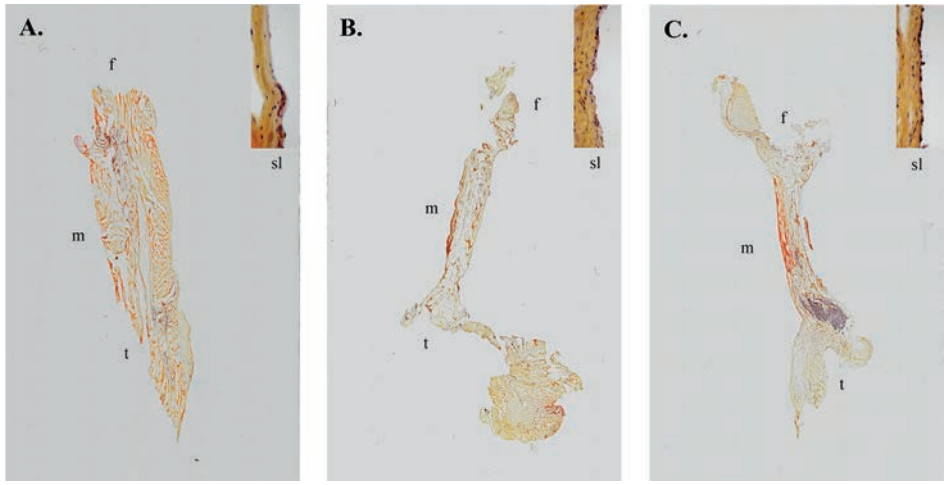

Figure 2. Histologic sections of a normal ACL (A), sutured ACL (B) and sutured ACL with SIS (C) with magnification of subintimal synovial layer at the top right (×100). The sections are stained with Lendrum Masson's trichrome; the collagen fibers are stained in yellow, the cytoplasm in red and the nuclei in blue.

Extracellular Matrix

H&E and Lendrum's Masson's trichrome shows that the ECM in the normal ACL was densely packed with aligned collagen fibers and a crimp pattern. No apparent capillaries, voids or lipid vacuoles can be observed (figure 3A, 4A). Immunostaining of collagen type 3 shows that there was limited staining, scoring 1 (figure 6A). In the Suture group the collagen fibers are aligned but loosely packed and with patches of more compact fibers but with no crimp pattern at the midsubstance (figure 3B, 4B). Voids and lipid vacuoles can be observed. Many capillaries can be observed between the fibers, and in some slides the capillaries can be traced through the ACL. Collagen type 3 was present with a score of 2 (figure 6B). In the Suture-SIS group the collagen fibers were aligned and more compact organized than the Suture group, but with no crimp pattern at the midsubstance (figure 3C, 4C). Voids and lipid vacuoles can also be observed but was less present than in the Suture group. Many capillaries can be observed between the fibers, and in some slides the capillaries can also be traced through the ACL. Collagen type 3 is present with a score of 2 (figure 6C). In all groups, the ACLs were vital and there were no necrotic areas.

Fibroblast morphology, cell and myofibroblast density

In the control groups, normal nucleus morphology and cell distribution can be observed within the ACL. Generally, ovoid fibroblast nuclei were located at the proximal ACL, rod-like fibroblast nuclei were located in the midsubstance (figure 4A, 5A). Round to ovoid shaped nuclei were located at the distal part. Some "chrondroblasts" were

observed at the distal part of the ACL. Quantification of the cells with the DIA shows that the cell density in the midsubstance of the Suture control group and Suture-SIS control group was 254 ± 92 cells/mm^2 and 204 ± 93 cells/mm^2, respectively. The ratio of α-SMA positive cells in the control groups was 19% and 20%, respectively (table 1).

In the Suture group, nucleus morphology and cell distribution were different than in the control group. Limited variation in nucleus morphology was observed. Generally, the nuclei were elongated with more of a spindle shape and were scattered over the whole ACL. The cell density was 1265 ± 1034 and the ratio of α-SMA positive cells over total cell count was 49% (table 1). The difference in cellularity and the difference in the ratio of the number of α-SMA positive cells over the total number of cells between the Suture group and its control group was statistically not significant ($p > 0.05$).

In the Suture-SIS group, nucleus morphology and cell distribution also differ from the control group and were comparable to the Suture group (figure 4C, 5C). The healing ACLs in the Suture-SIS group were hypercellular with a cell density of 954 ± 378 cells/mm^2. The difference in cellularity between the Suture-SIS group and its control group was statistically significant ($p = 0.048$) (table 1). The ratio of α-SMA positive cells of the Suture-SIS group was 26% and neared the control group (table 1). Comparing the cellularity and the ratio of α-SMA positive between the Suture group and the Suture-SIS group, shows that there were no statistically significant differences.

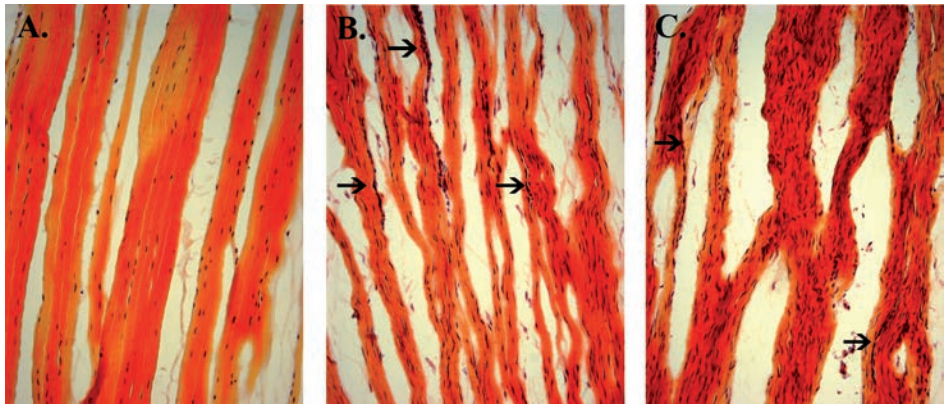

Figure 3. Histologic sections of a normal ACL (A), sutured ACL (B) and sutured ACL with SIS (C). The sections are stained with Lendrum Masson's trichrome; the collagen fibers are stained in yellow, the cytoplasm in red and the nuclei in blue. The ECM of both the Suture and Suture-SIS group have aligned collagen fibers, the collagen fibers in the Suture-SIS group stained denser, more compact arranged and contained less voids and less fat vacuoles. Neovasculature running parallel between the collagen fibers could be observed in both experimental groups. ×100

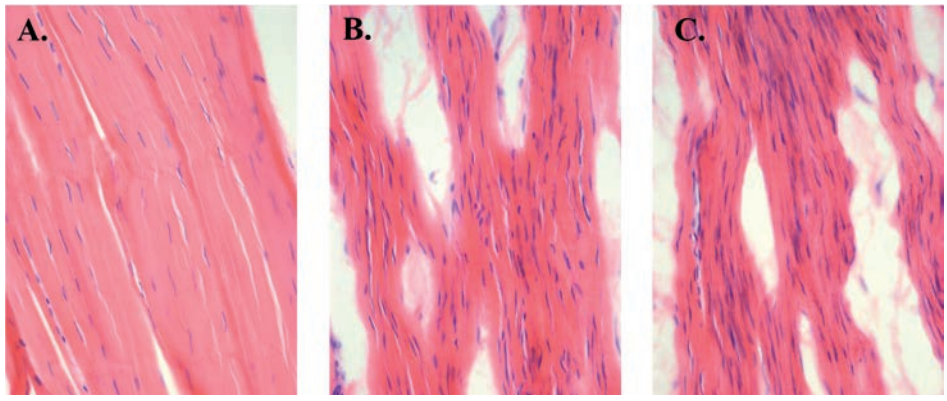

Figure 4. Histologic sections of a normal ACL (A), sutured ACL (B) and sutured ACL with SIS (C). The sections are stained with H&E. Note that the tissue is hypercellular in both the sutured and Suture & SIS ACL and that the nuclei are elongated while in the intact ACL the nuclei are rod-like shaped. ×200

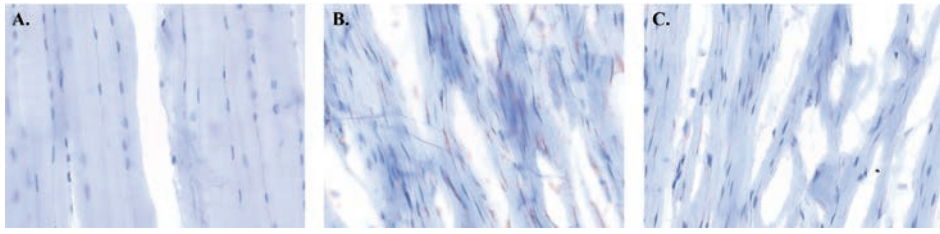

Figure 5. Immunohistologic sections of a normal ACL (A), sutured ACL (B) and sutured ACL with SIS (C). Example of a digital image analysis of α-smooth muscle actin expressing cells. Nuclei stained in blue and α- smooth muscle actin stained in red-brown, identifying α- smooth muscle actin expressing cells. (× 400)

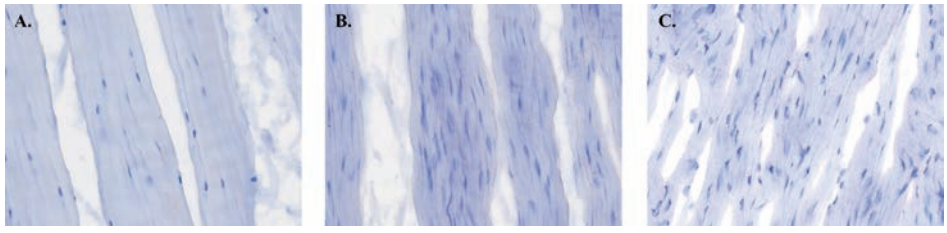

Figure 6. Immunohistologic sections of a normal ACL (A), sutured ACL (B) and sutured ACL with SIS (C). B and C show moderate red-brown staining of collagen type 3. (× 400)

Table 1. Total cell density and myofibroblast cell density in the samples of healing ACL tissue (mean±sd).

	Suture		Suture-SIS	
	Healing	Control	Healing	Control
Number of cells per mm^2	1265 ± 1034	254 ± 92	954 ± 378*	204 ± 93*
Number of myofibroblast per mm^2	642 ± 564	52 ± 22	266 ± 229	36 ± 15
Ratio myofibroblast/total cell density	49%	20%	26%	19%

The difference between Suture-SIS and Control was statistically significant (*paired Student t-test, $p<0.05$). There was no statistical difference between the Suture and Suture-SIS group.

DISCUSSION

Previously, our research group has shown that a new suture technique alone or combined with SIS bioscaffold resulted in healing of the transected goat ACL. (9) Knee laxity and ligament stiffness did not return to normal values. The difference between the Suture, Suture-SIS and intact control group was 53% and 51% respectively. However, the outcome was close to previously reported results of bone-patellar tendon-bone ACL reconstructions in goats. (25, 26) The results of this study shows that the healing ACL in the Suture group displayed typical histological characteristics like those observed in spontaneously-healing ligaments, such as the medial collateral ligament (MCL). The MCL's histological characteristics include, for example, disorganized and less compact organized collagen fibers, increased neovascularization, voids (e.g. lipid vacuoles), increased number of myofibroblasts and elevated content of collagen type 3. (11, 27-29) Therefore, it can be concluded that the ACL has a healing response. Adding SIS to the Suture repair seems to biologically enhance the healing as the collagen fibers were more compactly arranged, contain less collagen type 3, and fewer voids and fat vacuoles. The ratio of myofibroblasts to total cell count was more normal.

Although this study was not designed to elucidate the mechanism behind the effects of SIS on the healing of the ACL, it was likely that the same mechanisms were involved as previously reported. In previous MCL healing studies, it was also shown that SIS acted as a provisional scaffold to promote cell migration and to enhance revascularization and repair. (15-19) SIS treatment resulted in a greater alignment of collagen fibers and cells. Ultrastructurally, the SIS-treated group had larger collagen fibrils, and the gene expression of collagen type V, decorin, biglycan, and lumican in the SIS-treated group were significantly down-regulated, correlating with the improved morphological characteristics and mechanical properties. (16) Other studies have indicated that the hypocellularity of the normal ACL might be a limiting factor leading to the failure of healing of the ACL. However, in this study it was shown that the ACL in the Suture-SIS group can become hypercellular. Thus, hypercellularity may be a positive indicator of ACL healing. Additionally, the fibroblasts in the healing ACLs were not

rodlike-shaped but elongated and arranged in an aligned network. This reticular arrangement, hypercellularity, and phenotype may facilitate cell-to-cell communication and aligned deposition of newly formed collagen. (30-32). The cells that contribute to the healing may originate from the proliferating internal ligament fibroblasts or may be bone marrow-derived or a combination of these. (17, 33, 34) The ratio of myofibroblasts in the SIS treated ACLs neared that of the normal ACL. Whether this normalization represents a good healing response cannot be answered by this study. It may be a positive indicator, as a decrease in myofibroblasts may indicate that the fibroblasts within the SIS-treated ACLs did not need to maintain the contractile phenotype as they experienced less strain within a larger cross-sectional area. Regarding the vasculature, in both experimental groups, neovasculature through the healing ACL was clearly present. In summary, all these histological observations indicate that the whole ACL was involved in the healing of the injury site.

While this study provides some new insights into the histological morphology of the healing ACLs after Suture and Suture-SIS treatment, there were several limitations. The ACLs were not directly frozen into -80˚C which may have influenced and reduced the immunohistological stainings of collagen type 3. Furthermore, the evaluation of the H&E and Lendrum's Masson's trichrome was qualitative, though standard histology is commonly used as it provides a representative impression. Finally, the healing ACLs were examined at one time point which does not allow the evaluation of the healing process over time and there was a limited sample size.

Comparing the histological observations of the healing ACL to the ligamentization of tendon grafts in ACL reconstruction, it was shown that the healing ACLs were vital, while it has been reported that necrotic areas within the core of tendon grafts can still be observed during the ligamentization process at 12 weeks. (35)

Future studies will include rehabilitation protocols in order to prevent excessive loads on the ACL for potentially a better healing, by e.g. (short-term) casting or internal augmentation devices. (6, 10)

In conclusion, the healing ACL in both treated groups showed histological characteristics which are comparable to the spontaneously healing medial collateral ligament and shows that the ACL has a similar intrinsic healing response. The addition of SIS appears to biologically enhance the healing process as shown by a continuous fibrous synovial layer, more compact ECM, fewer voids, more aligned collagen fibers, less collagen type 3, and a decreased ratio of myofibroblasts. Though, no definitive conclusions on the beneficial effects of the SIS scaffold on the healing process can be made.

ACKNOWLEDGEMENTS

The authors are grateful for the technical assistance of Maarten de Boer and advice of Tamara Ramwadhdoebe with the immunohistochemistry experiments. The study was sponsored by Mozaïek PhD training grant 017.004.076 from the Netherlands Organization for Scientific Research (NWO) and the Marti-Keuning Eckhart foundation.

Author Disclosure Statement

The SIS material was provided by Cook Biotech Inc., West Lafayette, IN, USA, under a Material Use Agreement, without any monetary compensation and without any condition. None of the authors had any relation with any other third parties, commercial or otherwise, that has interest in the study or could have influenced the study.

REFERENCES

1. Beynnon BD, Johnson RJ, Abate JA, Fleming BC, Nichols CE. Treatment of anterior cruciate ligament injuries, part 2. Am J Sports Med. 2005;33(11):1751-67. Epub 2005/10/19.
2. Woo SL, Abramowitch SD, Kilger R, Liang R. Biomechanics of knee ligaments: injury, healing, and repair. Journal of biomechanics. 2006;39(1):1-20. Epub 2005/11/08.
3. Busam ML, Provencher MT, Bach BR, Jr. Complications of anterior cruciate ligament reconstruction with bone-patellar tendon-bone constructs: care and prevention. Am J Sports Med. 2008;36(2):379-94. Epub 2008/01/19.
4. Drogset JO, Strand T, Uppheim G, Odegard B, Boe A, Grontvedt T. Autologous patellar tendon and quadrupled hamstring grafts in anterior cruciate ligament reconstruction: a prospective randomized multicenter review of different fixation methods. Knee surgery, sports traumatology, arthroscopy : official journal of the ESSKA. 2010;18(8):1085-93. Epub 2009/12/04.
5. von Porat A, Roos EM, Roos H. High prevalence of osteoarthritis 14 years after an anterior cruciate ligament tear in male soccer players: a study of radiographic and patient relevant outcomes. Ann Rheum Dis. 2004;63(3):269-73. Epub 2004/02/14.
6. Fisher MB, Liang R, Jung HJ, Kim KE, Zamarra G, Almarza AJ, et al. Potential of healing a transected anterior cruciate ligament with genetically modified extracellular matrix bioscaffolds in a goat model. Knee surgery, sports traumatology, arthroscopy : official journal of the ESSKA. 2012;20(7):1357-65. Epub 2011/12/07.
7. Fleming BC, Spindler KP, Palmer MP, Magarian EM, Murray MM. Collagen-platelet composites improve the biomechanical properties of healing anterior cruciate ligament grafts in a porcine model. Am J Sports Med. 2009;37(8):1554-63. Epub 2009/04/02.
8. Murray MM, Spindler KP, Abreu E, Muller JA, Nedder A, Kelly M, et al. Collagen-platelet rich plasma hydrogel enhances primary repair of the porcine anterior cruciate ligament. J Orthop Res. 2007;25(1):81-91. Epub 2006/10/13.
9. Nguyen DT, Geel J, Schulze M, Raschke MJ, Woo SL, van Dijk CN, et al. Healing of the goat anterior cruciate ligament after a new suture repair technique and bioscaffold treatment. Tissue engineering Part A. 2013;19(19-20):2292-9. Epub 2013/06/04.
10. Kohl S, Evangelopoulos DS, Kohlhof H, Hartel M, Bonel H, Henle P, et al. Anterior crucial ligament rupture: self-healing through dynamic intraligamentary stabilization technique. Knee surgery, sports traumatology, arthroscopy : official journal of the ESSKA. 2013;21(3):599-605. Epub 2012/03/23.
11. Menetrey J, Laumonier T, Garavaglia G, Hoffmeyer P, Fritschy D, Gabbiani G, et al. alpha-Smooth muscle actin and TGF-beta receptor I expression in the healing rabbit medial collateral and anterior cruciate ligaments. Injury. 2011;42(8):735-41. Epub 2010/08/31.
12. Hodde JP, Badylak SF, Brightman AO, Voytik-Harbin SL. Glycosaminoglycan content of small intestinal submucosa: a bioscaffold for tissue replacement. Tissue Eng. 1996;2(3):209-17. Epub 1996/10/01.
13. Hodde JP, Ernst DM, Hiles MC. An investigation of the long-term bioactivity of endogenous growth factor in OASIS Wound Matrix. Journal of wound care. 2005;14(1):23-5. Epub 2005/01/20.
14. Voytik-Harbin SL, Brightman AO, Kraine MR, Waisner B, Badylak SF. Identification of extractable growth factors from small intestinal submucosa. J Cell Biochem. 1997;67(4):478-91. Epub 1998/01/24.

15. Gilbert TW, Stewart-Akers AM, Simmons-Byrd A, Badylak SF. Degradation and remodeling of small intestinal submucosa in canine Achilles tendon repair. The Journal of bone and joint surgery American volume. 2007;89(3):621-30. Epub 2007/03/03.
16. Liang R, Woo SL, Nguyen TD, Liu PC, Almarza A. Effects of a bioscaffold on collagen fibrillogenesis in healing medial collateral ligament in rabbits. Journal of orthopaedic research : official publication of the Orthopaedic Research Society. 2008;26(8):1098-104. Epub 2008/03/11.
17. Zantop T, Gilbert TW, Yoder MC, Badylak SF. Extracellular matrix scaffolds are repopulated by bone marrow-derived cells in a mouse model of achilles tendon reconstruction. J Orthop Res. 2006;24(6):1299-309. Epub 2006/05/02.
18. Liang R, Fisher M, Yang G, Hall C, Woo SL. Alpha1,3-galactosyltransferase knockout does not alter the properties of porcine extracellular matrix bioscaffolds. Acta biomaterialia. 2011;7(4):1719-27. Epub 2011/01/11.
19. Raeder RH, Badylak SF, Sheehan C, Kallakury B, Metzger DW. Natural anti-galactose alpha1,3 galactose antibodies delay, but do not prevent the acceptance of extracellular matrix xenografts. Transplant immunology. 2002;10(1):15-24. Epub 2002/08/17.
20. Becker H, Davidoff M. Eliminating the gap in flexor tendon surgery. A new method of suture. The Hand. 1977;9(3):306-11. Epub 1977/10/01.
21. Hatanaka H, Zhang J, Manske PR. An in vivo study of locking and grasping techniques using a passive mobilization protocol in experimental animals. J Hand Surg Am. 2000;25(2):260-9. Epub 2000/03/21.
22. van der Hall PO, Kraan MC, Tak PP. Quantitative image analysis of synovial tissue. Methods in molecular medicine. 2007;135:121-43. Epub 2007/10/24.
23. Haringman JJ, Vinkenoog M, Gerlag DM, Smeets TJ, Zwinderman AH, Tak PP. Reliability of computerized image analysis for the evaluation of serial synovial biopsies in randomized controlled trials in rheumatoid arthritis. Arthritis research & therapy. 2005;7(4):R862-7. Epub 2005/07/01.
24. Tak PP, Thurkow EW, Daha MR, Kluin PM, Smeets TJ, Meinders AE, et al. Expression of adhesion molecules in early rheumatoid synovial tissue. Clinical immunology and immunopathology. 1995;77(3):236-42. Epub 1995/12/01.
25. Spindler KP, Murray MM, Carey JL, Zurakowski D, Fleming BC. The use of platelets to affect functional healing of an anterior cruciate ligament (ACL) autograft in a caprine ACL reconstruction model. J Orthop Res. 2009;27(5):631-8. Epub 2008/11/15.
26. Abramowitch SD, Papageorgiou CD, Withrow JD, Gilbert TW, Woo SL. The effect of initial graft tension on the biomechanical properties of a healing ACL replacement graft: a study in goats. J Orthop Res. 2003;21(4):708-15. Epub 2003/06/12.
27. Frank C, Woo SL, Amiel D, Harwood F, Gomez M, Akeson W. Medial collateral ligament healing. A multidisciplinary assessment in rabbits. Am J Sports Med. 1983;11(6):379-89. Epub 1983/11/01.
28. Faryniarz DA, Chaponnier C, Gabbiani G, Yannas IV, Spector M. Myofibroblasts in the healing lapine medial collateral ligament: possible mechanisms of contraction. J Orthop Res. 1996;14(2):228-37. Epub 1996/03/01.
29. Amiel D, Frank CB, Harwood FL, Akeson WH, Kleiner JB. Collagen alteration in medial collateral ligament healing in a rabbit model. Connective tissue research. 1987;16(4):357-66. Epub 1987/01/01.

30. Nguyen TD, Liang R, Woo SL, Burton SD, Wu C, Almarza A, et al. Effects of cell seeding and cyclic stretch on the fiber remodeling in an extracellular matrix-derived bioscaffold. Tissue engineering Part A. 2009;15(4):957-63. Epub 2008/09/12.
31. Wang JH, Jia F, Gilbert TW, Woo SL. Cell orientation determines the alignment of cell-produced collagenous matrix. Journal of biomechanics. 2003;36(1):97-102. Epub 2002/12/18.
32. Birk DE, Zycband E. Assembly of the tendon extracellular matrix during development. Journal of anatomy. 1994;184 (Pt 3):457-63. Epub 1994/06/01.
33. Badylak SF, Park K, Peppas N, McCabe G, Yoder M. Marrow-derived cells populate scaffolds composed of xenogeneic extracellular matrix. Experimental hematology. 2001;29(11):1310-8. Epub 2001/11/08.
34. Beattie AJ, Gilbert TW, Guyot JP, Yates AJ, Badylak SF. Chemoattraction of progenitor cells by remodeling extracellular matrix scaffolds. Tissue engineering Part A. 2009;15(5):1119-25. Epub 2008/10/08.
35. Kondo E, Yasuda K, Katsura T, Hayashi R, Kotani Y, Tohyama H. Biomechanical and histological evaluations of the doubled semitendinosus tendon autograft after anterior cruciate ligament reconstruction in sheep. Am J Sports Med. 2012;40(2):315-24. Epub 2011/11/18.

Chapter 10

Discussion and Conclusions

"Man surprised me most about humanity. Because he sacrifices his health in order to make money. Then he sacrifices money to recuperate his health..." - Dalai Lama XIV

The main objective of the studies presented in this doctoral thesis is to improve the clinical outcome of patients who have torn their anterior cruciate ligament (ACL) by optimizing the current ACL reconstruction technique and by developing a bio-enhanced end-to-end ACL repair technique to heal the ACL. This main objective led to specific aims as described in chapter 1 and can be categorized into four themes: 1) obtaining near-objective and detailed information of the ACL's anatomy, 2) the development of the Arthroscopic Fluorescence Imaging system, 3) *in vitro* and *in vivo* evaluation of Small Intestine Submucosa bioscaffold, and finally 4) the development of a bio-enhanced end-to-end ACL repair technique to heal the ACL. The main findings and implications of this thesis are discussed in this chapter and recommendations for future research are given.

MAIN FINDINGS & IMPLICATIONS

Anatomy

Objective and detailed information of the ACL's anatomy is fundamental for understanding of its function as well as for developing effective treatments. Previously, researchers have manually dissected the ACL and illustrated the fiber orientation. (*1-6*) Manual digitizing systems have also been used to obtain the fiber bundle orientation, though the user of this system visually traces selected fiber bundles at a macroscopic scale. (*7*) Other researchers have used three dimensional representations of ligaments by quantifying the geometry of the bundle volume using MRI. (*8, 9*) Although, the resolution of these imaging modalities is insufficient to visualize the detailed fiber architecture of the ACL. On the other hand, current high resolution imaging modalities such as scanning electron microscopy (SEM), transmission electron microscopy (TEM), confocal microscopy, 3-D histology, and small angle light scattering are limited in the sample volume. (*10-13*) In order to quantify the whole ACL at a high resolution a new methodology was developed and validated (**chapter 2**). This methodology enabled us to obtain the 3-D collagen fiber anatomy and answer the clinical question whether the ACL consists of anatomically distinct fiber bundles. The methodology combined fluorescence imaging, the imaging cryomicrotome and fiber tracking software which provides unique and novel features. It allowed for obtaining: 1) near-objective anatomical data, 2) accurate data collection, 3) data collection at a high-resolution and 4) reconstruction of the 3-D collagen fiber tracts, length and connectivity maps. The implication of this study is that a new research platform was developed to obtain accurate, near-objective and detailed anatomical information of the ACL which can also be used for other ligaments and collagenous load bearing tissues, such as menisci, intervertebral discs, heart valves, etc.

The existing literature on the fiber anatomy of the ACL is contradictory. Some researchers report that the ACL is a single broad continuum of fascicles, with different

portions taut throughout the range of motion. (*1, 5*) Others report that the ACL is divisible into two bundles, namely an anteromedial bundle (AMB) and a posterolateral bundle (PLB). (*2, 3*) Others defined three functional bundles, namely anteromedial AMB, a PLB and an intermediate bundle (IMB). A conceivable explanation for this discrepancy is the subjective methodology used in these studies. With the aid of the near-objective methodology developed in chapter 2, the 3-D collagen fiber anatomy in three human knees was quantified (**chapter 3**). The preliminary finding is that the ACL is a single continuous construct of collagen fibers with short fibers posterolaterally and gradually longer fibers towards anteromedially. This preliminary conclusion does not support the current concept that the ACL has two or three anatomically distinct bundles and consequently the concept of anatomic double or triple bundle ACL reconstructions. (*14-19*) However, anatomic double or triple bundle ACL reconstruction does effectively mimic the anatomy of the ACL by placing the shorter tendon graft posterolaterally and the longer tendon graft anteromedially. Thus, anatomic double or triple bundle ACL reconstructions are encouraged but with a different rationale. The careful implication of this pilot study is that it provides basic knowledge of the ACL and that the acquired 3-D collagen fiber anatomy can be used as a blueprint for developing bio-enhanced end-to-end ACL repair techniques, finite element modeling and rehabilitation protocols.

ARTHROSCOPIC FLUORESCENCE IMAGING SYSTEM

The surgical outcome after ACL reconstruction is largely dependent on accurate tendon graft placement at the native insertion sites of the ruptured ACL. (*14, 20-27*) Graft misplacement is the most common cause for revision surgery. (*23-27*) Small deviations can result in large changes in knee stability. (*28-30*) Previous morphometric studies by Bernard and Hertel and by Amis and Jakob have been performed to guide graft placement. (*31, 32*) However, arthroscopic graft placement is still challenging due to visual and technical limitations. In the late 1980's, the so-called "transtibial" ACL reconstruction technique along with a guiding instrument was introduced. This technique allowed for standardized and fast graft placement and has since been the most used technique. (*33, 34*) However, the transtibial technique has been criticized for being inaccurate. (*20, 35, 36*) In a commentary, Howell, Hull and McAllister stated: "…we should be sensible and cautious about criticizing the placement of tunnels by other surgeons until instrumentation for placing the tunnels with greater precision is available and until the intended targets have been universally agreed on". (*37*) It is reported that around 5% of the transtibial ACL reconstruction fails and that around 50% of these failures is caused by graft misplacement. (*23-27*) A recent meta-analysis shows that only 41% of patients reported their reconstructed knee as normal. (*38*) More recently, long-term clinical follow up studies revealed that 70-80% of the ACL

reconstructed patients developed early osteoarthrosis. (*28-30, 39, 40*) Although the mechanisms that contribute to this early joint degeneration are likely multifactorial, several studies suggest that the inability of transtibial ACL reconstructions to restore normal joint kinematics plays an important role in the development of early OA. These perturbing studies prompted additional research effort to optimize the transtibial ACL reconstruction technique. Some surgeons have modified the transtibial technique while others abandoned this technique and rely on arthroscopic visualization of anatomical landmarks such as the posterior wall, cartilage edge, the lateral intercondylar ridge, and bifurcate ridge to locate the native insertion sites. (*18, 41-45*) These methods though, are time consuming and demanding due to the visual limitations, careful dissection, biological variability, and additional visual impairment in the injured and degenerated joint. Hence, the "transtibial" technique was introduced to circumvent these difficulties. Despite these difficulties, an increasing number of surgeons are recognizing the importance of the anatomic ACL reconstruction technique. Previous laboratory studies have shown that the anatomic ACL reconstruction is better in restoring the intact knee kinematics. (*46-49*) Recently, Abebe et al., showed in a clinical study that the anatomic ACL reconstruction is superior to the transtibial ACL reconstruction technique in restoring the in-vivo knee kinematics. (*50*) Several aides for arthroscopic visualization have been proposed to assist anatomic ACL reconstructions, including intraoperative fluoroscopic (*51-54*) and computer-aided navigation systems. (*55-57*) The use of these systems, however are often criticized for expensive, time consuming, and ionizing hazards. (*37, 58, 59*)

Another strategy to aid arthroscopic visualization objectively is by fluorescence imaging of the insertion sites (**chapter 4**). Fluorescence imaging is based on the detection of emitted photons after excitation of a fluorphore by photons of a certain wavelength. Using fluorescent markers against precancerous, tumors and metastasis researchers have previously shown to real time visualize the targeted structures in contrasting pseudo-colors. The visualization enabled for more complete tumor resection and even resection of precancerous tissues that would not have been detected with white-light. (*60, 61*) As the ACL is mainly made up of collagen which is autofluorescent, imaging of the collagen's autofluorescence turned out to be advantageous in visualizing joint structures. The difference in spectral responses could be separated by spectral unmixing. The difference could be displayed in contrasting pseudo-colors to discern the native ACL insertion site from its background. The arthroscopic fluorescence imaging (AFI) system have demonstrated its feasibility and potential in being a fast, easy, cheap, real-time, patient-specific method to accurate visualize of the native ACL insertion sites. Currently, the AFI system is further developed for the use in patients. Its value will be evaluated in future clinical trials. The clinical implication is that around 50% of the revision surgeries caused by misplacement may be prevented and

the AFI system may facilitate the paradigm shift towards anatomical ACL reconstruction which eventually may prevent early osteoarthrosis. Additionally, the AFI system may also be the platform for color-guided arthroscopic surgery in other joints and may be valuable in diagnosis and staging of degeneration of other collagenous tissues.

A TISSUE ENGINEERING APPROACH

Previously, surgeons have tried to heal the ruptured ACL by suturing the ends together with multiple U-loops. (*62-66*) The initial results were fairly good though the outcome was unpredictable. The long-term results were not satisfactory. (*65, 67-69*) In time this has led to the common opinion that the torn ACL does not heal. Though, the idea of healing the ACL remained appealing. To find a solution to heal the ACL, many researchers started to study the healing of the medial collateral ligament (MCL) to unravel the mechanisms involved in ligament healing. (*70-84*) Its spontaneous healing potential, accessibility and high aspect ratio make the MCL an ideal study model. Researchers have shown that MCL healing goes through three dynamic healing phases though the biomechanical properties, histomorphological appearance, and biochemical composition of the healed MCL remain abnormal when compared to those of the normal MCL. (*70-82*) Additionally, (developmental) research on other ligaments & tendons has led to an increase of fundamental knowledge during the past decades. (*85-92*) Along these milestones, new Functional Tissue Engineering (FTE) approaches such as the use of growth factors, gene therapy, cell therapy and scaffolds were developed to improve the healing of ligaments and tendons. (*93-102*) Especially, bioactive scaffolds such as porcine Small Intestine Submucosa (SIS) have recently been extensively researched and has shown good results in improving the healing of the MCL. (*96, 103, 104*) SIS is mainly composed of collagen type I and contains bioactive factors. In the rabbit model, the application of SIS to the healing medial collateral ligament (MCL) resulted in improved mechanical and histomorphological properties. These positive effects have been attributed to its ability to act as a provisional scaffold and its growth and chemotactic factors that can promote cell migration into the healing site to enhance revascularization and tissue repair. (*105-108*) The early effects of SIS on the collagen fibrillogenesis in the healing ligaments remained to be elucidated (**chapter 5**). The main finding is that the quantitative real-time PCR showed that the mRNAs of collagen type V, decorin, biglycan, and lumican in the SIS-treated group were 41, 58, 51, and 43% significantly lower than those in the nontreated group, respectively. Such significant reduction in the gene expressions are closely related to the improved morphological characteristics, which are known to be coupled with better mechanical properties, as previously reported in longer term studies. The implication of this study was that SIS is a good candidate to be used ACL healing based on its bioactive agents and conductive properties.

The SIS bioscaffolds can be further improved by altering their ultrastructure to be closer to that of the highly aligned collagen fiber orientation of native ligaments. An approach to achieve this goal is to seed the SIS with fibroblasts and cyclic stretch the construct (**chapter 6**). Studies have shown that cells have the tendency to avoid axial surface strain. (*109-111*) When cells were embedded in a fibrous substrate, the cells tended to align along the fibers in the stretching direction (stress shielding) and remodel the matrix rapidly by upregulating matrix metalloproteinases (MMPs). (*112-114*) Additionally, aligned fibroblast along the stretch direction deposit aligned *de novo* collagen fibers. (*115, 116*) The main finding of this study was that a combination of fibroblast seeding and cyclic uniaxial stretch can effectively improve the collagen fiber alignment in the ECM-SIS bioscaffold toward the axis of the applied stretch, while mechanical stretch or cell seeding alone was not sufficient to affect the ultrastructure of the scaffold. These findings emphasized the importance of the synergistic effects of cells and mechanical stimuli in the process of matrix remodeling.

BIO-ENHANCED END-TO-END ACL REPAIR

Healing of the torn ACL is a potential strategy to restore the function of the ACL, eliminate the need for a tendon graft harvest and circumvent other ACL reconstruction surgery specific issues. The thought of healing the ACL became recently more feasible and at the right time thanks to the exciting results of FTE approaches and due to the suboptimal results of ACL reconstructions. (*117-121*) Although, the common opinion is that the ACL does not have an intrinsic healing potential, case-reports have previously indicated the spontaneous healing potential of the ruptured ACL (*119, 122-124*) Surgeons also experimented with surgical interventions to stimulate the healing of the ACL. (*117, 125, 126*) Dr. Steadman reinserted proximal ACL tears near the femoral insertion site while additional blood and bone marrow cells were recruited by microfracturing the adjacent bone to elicit a healing response. He showed that the "healing response" technique resulted in ACL healing and improved knee stability. (*117*) However, 23% of these patients had a reinjury that required an ACL reconstruction. A limitation that was reported was the careful patient selection. Along these clinical studies, laboratory studies have found and hypothesized that many factors such as the local environment and intrinsic factors have a profound effect on ACL healing. (*78*) Follow up studies showed that ACL fibroblasts can be stimulated through the use of growth factors, platelet-rich plasma (PRP) and a scaffold (*120, 127-129*) Additionally, researchers have evaluated the failure of primary ACL repair and speculated that the suture repair technique and rehabilitation were not adequate. (*67, 130*) In 2007, Murray, Fleming et al. showed the feasibility of a bio-enhanced ACL repair technique with the use of PRP to treat ACL injuries. In a porcine model, the transected ACL was suture repaired with U-loops and augmented with non-absorbable sutures as reinforcement.

The results showed improved biomechanical results. However, the results were still below the normal ACL. (*120, 131*) Fisher et al., developed a bio-enhanced ACL repair with the use of PRP, SIS and U-loops with non-absorbable sutures. (*118*) The results showed improved biomechanical results, though the results also did not match the normal ACL. Our study was aimed at addressing two major constraining factors by using a new suture technique with absorbable sutures in combination with the SIS bioscaffold (**Chapter 7**). The first objective was to apply a new suture technique that has a higher tensile and pull-out strength then previously used suture techniques such as the grasping U-loops or multiple depth suture. It was postulated that the new suture technique will approximate and keep the ACL torn ends together and thus will lead to healing. The second objective is to evaluate the effect of small intestinal submucosa (SIS) bioscaffold as an initiator and enhancer on the healing of the ACL. Others studies have shown that SIS can provide a collagenous matrix to promote cell migration into the healing site to enhance revascularization and repair. (*17-19*) The main finding shows that the transected ACL in a goat model can heal with the new approach and that contact is a requirement for healing of the intra-articular situated ACL. Compared to recent research that focused on suture repair of the ACL in combination with platelet-rich plasma (PRP) delivery and scaffolds, (*118, 120*) the results of our study are similar in terms of the functional outcomes. The total AP translations of the treated ACL was four times greater than of the intact control under 67N anterior and posterior tibial load. Fisher et al., found a three times increase with the same AP load and Fleming, Murray et al., found a 3.5 fold increase in anterior tibial translation with a 35N anterior tibial load. The stiffnesses of the healed ACL, as compared to control, was respectively 23% in our study, 42% for Fisher et al., and 25% for Fleming, Murray et al. Besides similarities there are also differences between these studies. For example, the other studies used an augmentation, where the current study was relying only on the locking suture technique with absorbable sutures. Comparing, the results of these bio-enhanced ACL repair studies to the previously reported results of bone-patellar tendon-bone ACL reconstructions in goats. It can be concluded that the outcome was comparable to the ACL reconstruction. (*132, 133*) Most recently, Kohl et al., devised another approach to heal the ACL. A dynamic intraligamentary stabilization (DIS) device was developed to string the ACL ends while holding the knee in constant posterior translation. Self-healing of the ACL would be facilitated with the ACL ends in proximity. Additionally, a collagen sheath was placed around the ACL, PRP was applied and bone marrow stimulation at the femoral insertion site was used. The results were promising but the results were lower than the previously reported bio-enhanced (end-to-end) ACL repair techniques. Next to ACL healing studies that transect the ACL in its midsubstance there are studies that transect the ACL at its

femoral insertion site. (*121, 134*) The results of these studies demonstrate that the ACL has also a healing response at the femoral insertion site.

Histological studies on the healing ACL have not been often reported. (*118, 120*) Therefore, it was of interest to evaluate the healing ACLs in terms of the appearance of the synovial layer, the extracellular matrix (ECM), collagen fiber orientation, cellularity, ratio of myofibroblasts and collagen type 3 staining (**Chapter 8**). The main finding is that the healing ACL is hypercellular and appeared to be hypervascular. Additionally, the healing ACLs displayed typical histological characteristics which can also be observed in healing ligaments that can spontaneously heal such as the MCL. (*81*)

Previously, it was sometimes observed that the human tibial remnant of the ruptured ACL was attached to PCL or the intercondylar notch. This reattachment phenomenon implies that the ACL does have a healing potential even without any suturing. However there were no histologic evaluations from these reattachments to further backbone this conclusion. (*135-137*) In **Chapter 9** further evidence is provided that the human ACL does have an intrinsic healing potential. The results not only demonstrate the healing potential based on gross morphological characteristics but additionally show the typical histological characteristics that are seen in the healing process in the MCL. The implication of this study together with the Chapter 7, 8 and the existing literature is that there is sufficient support to warrant future translational studies to develop and evaluate the bio-enhanced end-to-end suture repair of the torn ACL in humans. However, we have to keep in mind that the torn ACL within the injured knee is not the only and sole cause for knee instability. It might be possible that instability remains in an injured knee even after a seamless healed ACL. A quantitative diagnostic tool for multi-directional knee instability would be of great value in identifying and grading the degree of other injured or outstretched knee stabilizers. Most recently, additional treatments such as extra-articular procedures have been revisited and proposed in order to improve the patient outcome with ACL reconstructions. (*138*)

RECOMMENDATIONS FOR FUTURE RESEARCH

In this doctoral thesis several experimental and translational studies were performed. The methodology to quantify the 3-D collagen fiber orientation of the ACL may also be a useful tool to obtain the fiber architecture of other collagenous structures such as menisci, the intervertebral disc, heart valves, etc. The knowledge of the detailed fiber anatomy of the load bearing structures may increase our understanding of the function and pathophysiology of these structures. The fiber anatomy can be a blueprint to guide the development of new treatments. A follow-up study with a larger sample size would be helpful to further support and generalize the conclusion made in chapter 3 on the ACL fiber anatomy.

Regarding the fluorescence arthroscopy. Currently, the AFI system is further developed for clinical use and its value for anatomical ACL reconstruction in patients has yet to be evaluated. The AFI system may also be used as a clinical platform for color-guided arthroscopic surgery in other joints and may be valuable in diagnosis and staging of degeneration of other collagenous tissues.

The experimental and pre-translational studies were performed in order to warrant future translational studies to heal the human ACL. A semi-automatic suturing device for relatively fast, fine and meticulously end-to-end suturing of the torn ACL while respecting the ACL's anatomy and biology may be needed. As it is of utmost importance to have a grossly end-to-end ACL repair with a high pull-out strength. Furthermore, a proper rehabilitation protocol needs to be devised. Finally, feel free to contact me for questions, advice, and brainstorming for future research.

CONCLUSIONS

The research performed in this doctoral thesis aimed at developing new methods to optimize the surgical treatment of patients with anterior cruciate ligament (ACL) tears. The first conclusion is that the cryo-imaging system combined with tractography is a near objective and accurate methodology to quantify the 3-D fiber orientation of the ACL. The second conclusion though preliminary is that the ACL is a single continuous construct of collagen fibers with short fibers posterolaterally and gradually longer fibers towards anteromedially. The third conclusion is that the AFI system can accurately and real-time visualize the native insertion site. The AFI system will soon be evaluated in patients. The fourth conclusion is that SIS can enhance the collagen fibrillogenesis. The fifth conclusion is that only the combination of cyclic stretch and cell-seeding is effective in remodeling the ultrastructure of SIS. The sixth conclusion is that the transected goat ACL can heal after the experimental bio-enhanced end-to-end ACL repair technique with the triple X locking suture technique and SIS. The seventh conclusion is that the healing goat ACL shows histological characteristics which are comparable to the spontaneously healing medial collateral ligament and shows that the ACL has a similar intrinsic healing potential. The eighth and final conclusion is that the human ACL has an intrinsic healing response. The combination of conclusions six, seven and eight shows the feasibility of translating the bio-enhanced end-to-end ACL repair technique to humans. Yet, healing the ACL may not be the whole solution due to the fact that other passive knee stabilizers may be injured and that the active stabilizers may not be suffice. As such, one should be mindful as there is still no panacea. Therefore, prevention where possible is the only and best treatment! Not only for ACL injuries but for human health in general.

REFERENCES

1. F. K. Fuss, Anatomy of the cruciate ligaments and their function in extension and flexion of the human knee joint. *The American journal of anatomy* 184, 165 (Feb, 1989).
2. F. G. Girgis, J. L. Marshall, A. Monajem, The cruciate ligaments of the knee joint. Anatomical, functional and experimental analysis. *Clinical orthopaedics and related research*, 216 (Jan-Feb, 1975).
3. K. Hara *et al.*, Anatomy of normal human anterior cruciate ligament attachments evaluated by divided small bundles. *The American journal of sports medicine* 37, 2386 (Dec, 2009).
4. L. A. Norwood, M. J. Cross, Anterior cruciate ligament: functional anatomy of its bundles in rotatory instabilities. *The American journal of sports medicine* 7, 23 (Jan-Feb, 1979).
5. M. Odensten, J. Gillquist, Functional anatomy of the anterior cruciate ligament and a rationale for reconstruction. *The Journal of bone and joint surgery. American volume* 67, 257 (Feb, 1985).
6. A. Chhabra *et al.*, Anatomic, radiographic, biomechanical, and kinematic evaluation of the anterior cruciate ligament and its two functional bundles. *The Journal of bone and joint surgery. American volume* 88 Suppl 4, 2 (Dec, 2006).
7. T. J. Mommersteeg *et al.*, The fibre bundle anatomy of human cruciate ligaments. *Journal of anatomy* 187 (Pt 2), 461 (Oct, 1995).
8. H. Steckel, G. Vadala, D. Davis, F. H. Fu, 2D and 3D 3-tesla magnetic resonance imaging of the double bundle structure in anterior cruciate ligament anatomy. *Knee surgery, sports traumatology, arthroscopy : official journal of the ESSKA* 14, 1151 (Nov, 2006).
9. M. J. Breitenseher, M. E. Mayerhoefer, Oblique MR imaging of the anterior cruciate ligament based on three-dimensional orientation. *Journal of magnetic resonance imaging : JMRI* 26, 794 (Sep, 2007).
10. M. S. Sacks, D. B. Smith, E. D. Hiester, A small angle light scattering device for planar connective tissue microstructural analysis. *Annals of biomedical engineering* 25, 678 (Jul-Aug, 1997).
11. P. P. Provenzano, C. Hurschler, R. Vanderby, Jr., Microstructural morphology in the transition region between scar and intact residual segments of a healing rat medial collateral ligament. *Connective tissue research* 42, 123 (Oct, 2001).
12. P. T. Hadjicostas, P. N. Soucacos, N. Koleganova, G. Krohmer, I. Berger, Comparative and morphological analysis of commonly used autografts for anterior cruciate ligament reconstruction with the native ACL: an electron, microscopic and morphologic study. *Knee surgery, sports traumatology, arthroscopy : official journal of the ESSKA* 16, 1099 (Dec, 2008).
13. M. P. Rubbens *et al.*, Quantification of the temporal evolution of collagen orientation in mechanically conditioned engineered cardiovascular tissues. *Annals of biomedical engineering* 37, 1263 (Jul, 2009).
14. P. S. Cha *et al.*, Arthroscopic double-bundle anterior cruciate ligament reconstruction: an anatomic approach. *Arthroscopy : the journal of arthroscopic & related surgery : official publication of the Arthroscopy Association of North America and the International Arthroscopy Association* 21, 1275 (Oct, 2005).
15. H. W. Mott, Semitendinosus anatomic reconstruction for cruciate ligament insufficiency. *Clinical orthopaedics and related research*, 90 (Jan-Feb, 1983).
16. T. Muneta *et al.*, Two-bundle reconstruction of the anterior cruciate ligament using semitendinosus tendon with endobuttons: operative technique and preliminary results. *Arthroscopy : the journal of arthroscopic & related surgery : official publication of the Arthroscopy Association of North America and the International Arthroscopy Association* 15, 618 (Sep, 1999).

17. N. K. Shino K, Nakamura N, Mae T, Ohtsubo H, Iwahashi T, Nakagawa S, Anatomic anterior cruciate ligament reconstruction using two double-looped hamstring tendon grafts via twin femoral and triple tibial tunnels. *Oper Tech Orthop* 15, 130 (2005).
18. K. Yasuda *et al.*, Anatomic reconstruction of the anteromedial and posterolateral bundles of the anterior cruciate ligament using hamstring tendon grafts. *Arthroscopy : the journal of arthroscopic & related surgery : official publication of the Arthroscopy Association of North America and the International Arthroscopy Association* 20, 1015 (Dec, 2004).
19. T. Rosenberg, B. Graf. (Mansfield, MA: Acufex Microsurgical, 1994).
20. M. P. Arnold, J. Kooloos, A. van Kampen, Single-incision technique misses the anatomical femoral anterior cruciate ligament insertion: a cadaver study. *Knee surgery, sports traumatology, arthroscopy : official journal of the ESSKA* 9, 194 (Jul, 2001).
21. E. Lopez-Vidriero, D. Hugh Johnson, Evolving concepts in tunnel placement. *Sports medicine and arthroscopy review* 17, 210 (Dec, 2009).
22. C. F. van Eck *et al.*, Evidence to support the interpretation and use of the anatomic anterior cruciate ligament reconstruction checklist. *The Journal of bone and joint surgery. American volume* 95, e1531 (Oct 16, 2013).
23. L. Rahr-Wagner, T. M. Thillemann, A. B. Pedersen, M. C. Lind, Increased risk of revision after anteromedial compared with transtibial drilling of the femoral tunnel during primary anterior cruciate ligament reconstruction: results from the Danish Knee Ligament Reconstruction Register. *Arthroscopy : the journal of arthroscopic & related surgery : official publication of the Arthroscopy Association of North America and the International Arthroscopy Association* 29, 98 (Jan, 2013).
24. J. A. Morgan, D. Dahm, B. Levy, M. J. Stuart, Femoral tunnel malposition in ACL revision reconstruction. *The journal of knee surgery* 25, 361 (Nov, 2012).
25. P. E. Greis, D. L. Johnson, F. H. Fu, Revision anterior cruciate ligament surgery: causes of graft failure and technical considerations of revision surgery. *Clinics in sports medicine* 12, 839 (Oct, 1993).
26. C. Sommer, N. F. Friederich, W. Muller, Improperly placed anterior cruciate ligament grafts: correlation between radiological parameters and clinical results. *Knee surgery, sports traumatology, arthroscopy : official journal of the ESSKA* 8, 207 (2000).
27. C. Trojani *et al.*, Causes for failure of ACL reconstruction and influence of meniscectomies after revision. *Knee surgery, sports traumatology, arthroscopy : official journal of the ESSKA* 19, 196 (Feb, 2011).
28. K. P. Spindler *et al.*, Prognosis and predictors of ACL reconstructions using the MOON cohort: a model for comparative effectiveness studies. *J Orthop Res* 31, 2 (Jan, 2013).
29. L. J. Salmon *et al.*, Long-term outcome of endoscopic anterior cruciate ligament reconstruction with patellar tendon autograft: minimum 13-year review. *The American journal of sports medicine* 34, 721 (May, 2006).
30. A. von Porat, E. M. Roos, H. Roos, High prevalence of osteoarthritis 14 years after an anterior cruciate ligament tear in male soccer players: a study of radiographic and patient relevant outcomes. *Ann Rheum Dis* 63, 269 (Mar, 2004).
31. M. Bernard, P. Hertel, H. Hornung, T. Cierpinski, Femoral insertion of the ACL. Radiographic quadrant method. *The American journal of knee surgery* 10, 14 (Winter, 1997).
32. A. A. Amis, R. P. Jakob, Anterior cruciate ligament graft positioning, tensioning and twisting. *Knee surgery, sports traumatology, arthroscopy : official journal of the ESSKA* 6 Suppl 1, S2 (1998).

33. M. P. Arnold, N. F. Friederich, W. Muller, M. T. Hirschmann, From open to arthroscopic anatomical ACL-reconstructions: the long way round. A statement paper. *Knee surgery, sports traumatology, arthroscopy : official journal of the ESSKA* 21, 1478 (Jul, 2013).
34. T. R. Duquin, W. M. Wind, M. S. Fineberg, R. J. Smolinski, C. M. Buyea, Current trends in anterior cruciate ligament reconstruction. *The journal of knee surgery* 22, 7 (Jan, 2009).
35. E. J. Strauss *et al.*, Can anatomic femoral tunnel placement be achieved using a transtibial technique for hamstring anterior cruciate ligament reconstruction? *The American journal of sports medicine* 39, 1263 (Jun, 2011).
36. D. E. Meuffels, M. Reijman, J. A. Verhaar, Computer-assisted surgery is not more accurate or precise than conventional arthroscopic ACL reconstruction: a prospective randomized clinical trial. *The Journal of bone and joint surgery. American volume* 94, 1538 (Sep 5, 2012).
37. S. M. Howell, M. Hull, D. McAllister, Be sensible and cautious about criticizing tunnel placement in ACL reconstruction. *The Journal of bone and joint surgery. American volume* 94, e133 (Sep 5, 2012).
38. D. J. Biau, C. Tournoux, S. Katsahian, P. Schranz, R. Nizard, ACL reconstruction: a meta-analysis of functional scores. *Clinical orthopaedics and related research* 458, 180 (May, 2007).
39. J. O. Drogset *et al.*, Autologous patellar tendon and quadrupled hamstring grafts in anterior cruciate ligament reconstruction: a prospective randomized multicenter review of different fixation methods. *Knee surgery, sports traumatology, arthroscopy : official journal of the ESSKA* 18, 1085 (Aug, 2010).
40. L. A. Pinczewski *et al.*, A 10-year comparison of anterior cruciate ligament reconstructions with hamstring tendon and patellar tendon autograft: a controlled, prospective trial. *The American journal of sports medicine* 35, 564 (Apr, 2007).
41. C. G. Ziegler *et al.*, Arthroscopically pertinent landmarks for tunnel positioning in single-bundle and double-bundle anterior cruciate ligament reconstructions. *The American journal of sports medicine* 39, 743 (Apr, 2011).
42. M. Ferretti, M. Ekdahl, W. Shen, F. H. Fu, Osseous landmarks of the femoral attachment of the anterior cruciate ligament: an anatomic study. *Arthroscopy : the journal of arthroscopic & related surgery : official publication of the Arthroscopy Association of North America and the International Arthroscopy Association* 23, 1218 (Nov, 2007).
43. L. D. Farrow, M. R. Chen, D. R. Cooperman, B. N. Victoroff, D. B. Goodfellow, Morphology of the femoral intercondylar notch. *The Journal of bone and joint surgery. American volume* 89, 2150 (Oct, 2007).
44. T. Mae *et al.*, Anatomic double-bundle anterior cruciate ligament reconstruction using hamstring tendons with minimally required initial tension. *Arthroscopy : the journal of arthroscopic & related surgery : official publication of the Arthroscopy Association of North America and the International Arthroscopy Association* 26, 1289 (Oct, 2010).
45. C. F. van Eck, B. P. Lesniak, V. M. Schreiber, F. H. Fu, Anatomic single- and double-bundle anterior cruciate ligament reconstruction flowchart. *Arthroscopy : the journal of arthroscopic & related surgery : official publication of the Arthroscopy Association of North America and the International Arthroscopy Association* 26, 258 (Feb, 2010).
46. T. Zantop *et al.*, Anatomical and nonanatomical double-bundle anterior cruciate ligament reconstruction: importance of femoral tunnel location on knee kinematics. *The American journal of sports medicine* 36, 678 (Apr, 2008).

47. Y. Yamamoto *et al.*, Knee stability and graft function after anterior cruciate ligament reconstruction: a comparison of a lateral and an anatomical femoral tunnel placement. *The American journal of sports medicine* 32, 1825 (Dec, 2004).
48. M. Herbort, S. Lenschow, F. H. Fu, W. Petersen, T. Zantop, ACL mismatch reconstructions: influence of different tunnel placement strategies in single-bundle ACL reconstructions on the knee kinematics. *Knee surgery, sports traumatology, arthroscopy : official journal of the ESSKA* 18, 1551 (Nov, 2010).
49. V. Musahl *et al.*, Varying femoral tunnels between the anatomical footprint and isometric positions: effect on kinematics of the anterior cruciate ligament-reconstructed knee. *The American journal of sports medicine* 33, 712 (May, 2005).
50. E. S. Abebe *et al.*, The effects of femoral graft placement on in vivo knee kinematics after anterior cruciate ligament reconstruction. *Journal of biomechanics* 44, 924 (Mar 15, 2011).
51. B. J. Larson, J. Egbert, E. M. Goble, Radiation exposure during fluoroarthroscopically assisted anterior cruciate reconstruction. *The American journal of sports medicine* 23, 462 (Jul-Aug, 1995).
52. G. Moloney *et al.*, Use of a fluoroscopic overlay to assist arthroscopic anterior cruciate ligament reconstruction. *The American journal of sports medicine* 41, 1794 (Aug, 2013).
53. Y. Kawakami *et al.*, The accuracy of bone tunnel position using fluoroscopic-based navigation system in anterior cruciate ligament reconstruction. *Knee surgery, sports traumatology, arthroscopy : official journal of the ESSKA* 20, 1503 (Aug, 2012).
54. T. V. Klos *et al.*, Computer assistance in arthroscopic anterior cruciate ligament reconstruction. *Clinical orthopaedics and related research*, 65 (Sep, 1998).
55. S. Zaffagnini, T. V. Klos, S. Bignozzi, Computer-assisted anterior cruciate ligament reconstruction: an evidence-based approach of the first 15 years. *Arthroscopy : the journal of arthroscopic & related surgery : official publication of the Arthroscopy Association of North America and the International Arthroscopy Association* 26, 546 (Apr, 2010).
56. A. Burkart *et al.*, Precision of ACL tunnel placement using traditional and robotic techniques. *Computer aided surgery : official journal of the International Society for Computer Aided Surgery* 6, 270 (2001).
57. V. Dessenne *et al.*, Computer-assisted knee anterior cruciate ligament reconstruction: first clinical tests. *Journal of image guided surgery* 1, 59 (1995).
58. G. Rivkin, M. Liebergall, Challenges of technology integration and computer-assisted surgery. *The Journal of bone and joint surgery. American volume* 91 Suppl 1, 13 (Feb, 2009).
59. P. Kasten *et al.*, What is the role of intra-operative fluoroscopic measurements to determine tibial tunnel placement in anatomical anterior cruciate ligament reconstruction? *Knee surgery, sports traumatology, arthroscopy : official journal of the ESSKA* 18, 1169 (Sep, 2010).
60. Q. T. Nguyen, R. Y. Tsien, Fluorescence-guided surgery with live molecular navigation--a new cutting edge. *Nature reviews. Cancer* 13, 653 (Sep, 2013).
61. A. L. Vahrmeijer, M. Hutteman, J. R. van der Vorst, C. J. van de Velde, J. V. Frangioni, Image-guided cancer surgery using near-infrared fluorescence. *Nature reviews. Clinical oncology* 10, 507 (Sep, 2013).
62. D. H. O'Donoghue, C. A. Rockwood, Jr., G. R. Frank, S. C. Jack, R. Kenyon, Repair of the anterior cruciate ligament in dogs. *The Journal of bone and joint surgery. American volume* 48, 503 (Apr, 1966).
63. H. E. Cabaud, J. A. Feagin, W. G. Rodkey, Acute anterior cruciate ligament injury and augmented repair. Experimental studies. *The American journal of sports medicine* 8, 395 (Nov-Dec, 1980).

64. J. K. Weaver *et al.*, Primary knee ligament repair--revisited. *Clinical orthopaedics and related research*, 185 (Oct, 1985).
65. T. Strand *et al.*, Knee function following suture of fresh tear of the anterior cruciate ligament. *Acta orthopaedica Scandinavica* 55, 181 (Apr, 1984).
66. J. L. Marshall, R. F. Warren, T. L. Wickiewicz, B. Reider, The anterior cruciate ligament: a technique of repair and reconstruction. *Clinical orthopaedics and related research*, 97 (Sep, 1979).
67. J. A. Feagin, Jr., W. W. Curl, Isolated tear of the anterior cruciate ligament: 5-year follow-up study. *The American journal of sports medicine* 4, 95 (May-Jun, 1976).
68. N. Kaplan, T. L. Wickiewicz, R. F. Warren, Primary surgical treatment of anterior cruciate ligament ruptures. A long-term follow-up study. *The American journal of sports medicine* 18, 354 (Jul-Aug, 1990).
69. M. F. Sherman, L. Lieber, J. R. Bonamo, L. Podesta, I. Reiter, The long-term followup of primary anterior cruciate ligament repair. Defining a rationale for augmentation. *The American journal of sports medicine* 19, 243 (May-Jun, 1991).
70. C. Niyibizi, K. Kavalkovich, T. Yamaji, S. L. Woo, Type V collagen is increased during rabbit medial collateral ligament healing. *Knee surgery, sports traumatology, arthroscopy : official journal of the ESSKA* 8, 281 (2000).
71. S. L. Woo, M. A. Gomez, Y. K. Woo, W. H. Akeson, Mechanical properties of tendons and ligaments. II. The relationships of immobilization and exercise on tissue remodeling. *Biorheology* 19, 397 (1982).
72. R. C. Bray, C. A. Leonard, P. T. Salo, Correlation of healing capacity with vascular response in the anterior cruciate and medial collateral ligaments of the rabbit. *J Orthop Res* 21, 1118 (Nov, 2003).
73. J. Witkowski, L. Yang, D. J. Wood, K. L. Sung, Migration and healing of ligament cells under inflammatory conditions. *J Orthop Res* 15, 269 (Mar, 1997).
74. H. Sakai *et al.*, Type I and type III procollagen gene expressions in the early phase of ligament healing in rabbits: an in situ hybridization study. *J Orthop Res* 19, 132 (Jan, 2001).
75. D. A. Faryniarz, C. Chaponnier, G. Gabbiani, I. V. Yannas, M. Spector, Myofibroblasts in the healing lapine medial collateral ligament: possible mechanisms of contraction. *J Orthop Res* 14, 228 (Mar, 1996).
76. P. Sciore, R. Boykiw, D. A. Hart, Semiquantitative reverse transcription-polymerase chain reaction analysis of mRNA for growth factors and growth factor receptors from normal and healing rabbit medial collateral ligament tissue. *J Orthop Res* 16, 429 (Jul, 1998).
77. K. Ohno *et al.*, Healing of the medial collateral ligament after a combined medial collateral and anterior cruciate ligament injury and reconstruction of the anterior cruciate ligament: comparison of repair and nonrepair of medial collateral ligament tears in rabbits. *J Orthop Res* 13, 442 (May, 1995).
78. S. L. Woo, T. M. Vogrin, S. D. Abramowitch, Healing and repair of ligament injuries in the knee. *The Journal of the American Academy of Orthopaedic Surgeons* 8, 364 (Nov-Dec, 2000).
79. T. J. Ivie, R. C. Bray, P. T. Salo, Denervation impairs healing of the rabbit medial collateral ligament. *J Orthop Res* 20, 990 (Sep, 2002).
80. B. J. Loitz-Ramage, C. B. Frank, N. G. Shrive, Injury size affects long-term strength of the rabbit medial collateral ligament. *Clinical orthopaedics and related research*, 272 (Apr, 1997).
81. C. Frank *et al.*, Medial collateral ligament healing. A multidisciplinary assessment in rabbits. *The American journal of sports medicine* 11, 379 (Nov-Dec, 1983).

82. I. K. Lo *et al.*, The cellular networks of normal ovine medial collateral and anterior cruciate ligaments are not accurately recapitulated in scar tissue. *Journal of anatomy* 200, 283 (Mar, 2002).
83. C. N. Nagineni, D. Amiel, M. H. Green, M. Berchuck, W. H. Akeson, Characterization of the intrinsic properties of the anterior cruciate and medial collateral ligament cells: an in vitro cell culture study. *J Orthop Res* 10, 465 (Jul, 1992).
84. C. Agarwal, Z. T. Britton, D. A. Alaseirlis, Y. Li, J. H. Wang, Healing and normal fibroblasts exhibit differential proliferation, collagen production, alpha-SMA expression, and contraction. *Annals of biomedical engineering* 34, 653 (Apr, 2006).
85. X. Liu, H. Wu, M. Byrne, S. Krane, R. Jaenisch, Type III collagen is crucial for collagen I fibrillogenesis and for normal cardiovascular development. *Proceedings of the National Academy of Sciences of the United States of America* 94, 1852 (Mar 4, 1997).
86. T. F. Linsenmayer *et al.*, Type V collagen: molecular structure and fibrillar organization of the chicken alpha 1(V) NH2-terminal domain, a putative regulator of corneal fibrillogenesis. *The Journal of cell biology* 121, 1181 (Jun, 1993).
87. D. E. Birk, R. Mayne, Localization of collagen types I, III and V during tendon development. Changes in collagen types I and III are correlated with changes in fibril diameter. *European journal of cell biology* 72, 352 (Apr, 1997).
88. C. C. Banos, A. H. Thomas, C. K. Kuo, Collagen fibrillogenesis in tendon development: current models and regulation of fibril assembly. *Birth defects research. Part C, Embryo today : reviews* 84, 228 (Sep, 2008).
89. C. K. Kuo, R. S. Tuan, Mechanoactive tenogenic differentiation of human mesenchymal stem cells. *Tissue engineering. Part A* 14, 1615 (Oct, 2008).
90. N. Juncosa-Melvin *et al.*, Effects of cell-to-collagen ratio in stem cell-seeded constructs for Achilles tendon repair. *Tissue engineering* 12, 681 (Apr, 2006).
91. D. L. Butler *et al.*, Functional tissue engineering for tendon repair: A multidisciplinary strategy using mesenchymal stem cells, bioscaffolds, and mechanical stimulation. *J Orthop Res* 26, 1 (Jan, 2008).
92. N. A. Dyment *et al.*, The paratenon contributes to scleraxis-expressing cells during patellar tendon healing. *PloS one* 8, e59944 (2013).
93. T. Marui *et al.*, Effect of growth factors on matrix synthesis by ligament fibroblasts. *J Orthop Res* 15, 18 (Jan, 1997).
94. K. A. Hildebrand *et al.*, The effects of platelet-derived growth factor-BB on healing of the rabbit medial collateral ligament. An in vivo study. *The American journal of sports medicine* 26, 549 (Jul-Aug, 1998).
95. N. Nakamura *et al.*, Decorin antisense gene therapy improves functional healing of early rabbit ligament scar with enhanced collagen fibrillogenesis in vivo. *J Orthop Res* 18, 517 (Jul, 2000).
96. R. Liang *et al.*, Long-term effects of porcine small intestine submucosa on the healing of medial collateral ligament: a functional tissue engineering study. *J Orthop Res* 24, 811 (Apr, 2006).
97. S. C. Scherping, Jr. *et al.*, Effect of growth factors on the proliferation of ligament fibroblasts from skeletally mature rabbits. *Connective tissue research* 36, 1 (1997).
98. C. K. Kuo, J. E. Marturano, R. S. Tuan, Novel strategies in tendon and ligament tissue engineering: Advanced biomaterials and regeneration motifs. *Sports medicine, arthroscopy, rehabilitation, therapy & technology : SMARTT* 2, 20 (2010).
99. S. J. Kew *et al.*, Regeneration and repair of tendon and ligament tissue using collagen fibre biomaterials. *Acta biomaterialia* 7, 3237 (Sep, 2011).

100. F. Guilak, *Functional tissue engineering*. (Springer, New York, 2003), pp. xvi, 426 p.
101. Z. Ge, F. Yang, J. C. Goh, S. Ramakrishna, E. H. Lee, Biomaterials and scaffolds for ligament tissue engineering. *Journal of biomedical materials research. Part A* 77, 639 (Jun 1, 2006).
102. A. P. Breidenbach *et al.*, Functional tissue engineering of tendon: Establishing biological success criteria for improving tendon repair. *Journal of biomechanics*, (Oct 22, 2013).
103. S. L. Woo, Y. Takakura, R. Liang, F. Jia, D. K. Moon, Treatment with bioscaffold enhances the the fibril morphology and the collagen composition of healing medial collateral ligament in rabbits. *Tissue engineering* 12, 159 (Jan, 2006).
104. V. Musahl *et al.*, The use of porcine small intestinal submucosa to enhance the healing of the medial collateral ligament--a functional tissue engineering study in rabbits. *J Orthop Res* 22, 214 (Jan, 2004).
105. T. Zantop, T. W. Gilbert, M. C. Yoder, S. F. Badylak, Extracellular matrix scaffolds are repopulated by bone marrow-derived cells in a mouse model of achilles tendon reconstruction. *J Orthop Res* 24, 1299 (Jun, 2006).
106. T. W. Gilbert, A. M. Stewart-Akers, A. Simmons-Byrd, S. F. Badylak, Degradation and remodeling of small intestinal submucosa in canine Achilles tendon repair. *The Journal of bone and joint surgery. American volume* 89, 621 (Mar, 2007).
107. S. L. Voytik-Harbin, A. O. Brightman, M. R. Kraine, B. Waisner, S. F. Badylak, Identification of extractable growth factors from small intestinal submucosa. *Journal of cellular biochemistry* 67, 478 (Dec 15, 1997).
108. J. P. Hodde, R. D. Record, H. A. Liang, S. F. Badylak, Vascular endothelial growth factor in porcine-derived extracellular matrix. *Endothelium : journal of endothelial cell research* 8, 11 (2001).
109. P. C. Dartsch, H. Hammerle, Orientation response of arterial smooth muscle cells to mechanical stimulation. *European journal of cell biology* 41, 339 (Aug, 1986).
110. C. Neidlinger-Wilke, E. Grood, L. Claes, R. Brand, Fibroblast orientation to stretch begins within three hours. *J Orthop Res* 20, 953 (Sep, 2002).
111. J. H. Wang, E. S. Grood, The strain magnitude and contact guidance determine orientation response of fibroblasts to cyclic substrate strains. *Connective tissue research* 41, 29 (2000).
112. D. Huang, T. R. Chang, A. Aggarwal, R. C. Lee, H. P. Ehrlich, Mechanisms and dynamics of mechanical strengthening in ligament-equivalent fibroblast-populated collagen matrices. *Annals of biomedical engineering* 21, 289 (May-Jun, 1993).
113. M. Eastwood, V. C. Mudera, D. A. McGrouther, R. A. Brown, Effect of precise mechanical loading on fibroblast populated collagen lattices: morphological changes. *Cell motility and the cytoskeleton* 40, 13 (1998).
114. R. T. Prajapati, B. Chavally-Mis, D. Herbage, M. Eastwood, R. A. Brown, Mechanical loading regulates protease production by fibroblasts in three-dimensional collagen substrates. *Wound repair and regeneration : official publication of the Wound Healing Society [and] the European Tissue Repair Society* 8, 226 (May-Jun, 2000).
115. J. H. Wang, F. Jia, T. W. Gilbert, S. L. Woo, Cell orientation determines the alignment of cell-produced collagenous matrix. *Journal of biomechanics* 36, 97 (Jan, 2003).
116. E. T. den Braber, J. E. de Ruijter, L. A. Ginsel, A. F. von Recum, J. A. Jansen, Orientation of ECM protein deposition, fibroblast cytoskeleton, and attachment complex components on silicone microgrooved surfaces. *Journal of biomedical materials research* 40, 291 (May, 1998).
117. J. R. Steadman, M. L. Cameron-Donaldson, K. K. Briggs, W. G. Rodkey, A minimally invasive technique ("healing response") to treat proximal ACL injuries in skeletally immature athletes. *The journal of knee surgery* 19, 8 (Jan, 2006).

118. M. B. Fisher *et al.*, Potential of healing a transected anterior cruciate ligament with genetically modified extracellular matrix bioscaffolds in a goat model. *Knee surgery, sports traumatology, arthroscopy : official journal of the ESSKA* 20, 1357 (Jul, 2012).
119. E. Fujimoto, Y. Sumen, M. Ochi, Y. Ikuta, Spontaneous healing of acute anterior cruciate ligament (ACL) injuries - conservative treatment using an extension block soft brace without anterior stabilization. *Archives of orthopaedic and trauma surgery* 122, 212 (May, 2002).
120. M. M. Murray *et al.*, Collagen-platelet rich plasma hydrogel enhances primary repair of the porcine anterior cruciate ligament. *Journal of orthopaedic research : official publication of the Orthopaedic Research Society* 25, 81 (Jan, 2007).
121. M. Richter *et al.*, Acutely repaired proximal anterior cruciate ligament ruptures in sheep - by augmentation improved stability and reduction of cartilage damage. *Journal of materials science. Materials in medicine* 8, 855 (Dec, 1997).
122. M. Kurosaka, S. Yoshiya, T. Mizuno, K. Mizuno, Spontaneous healing of a tear of the anterior cruciate ligament. A report of two cases. *The Journal of bone and joint surgery. American volume* 80, 1200 (Aug, 1998).
123. M. Costa-Paz, M. A. Ayerza, I. Tanoira, J. Astoul, D. L. Muscolo, Spontaneous healing in complete ACL ruptures: a clinical and MRI study. *Clinical orthopaedics and related research* 470, 979 (Apr, 2012).
124. H. Ihara, M. Miwa, K. Deya, K. Torisu, MRI of anterior cruciate ligament healing. *Journal of computer assisted tomography* 20, 317 (Mar-Apr, 1996).
125. J. Wasmaier *et al.*, Proximal anterior cruciate ligament tears: the healing response technique versus conservative treatment. *The journal of knee surgery* 26, 263 (Aug, 2013).
126. A. Gobbi, L. Bathan, L. Boldrini, Primary repair combined with bone marrow stimulation in acute anterior cruciate ligament lesions: results in a group of athletes. *The American journal of sports medicine* 37, 571 (Mar, 2009).
127. D. Kobayashi, M. Kurosaka, S. Yoshiya, K. Mizuno, Effect of basic fibroblast growth factor on the healing of defects in the canine anterior cruciate ligament. *Knee surgery, sports traumatology, arthroscopy : official journal of the ESSKA* 5, 189 (1997).
128. M. M. Murray, Current status and potential of primary ACL repair. *Clinics in sports medicine* 28, 51 (Jan, 2009).
129. M. M. Murray, R. Bennett, X. Zhang, M. Spector, Cell outgrowth from the human ACL in vitro: regional variation and response to TGF-beta1. *J Orthop Res* 20, 875 (Jul, 2002).
130. W. J. Radford, A. A. Amis, F. W. Heatley, Immediate strength after suture of a torn anterior cruciate ligament. *The Journal of bone and joint surgery. British volume* 76, 480 (May, 1994).
131. B. C. Fleming, K. P. Spindler, M. P. Palmer, E. M. Magarian, M. M. Murray, Collagen-platelet composites improve the biomechanical properties of healing anterior cruciate ligament grafts in a porcine model. *The American journal of sports medicine* 37, 1554 (Aug, 2009).
132. S. D. Abramowitch, C. D. Papageorgiou, J. D. Withrow, T. W. Gilbert, S. L. Woo, The effect of initial graft tension on the biomechanical properties of a healing ACL replacement graft: a study in goats. *J Orthop Res* 21, 708 (Jul, 2003).
133. K. P. Spindler, M. M. Murray, J. L. Carey, D. Zurakowski, B. C. Fleming, The use of platelets to affect functional healing of an anterior cruciate ligament (ACL) autograft in a caprine ACL reconstruction model. *J Orthop Res* 27, 631 (May, 2009).
134. H. Seitz, W. Pichl, V. Matzi, T. Nau, Biomechanical evaluation of augmented and nonaugmented primary repair of the anterior cruciate ligament: an in vivo animal study. *International orthopaedics* 37, 2305 (Nov, 2013).

135. E. H. Crain, D. C. Fithian, E. W. Paxton, W. F. Luetzow, Variation in anterior cruciate ligament scar pattern: does the scar pattern affect anterior laxity in anterior cruciate ligament-deficient knees? *Arthroscopy : the journal of arthroscopic & related surgery : official publication of the Arthroscopy Association of North America and the International Arthroscopy Association* 21, 19 (Jan, 2005).
136. I. K. Lo, G. H. de Maat, J. W. Valk, C. B. Frank, The gross morphology of torn human anterior cruciate ligaments in unstable knees. *Arthroscopy : the journal of arthroscopic & related surgery : official publication of the Arthroscopy Association of North America and the International Arthroscopy Association* 15, 301 (Apr, 1999).
137. T. N. Vahey, D. R. Broome, K. J. Kayes, K. D. Shelbourne, Acute and chronic tears of the anterior cruciate ligament: differential features at MR imaging. *Radiology* 181, 251 (Oct, 1991).
138. S. Claes *et al.*, Anatomy of the anterolateral ligament of the knee. *Journal of anatomy* 223, 321 (Oct, 2013).

Chapter 11

Summary

INTRODUCTION

The anterior cruciate ligament (ACL) is a complex structure within the knee joint and it is important to maintain knee stability. The ACL is often injured after twisting the knee during sport or work. As sports participation under adults and teenagers is increasing worldwide, the incidence of ACL injuries has reached epidemic rates. It is estimated that annually more than 6,000 new ACL tears occur in the Netherlands and more than 200,000 new ACL tears occur in the United States - resulting in an estimated annual cost to the American society on the order of 3 billion dollars. (*1, 2*) The current surgical gold standard is the reconstruction of the torn ACL with a tendon graft. This surgical reconstruction is a difficult and technical challenging procedure. The results are generally satisfactory, but there are several drawbacks related to ACL reconstructions. According to a recent meta-analysis only 41% of the patients reported their knee as being normal after the ACL reconstruction. (*3*) Several variables in ACL reconstruction techniques have been and can be optimized such as graft selection, number of reconstructed bundles or additional anterolateral ligament reconstruction, graft placement, graft fixation, graft healing, donor site morbidity, and rehabilitation. (*4-7*) Alternatively, an ACL could be repaired, directly after the trauma by suturing the torn ends together. Theoretically, this may restore the function of the ACL, eliminate the need for tendon graft harvest and circumvent other issues related to ACL reconstruction surgery. To date this is seldom performed due to the previously poor outcome attained in the 1980's and the common opinion that the ACL cannot heal. (*8-10*) However, during the past decades new basic knowledge, advances in technology and developments in Tissue Engineering and Regenerative Medicine as well as new insights why the ACL did not heal in the previous studies, have led to a renewed interest in suture repair and the development of bio-enhanced (end-to-end) ACL repair techniques. (*11*) (*12*) (*13-15*) (*16*) (*17-19*) (*20-23*) (*24-26*)

This doctoral thesis aimed at improving the patient outcome by optimizing two important variables in the reconstruction technique and by developing a bio-enhanced end-to-end ACL repair technique to heal the ACL. The aims of this thesis are: 1) To develop a near-objective methodology to quantify the 3-D collagen fiber anatomy in ligaments; 2) To quantify the human ACL collagen fiber anatomy in 3-D; 3) To develop a new arthroscopic imaging methodology to per-operatively localize the original insertion sites of the ACL; 4) To investigate the effect of the bioscaffold small intestine submucosa (SIS) on MCL collagen fibrillogenesis; 5) To investigate the effect of cyclic stretch and cell-seeding on the fiber remodeling of SIS; 6) To investigate the effect of SIS and a new suture technique on ACL healing in a goat model; 7) To investigate whether the human ACL has a healing potential.

CHAPTER 2

3D Fiber Tractography of the Cruciate Ligaments of the Knee

The aim of this study is to develop and validate a novel near-objective methodology to study the complex three-dimensional collagen fiber architecture of the ACL. The main drawback of most existing techniques is that they distort the ligament geometry during analysis. In this study we propose to detect the collagen fiber anatomy in the knee by acquiring and processing a 3D volume of imaging data from a cryo-microtome imaging system. Methods: The ligament structure is visualized using the autofluorescent properties of collagen and analyzed by estimating the fiber orientations and performing a tractography along the ligaments. Specific image processing algorithms that suppress acquisition artifacts in the cryo-microtome data, while maintaining the fiber structure are presented and validated. The ligament tractography enabled the visualization of fiber distributions between two connected bones, autofluorescent fiber tracking (AFT). Results: Tract lengths were found to be 32.0 (6.1) mm, 29.4 (5.4) mm, and 39.5 (4.4) mm on average (standard deviations) for the anterior cruciate ligament (ACL) of the three donors and 35.7 (1.8) mm, 40.1 (2.9) mm, and 39.8 (5.2) for the posterior cruciate ligament (PCL) of the three. Furthermore, connectivity maps between were generated, that showed that adjacent tracts on the femur stayed adjacent for both ACL and PCL. Conclusion: A new method to quantify and visualize collagen fiber geometry in 3D was proposed and validated. The detected tracts can serve as a detailed input for biomechanical joint models and used for the optimization of ligament reconstruction procedures, bio-enhanced end-to-end ACL suture repair techniques, and tissue engineering.

CHAPTER 3

Analysis of the 3-D Collagen Fiber Anatomy of the Human Anterior Cruciate Ligament: a Preliminary Investigation

The aim of this study is to assess the applicability of autofluorescent fiber tracking (AFT) to obtain quantitative data on the 3-D collagen fiber anatomy of the human ACL. Based on the majority of the literature, the hypothesis is that the ACL has at least two anatomically distinct fiber bundles with different fiber orientations. Methods: AFT combines an imaging cryomicrotome for serial sectioning, collagen autofluorescence, image acquisition and fiber tracking software to reconstruct the fiber tracts in three dimensions and to analyze the fiber tract orientation, lengths of the fiber tracts and connectivity map of the ACLs. In this pilot study, three fresh-frozen human knees were processed, two in extension and one in flexion. Results: All fiber tracts of the ACL in extension are running parallel from the femoral insertion towards the tibial insertion. A twist of fiber tracts is observed with the knee in flexion. However, the twist is not caused by anatomically distinct fiber bundles as the length maps reveal a clear pattern

of gradual length change across the insertion sites with short fibers posterolateral and gradually longer fibers towards anteromedial direction. In addition, the connectivity maps confirm that neighboring fiber tracts remain neighbors. Conclusion: This pilot study demonstrates that autofluorescent fiber tracking is able to quantify the 3-D fiber anatomy of the ACL and shows that the 3-D fiber anatomy of the three specimens is a single broad continuum of collagen fibers with short fibers posterolateral and gradually longer fibers towards anteromedial

CHAPTER 4

The Development of the Arthroscopic Fluorescence Imaging System to Improve the Contrast between Joint Structures during Arthroscopic Surgery

Arthroscopic surgery has many advantages but remains difficult to master. This is primarily due to the suboptimal contrast between ligament, bone and cartilage when imaged with the current white light endoscopic systems. Many tissues are autofluorescent, potentially adding an extra source of contrast. Here we study the hypothesis that joint structures display different autofluorescent spectral responses based on differences in collagen content and distribution and therefor can be separately visualized. We report the development of an arthroscopic fluorescence imaging (AFI) system to real-time enhance the contrast between joint structures for visualization during arthroscopic surgery. Its validity was evaluated around the arthroscopic anterior cruciate ligament (ACL) reconstruction, specifically improving the contrast between the femoral insertion site and its background. Methods: The spectral responses of the femoral insertion site and its surrounding bone and cartilage were measured with a fluorospectrometer. A prototype AFI system was developed based on the spectral responses and test images of the insertion site. The accuracy was validated by evaluating the overlap between manually segmented insertion sites on the white light color images and on the corresponding spectral unmixed fluorescence images. The final prototype of the AFI system was tested during an arthroscopy in cadaveric knees. Results: Spectral unmixing was effective in improving the contrast. The insertion site was depicted in bright red and the bony and cartilage background, in contrasting green and dimmed red, respectively. Arthroscopy with the AFI system showed that the insertion site can be clearly distinguished from its background. Conclusion: We have developed the AFI system to improve the contrast between the insertion site and its background in real time and subject specific. In addition, the AFI system can facilitate arthroscopic procedures in other joints and can also be used as a diagnostic tool during a fluorescence arthroscopy.

CHAPTER 5

Effects of a Bioscaffold on Collagen Fibrillogenesis in Healing Medial Collateral Ligament in Rabbits

Bioscaffolds have been successfully used to improve the healing of ligaments and tendons. In a rabbit model, the application of porcine small intestine submucosa (SIS) to the healing medial collateral ligament (MCL) resulted in improved mechanical properties with the formation of larger collagen fibrils. Thus, the objective of the study was to find out whether the SIS bioscaffold could improve the gene expressions of fibrillogenesis-related molecules, specifically, collagen types I, III, V, and small leucine-rich proteoglycans including decorin, biglycan, lumican, and fibromodulin, as well as collagen fibril morphology and organization, in the healing rabbit MCL at an early time point (6 weeks post-injury). Methods: Twenty skeletally mature rabbits were equally divided into two groups. In the SIS-treated group, a 6-mm gap was surgically created and a layer of SIS was sutured to cover the gap, whereas the gap was left open in the nontreated group. Results: At 6 weeks post-injury, Masson's trichrome staining showed that the SIS-treated group had more regularly aligned collagen fibers and cells. Transmission electron microscopy revealed that the SIS-treated group had larger collagen fibrils with a diameter distribution from 24 to 120 nm, whereas the non-treated group had only small collagen fibrils (ranging from 26 to 87 nm, $p<0.05$). Finally, the quantitative real-time PCR showed that the mRNAs of collagen type V, decorin, biglycan, and lumican in the SIS-treated group were 41, 58, 51, and 43% lower than those in the non-treated group, respectively ($p<0.05$). Conclusion: The significant reduction in the gene expressions are closely related to the improved morphological characteristics, which are known to be coupled with better mechanical properties, as previously reported in longer term studies

CHAPTER 6

Effects of Cell Seeding and Cyclic Stretch on the Fiber Remodeling in an Extracellular Matrix–Derived Bioscaffold

The porcine small intestine submucosa, an extracellular matrix–derived bioscaffold (ECM-SIS), has been successfully used to enhance the healing of ligaments and tendons. Since the collagen fibers of ECM-SIS have an orientation of ±30°, its application in improving the healing of the parallel-fibered ligament and tendon may not be optimal. Therefore, the objective was to improve the collagen fiber alignment of ECM-SIS in vitro with fibroblast seeding and cyclic stretch. The hypothesis was that with the synergistic effects of cell seeding and mechanical stimuli, the collagen fibers in the ECM-SIS can be remodeled and aligned, making it an improved bioscaffold with enhanced conductive properties. Methods: Three experimental groups were established: group I (n=14), ECM-SIS was seeded with fibroblasts and cyclically stretched;

group II (n=13), ECM-SIS was seeded with fibroblasts but not cyclically stretched; and group III (n=8), ECM-SIS was not seeded with fibroblasts but cyclically stretched. After 5 days' experiments, the scaffolds from all the three groups (n=9 for group I; n=8 for groups II and III) were processed for quantification of the collagen fiber orientation with a small-angle light scattering (SALS) system. For groups I and II, in which the scaffolds were seeded with fibroblasts, the cell morphology and orientation and newly produced collagen fibrils were examined with confocal fluorescent microscopy (n=3/group) and transmission electronic microscopy (n=2/group). Results: The results revealed that the collagen fiber orientation in group I was more aligned closer to the stretching direction when compared to the other two groups. The mean angle decreased from 25.38 to 7.18 ($p < 0.05$), and the associated angular dispersion was also reduced (37.48 vs. 18.58, $p < 0.05$). In contrast, groups II and III demonstrated minimal changes. The cells in group I were more aligned in the stretching direction than those in group II. Newly produced collagen fibrils could be observed along the cells in both groups I and II. Conclusion: This study demonstrated that a combination of fibroblast seeding and cyclic stretch could remodel and align the collagen fiber orientation in ECM-SIS bioscaffolds. The better-aligned ECM-SIS has the prospect of eliciting improved effects on enhancing the healing of ligaments and tendons.

CHAPTER 7

Intrinsic Healing Response of the Human Anterior Cruciate Ligament: An Histological Study of Reattached ACL Remnants

A reattachment of the tibial remnant of the torn anterior cruciate ligament (ACL) to the posterior cruciate ligament is sometimes observed during surgery and apparently implies that the human ACL does have a healing response. The aim of this study was to investigate whether this reattachment tissue has similar histological characteristics of a healing response as the medial collateral ligament (MCL), which can heal spontaneously. Methods: Standard histology and immunostaining of a-smooth muscle actin and collagen type 3 was performed. Results: The results shows that the reattached tissue has typical characteristics of a healing response: the reattached ACL remnant could not be released by forceful traction; microscopy showed that the collagen fibers of the reattached tissue were disorganized with no preferred direction; increased neovascularization; the presence of lipid vacuoles; the mean number of cells within the biopsy tissue was 631_269 cells per mm2; and 68_20% was expressing α-SMA; semi-quantitative analysis of collagen type 3 expression showed that collagen type 3 had an high expression with an average score of 3. Conclusion: This study shows that the human proximal 1/3 ACL has an intrinsic healing response with typical histological characteristics similar to the MCL.

CHAPTER 8

Healing of the Goat Anterior Cruciate Ligament After a New Suture Repair Technique and Bioscaffold Treatment

Primary suture repair of the anterior cruciate ligament (ACL) has been used clinically in an attempt to heal the ruptured ACL. The results, however, were not satisfactory, which in retrospect can be attributed to the used suturing technique and the suboptimal healing conditions. These constraining conditions can be improved by introducing a new suturing technique and by using small intestinal submucosa (SIS) as a bioscaffold. It is hypothesized that the suturing technique keep the torn ends together and that SIS enhance and promote the healing of the ACL. Methods: The goat was used as the study model. In the Suture group, the left ACL was transected and suture repaired with a new locking suture repair technique (n = 5) allowing approximation and fixation under tension. The Suture-SIS group underwent the same procedure with the addition of SIS (n = 5). The right ACL served as control. After 12 weeks of healing, anterior–posterior translation and in situ force of the healing ACL were measured, followed by the measurement of the cross-sectional area and structural stiffness. Routine histology was performed on tissue samples. Results: Gross morphology showed that the healing ACL was continuous with collagenous tissue in both groups. The cross-sectional area of the Suture and the Suture-SIS group was 35% and 50% of the intact control, respectively. The anterior–posterior translations at different flexion angles were statistically not different between the Suture group and the Suture-SIS group. Only the in situ force at 30_ in the Suture-SIS group was higher than in the Suture group. Tensile tests showed that the stiffness for the Suture group was not different from the Suture-SIS group (31.1 – 8.1N/mm vs. 41.9 – 18.0N/mm [$p > 0.05$]). Histology showed longitudinally aligned collagen fibers from origo to insertion. More fibroblasts were present in the healing tissue than in the control intact tissue. Conclusion: The study demonstrated the proof of concept of ACL repair in a goat model with a new suture technique and SIS. The mechanical outcome is comparable to previously reported for ACL reconstruction. In conclusion, the approach of using a new suture technique, with or without a bioscaffold to heal the ACL is promising.

CHAPTER 9

Histological Evaluation of the Healing Goat Anterior Cruciate Ligament

The aim of this study was to histologically evaluate the healing anterior cruciate ligament (ACL) in terms of the appearance of the fibrous synovial layer, the extracellular matrix (ECM), collagen fiber orientation, cellularity, ratio of myofibroblasts and collagen type 3 staining. The hypothesis is that small intestine submucosa (SIS) enhances the healing due to the scaffolding effect, endogenous growth factors and chemoattractants. Methods: In the Suture group, the left ACL was transected and

sutured with the triple X locking suture repair technique (n=4). The Suture-SIS group underwent the same procedure with the addition of SIS (n=4). Standard histology and immunostaining of α-smooth muscle actin (SMA) and collagen type 3 were used. Results: Microscopy showed that the fibrous synovial layer around the ACL was reestablished in both groups. The collagen fibers in the Suture-SIS group stained denser, more compactly arranged and the ECM contained less voids and less fat vacuoles. Neovasculature running between the collagen fibers was observed in both groups. Collagen type 3 appeared to stain less in the Suture-SIS group. The cellularity in the Suture group and Suture-SIS group was 1265±1034 per mm^2 and 954±378 per mm^2; and 49% and 26% of the cells stained positive for α-SMA, respectively. Conclusion: The healing ACL in both treated groups showed histological characteristics which are comparable to the spontaneously healing medial collateral ligament and showed that the ACL has a similar intrinsic healing response. Though, no definitive conclusions on the beneficial effects of the SIS scaffold on the healing process can be made.

CHAPTER 10
Discussion & conclusions

The research described in this doctoral thesis aimed at developing new methods to optimize the surgical treatment of patients with anterior cruciate ligament (ACL) tears. The research projects can be categorized into four themes: 1) obtaining near-objective and detailed information of the anatomy of the ACL, 2) the development of the Arthroscopic Fluorescence Imaging system, 3) *in vitro* and *in vivo* evaluation of Small Intestine Submucosa bioscaffold, and finally 4) the development of a bio-enhanced end-to-end ACL repair technique to heal the ACL in an animal model. The main findings, conclusions, clinical implications, and suggestions for future research are given in this final chapter.

The first conclusion is that the cryo-imaging system combined with tractography is an near-objective and accurate methodology to quantify the 3-D fiber orientation of the ACL. This methodology may also be a useful tool to obtain the fiber architecture of other collagenous structures such as menisci, the intervertebral disc, heart valves, etc. The knowledge of the detailed fiber anatomy of the load bearing structures may increase our understanding of the function and pathophysiology of these structures. The implication is that the obtained fiber anatomy can be used a blueprint to guide the development of new treatments.

The main preliminary finding and conclusion of the second study is that the studied ACL's are a single continuous construct of collagen fibers with short fibers posterolaterally and gradually longer fibers towards anteromedially. This preliminary conclusion does not support the current concept that the ACL has two or three anatomically distinct bundles and consequently the concept of anatomic double or triple bundle ACL

reconstructions. (*27-32*) However, anatomic double or triple bundle ACL reconstruction does effectively mimic the anatomy of the ACL by placing the shorter tendon graft posterolaterally and the longer tendon graft anteromedially. Thus, anatomic double or triple bundle ACL reconstructions are encouraged but with a different rationale. The implication of this study is that it provides fundamental knowledge of the ACL. The acquired 3-D collagen fiber anatomy can be used as a blueprint for developing bio-enhanced end-to-end ACL repair techniques, optimize ACL reconstruction techniques and finite element modeling. The main finding and conclusion of the third study is that the arthroscopic fluorescence imaging (AFI) system can accurately visualize the native ACL insertion sites. Additionally, it demonstrates its feasibility and potential to be fast, easy, cheap, real-time, and enables patient-specific tendon graft placement. Currently, the AFI system is further developed for the use in patients. Its value will be evaluated in future clinical trials. The clinical implication is that around 50% of the revision surgeries which are caused by graft misplacement may be prevented and the AFI system may facilitate the paradigm shift towards anatomical ACL reconstruction which in turn may prevent early osteoarthrosis. Additionally, the AFI system may also be the platform for color-guided arthroscopic surgery in other joints and may be valuable in diagnosis and staging of degeneration of collagenous tissues.

The main finding and conclusion of the fourth study is that SIS can down-regulate collagenfibrillogenesis related genes such that the ultrastructure and morphology are improved, which are known to be coupled with better mechanical properties, as previously reported in long-term studies. The implication of this study was that SIS is a good candidate to be used for ACL healing based on its bioactive agents and conductive properties.

The main finding and conclusion of the fifth study is that a combination of fibroblast seeding and cyclic uniaxial stretch can effectively improve the collagen fiber alignment in the ECM-SIS bioscaffold toward the axis of the applied stretch, while mechanical stretch or cell seeding alone was not sufficient to affect the ultrastructure of the scaffold. These findings emphasized the importance of the synergistic effects of cells and mechanical stimuli in the process of matrix remodeling.

The main finding and conclusion of the sixth study is that the transected goat ACL can heal after the treatment of a bio-enhanced end-to-end ACL repair technique with the triple X locking suture technique and SIS. It can be concluded that, in a mechanical sense, the outcome was comparable to the previously reported results of bone-patellar tendon-bone ACL reconstructions in goats. (*33, 34*)

The main finding and conclusion of the seventh study is that the healing ACL in both treated groups showed histological characteristics which are comparable to the spontaneously healing medial collateral ligament and showed that the ACL has a similar

intrinsic healing response. (*35*) Though, no definitive conclusions on the beneficial effects of the SIS scaffold on the healing process can be made.

The main finding and conclusion of the eight study is that further evidence is provided that the human ACL does have an intrinsic healing potential. The results not only demonstrate the healing potential based on gross morphological characteristics but additionally show the typical histological characteristics that are seen in the healing process in the MCL. The implication of this study together with the Chapter 7, 8 and the existing literature is that there is sufficient support to warrant future translational studies to develop and evaluate the bio-enhanced end-to-end suture repair of the torn ACL in humans.

REFERENCES

1. R. C. Mather, 3rd *et al.*, Societal and economic impact of anterior cruciate ligament tears. *The Journal of bone and joint surgery. American volume* **95**, 1751 (Oct 2, 2013).
2. R. H. Brophy, R. W. Wright, M. J. Matava, Cost analysis of converting from single-bundle to double-bundle anterior cruciate ligament reconstruction. *The American journal of sports medicine* **37**, 683 (Apr, 2009).
3. D. J. Biau, C. Tournoux, S. Katsahian, P. Schranz, R. Nizard, ACL reconstruction: a meta-analysis of functional scores. *Clinical orthopaedics and related research* **458**, 180 (May, 2007).
4. S. Claes *et al.*, Anatomy of the anterolateral ligament of the knee. *Journal of anatomy* **223**, 321 (Oct, 2013).
5. B. D. Beynnon, R. J. Johnson, J. A. Abate, B. C. Fleming, C. E. Nichols, Treatment of anterior cruciate ligament injuries, part 2. *The American journal of sports medicine* **33**, 1751 (Nov, 2005).
6. B. D. Beynnon, R. J. Johnson, J. A. Abate, B. C. Fleming, C. E. Nichols, Treatment of anterior cruciate ligament injuries, part I. *The American journal of sports medicine* **33**, 1579 (Oct, 2005).
7. A. van Kampen, A. B. Wymenga, H. J. van der Heide, H. J. Bakens, The effect of different graft tensioning in anterior cruciate ligament reconstruction: a prospective randomized study. *Arthroscopy : the journal of arthroscopic & related surgery : official publication of the Arthroscopy Association of North America and the International Arthroscopy Association* **14**, 845 (Nov-Dec, 1998).
8. M. F. Sherman, L. Lieber, J. R. Bonamo, L. Podesta, I. Reiter, The long-term followup of primary anterior cruciate ligament repair. Defining a rationale for augmentation. *Am J Sports Med* **19**, 243 (May-Jun, 1991).
9. J. A. Feagin, Jr., W. W. Curl, Isolated tear of the anterior cruciate ligament: 5-year follow-up study. *The American journal of sports medicine* **4**, 95 (May-Jun, 1976).
10. L. Engebretsen, P. Benum, O. Fasting, A. Molster, T. Strand, A prospective, randomized study of three surgical techniques for treatment of acute ruptures of the anterior cruciate ligament. *The American journal of sports medicine* **18**, 585 (Nov-Dec, 1990).
11. S. L. Woo, T. M. Vogrin, S. D. Abramowitch, Healing and repair of ligament injuries in the knee. *The Journal of the American Academy of Orthopaedic Surgeons* **8**, 364 (Nov-Dec, 2000).
12. S. L. Hsu, R. Liang, S. L. Woo, Functional tissue engineering of ligament healing. *Sports Med Arthrosc Rehabil Ther Technol* **2**, 12 (2010).
13. Z. Ge, J. C. Goh, E. H. Lee, Selection of cell source for ligament tissue engineering. *Cell Transplant* **14**, 573 (2005).
14. J. M. McKean, A. H. Hsieh, K. L. Sung, Epidermal growth factor differentially affects integrin-mediated adhesion and proliferation of ACL and MCL fibroblasts. *Biorheology* **41**, 139 (2004).
15. C. N. Nagineni, D. Amiel, M. H. Green, M. Berchuck, W. H. Akeson, Characterization of the intrinsic properties of the anterior cruciate and medial collateral ligament cells: an in vitro cell culture study. *J Orthop Res* **10**, 465 (Jul, 1992).
16. W. J. Radford, A. A. Amis, F. W. Heatley, Immediate strength after suture of a torn anterior cruciate ligament. *The Journal of bone and joint surgery. British volume* **76**, 480 (May, 1994).
17. M. M. Murray *et al.*, Collagen-platelet rich plasma hydrogel enhances primary repair of the porcine anterior cruciate ligament. *J Orthop Res* **25**, 81 (Jan, 2007).
18. M. B. Fisher *et al.*, Potential of healing a transected anterior cruciate ligament with genetically modified extracellular matrix bioscaffolds in a goat model. *Knee surgery, sports traumatology, arthroscopy : official journal of the ESSKA* **20**, 1357 (Jul, 2012).

19. P. Vavken, M. M. Murray, Translational Studies in ACL repair. *Tissue Eng Part A*, (Jul 21, 2009).
20. T. Zantop, T. W. Gilbert, M. C. Yoder, S. F. Badylak, Extracellular matrix scaffolds are repopulated by bone marrow-derived cells in a mouse model of achilles tendon reconstruction. *J Orthop Res* **24**, 1299 (Jun, 2006).
21. T. W. Gilbert, A. M. Stewart-Akers, A. Simmons-Byrd, S. F. Badylak, Degradation and remodeling of small intestinal submucosa in canine Achilles tendon repair. *The Journal of bone and joint surgery. American volume* **89**, 621 (Mar, 2007).
22. S. L. Voytik-Harbin, A. O. Brightman, M. R. Kraine, B. Waisner, S. F. Badylak, Identification of extractable growth factors from small intestinal submucosa. *J Cell Biochem* **67**, 478 (Dec 15, 1997).
23. J. P. Hodde, R. D. Record, H. A. Liang, S. F. Badylak, Vascular endothelial growth factor in porcine-derived extracellular matrix. *Endothelium : journal of endothelial cell research* **8**, 11 (2001).
24. S. L. Woo, Y. Takakura, R. Liang, F. Jia, D. K. Moon, Treatment with bioscaffold enhances the the fibril morphology and the collagen composition of healing medial collateral ligament in rabbits. *Tissue Eng* **12**, 159 (Jan, 2006).
25. V. Musahl *et al.*, The use of porcine small intestinal submucosa to enhance the healing of the medial collateral ligament--a functional tissue engineering study in rabbits. *Journal of orthopaedic research : official publication of the Orthopaedic Research Society* **22**, 214 (Jan, 2004).
26. R. Liang *et al.*, Long-term effects of porcine small intestine submucosa on the healing of medial collateral ligament: a functional tissue engineering study. *Journal of orthopaedic research : official publication of the Orthopaedic Research Society* **24**, 811 (Apr, 2006).
27. P. S. Cha *et al.*, Arthroscopic double-bundle anterior cruciate ligament reconstruction: an anatomic approach. *Arthroscopy : the journal of arthroscopic & related surgery : official publication of the Arthroscopy Association of North America and the International Arthroscopy Association* **21**, 1275 (Oct, 2005).
28. H. W. Mott, Semitendinosus anatomic reconstruction for cruciate ligament insufficiency. *Clinical orthopaedics and related research*, 90 (Jan-Feb, 1983).
29. T. Muneta *et al.*, Two-bundle reconstruction of the anterior cruciate ligament using semitendinosus tendon with endobuttons: operative technique and preliminary results. *Arthroscopy : the journal of arthroscopic & related surgery : official publication of the Arthroscopy Association of North America and the International Arthroscopy Association* **15**, 618 (Sep, 1999).
30. N. K. Shino K, Nakamura N, Mae T, Ohtsubo H, Iwahashi T, Nakagawa S, Anatomic anterior cruciate ligament reconstruction using two double-looped hamstring tendon grafts via twin femoral and triple tibial tunnels. *Oper Tech Orthop* **15**, 130 (2005).
31. K. Yasuda *et al.*, Anatomic reconstruction of the anteromedial and posterolateral bundles of the anterior cruciate ligament using hamstring tendon grafts. *Arthroscopy : the journal of arthroscopic & related surgery : official publication of the Arthroscopy Association of North America and the International Arthroscopy Association* **20**, 1015 (Dec, 2004).
32. T. Rosenberg, B. Graf. (Mansfield, MA: Acufex Microsurgical, 1994).
33. S. D. Abramowitch, C. D. Papageorgiou, J. D. Withrow, T. W. Gilbert, S. L. Woo, The effect of initial graft tension on the biomechanical properties of a healing ACL replacement graft: a study in goats. *Journal of orthopaedic research : official publication of the Orthopaedic Research Society* **21**, 708 (Jul, 2003).
34. K. P. Spindler, M. M. Murray, J. L. Carey, D. Zurakowski, B. C. Fleming, The use of platelets to affect functional healing of an anterior cruciate ligament (ACL) autograft in a caprine ACL

reconstruction model. *Journal of orthopaedic research : official publication of the Orthopaedic Research Society* **27**, 631 (May, 2009).

35. C. Frank *et al.*, Medial collateral ligament healing. A multidisciplinary assessment in rabbits. *Am J Sports Med* **11**, 379 (Nov-Dec, 1983).

Chapter 12

Samenvatting

INTRODUCTIE

De voorste kruisband (VKB) is een complex structuur binnen het kniegewricht en is een belangrijke stabilisator. De VKB scheurt regelmatig na een knietrauma tijdens het sporten of het werken. De incidentie van voorste kruisbandscheuren nadert epidemische getallen omdat sportparticipatie onder jongeren en volwassen wereldwijd toeneemt. Er wordt geschat dat jaarlijks meer dan 6000 nieuwe kruisbandscheuren in Nederland bijkomen. In de Verenigde Staten is dit getal zelfs hoger en de schatting is dat meer dan 200.000 nieuwe kruisbandscheuren jaarlijks bijkomen. Dit resulteert in een geschatte kostenplaatje van meer dan 3 miljard Amerikaanse dollars*. (1, 2)* De huidige standaard chirurgische behandeling is een arthroscopische VKB-reconstructie met een donorpees van de patiënt. Deze procedure is door de vele chirurgische stappen en variabelen een lastig en technisch uitdagende procedure. De resultaten zijn in het algemeen bevredigend, echter er blijven nadelen verbonden aan de VKB-reconstructies. Volgens een recente meta-analyse vinden slechts 41% van de geopereerde patiënten dat hun knie weer normaal functioneert. *(3)* Verscheidene variabelen in de VKB-reconstructie techniek zijn reeds geoptimaliseerd en gestandaardiseerd, echter andere variabelen blijven nog een punt van discussie zoals: de type donorpees, het aantal boortunnels, de boortunnel locatie, additionele extra-articulaire anterolaterale ligament reconstructie, de wijze van peesfixatie, de mate van donorpees herstel, de donorlocatie morbiditeit en de wijze van het revalideren, etc. *(4-7)*

Een alternatief voor de chirurgische behandeling zou de heling van de gescheurde kruisband kunnen zijn. Theoretisch zal laatstgenoemde techniek de functie van de kruisband kunnen herstellen, alsmede de hierboven genoemde variabelen in de VKB-reconstructie techniek omzeilen. In het verleden was reeds getracht om de gescheurde VKB te helen door middel van direct herstel met parallel gehechte hechtdraden. Echter de resultaten waren onbevredigend en zorgden ervoor dat er een algemene opvatting ontstond dat de kruisband niet kon helen en herstellen. (*8-10*) Recentelijk is er een hernieuwde interesse gekomen om de kruisband te helen. Deze opleving wordt niet alleen veroorzaakt door de suboptimale resultaten van de VKB-reconstructies, maar ook door nieuw verworven fundamentele kennis, alsmede de technologische vooruitgang en de nieuwe ontwikkelingen in de Tissue Engineering en Regeneratieve Geneeskunde. Daarnaast zijn er nieuwe inzichten in de redenen waarom het direct herstel in het verleden niet succesvol was. *(11, 12)(8, 9) (13-15) (16) (17-19) (20-23) (24-26).*

Dit proefschrift heeft als doel om de patiënten uitkomst na een VKB letsel te verbeteren door twee belangrijke variabelen in de VKB-reconstructie techniek te optimaliseren alsmede om een “bio-enhanced ACL end-to-end” direct herstel te ontwikkelen met het doel om de kruisband te helen. De deeldoelstellingen zijn: 1) het ontwikkelen van een objectievere methode om de 3-D collageenvezel anatomie van ligamenten

te kwantificeren; 2) het kwantificeren van de 3-D collageenvezel anatomie van de menselijke VKB; 3) het ontwikkelen van een nieuwe kijkoperatie systeem dat het mogelijk maakt om tijdens de kijkoperatie de insertieplaatsen van de VKB nauwkeurig te lokaliseren; 4) het onderzoeken van het effect van het biomateriaal "small intestine submucosa" (SIS) op de collageenvezelvorming in de mediaal collateraal ligament; 5) het onderzoeken van het effect van cyclische rek en celpopulatie op de collageenvezel remodelering van SIS; 6) het onderzoeken van het effect van SIS en een nieuwe hechttechniek op de kruisbandheling in een diermodel; 7) het onderzoeken of de humane kruisband een helingspotentieel heeft.

HOOFDSTUK 2

3D Fiber Tractography of the Cruciate Ligaments of the Knee

De doelstelling van deze studie is om een methode te ontwikkelen en te valideren die het mogelijk maakt om de complexe 3-D collageenvezel anatomie van de kruisband objectiever te kwantificeren. Het grootste nadeel van de bestaande technieken is dat ze de ligamentgeometrie verstoren tijdens de bewerking en de analyse.

In deze studie stellen we een nieuwe methode voor om de kruisband objectiever te kwantificeren, de autofluorescent fiber tracking (AFT). Methodes: Ligamenten kunnen worden gevisualiseerd door gebruik te maken van de autofluorescente eigenschap van collageen. Specifieke beeldbewerkingsalgoritmes die acquisitie artefacten in het cryo-microtoom data filteren en tegelijkertijd de vezelstructuur bewaren worden hier ook gevalideerd. Deze data wordt vervolgens geanalyseerd m.b.v. de vezeloriëntatie estimatie en vezeltractografie. Ligament tractografie maakt het mogelijk om vezelbanen tussen twee structuren te visualiseren alsmede om de vezelbaanoriëntatie, lengte en connectiviteit te berekenen. Resultaten: de gemiddelde vezelbaanlengte van de drie voorste kruisbanden (VKB) waren respectievelijk 32.0 (6.1) mm, 29.4 (5.4) mm en 39.5 (4.4) mm. De gemiddelde vezelbaanlengte van de drie achterste kruisbanden (AKB) waren respectievelijk 35.7 (1.8) mm, 40.1 (2.9) mm en 39.8 (5.2). De connectiviteitsmappen lieten zien dat de aan elkaar grenzende vezelbanen voor zowel de VKB als de AKB vezelbanen parallel blijven lopen. Conclusie: We hebben in deze studie een nieuwe methode beschreven en gevalideerd om de 3-D collageenvezel anatomie objectiever te kwantificeren. De gedetecteerde vezelbanen kunnen gebruikt worden als invoerparameters voor biomechanische gewrichtsmodellen, tissue engineering blauwdrukken, alsmede om ligament reconstructietechnieken te optimaliseren en om de "bio-enhanced end-to-end ACL" hersteltechniek verder te ontwikkelen.

HOOFDSTUK 3

Analysis of the 3-D Collagen Fiber Anatomy of the Human Anterior Cruciate Ligament: a Preliminary Investigation

De doelstelling van deze studie is om te onderzoeken of de toepassing van autofluorescent fiber tracking (AFT) een geschikte methode is om de 3-D collageenvezel anatomie van de humane voorste kruisband (VKB) te kwantificeren. Baserend op de bestaande literatuur, is de hypothese dat VKB uit minimaal twee anatomisch verschillende bundels bestaat. Methodes: De AFT methode maakt gebruik van gecombineerde technieken (de imaging cryo-microtoom, de autofluorescente eigenschap van collageen, beeldacquisitie en fiber tracking software) om de collageenvezelbanen in 3D te reconstrueren. Uit de 3-D reconstructie kunnen vervolgens de vezelbaanoriëntatie, de vezelbaanlengte en de connectiviteitsmap van de VKB worden berekend. In deze pilot studie werden drie fresh-frozen humane knieën geanalyseerd: twee knieën met het kniegewricht in extensie en één knie in flexie. Resultaten: alle collageenvezels van de voorste kruisband waarvan de knie in extensie is gesneden lopen parallel. De collageenvezels van de voorste kruisband waarvan de knie in flexie is gesneden liet een twist zien. Deze twist wordt veroorzaakt door de flexie stand van de knie. De lengte map laat zien dat er een patroon is van een geleidelijke lengte overgang. Korte collageenvezelbanen zijn posterolateraal gelokaliseerd en richting anteromediaal nemen de collageenvezelbanen in lengte toe. Daarnaast bevestigen de connectiviteitsmappen dat aangrenzende collageenvezelbanen parallel blijven lopen. Verschillende anatomische bundels werd niet geobserveerd. Conclusie: Deze pilot studie laat zien dat autofluorescent fiber tracking een geschikte methode is om de 3-D collageenvezel anatomie van de humane voorste kruisband te kwantificeren. Daarnaast blijkt uit deze studie dat de drie onderzochte voorste kruisbanden één continuum is van collageenvezels waarbij de korte vezels posterolateraal zijn gelokaliseerd en richting anteromediaal geleidelijk langer worden.

HOOFDSTUK 4

The Development of the Arthroscopic Fluorescence Imaging System to Improve the Contrast between Joint Structures during Arthroscopic Surgery

Arthroscopische chirurgie met de huidige wit licht endoscopie systemen heeft vele voordelen, maar blijft technisch lastig. Dit is mede te wijten aan het suboptimale contrast tussen het witte kruisbandweefsel, het bot en het kraakbeen. Veel weefsels zijn autofluorescent en deze eigenschap zou mogelijkerwijs een extra mogelijkheid verschaffen om het contrast te verbeteren. De hypothese is dat de respectievelijk gewrichtsweefsels verschillende collageen hoeveelheden en spreiding hebben waardoor ze verschillen in het spectrale respons en derhalve gesepareerd kunnen worden om het contrast te verbeteren. De autofluorescentie arthroscopie (AFI) systeem werd

rond de arthroscopische voorste kruisband (VKB) ontwikkeld waarbij de doelstelling is om het contrast tussen de femorale insertieplaats en de achtergrond te verbeteren. Methodes: het spectrale respons van de femorale insertie, omringende bot en kraakbeen werd met een fluorospectrometer gemeten. Vervolgens werd op basis van de spectrale responsen en testbeelden van de femorale insertieplaatsen een prototype van de AFI systeem ontwikkeld. De nauwkeurigheid werd berekend d.m.v. de Dice index van de overlap tussen de handmatig gesegmenteerde insertieplaats op de normale witlicht beelden en de spectraal unmixed fluorescentie beelden. De prototype van de AFI systeem werd vervolgens arthroscopisch getest in kadaver knieën. Resultaten: de resultaten laten zien dat spectraal unmixen van de autofluorescerende weefsels een effectieve manier is om de contrast te verbeteren. De femorale insertieplaats kon contrasterend worden weergegeven in helder rood, het bot en kraakbeen in respectievelijk groen en gedimd rood. De arthroscopie in de humane kadaver knieën liet zien dat de insertieplaats met de AFI duidelijk kon worden onderscheiden van de achtergrond. Conclusie: we hebben in deze studie laten zien dat de AFI systeem in staat is om het contrast tussen de femorale insertieplaats en de achtergrond real-time en subject specifiek te verbeteren. De AFI systeem zou mogelijk andere arthroscopische procedures kunnen vergemakkelijken alsmede gebruikt kunnen worden als een diagnostische instrument tijdens een fluorescentie arthroscopie.

HOOFDSTUK 5

Effects of a Bioscaffold on Collagen Fibrillogenesis in Healing Medial Collateral Ligament in Rabbits

Biomaterialen zijn succesvol gebruikt om de heling van ligamenten en pezen te verbeteren. In een dierexperimenteel onderzoek werd aangetoond dat het biomateriaal small intestine submucosa (SIS) de mechanische eigenschappen en de collageenfibril diameter van de helende mediaal collateraal ligament (MCL) significant verbetert. De doelstelling van deze studie is derhalve om de genexpressie van de fibrillogenese-gerelateerde moleculen, i.e. collageen types I, III, V, en small leucine-rich proteoglycanen, inclusief decorin, biglycan, lumican, en fibromodulin, alsmede de collageenfibril morfologie en organisatie te onderzoeken. Methodes: twintig skeletaal volwassen konijnen werden gelijk verdeeld in twee groepen. In de SIS-behandelde groep werd een 6 mm defect in de MCL gemaakt en over het defect werd een laag SIS gehecht. In de Onbehandelde groep werd het defect zo gelaten. Resultaten: de Masson's trichrome kleuring liet zien de SIS-behandelde groep meer regelmatig gealigneerde collageenvezels en cellen bevatte. De transmissie elektronen microscopie liet zien dat de SIS-behandelde groep grotere collageenfibril diameters heeft met een distributie van 24 tot 120 nm. Dit in tegenstelling van de Onbehandelde groep, deze had dunnere collageen fibrillen variërend van 26 tot 87 nm, $p<0.05$. De quantitative real-time PCR

liet zien dat de mRNA expressie van collageen type V, decorin, biglycan, en lumican in de SIS-behandelde groep, respectievelijk 41%, 58%, 51%, en 43% lager waren dan in de Onbehandelde groep ($p<0.05$). Conclusie: de significante verlaging van de genexpressie in de SIS-behandelde groep zijn nauw gerelateerd aan de morfologische verbeteringen en de mechanische eigenschappen zoals eerder gerapporteerd.

HOOFDSTUK 6

Effects of Cell Seeding and Cyclic Stretch on the Fiber Remodeling in an Extracellular Matrix–Derived Bioscaffold

Small intestine submucosa, een uit extracellulair matrix verkregen biomateriaal (ECM-SIS), is met goede resultaten gebruikt om de heling van ligamenten en pezen te verbeteren. ECM-SIS heeft een vezeloriëntatie van ±30˚ waardoor zijn applicatie mogelijk niet helemaal optimaal voor het herstel van ligamenten en pezen is. De doelstelling van deze studie is derhalve om de collageenvezel oriëntatie van het ECM-SIS in vitro te verbeteren door middel van celpopulatie en cyclisch rek. De hypothese is dat het synergetische effect van celpopulatie en cyclisch rek zullen resulteren in het remodeleren van collageenvezels in het ECM-SIS tot gealigneerde vezels. Deze gealigneerde ECM-SIS zou mogelijk verbeterde conductieve eigenschappen hebben. Methodes: drie experimentele groepen werden opgezet: groep I (n=14), het ECM-SIS werd gezaaid met fibroblasten en cyclisch gerekt; groep II (n=13), het ECM-SIS werd gezaaid met fibroblasten, maar werd niet cyclisch gerekt; en groep III (n=8), ECM-SIS werd niet gezaaid met fibroblasten, maar wel cyclisch gerekt. Na 5 dagen werden de ECM-SIS biomaterialen verwerkt om de collageenvezelorientatie te kwantificeren middels de small-angle light scattering (SALS), (n=9 voor groep I; n=8 voor groepen II en III). Voor groepen I en II, waarin de ECM-SIS werden gezaaid met fibroblasten, werd de celmorfologie en celorientatie en de nieuw geproduceerde collageen onderzocht met de confocale fluorescentie microscopie (n=3 per groep) en transmissie elektronen microscopie (n=2 per groep). Resultaten: de resultaten laten zien dat de collageenvezeloriëntatie in groep I, meer in de rekrichting was gealigneerd dan de andere twee groepen. De gemiddeld hoek daalde van 25.38 naar 7.18 ($p < 0.05$), de angular dispersion was ook verminderd (37.48 vs. 18.58, $p < 0.05$). In tegenstelling tot groep I lieten Groep II en III minimale veranderingen zien. De fibroblasten in groep I was meer in de rekrichting gealigneerd dan in groep II. En nieuw geproduceerde collageenfibrillen werden in beide groepen geobserveerd. Conclusie: Deze studie laat zien dat de combinatie van celpopulatie en cyclisch rek het ECM-SIS kunnen remodeleren en de collageenvezels in de rekrichting kunnen aligneren. De applicatie van de gealigneerde ECM-SIS heeft het vooruitzicht om tot een betere heling te bekomen in ligamenten en pezen.

HOOFDSTUK 7

Intrinsic Healing Response of the Human Anterior Cruciate Ligament: An Histological Study of Reattached ACL Remnants

Een verbinding tussen de distale tibiale gescheurde kruisband met de achterste kruisband wordt dikwijls tijdens een kijkoperatie geobserveerd. Deze verbinding zou mogelijk een aanwijzing kunnen zijn dat de voorste kruisband wel een helingsrepons heeft. De doelstelling van deze studie is om te onderzoeken of deze verbindingsweefsel histologische karakteristieken vertoont die vergelijkbaar is het helingsweefsel van het mediale collaterale ligament, een ligament dat bekend staat spontaan te kunnen helen. Methodes: Een biopt van het verbindingsweefsel werd afgenomen in vijf patiënten en door middel van standaard histologie en immunokleuring op α-smooth muscle actin en collageen type 3 onderzocht. Resultaten: De resultaten laten zien dat het verbindingsweefsel typische helingsresponse karakteristieken vertoont: de verbinding van distale voorste kruisband aan de achterste kruisband kon niet door middel van krachtige tractie worden verbroken; het microscopisch beeld van het bioptweefsel liet een gedesorganiseerde weefsel zien met toegenomen vasculariteit en aanwezigheid van vet vacuoles. De gemiddelde celpopulatie bedroeg 631±269 cellen per mm^2 waarvan 68±20% positief kleurde voor α-SMA. Semi-kwantitatieve analyse liet een verhoogde collageen type 3 hoeveelheid zien met een gemiddelde score van 3. Conclusie: Deze studie toont aan dat het proximale eenderde deel van de humane voorste kruisband een intrinsieke helingsrespons heeft die vergelijkbaar is met de helingsrespons van de MCL.

HOOFDSTUK 8

Healing of the Goat Anterior Cruciate Ligament After a New Suture Repair Technique and Bioscaffold Treatment

Direct herstel van de voorste kruisband (VKB) is in het verleden toegepast om te proberen de gescheurde kruisband te helen. Helaas waren de resultaten niet bevredigend die retrospectief te wijten zijn aan de hechttechniek en suboptimale helingscondities. Deze suboptimale condities zou mogelijk kunnen worden verbeterd door gebruik te maken van een nieuwe hechttechniek en het biomateriaal small intestinal submucosa (SIS). De hypothese is dat de nieuwe hechttechniek de gescheurde uiteinden van de kruisband onder tractie bij elkaar kan houden en dat SIS de heling van de kruisband zal stimuleren. Methodes: Een geitenstudiemodel werd in deze studie gebruikt. In de Hecht groep, werd de linker kruisband volledig doorgenomen en gehecht met de nieuwe “triple X locking” hechttechniek (n = 5) die approximatie en fixatie onder tractie mogelijk maken. De kruisbanden in de Hecht-SIS ondergingen dezelfde procedure zoals in de Hecht groep met daarbij de toevoeging van SIS (n = 5). De rechter niet-geopereerde kruisband fungeerde als controle groep. Na 12 weken werd de voor-

achterwaartse translatie, in situ krachten van de helende kruisband, de diameter en de stijfheid van de kruisband gemeten. Tot slot werd routine histologie verricht op de weefsels. Resultaten: Morfologisch onderzoek liet zien dat de helende kruisband continue is en collagene structuur is. De "cross-sectional area" van de Hecht groep en de Hecht-SIS groep was respectievelijk 35% en 50% ten opzichte van de controle groep. De voor-achterwaartse translaties waren niet significant verschillend tussen de Hecht en Hecht-SIS groep, behalve op 30° was de in situ kracht van de Hecht-SIS groep hoger dan in de Hecht groep. De trekproeven lieten zien dat de stijfheid tussen de Hecht groep en Hecht-SIS groep significant niet verschillend van elkaar waren (31.1 ± 8.1N/mm vs. 41.9 ± 18.0N/mm [$p > 0.05$]). Histologisch onderzoek liet zien dat de collageenvezels longitudinaal van origo naar insertie gealigneerd waren. Veel meer fibroblasten waren aanwezig in de helende weefsel dan in de normale weefsel. Conclusie: Deze studie laat zien dat het mogelijk is om de geiten kruisband te helen met de nieuwe hechttechniek en SIS. De mechanische resultaten is vergelijkbaar met de resultaten die behaald worden met een voorste kruisbandreconstructie. Concluderend is deze nieuwe methode om de kruisband met of zonder SIS te helen veelbelovend.

HOOFDSTUK 9

Histological Evaluation of the Healing Goat Anterior Cruciate Ligament

De doelstelling van deze studie is om het weefsel van de helende geiten voorste kruisband histologisch te onderzoeken op de fibreuze synoviale membraan, de extracellulaire matrix (ECM), de collageenvezelorientatie, de cellulariteit, de myofibroblasten ratio en mate van collageen type 3 kleuring. De hypothese is dat small intestine submucosa (SIS) de heling verbetert dankzij het scaffolding effect en de groeifactoren. Methodes: In de Hecht groep werd de linker VKB volledig doorgenomen en gehecht met de "triple X locking suture repair" techniek (n=4). De Hecht-SIS group onderging dezelfde procedure met de toevoeging van SIS (n=4). De helende kruisbanden werden geanalyseerd door middel van standaard histologie en immunokleuring op α-smooth muscle actin (SMA) en collageen type 3. Resultaten: Microscopisch onderzoek liet zien dat de fibreuze synoviale membraan rond de VKB in beide groepen was hersteld. De collageenvezels in de Hecht-SIS groep waren compacter georganiseerd, kleurden donkerder, en bevatten minder voids en vet vacuoles. Daarnaast werd neovascularisatie die tussen de collageenvezels liep in beide groepen geobserveerd. Collageen type 3 leek minder te kleuren in de Hecht-SIS groep. De cellulariteit in de Hecht en Hecht-SIS groep was respectievelijk 1265±1034 per mm^2 en 954±378 per mm^2; en 49% en 26% van de cellen kleurden positief voor α-SMA. Conclusie: De helende voorste kruisbanden in beide experimentele groepen lieten histologische karakteristieken zien die vergelijkbaar zijn met de helende mediale collaterale band. Derhalve kan geconcludeerd worden dat de voorste kruisband een intrinsieke helingsrespons heeft.

Een definitief oordeel of SIS een verbeterende effect op de heling heeft, kan nog niet worden gegeven.

HOOFDSTUK 10

Discussie & conclusies

De doelstelling van dit proefschrift is om nieuwe chirurgische methodes te ontwikkelen om patiënten met een voorste kruisbandscheur te behandelen. De beschreven onderzoeksprojecten kunnen in vier thema's onder worden verdeeld: 1) het verkrijgen van gedetailleerder en objectievere informatie over de anatomie van de voorste kruisband; 2) de ontwikkeling van de Arthroscopic Fluorescence Imaging system; 3) het in vitro en in vivo evalueren van Small Intestine Submucosa en tot slot 4) het ontwikkelen van het "bio-enhanced end-to-end ACL repair" techniek om de kruisband te helen. De hoofdbevindingen, conclusies, klinische implicaties en suggesties voor vervolgonderzoek zijn in dit laatste hoofdstuk beschreven.

De eerste conclusie is dat de combinatie van de cryo-imaging systeem met tractografie een objectievere en accurate methode is om de 3-D collageenvezel anatomie van de voorste kruisband te kwantificeren. Deze methode zou ook van toepassing kunnen komen om de collageenvezel architectuur van de andere collagene structuren te kwantificeren zoals de meniscus, tussenwervelschijven, hartkleppen, etc. De gedetailleerde informatie zou onze inzichten over de functie en pathofysiologie van deze gewicht dragende structuren kunnen vergroten. De implicatie zou kunnen zijn dat de verkregen vezelanatomie als een blauwdruk kan worden gebruikt voor nieuwe behandelingen.

De voorlopige hoofdbevinding en conclusie van de tweede studie is dat de onderzochte voorste kruisbanden een enkelvoudige band is met korte vezels posterolateraal die richting anteromediaal geleidelijk langer worden. Deze voorlopige conclusie ondersteunt niet het concept dat de voorste kruisband uit twee of drie anatomische verschillende bundels bestaat. Het voorgaande geldt derhalve eveneens voor het concept van dubbel of driedubbele boortunnel voorste kruisband reconstructies. (27-32) Echter, dubbel of driedubbele boortunnel voorste kruisband reconstructies reconstrueert effectief wel de globale anatomie door de korte vervangpees posterolateraal te plaatsen en de langere anteromediaal. Derhalve wordt de anatomische dubbel of driedubbele boortunnel VKB reconstructies aangemoedigd maar gebaseerd op een andere rationale. De implicatie van deze studie is dat het basale informatie verschaft over de VKB anatomie en voor verschillende doeleinden kan worden gebruikt zoals een blauwdruk om de "bio-enhanced end-to-end ACL repair" techniek ver te ontwikkelen, VKB-reconstructies optimaliseren en voor het gebruik bij oneindige elementen modelering.

De hoofdbevinding en conclusie van de derde studie is dat het arthroscopic fluorescence imaging (AFI) systeem de femorale voorste kruisband insertie nauwkeurig kan visualiseren. Daarnaast heeft het AFI systeem laten zien dat het snel, makkelijk, goedkoop, real-time en gepersonaliseerd is. Momenteel wordt het AFI systeem verder ontwikkeld voor het gebruik in patiënten en de waarde ervan zal in toekomstige klinische onderzoeken worden geëvalueerd. De klinische implicatie is dat mogelijk 50% van de revisiechirurgie, veroorzaakt door het niet optimaal plaatsen van de donorpees, zou kunnen worden voorkomen. Mogelijk zou het AFI systeem ook de paradigma van de anatomische voorste kruisband reconstructie kan faciliteren waardoor vroegtijdige arthrose kan worden voorkomen. Daarnaast zou de AFI systeem een platform kunnen zijn voor kleurgeleide arthroscopische chirurgie in andere gewrichten alsmede om de diagnose en gradatie van degeneratie in collagene structuren.

De hoofbevinding en conclusie van de vierde studie is dat SIS de fibrillogenese gerelateerde genexpressie kan onderdrukken zodat de ultrastructuur, morfologie en mechanische eigenschappen wordt verbeterd. De implicatie van deze studie is dat SIS een geschikte kandidaat is om gebruikt te worden voor de VKB heling gebaseerd op de bioactieve stoffen en conductieve eigenschappen.

De hoofdbevinding en conclusie van de vijfde studie dat de combinatie van fibroblastpopulatie en cyclisch rek een effectieve methode is om de collageenvezeloriëntatie van het biomateriaal ECM-SIS te verbeteren. Terwijl alleen fibroblastpopulatie of cyclisch rek niet voldoende was om de ultrastructuur te veranderen. Deze bevindingen benadrukken het belang van het synergetische effecten van fibroblasten en mechanische stimuli in de matrix modelering.

De hoofdbevinding en conclusie van de zesde studie is dat de geiten VKB kan helen door gebruik te maken van de “bio-enhanced end-to-end ACL repair” met de triple X hechttechniek en SIS. Daarnaast kan geconcludeerd worden dat de mechanische eigenschappen van de helende kruisband vergelijkbaar is met de VKB reconstructie in een geitenmodel. (33, 34)

De hoofdbevinding en de conclusie van de zevende studie is dat de helende voorste kruisband in beide groepen histologische karakteristieken vertoont die vergelijkbaar is met de spontane heling van het mediale collaterale ligament. Derhalve kan geconcludeerd worden dat de geiten VKB een intrinsieke helingsresponse heeft. (35) De conclusie dat SIS mogelijkerwijs positief aan de heling heeft bijgedragen, kon nog niet worden gemaakt.

De hoofdbevinding en conclusie van de achtste studie is dat additioneel bewijs is gevonden voor het intrinsieke helingspotentieel van de voorste kruisband. De implicatie van deze studie samen met de vorige twee is dat er voldoende basis is om translationele studies te garanderen om de “bio-enhanced end-to-end ACL repair” door te ontwikkelen in patiënten.

REFERENTIES

1. R. C. Mather, 3rd *et al.*, Societal and economic impact of anterior cruciate ligament tears. *The Journal of bone and joint surgery. American volume* **95**, 1751 (Oct 2, 2013).
2. R. H. Brophy, R. W. Wright, M. J. Matava, Cost analysis of converting from single-bundle to double-bundle anterior cruciate ligament reconstruction. *The American journal of sports medicine* **37**, 683 (Apr, 2009).
3. D. J. Biau, C. Tournoux, S. Katsahian, P. Schranz, R. Nizard, ACL reconstruction: a meta-analysis of functional scores. *Clinical orthopaedics and related research* **458**, 180 (May, 2007).
4. S. Claes *et al.*, Anatomy of the anterolateral ligament of the knee. *Journal of anatomy* **223**, 321 (Oct, 2013).
5. B. D. Beynnon, R. J. Johnson, J. A. Abate, B. C. Fleming, C. E. Nichols, Treatment of anterior cruciate ligament injuries, part 2. *The American journal of sports medicine* **33**, 1751 (Nov, 2005).
6. B. D. Beynnon, R. J. Johnson, J. A. Abate, B. C. Fleming, C. E. Nichols, Treatment of anterior cruciate ligament injuries, part I. *The American journal of sports medicine* **33**, 1579 (Oct, 2005).
7. A. van Kampen, A. B. Wymenga, H. J. van der Heide, H. J. Bakens, The effect of different graft tensioning in anterior cruciate ligament reconstruction: a prospective randomized study. *Arthroscopy : the journal of arthroscopic & related surgery : official publication of the Arthroscopy Association of North America and the International Arthroscopy Association* **14**, 845 (Nov-Dec, 1998).
8. J. A. Feagin, Jr., W. W. Curl, Isolated tear of the anterior cruciate ligament: 5-year follow-up study. *The American journal of sports medicine* **4**, 95 (May-Jun, 1976).
9. M. F. Sherman, L. Lieber, J. R. Bonamo, L. Podesta, I. Reiter, The long-term followup of primary anterior cruciate ligament repair. Defining a rationale for augmentation. *The American journal of sports medicine* **19**, 243 (May-Jun, 1991).
10. L. Engebretsen, P. Benum, O. Fasting, A. Molster, T. Strand, A prospective, randomized study of three surgical techniques for treatment of acute ruptures of the anterior cruciate ligament. *The American journal of sports medicine* **18**, 585 (Nov-Dec, 1990).
11. S. L. Woo, T. M. Vogrin, S. D. Abramowitch, Healing and repair of ligament injuries in the knee. The Journal of the American Academy of Orthopaedic Surgeons 8, 364 (Nov-Dec, 2000).
12. S. L. Hsu, R. Liang, S. L. Woo, Functional tissue engineering of ligament healing. *Sports Med Arthrosc Rehabil Ther Technol* **2**, 12 (2010).
13. Z. Ge, J. C. Goh, E. H. Lee, Selection of cell source for ligament tissue engineering. *Cell Transplant* **14**, 573 (2005).
14. J. M. McKean, A. H. Hsieh, K. L. Sung, Epidermal growth factor differentially affects integrin-mediated adhesion and proliferation of ACL and MCL fibroblasts. *Biorheology* **41**, 139 (2004).
15. C. N. Nagineni, D. Amiel, M. H. Green, M. Berchuck, W. H. Akeson, Characterization of the intrinsic properties of the anterior cruciate and medial collateral ligament cells: an in vitro cell culture study. *J Orthop Res* **10**, 465 (Jul, 1992).
16. W. J. Radford, A. A. Amis, F. W. Heatley, Immediate strength after suture of a torn anterior cruciate ligament. *The Journal of bone and joint surgery. British volume* **76**, 480 (May, 1994).
17. M. M. Murray *et al.*, Collagen-platelet rich plasma hydrogel enhances primary repair of the porcine anterior cruciate ligament. *J Orthop Res* **25**, 81 (Jan, 2007).
18. M. B. Fisher *et al.*, Potential of healing a transected anterior cruciate ligament with genetically modified extracellular matrix bioscaffolds in a goat model. *Knee surgery, sports traumatology, arthroscopy : official journal of the ESSKA* **20**, 1357 (Jul, 2012).

19. P. Vavken, M. M. Murray, Translational Studies in ACL repair. *Tissue Eng Part A*, (Jul 21, 2009).
20. T. Zantop, T. W. Gilbert, M. C. Yoder, S. F. Badylak, Extracellular matrix scaffolds are repopulated by bone marrow-derived cells in a mouse model of achilles tendon reconstruction. *J Orthop Res* **24**, 1299 (Jun, 2006).
21. T. W. Gilbert, A. M. Stewart-Akers, A. Simmons-Byrd, S. F. Badylak, Degradation and remodeling of small intestinal submucosa in canine Achilles tendon repair. *The Journal of bone and joint surgery. American volume* **89**, 621 (Mar, 2007).
22. S. L. Voytik-Harbin, A. O. Brightman, M. R. Kraine, B. Waisner, S. F. Badylak, Identification of extractable growth factors from small intestinal submucosa. *Journal of cellular biochemistry* **67**, 478 (Dec 15, 1997).
23. J. P. Hodde, R. D. Record, H. A. Liang, S. F. Badylak, Vascular endothelial growth factor in porcine-derived extracellular matrix. *Endothelium : journal of endothelial cell research* **8**, 11 (2001).
24. S. L. Woo, Y. Takakura, R. Liang, F. Jia, D. K. Moon, Treatment with bioscaffold enhances the the fibril morphology and the collagen composition of healing medial collateral ligament in rabbits. *Tissue engineering* **12**, 159 (Jan, 2006).
25. V. Musahl *et al.*, The use of porcine small intestinal submucosa to enhance the healing of the medial collateral ligament--a functional tissue engineering study in rabbits. *J Orthop Res* **22**, 214 (Jan, 2004).
26. R. Liang *et al.*, Long-term effects of porcine small intestine submucosa on the healing of medial collateral ligament: a functional tissue engineering study. *J Orthop Res* **24**, 811 (Apr, 2006).
27. P. S. Cha *et al.*, Arthroscopic double-bundle anterior cruciate ligament reconstruction: an anatomic approach. *Arthroscopy : the journal of arthroscopic & related surgery : official publication of the Arthroscopy Association of North America and the International Arthroscopy Association* **21**, 1275 (Oct, 2005).
28. H. W. Mott, Semitendinosus anatomic reconstruction for cruciate ligament insufficiency. *Clinical orthopaedics and related research*, 90 (Jan-Feb, 1983).
29. T. Muneta *et al.*, Two-bundle reconstruction of the anterior cruciate ligament using semitendinosus tendon with endobuttons: operative technique and preliminary results. *Arthroscopy : the journal of arthroscopic & related surgery : official publication of the Arthroscopy Association of North America and the International Arthroscopy Association* **15**, 618 (Sep, 1999).
30. N. K. Shino K, Nakamura N, Mae T, Ohtsubo H, Iwahashi T, Nakagawa S, Anatomic anterior cruciate ligament reconstruction using two double-looped hamstring tendon grafts via twin femoral and triple tibial tunnels. *Oper Tech Orthop* **15**, 130 (2005).
31. K. Yasuda *et al.*, Anatomic reconstruction of the anteromedial and posterolateral bundles of the anterior cruciate ligament using hamstring tendon grafts. *Arthroscopy : the journal of arthroscopic & related surgery : official publication of the Arthroscopy Association of North America and the International Arthroscopy Association* **20**, 1015 (Dec, 2004).
32. T. Rosenberg, B. Graf. (Mansfield, MA: Acufex Microsurgical, 1994).
33. S. D. Abramowitch, C. D. Papageorgiou, J. D. Withrow, T. W. Gilbert, S. L. Woo, The effect of initial graft tension on the biomechanical properties of a healing ACL replacement graft: a study in goats. *J Orthop Res* **21**, 708 (Jul, 2003).
34. K. P. Spindler, M. M. Murray, J. L. Carey, D. Zurakowski, B. C. Fleming, The use of platelets to affect functional healing of an anterior cruciate ligament (ACL) autograft in a caprine ACL reconstruction model. *J Orthop Res* **27**, 631 (May, 2009).
35. C. Frank *et al.*, Medial collateral ligament healing. A multidisciplinary assessment in rabbits. *Am J Sports Med* **11**, 379 (Nov-Dec, 1983).

CHAPTER 13

Tóm tắt tiếng Việt

"Con người làm tôi ngạc nhiên về nhân tính. Bởi vì họ hy sinh sức khỏe để làm tiền. Rồi sau đó họ hy sinh tiền để tái tạo sức khỏe..." - Dalai Lama XIV

CHƯƠNG 13

Mục tiêu chính của những nghiên cứu này trình bày trong luận án này là để cải thiện kết quả lâm sàng của bệnh nhân bị rách Dây Chằng Chéo Trước của họ bằng cách tối ưu hóa sự tái tạo Dây Chằng Chéo Trướ chiện nay và phát triển kỹ thuật sửa chữa Dây Chằng Chéo Trước Dây Chằng Chéo Trước bằng cách nối tận tận có củng cố sinh học giúp mau lành Dây Chằng Chéo Trước.

Mục tiêu chính này dẫn đến những mục đích được mô tả trong chương 1 và có thể được chia thành bốn đề tài: 1) đạt được mục tiêu gần và thông tin chi tiết về giải phẫu học của Dây Chằng Chéo Trước, 2) phát triển Hình Ảnh Học Huỳnh Quang Nội Soi, 3) đánh giá qua thực nghiệm và trên lâm sàng sườn sinh học dưới niêm mạc ruột non, và cuối cùng 4) sự phát triển của kỹ thuật sửa chữa Dây Chằng Chéo Trước bằng cách nối tận tận có củng cố sinh học giúp mau lành Dây Chằng Chéo Trước. Những điều tìm thấy và hàm ẩn trong luận án này sẽ được thảo luận và cho những lời khuyên cho sự nghiên cứu trong tương lai.

NHỮNG ĐIỀU TÌM THẤY VÀ Ý NGHĨA GIẢI PHẪU HỌC

Mục tiêu và những thông tin chi tiết của giải phẫu học của Dây Chằng Chéo Trước là căn bản cho sự hiểu biết chức năng của nó cũng như việc phát triển những phương pháp điều trị hữu hiệu. Trước đây, những nhà nghiên cứu đã phẫu tích bằng tay và đã minh họa hướng các sợi. (1-6). Hệ thống vi tính hóa bằng tay cũng đã được dùng để đạt được hướng của các bó sợi, mặc dầu người dùng của hệ thống này vạch ra hình ảnh thấy được những bó sợi chọn lọc nơi cấp độ kiếng hiển vi. (7) Những nhà nghiên cứu khác dung sự trình bày trong không gian ba chiều của dây chằng bằng cách lượng hóa hình học của thể tích bó sợi sử dụng Hình Ảnh Cộng Hưởng Từ. (8, 9). Mặc dầu giải pháp của những mô hình hình ảnh này thì không đủ để thấy cấu trục sợi một cách chi tiết của Dây Chằng Chéo Trước.

Mặt khác, những kiểu mẫu hình ảnh học giải pháp cao hiện nay như kiếng hiển vi điện tử cắt lớp - SEM, kiếng hiển vi truyền điện tử (electron) (TEM), kiếng hiển vi đồng tiêu (CFM), Mô học ba chiều 3-DH, khảo sát phân tán ánh sáng góc nhỏ- SA(X)S còn bị giới hạn trong những thể tích nhỏ. (*10-13*).

Nhằm lượng giá toàn bộ Dây Chằng Chéo Trước với giải pháp kỹ thuật cao một phương pháp mới được phát triển và hiệu lực hóa. (chương 2). Phương pháp luận này giúp chúng ta có thể đạt được hình ảnh giải phẫu sợi 3 chiều và trả lời câu hỏi lâm sàng liệu Dây Chằng Chéo Trước có chứa những bó sợi khác biệt về nặt giải phẫu không. Phương pháp luận bao gồm hình ảnh huỳnh quang, máy cắt lạnh siêu nhỏ cho hình ảnh, và phần mềm theo dấu sợi cung cấp những điểm nổi bật mới và nhất quán. Nó cho phép đạt được: 1- tư liệu giải phẫu gần mục tiêu nhất, 2- thu thập tư liệu chính xác nhất, 3- thu thập tư liệu ở cấp giải pháp cao và 4- tái tạo mô sợi collagen 3 chiều, chiều dài và bảng đồ kết nối. Sự hàm chứa trong nghiên cứ này là phạm trú nghiên cứu mới được phát

triển để đạt sự chính xác, cận mục tiêu và thông tin chi tiết giải phẫu học về Dây Chằng Chéo Trước có thể được dùng cho các loại dây chằng khác và mô liên kết chịu lực, chẳng hạn như sụn nêm gối, đĩa sống, van tim v...v...

Y văn hiện nay trên giải phẫu học sợi của Dây Chằng Chéo Trước rất mâu thuẫn. Những nhà nghiên cứu báo cáo rằng Dây Chằng Chéo Trước dải liên tục đơn độc của các bó sợi, với những phần khác nhau kéo căng qua biên độ cử động. (1,5). Những báo cáo khác cho rằng Dây Chằng Chéo Trướccó thể chia thành hai bó, có tên là bó trước trong (AMB) và bó sau ngoài (PLB). (2,3). Những người khác cho rằng có ba bó chức năng khác nhau, đặt tên là bó trước trong (AMB), bó sau ngoài (PLB) và bó trung gian (IMB). Sự giải thích nhận thức về sự không nhất quán này là phương pháp luận chủ quan dùng trong những nghiên cứu trên. Với sự trợ giúp của phương pháp luận các mục tiêu trình bày trang chương 2, giải phẫu học bó sợi collagen 3 chiều trong ba khớp gối con người được định tính (chương 3). Những khám phá ban đầu cho thấy Dây Chằng Chéo Trước là một cấu trúc sợi collagen liên tục duy nhất với sợi ngắn sau ngoài và sợi dài chuyển dần vào trước trong. Kết luận sơ khởi không ủng hộ quan niệm hiện nay cho rằng Dây Chằng Chéo Trước có cấu hình là hai hay ba bó sợi. (14-19).

Tuy nhiên, sự tái tạo hai hay ba bó dân chằng chéo trước hai hay ba bó sợi giải phẫu học không hoàn toàn giống với giải phẫu học của Dây Chằng Chéo Trước khi đặt ghép gân ngắn hơn sau ngoài và ghép gân dài hơn trước trong. Như thế, sự tái tạo hai hay ba bó Dây Chằng Chéo Trước hai hay ba bó sợi giải phẫu học được khuyến khích nhưng với phân tích cơ bản khác. Sự hàm ý cẩn thận của nghiên cứu hoa tiêu là cung cấp kiến thức căn bản cua Dây Chằng Chéo Trước và rằng giải phẫu học bó sợi collagen hoạch đắc trong không gian ba chiều có thể được dùng như một kế hoạch phát triển kỹ thuật nối tận tận sinh học của Dây Chằng Chéo Trước, mô hình yếu tố giới hạn và chương trình phục hồi chức năng.

HỆ THỐNG HÌNH ẢNH HỌC HUỲNH QUANG NỘI SOI

Kết quả phẫu thuật sau khi tái tạo Dây Chằng Chéo Trước lệ thuộc rất lớn vào sự đặt gân ghép chính xác vào nơi đính nguyên thủy của Dây Chằng Chéo Trước bị rách. (14,20-27). Sự đặt sai gân ghép là nguyên nhân thường thấy trong phẫu thuật lại. (23-27). Sự lệch hướng nhỏ có thể đem lại sự thay đổi lớn trong sự vững khớp gối. (28-30). Những nghiên cứu hình thái học trước đây bởi Bernard và Hertel và bởi Amis và Jakob đã hoàn thiện để hướng dẫn cách đặt ghép. (31-32).

Tuy nhiên, đặt ghép dưới nội soi hãy còn là một thách đố sự giới hạn kỹ thuật và hình ảnh. Trong những năm cuối 1980, Cái gọi là kỹ thuật tái tạo Dây Chằng Chéo Trước xuyên qua xương quyển kèm theo dụng cụ đã được giới thiệu. Kỹ thuật này cho phép cách đặt ghép chuẩn và nhanh hơn và đã trở thành kỹ thuật hay áp dụng nhất. (33,34). Tuy nhiên kỹ thuật xuyên xương quyển này bị chỉ trích là thiếu chính xác. (20,35,36).

Treong một bình luận, Howel, Hull và McAllister cho rằng:.. "chúng ta phải nhạy bén và cảnh giác về sự chỉ trích việc đặt đường hầm bởi các phẫu thuật viên khác cho tới khi dụng cụ đặt đường hầm bởi những với sự chính xác hơn nữa được áp dụng và cho tới khi những mục tiêu mong muốn đã được chấp thuận phổ quát hơn". (37). Đã có báo cáo rằng khoảng 5% tái tạo Dây Chằng Chéo Trước xuyên qua xương quyển thất bại và rằng khoảng 50% của những thất bại này do đặt ghép sai vị trí. (23-27). Sự phân tích meta gần đây cho thấy chỉ 41% bệnh nhân báo cáo khớp gối được tái tạo của họ bình thường. (38). Gần đây hơn, những nghiên cứu lâm sàng theo dõi lâu dài khám phá khoảng 70- 80% bệnh nhân được tái tạo Dây Chằng Chéo Trước phát triển thoái hóa khớp gối sớm. (28- 30, 39, 40).

Mặc dầu những cơ chế góp phần vào sự thoái hóa khớp sớm này do nhiều yếu tố khác nhau, nhiều nghiên cứu gợi ý rằng sự bất khả thi của sự tái tạo Dây Chằng Chéo Trước xuyên qua xương quyển để tái lập động học khớp gối bình thường đóng vai trò quan trọng trong việc gây ra thoái hóa khớp gối sớm. Những nghiên cứu gây xáo trộn này thúc đẩy cố gắng nghiên cứu tiếp theo để tối ưu hóa kỹ thuật tái tạo dây chằng chéo xuyên qua xương quyển. Vài phẫu thuật viên đã cải biên kỹ thuật tái tạo dây chằng chéo xuyên qua xương quyển trong khi những người khác bỏ kỹ thuật này và tin cậy vào sự nhìn rõ qua nội soi các mốc cơ thể học như thành sau, bờ sụn, gờ liên lồi cầu ngoài, và gờ chẻ đôi để định vị nới bám tận nguyên thủy. (18, 41-45).

Những phương pháp này tuy đòi hỏi kỹ thuật và tốn nhiều thời gian do sự giới hạn hình ảnh, phẫu thích cẩn thận, thay đổi sinh học, và sự yếu kém hình ảnh thêm trong khớp bị chấn thương và thoái hóa. Do đó, kỹ thuật tái tạo Dây Chằng Chéo Trước xuyên qua xương quyển được giới thiệu như vượt qua những khó khăn này. Bất chấp những khó khăn này, con số những phẫu thuật viên gia tăng đã nhìn nhận tầm quan trọng của kỹ thuật tái tạo giải phẫu của Dây Chằng Chéo Trước. Những nghiên cứu trong phòng thí nghiệm trước đây chứng minh rằng sự tái tạo giải phẫu của Dây Chằng Chéo Trước tốt hơn trong việc tái lập chuyển động học khớp gối bình thường. (46-49). Mới đây, Abe và CS đã chứng minh trong một nghiên cứu lâm sàng rằng tái tạo giải phẫu Dây Chằng Chéo Trước tốt hơn cho kỹ thuật tái tạo giải phẫu của Dây Chằng Chéo Trước khi tái lập chuyển động học trong lâm sàng khớp gối. (50). Nhiều hỗ trợ trong hình ảnh học nội soi đã được đề nghị giúp sự tái tạo giải phẫu Dây Chằng Chéo Trước bao gồm cả hệ thống huỳnh quang trong mổ (51-54) và định vị với trợ giúp điện toán (55-57). Sự ứng dụng của những hệ thống này tuy nhiên đã bị chỉ trích là mắc tiền, tốn thời gian, và rủi ro ảnh hưởng ion. (37, 58, 59).

Chiến lược khác giúp hình ảnh hội soi một cách khách quan là hình ảnh học huỳnh quang nơi bám tận. (chương 4). Hình ảnh học huỳnh quang dựa trên sự khám phá của các photons phát ra sau khi kích thích Fluorphore bằng photon của và chiều dài sóng. Dùng những chất đánh dấu huỳnh quang chống tiền ung thư, bướu, và K di căn những nhà nghiên cứu trước đây đã chứng minh thời gian thực hình ảnh nhìn cấu trúc tiêu

điểm trong những màu sắc giả tương phản. Hình ảnh hóa có thể giúp lấy khối bướu hoàn toàn hơn và ngay cả lấy cả các mô tổn thương tiền ung thư không thể nhìn thấy với ánh sáng trắng. (60, 61).

Do Dây Chằng Chéo Trước chủ yếu làm bằng các sợi collagen tự phát huỳnh quang, hình ảnh của sự tự phát huỳnh quang của sợi collagen biến thành ra sự thuận lợi khi nhìn thấy cấu trúc khớp. Sự khác biệt trong đáp ứng quang phổ có thể tách ra bởi sự không pha trộn quang phổ. Sự khác biệt này có thể được trình bày bằng màu sắc giả tương phản giúp phân biệt nơi bám tận nguyên thủy của Dây Chằng Chéo Trước ra khỏi khung nền. Hệ thống hình ảnh huỳnh quang nội soi (AFI) đã chứng minh sự khả thi và khả năng tiềm tàng của phương pháp nhanh chóng, dễ dàng, rẻ tiền, đúng thời gian, bệnh nhân chuyên biệt để nhìn rõ nhất nơi gốc bám tận của Dây Chằng Chéo Trước. Hiện nay, hệ thống AFI được phát triển hơn nữa dùng cho bệnh nhân. Giá trị của nó sẽ được lượng giá trong các nghiên cứu lâm sàng tương lai. Ý nghĩa lâm sàng cho thấy khoảng 50% các phẫu thuật lại do sự đặt sai có thể được phòng ngừa và hệ thống AFI có thể giúp thuận lợi cho sự tái tạo giải phẫu Dây Chằng Chéo Trước nhằm có thể phòng ngừa thoái hóa khớp gối sớm. Ngoài ra, hệ thống AFI cũng có thể là nền tảng cho phẫu thuật nội soi hướng dẫn hình ảnh trong những khớp khác và có thể có giá trị chẩn đoán và phân loại thoái hóa của các mô liên kết khác.

TIẾP CẬN CÔNG NGHỆ MÔ HỌC

Trước đây các phẫu thuật viên cố gắng làm lành đứt Dây Chằng Chéo Trước bằng cách nối tận tận nhau với nhiều mối hình chữ U. (62-66). Kết quả ban đầu khá tốt dù kết quả cuối cùng không thể tiên đoán được. Kết quả theo dõi lâu dài không thỏa đáng. (65, 670 69). Thời đó, điều này dẫn đến ý kiến thường thấy cho rằng đau Dây Chằng Chéo Trước không lành. Mặc dầu vậy, ý tưởng lành Dây Chằng Chéo Trước vẫn còn lôi cuốn. Để tìm giải pháp cho sự lành Dây Chằng Chéo Trước, nhiều nhà khoa học đã bắt đầu nghiên cứu sự lành của dây chằng bên trong nhằm làm sáng tỏ cơ chế ảnh hưởng sự lành dây chằng. (70-84).

Khả năng lành tự nhiên, sự dễ tiếp cận và tần suất gặp phải tổn thương cao khiến dây chằng bên trong thành mô hình nghiên cứu lý tưởng. Các nhà nghiên cứu đã chỉ ra rằng dây chằng bên trong lành qua 3 giai đoạn lành động, mặc dù với những đặc tính sinh cơ học, sự biểu hiện hình thái mô học và thành phần sinh hóa vẫn còn bất thường so với những đặc tính trên của Dây chằng bên trong bên lành. (70-82)

Ngoài ra, nghiên cứu bổ túc trên những dây chằng và gân cơ khác đã dẫn đến một sự gia tăng những kiến thức cơ bản trong những thập kỷ qua. (85-92)

Cùng những cột trụ này, những tiếp cận Công Nghệ Mô Học Chức Năng Mới (FTE) như việc sử dụng các yếu tố tăng trưởng, liệu pháp gen, liệu pháp tế bào và sử dụng giá đỡ đã được phát triển để cải thiện sự lành dây chằng và gân cơ (93-102).

Đặc biệt, giá đỡ sinh học như Niêm Mạc Dưới Ruột Non Heo (SIS) đã mở rộng nghiên cứu gần đây và cho thấy kết quả tốt trong quá trình lành dây chằng bên trong. (96, 103, 104)

Niêm Mạc Dưới Ruột Non Heo (SIS) chủ yếu được tạo bởi collagen loại I và các yếu tố hoạt động sinh học. Khi ứng dụng SIS nghiên cứu trên thỏ vào sự lành dây chằng bên trong cho thấy kết quả cải thiện những đặc tính cơ học và hình thái mô học. Những tác động có lợi này đã khẳng định khả năng tác động như cung cấp giá đỡ và sự tăng trưởng của nó và những yếu tố hóa tinh có thể vừa thúc đẩy sự di trú của tế bào vào nơi lành dây chằng, vừa thúc đẫy cự tái tưới máu và sửa chữa các mô tổn thương. (105-108)

Tác động sớm của SIS trên sự tổng hợp sợi collagen trong sự lành dây chằng vẫn cần được làm sáng tỏ (chương 5). Khám phá chủ yếu là khi định lượng thời gian thực PCR đã chứng tỏ rằng lượng mRNAs của collagen loại V, decorin, biglycan và lumican trong nhóm sử dụng SIS lần lượt là 41, 58, 51, và 43%, thấp hơn có ý nghĩa tương ứng với từng loại trong nhóm không dùng SIS.

Những khác biệt đáng chú ý trong biểu hiện gen có liên quan mật thiết đến đặc tính hình thái được cải thiện, thường đi kèm với sự đặc tính cơ học tốt hơn, như đã được báo cáo trong những nghiên cứu trước đây với thời gian nghiên cứu dài hạn.

Nghiên cứu này gợi ý rằng SIS là một ứng viên tốt được dùng trong sự lành của Dây Chằng Chéo Trước dựa trên hoạt tính sinh học và các đặc tính dẫn truyền.

Giá đỡ sinh học SIS có thể được cải thiện hơn nữa bằng cách thay đổi siêu cấu trúc của nó gần giống với sự định hướng sợi collagen được dóng hàng tốt nhất của dây chằng tự nhiên. Một cách tiếp cận để đạt mục tiêu này là phân rãi nguyên bào sợi lên cấu trúc SIS và tạo lực căng đồng tâm lên cấu hình này (chương 6).

Các nghiên cứu đã chỉ ra rằng các tế bào có khuynh hướng tránh lực căng mặt ngoài theo trục (109-111). Khi các tế bào gắn vào chất nền sợi, nó có khuynh hướng dóng hàng theo những sợi theo hướng bị kéo căng (ứng suất căng trên tế bào) và tu chỉnh chất nền nhanh chóng bằng cách tăng điều hòa metalloproteinases (MMPs) của chất nền (112-114). Ngoài ra, nguyên bào sợi dóng hàng theo hướng kéo căng tạo thành những sợi colagen de novo. (115, 116)

Sự tìm thấy chủ yếu của nghiên cứu này là sự kết hợp giữa việc phân rãi nguyên bào sợi và sự căng đồng tâm theo một trục có thể cải thiện hiệu quả sự dóng hàng của sợi collagen trong giá đỡ sinh học ECM-SIS hướng theo trục tác động lực căng, trong khi kéo căng cơ học hoặc phân rải tế bào đơn thuần không đủ để tác động lên siêu cấu trúc của giá đỡ. Những điều tìm thấy này nhấn mạnh tầm quan trọng của tác động đồng vận giữa tế bào và kích thích cơ học trong qua trình tu chỉnh chất nền.

NỐI TẬN TẬN DÂY CHẰNG CHÉO TRƯỚC VỚI TĂNG CƯỜNG SINH HỌC

Sự lành Dây Chằng Chéo Trước bị đứt là một khả năng chiến lược nhằm phục hồi chức năng cho Dây Chằng Chéo Trước, loại bỏ sự cần thiết cho sự thu hoạch gân ghép hay làm tổn thương mô đặc biệt trong phẫu thuật tái tạo Dây Chằng Chéo Trước khác.

Ý tưởng của việc lành Dây Chằng Chéo Trước giờ đây đã có thể thực hiện được và đúng vào lúc này nhờ vào kết quả lý thú của sự tiếp cận Công Nghệ Mô Học Chức Năng Mới -FTE và vào những kết quả khá tốt của việc tái tạo Dây Chằng Chéo Trước. (*117-121*).

Mặc dù ý kiến thường thấy cho rằng Dây Chằng Chéo Trước không có khả năng lành nội tại, những nghiên cứu báo cáo hàng loạt ca trước đây đã chỉ ra khả năng lành tự nhiên của Dây Chằng Chéo Trước bị đứt. (*119, 122-124*)

Các phẫu thuật viên cũng đã thử nghiệm can thiệp phẫu thuật nhằm kích thích quá trình lành Dây Chằng Chéo Trước. (*117, 125, 126*)

Bác sĩ Steadman đã cố định lại đầu gần của Dây Chằng Chéo Trước bị đứt vào gần điểm bám chỗ xương đùi, khi máu nuôi phụ và các tế bào tủy xương được phục hồi bởi làm gãy xương vi thể xương kế cận để tạo *phản ứng lành*. Ông đã chứng minh rằng kỹ thuật "phản ứng lành" tạo ra sự lành Dây Chằng Chéo Trước và cải thiện độ vững khớp gối. (*117*)

Tuy nhiên, 23% các bệnh nhân này bị tái chấn thương và cần phải tái tạo lại Dây Chằng Chéo Trước. Một điểm hạn chế được báo cáo là sự lựa chọn bệnh nhân cẩn thận. Cùng với những nghiên cứu lâm sàng, các nghiên cứu trong phòng thí nghiệm đã tìm ra và nêu giả thuyết rằng nhiều yếu tố như môi trường tại chỗ và các yếu tố nội tại có ảnh hưởng hết sức sâu sắc lên quá trình lành Dây Chằng Chéo Trước. (78) Những nghiên cứu tiếp theo cũng cho thấy nguyên bào sợi Dây Chằng Chéo Trước có thể được kích thích thông qua việc sử dụng các yếu tố tăng trưởng, huyết tương tươi giàu tiểu cầu (PRP) và giá đỡ. (120, 127-129)

Ngoài ra, các nhà nghiên cứu cũng đánh giá thất bại của việc tái tạo Dây Chằng Chéo Trước thì đầu và cho rằng kỹ thuật khâu tái tạo và việc tập PHCN là chưa đủ. (67, 130) Vào năm 2007, Murray, Fleming và cộng sự chứng minh tính khả thi của kỹ thuật tái tạo D Dây Chằng Chéo Trước có tăng cường sinh học bằng việc dùng PRP trong điều trị các tổn thương Dây Chằng Chéo Trước. Trong một nghiên cứu trên heo, Dây Chằng Chéo Trước bị cắt ngang được may lại bằng mũi chữ U và tăng cường bằng chỉ không tan. Kết quả cho thấy sự cải thiện về sinh cơ học, tuy nhiên, kết quả vẫn dưới mức Dây Chằng Chéo Trước bình thường. (120, 131)

Fisher và cộng sự phát triển kỹ thuật tái tạo Dây Chằng Chéo Trước có tăng cường sinh học với sự ứng dụn PRP, SIS và mũi chữ U khâu bằng chỉ không tan. (*118*). Kết quả cho thấy sự cải thiện về sinh cơ học, mặc dù vẫn không đạt được Dây Chằng Chéo Trước bình thường. Nghiên cứu của chúng tôi với mục tiêu nhằm vào hai yếu tố chính, bằng cách dung kỹ thuật may mới với chỉ tan kết hợp với giá đỡ sinh học SIS (**Chapter 7**).

Mục tiêu đầu tiên là áp dụng kỹ thuật may mới có lực căng cao hơn và sức kéo đứt mối chỉ cao hơn so với những kỹ thuật may đã dùng trước đây như mũi chữ U hoặc may nhiều mũi móc sâu. Hiển nhiên là kỹ thuật may nối mới sẽ áp sát và giữ được hai đầu gân đứt lại nhau và như thế dẫn đến sự lành dây chằng. Mục tiêu thứ hai nhằm đánh giá hiệu quả của giá đỡ sinh học dung giá đỡ kép lớp dưới niêm mạc của ruột non (SIS) trong vai trò yếu tố kích hoạt và yếu tố tăng cường sự lành Dây Chằng Chéo Trước. Những nghiên cứu khác cho thấy SIS có thể cung cấp chất nền collagen nhằm thúc đẩy sự di chuyển của các tới bào tới vùng lành dây chằng để tăng tái tưới máu và sửa chữa tổn thương. (*17-19*).

Sự tìm thấy chủ yếu cho thấy rằng Dây Chằng Chéo Trước cắt ngang trong mô hình trên dê có thể lành với sự tiếp cận mới này và rằng sự tiếp xúc bề mặt dây chằng là một điều kiện cần cho sự lành Dây Chằng Chéo Trước bên trong khớp gối. So với nghiên cứu mới đây tập trung trên sự may nối Dây Chằng Chéo Trước kết hợp với sự cung cấp huyết tương giàu tiểu cầu (PRP) và giá đỡ sinh học, (*118, 120*), nghiên cứu của chúng tôi cho thấy kết quả tương tự về mặt kết quả chức năng.

Tổng xê dịch trong mặt phẳng trước sau của Dây Chằng Chéo Trước được tái tạo lớn gấp 4 lần so với xê dịch của bên lành, dưới tải lực trước và sau qua xương chày là 67N.

Fisher và cộng sự tìm thấy độ lớn gấp ba lần với cùng tải lực trước sau và Fleming, Murray cùng cộng sự thấy gấp 3.5 lần xê dịch trước xương quyển với tải lực 35 N.

Sự vững chắc của Dây Chằng Chéo Trước đã lành, so với nhóm chứng, lần lượt là 23% trong nghiên cứu của chúng tôi, 42% trong nghiên cứu của Fisher và cộng sự, và 25% trong nghiên cứu của Fleming, Murray và cộng sự. Ngoài những điểm tương đồng, có những khác biệt được ghi nhận giữa các nghiên cứu. Ví dụ, những nghiên cứu khác dùng mũi tăng cường trong khi nghiên cứu chúng tôi chỉ dựa trên kỹ thuật may mũi khóa với chỉ tan. So với những kết quả của những nghiên cứu tái tạo Dây Chằng Chéo Trước có tăng cường sinh học với những kết quả báo cáo trước đây về sự tái tạo Dây Chằng Chéo Trước Trên Dê với ghép gân- xương lấy từ xương bánh chè. Có thể kết luận được rằng, kết quả tương đương với sự tái tạo Dây Chằng Chéo Trước. (132, 133)

Mới đây nhất, Kohl và cộng sự đã tìm ra một cách tiếp cận khác để mang lại sự lành Dây Chằng Chéo Trước. Một dụng cụ cố định động bên trong gân (DIS) đã được phát triển nhằm buộc hai đầu Dây Chằng Chéo Trước đứt trong khi giữ gối trong tư thế chuyển dịch ra sau cố định.

Sự tự lành Dây Chằng Chéo Trước được hỗ trợ với hai đầu dây chằng áp sát với nhau. Ngoài ra, một lớp bao collagen được đặt quanh Dây Chằng Chéo Trước, PRP được áp dụng và sự kích thích tủy xương tại điểm bám xương đùi được sử dụng. Nhưng kết quả nghiên cứu này đầy hứa hẹn, nhưng kết quả thấp hơn so với kkỹ thuật tái tạo Dây Chằng Chéo Trước may nối tận tận với tăng cường sinh học. Bên cạnh những nghiên cứu về sự lành Dây Chằng Chéo Trước được cắt ngang Dây Chằng Chéo Trước ở đoạn giữa còn có

những nghiên cứu cắt ngang Dây Chằng Chéo Trước ở điểm bám tận phía xương đùi. (*121, 134*).

Kết quả những nghiên cứu này cho thấy Dây Chằng Chéo Trước cũng vẫn lành ngang điểm bám. Kết quả nghiên cứu mô học trên sự lành dây chằng không được báo cáo thường xuyên. (*118, 120*)

Từ đó, thật thú vị để đánh giá sự lành của Dây Chằng Chéo Trước qua sự xuất hiện của màng hoạt dịch, chất nền ngoại bào (ECM), sự định hướng các sợi collagen, các tế bào, tỉ lệ bắt màu nhuộm giữa myofibroblasts và collagen loại 3 (Chương 8).

Sự tìm thấy chủ yếu là Dây Chằng Chéo Trước lành với đa tế bào và tăng tưới máu. Ngoài ra, sự lành Dây Chằng Chéo Trước biểu hiện những đặc tính mô học đặc trưng cũng có thể quan sát thấy ở quá trình lành tự nhiên những dây chằng khác, chẳng hạn như Dây Chằng Bên Trong. (81)

Trước đây, có vài quan sát nhận định rằng dấu vết còn lại phía xương quyển người của Dây Chằng Chéo Trước đứt có thể dính vào Dây Chằng Chéo Sau hoặc hố khuyết gian lồi cầu. Hiện tượng đính lại này hàm ý rằng Dây Chằng Chéo Trước có khả năng lành ngay cả khi không có mũi may nối nào. Tuy nhiên, không có bất cứ đánh giá mô học nào từ việc tạo dính lại dây chằng vào xương trong kết luận này. (135-137)

Trong Chương 9, bằng chứng hiển nhiên đã cho thấy Dây Chằng Chéo Trước người có khả năng lành nội tại. Kết quả không chỉ chứng minh khả năng lành dựa trên những đặc tính hình thái học đại thể mà còn cho thấy nhưng đặc tính mô học đặc trưng thấy được trong tiến trình lành Dây Chằng Bên Trong.

Hàm ý của nghiên cứu này cùng với chương 7, 8 và y văn hiện hành cho thấy có những căn cứ đầy đủ để đảm bảo cho những nghiên cứu xa hơn để phát triển và đánh giá kỹ thuật tái tạo Dây Chằng Chéo Trước nối tận tận có tăng cường sinh học cho Dây Chằng Chéo Trước bị đứt ở người.

Tuy nhiên, chúng ta cần nhớ rằng, Dây Chằng Chéo Trước đứt do chấn thương khớp gối không phải là nguyên nhân đơn độc và duy nhất gây mất vững khớp gối. Mất vững khớp gối vẫn có thể xảy ra ở gối bị chấn thương ngay sau khi Dây Chằng Chéo Trước có vẽ không lành. Công cụ chẩn đoán định lượng cho mất vững đa hướng khớp gối sẽ rất có giá trị trong việc xác định và phân loại mức độ của những phương tiện làm vững gối bị căng dãn hay tổn thương khác. Gần đây, những cách điều trị hỗ trợ như các thủ thuật ngoài khớp đã được nhắc đến và đề nghị nhằm cải thiện dự hậu cho những bệnh nhân tái tạo Dây Chằng Chéo Trước. (138)

NHỮNG KHUYẾN CÁO CHO NGHIÊN CỨU TRONG TƯƠNG LAI

Trong luận án Tiến Sĩ này, nhiều nghiên cứu thực nghiệm và nghiên cứu chuyển vị đã được thực hiện. Phương pháp luận để định lượng hướng các sợi collagen trong không gian ba chiều của Dây Chằng Chéo Trước có thể là một công cụ hữu ích để xác định kiến trúc sợi của các cấu trúc collagen khác như sụn chêm, đĩa lên sống, van tim, v.v... Kiến

thức giải phẫu học chi tiết của các cấu trúc chịu lực này có thể gia tăng sự hiểu biết của chúng ta về chức năng cũng như sinh lý bệnh của các cấu trúc này. Giải phẫu sợi có thể là dấu nhận dạng hương dẫn sự phát triển các kiểu điều trị mới. Nghiên cứu theo dõi với mẫu lớn hơn có thể hữu ích cho căn cứ xa hơn và tổng quá hóa sự kết luận trong chương ba về giải phẫu học sơi Dây Chằng Chéo Trước.

Liên quan đến nội soi huỳnh quang, hiện nay, hệ thống AFI sẽ còn được phát triển them cho sử dụng lâm sàng và giá trị của nó trong sự tái tạo Dây Chằng Chéo Trước theo giải phẫu học trên bệnh nhân còn chưa được lượng giá.

Hệ thống AFI có thể cũng sẽ được sử dụng như nên tảng lâm sàng cho phẫu thuật nội soi hướng dẫn bởi màu sắc trong những khớp khác và có thể có giá trị trong chẩn đoán hay phân loại sự thoái hóa của môi collagen khác.

Những nghiên cứu trước chuyển vị và thực nghiệm đã được thực hiện để đãm bảo nghiên cứu chuyển vị trong tương lai để làm lành Dây Chằng Chéo Trước Người.

Thiết bị may nối bán tự động cho kiểu may nối tận- tận tỉ mỉ, tinh tế và tương đối nhanh của Dây Chằng Chéo Trước Rách trong khi vẫn tôn trọng giải phẫu học và sinh học của Dây Chằng Chéo Trước có thể cần thiết.

Một điều cực kỳ quan trọng là phải có sự tái tạo may nối tận tận đại thể với lực kéo đứt rất cao. Hơn nữa, một chương trình Phục Hồi Chức Năng cần phải được đặt ra.

Cuối cùng, hãy thoải mái tiếp xúc với tôi để đặt câu hỏi, tham vấn, và giúp động não cho nghiên cứu tương lai.

KẾT LUẬN

Nghiên cứu được thực hiện trong Luận Án Tiến Sĩ này nhằm phát triển phương pháp mới, lạc quan hóa việc điều trị phẫu thuật cho bệnh nhân bị đứt Dây Chằng Chéo Trước (ACL).

Kết luận đầu tiên là hệ thống hình ảnh lạnh kết hợp với biểu đồ bó sợi là mục tiêu gần và là phương pháp luận chính xác để xác định hướng sợi collagen của Dây Chằng Chéo Trước trong không gian 3 chiều.

Kết luận sơ bộ thứ hai là, Dây Chằng Chéo Trước là một cấu trúc sợi collagen liên tục duy nhất với những sợi collagen ngắn chạy theo hướng sau ngoài và dần dần biến thành sợi dài chạy theo hướng trước trong.

Kết luận thứ ba là, hệ thống AFI có thể hình ảnh hóa chính xác và đúng thời điểm điểm bám gốc tự nhiên của dây chằng vào xương. Hệ thống AFI sẽ sớm được sử dụng đánh giá trên bệnh nhân đứt Dây Chằng Chéo Trước.

Kết luận thứ tư là, SIS có thể thúc đẩy tiến trình tổng hợp sợi collagen.

Kết luận thứ năm là, chỉ có sự kết hợp giữa lực căng đồng tâm và phân rãi tế bào mới hiệu quả trong việc tu chỉnh siêu cấu trúc của SIS.

Kết luận thứ sáu là, Dây Chằng Chéo Trước cắt ngang ở dê có thể lành sau thực nghiệm dùng kỹ thuật may nối tận-tận có tăng cường sinh học với mũi may khóa 3 chữ X và SIS.

Kết luận thứ bảy là, Dây Chằng Chéo Trước lành ở dê chứng tỏ những đặc điểm mô học tương đồng với sự lành của Dây Chằng Bên Trong tự nhiên, cho thấy Dây Chằng Chéo Trước có khả năng lành nội tại tương tợ.

Kết luận thứ tám, cũng là kết luận cuối cùng là, Dây Chằng Chéo Trước ở người có đáp ứng lành nội tại.

Tổng hợp các kết luận thứ sáu, bảy và tám cho thấy khả năng sửa chữa Dây Chằng Chéo Trước của kỹ thuật may nối tái tạo tận-tận có tăng cường sinh học trên người.

Tuy vậy, sự lành Dây Chằng Chéo Trước không phải là giải pháp tổng thể do sự thật là những cấu trúc làm vững khớp gối thụ động khác có thể bị tổn thương và rằng những cấu trúc làm vững khớp gối hoạt động khác không đủ. Như thế, cần nhớ rằng, không có phương pháp nào triệt để. Từ đó, sự phòng tránh tổn thương khi có thể là biện pháp duy nhất và tốt nhất! Không chỉ dành cho Dây Chằng Chéo Trước mà còn cho sức khỏe con người nói chung.

ADDENDA

Addendum I: About the author

Addendum II: PhD portfolio

Addendum III: Acknowledgements/ Dankwoord

About the author

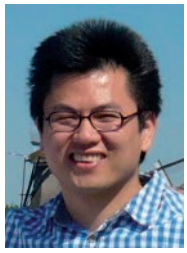

Nguyen Duy Tan was born on December 18th, 1979 in Naarden, the Netherlands. In 1998 he graduated from the Jacobus college high school in Enschede and consecutively started with medical school at the Rijksuniversiteit Groningen. During his study he was a student assistant at the department of Anatomy & Embryology. He completed his research electives at the Molecular Genetics Laboratory at the Universitat de Barcelona under the supervision of prof. dr. Jovita Mezquita and at the Musculoskeletal Research Center (MSRC) at the University of Pittsburgh under the supervision of prof.dr. Savio L-Y. Woo. After graduation from medical school in 2005, he started a 2 ½ years research fellowship at the MSRC. In 2007 he was granted the NWO Mozaïek grant to initiate multidisciplinary research projects to heal the ACL. In 2011 he was granted a starting grant from the Annafonds | NOREF to develop the Arthroscopic Fluorescence Imaging System. The research was performed under the supervision of prof.dr. Savio L-Y. Woo, prof.dr. Niek van Dijk and dr.ir. Leendert Blankevoort of which the results are presented in this PhD thesis.

PhD Portfolio

Name	D.T. Nguyen
Research schools	Musculoskeletal Research Center, Department of Bioengineering, University of Pittsburgh
	AMC Graduate School for Medical Sciences, University of Amsterdam
PhD period	2005-2007 and 2007-2011
Promotor	Prof. dr. C.N. van Dijk
	Prof. dr. S. L-Y. Woo
Copromotor	Dr.ir. L. Blankevoort

1. PHD TRAINING

Courses	Year	workload (ECTS)
NVA knie-arthroscopiecursus	2011	0.25
The Principles and Practice of Clinical Research, OTC foundation	2008	0.5
Proefdierkunde, artikel 9. Wet op de Dierproeven	2007	4
Good Clinical Practice/ Basiscursus, AMC	2007	1
Dangerous goods regulations/IATA training	2005	0.25
Laboratory Animal Research Module The University of Pittsburgh, Education and Certification Program in Research & Practice Fundamentals	2004	0.25
Research Integrity Module. The University of Pittsburgh, Education and Certification Program in Research & Practice Fundamentals	2004	0.25
Seminars, workshops and master classes		
Weekly department seminars	2005-2007 2007-2011	6
Ruysch lectures	2007-2011	1
NWO Mozaïek workshops: media training, networking, negotiating, career planning, NWO Talent Class People, Politics and Power	2007-2010	1.25

Presentations oral and poster presentations

	Year	ECTS
Nguyen TD, Raschke MJ, Tak PP, Woo S.L-Y, Van Dijk CN, Blankevoort L. Biomechanical and Histological Evaluation of the Healing Goat Anterior Cruciate Ligament after a New Repair Technique and Bioscaffold Treatment European Society of Sports Traumatology, Knee Surgery and Arthroscopy, ESSKA, (poster)	2014	0.5
Nguyen TD, Ramwadhdoebe T, van der Hart CP, Tak PP, Blankevoort L, van Dijk CN. Intrinsic Healing Response of the Human Anterior Cruciate Ligament: a Histological Study of Reattached ACL Remnants. ESSKA, (poster)	2014	0.5
Nguyen TD, Ramwadhdoebe T, van der Hart CP, Tak PP, Blankevoort L, van Dijk CN. Intrinsic Healing Response of the Human Anterior Cruciate Ligament: a Histological Study of Reattached ACL Remnants. Int'l Symp on Ligaments & Tendons, (oral)	2013	0.5
Nguyen TD, Geel J, Schulze M, Zantop T, Woo S. L-Y., Van Dijk CN, Blankevoort L. Enhanced Healing of the Ruptured Goat Anterior Cruciate Ligament after Suture Repair Combined with a Bioscaffold Orthopaedic Research Society, (oral)	2011	0.5
Nguyen TD, van de Giessen M, van den Wijngaard J, van Horssen P, Streekstra G, Spaan, JA, Van Dijk C, Blankevoort L. A Novel Method to Quantify the Anatomy of the Anterior Cruciate Ligament: An Experimental study in Goats. Int'l Symp on Ligaments & Tendons, (oral)	2011	0.5
Nguyen TD, Geel J, Schulze M, Zantop T, Woo S. L-Y., Van Dijk CN, Blankevoort L. Heling van de voorste kruisband van de geit na een nieuwe gemodificeerde hechttechniek en biomateriaalbehandeling, SEOHS, (oral)	2010	0.5
Nguyen TD, Geel J, Schulze M, Zantop T, Woo S. L-Y., Van Dijk CN, Blankevoort L. Heling van de voorste kruisband van de geit na een nieuwe gemodificeerde hechttechniek en biomateriaalbehandeling, NOV najaarsvergadering, (oral)	2010	0.5
Nguyen TD, Geel J, Schulze M, Zantop T, Woo S. L-Y., Van Dijk CN, Blankevoort L. Enhanced Healing of the Ruptured Goat Anterior Cruciate Ligament after Suture Repair Combined with a Bioscaffold , 6th World Congress on Biomechanics (oral)	2010	0.5
Nguyen TD, van de Giessen M, van den Wijngaard J, van Horssen P, Streekstra G, Van Dijk C, Blankevoort L. Quantifying the Collagen Fiber Orientation of the Caprine Cruciate Ligaments, 55th Annual Meeting of the Orthopaedic Research Society, (poster)	2009	0.5
Nguyen TD, Burton SD, Liang R, Almarza A, Sacks MS, Woo S.L-Y " A Quantitative analysis of the effects of cyclic loading and cell-seeding on the remodeling of an extracellular matrix based bioscaffold" Nordic Orthopaedic Federation Congress, (oral)	2008	0.5
Nguyen TD, Burton SD, Liang R, Almarza A, Sacks MS, Woo S.L-Y "Een kwantitatieve analyse van het effect van cyclische rek op extracellulaire matrix remodellering" Nederlandse Orthopaedische Vereniging Jaarvergadering, (oral)	2008	0.5

Liang R, Nguyen TD, Nola R, Almarza A, Woo S.L-Y. A Bioscaffold to Enhance the Fibrillogenesis in Healing Ligaments. 54th Annual Meeting of the Orthopaedic Research Society, (oral)	2008	0.5
Liang R, Nguyen T, Nola R, Almarza A, Woo SLY. Effects of a Bioscaffold on the Fibrillogenesis the Healing Medial Collateral Ligament. 2007 National Science Foundation Mathematical and Bioscience Institute's Workshop on Cell and Tissue Engineering, (oral)	2007	0.5
Nguyen TD, Burton SD, Liang R, Almarza A, Sacks MS, Woo S.L-Y. A Quantitative analysis of the effect of cyclic loading on extracellular matrix remodeling. 53rd Annual Meeting of the Orthopaedic Research Society, (oral)	2007	0.5
Nguyen TD, Liang R, Fu YC, Almarza A, Abramowitch SD, Woo S. L-Y. A Bioscaffold to Enhance Neo-tissue Formation in the Patellar Tendon Donor Site and to Limit Adhesion Formation with the Fat Pad: a Morphological Study. ISAKOS, (oral)	2007	0.5
Fu YC, Liang R, Moon DK, Nguyen DT, Abramowitch SD, Woo S.L-Y. Potential of Bioscaffold Treatment to Improve the Healing of a Patellar Tendon Defect. Biomedical Engineering Society, (poster)	2005	0.5

(Inter)national conferences visitor

Photonics Event and Vison, Robotics & Mechatronics Event	2014	0.5
Innovation for Health	2014	0.25
LEDExpo	2014	0.25
Technology for Health	2013	0.25
3rd International Symposium Stem Cells, Development and Regulation, Amsterdam	2009	0.25
2nd International Symposium Stem Cells, Development and Regulation, Amsterdam	2008	0.25
4th Dutch Program Tissue Engineering Symposium	2008	0.25
Regenerate, World Congress on Tissue Engineering and Regenerative Medicine, Pittsburgh	2006	0.25

2. TEACHING

Supervising master thesis and summer courses

Shawn Burton, BS	2005	1
Maarten van den Berg, BS	2007	1
Jurre Geel, BS	2008	1
Sietske Dellbrugge, BS	2009	1
Leon Buirs	2010	1
Hans Derriks, BS	2011	1

Other

Guest lecture at TU Delft: Tissue Engineering in Orthopaedics	2010	0.5
Guest lecture at TU Delft: Tissue Engineering of the ACL	2011	0.5

3. PARAMETERS OF ESTEEM

Grants	Year
Annafonds | NOREF subsidie	2011
Marti-Keuning Eckhart stichting onderzoekssubsidie	2011
Nederlandse Organisatie voor Wetenschappelijk Onderzoek, Mozaïekbeurs	2007
Dr. and Mrs. Savio L-Y. Woo research Scholarship	2007
Musculoskeletal Research Center, Research fellowship	2005
Travel grants from: stichting Annafonds, Reumafonds, J.K. de Cock stichting, Marti-Keuning Eckhart stichting, Amsterdams universiteitsfonds	2004-2011

Awards & Prizes

Collegium Chirurgicum Neerlandicum 1e prijs	2010
NOV Best Free Paper Award, Nordic Orthopaedic Federation Congres	2008

4. PUBLICATIONS

Peer reviewed

Nguyen TD, van de Giessen M, van den Wijngaard J, van Horssen P, Streekstra GJ, Spaan JA, van Dijk CN, Blankevoort L. Analysis of the 3-D Collagen Fiber Anatomy of the Human Anterior Cruciate Ligament: a Preliminary Investigation, submitted	2015
Nguyen TD, van Horssen P, van de Giessen M, Derriks H, van Leeuwen TG. Fluorescence Imaging for Improved Visualization of Joint Structures during Arthroscopic Surgery, submitted	2015
Nguyen TD, Dellbruegge S, Blankevoort L, Tak PP, van Dijk CN. Histological Characteristics of Ligament Healing after Bio-enhanced repair of the Transected Goat ACL, accepted in Journal of Experimental Orthopaedics	2015
Nguyen TD, Ramwadhdoebe T, van der Hart C, Blankevoort L, Tak PP, van Dijk CN. Intrinsic Healing Response of the Human Anterior Cruciate Ligament: a Histological Study of Reattached ACL Remnants, Journal of Orthopaedic Research	2013
Nguyen TD, Geel J, Schulze M, Zantop T, Woo S. L-Y., Van Dijk CN, Blankevoort L. Enhanced Healing of the Ruptured Goat Anterior Cruciate Ligament after Suture Repair Combined with a Bioscaffold, Tissue Engineering	2013
Van Eck CF, Nguyen TD, Fu FH, van Dijk CN. Dubbeletunnelreconstructie van de voorste kruisband: de nieuwe standaard? Sport & Geneeskunde	2009
Nguyen TD, Liang R, Woo S.L-Y, Burton SD, Almarza A, Sacks MS, Abramowitch S. Effects of Cell-seeding and Cyclic stretch on the Remodeling of an Extracellular Matrix derived Bioscaffold. Tissue Engineering	2009

Almarza, AJ, Yang, GG, Woo, S.L-Y., Nguyen,T., Abramowitch, SD. Positive Changes in Response of Bone Marrow Derived Cells to Culture on an Aligned Bioscaffold. Tissue Engineering	2008
Liang R, Woo S.L-Y, Nguyen TD, Lui PC, Almarza A. A Bioscaffold to Enhance the Collagen Fibrillogenesis in Healing Medial Collateral Ligament in Rabbits. Journal of Orthopaedic Research	2008
Gilbert TW, Stewart-Akers A, Sydeski J, Nguyen TD, Badylak S, Woo S.L-Y. Gene expression by fibroblasts seeded on small intestine submucosa and subjected to cyclic stretching. Tissue Engineering	2007
Woo SL-Y, Moon DK, Miura K, Fu YC, Nguyen TD. Basic science of ligament healing: Anterior cruciate ligament graft biomechanics and knee kinematics. Sports Medicine and Arthroscopy Review	2005

Other

Patent application: Nguyen TD, van Leeuwen TG, Horssen P. Arthroscopic Instrument Assembly, and Method of Localizing Musculoskeletal Structures during Arthroscopic Surgery	2014
Bookchapter: Woo, S.L-Y., Nguyen, T.D., Papas, N., and Liang, R.: Tissue Mechanics of Ligaments and Tendons, in Biomechanics in Ergonomics. Ed. S. Kumar, Taylor & Francis, Ltd., London	2007

Acknowledgements/ Dankwoord

Terugkijkend op de afgelopen jaren, prijs ik me gelukkig door de gekregen steun, vriendschappen, plezierige samenwerkingen, toevalligheden en de financiële steun. Ik wil iedereen hiervoor nogmaals hartelijk bedanken. Zonder jullie zou dit boekje er niet zijn.

BEDANKT!

Een aantal personen wil ik hieronder in het bijzonder noemen.

Prof.dr. Savio L-Y. Woo, D.Sc., dear dr. Woo, I think I have already said and wrote to you more than two hundred times "thank you". Not only to thank you for granting me the opportunities, your great teachings, your Nestorian advises, but also for the delicious food and fun during the many dinners and other memorable occasions. Reading the book, "*The flow of a long river – tributes to Savio L-Y. Woo on his 70th birthday*" emphasizes again how generous and important you have been to me but also to numerous other students and fellows. Thank you my teacher.

Prof.dr. Niek van Dijk, geachte professor van Dijk, veel dank dat u mijn promotor wilt zijn en voor de gegeven mogelijkheden. Ik wil u ook hartelijk danken voor de klinische lessen en leermomenten tijdens uw operaties. Het is bewonderingswaardig hoeveel patiënten door uw befaamde enkel arthroscopie technieken zijn geholpen. Een aantal die mede dankzij uw jaarlijkse enkelcursus exponentieel toeneemt.

Dr. ir. Leendert, beste Leendert, na een transatlantische telefoontje had je je sterke bedenkingen over de haalbaarheid om de kruisband te helen. Geleidelijk verdwenen ze en kreeg ik je zegen en volledige steun. Als nieuweling stelde je me voor aan andere onderzoekers en professoren waarna er mooie multidisciplinaire projecten konden worden geïnitieerd. Alsmede het vrijmaken van extra financiële middelen binnen de afdeling zijn hiervoor onmisbaar geweest. Elke woensdag, een werkbespreking, niet alleen om bij te sturen maar ook om af te remmen. Die total body cryomicrotoom project moeten we toch nog een keer gaan doen. Gezond eigenwijs, zoals je het een keer benoemde. En die pinda's ook altijd! [dĩ. pĩndã:s õ:k ãltɛĩt]! Lennie, de basis was in Pittsburgh gelegd, maar zonder jou zou het niet verder tot bloei zijn gekomen. Hartelijk dank vanaf het begin tot het eind!

Overige leden van de promotiecommissie, prof. dr. A. van Kampen, prof. dr. F. Nollet, prof. dr. R.J. Oostra, prof. dr. D.B.F. Saris, en prof. dr. ir. T.H. Smit, hartelijk dank voor het plaats nemen in de promotiecommissie en voor het beoordelen van het manuscript.

The Musculoskeletal Research Center, the MSRC was like a playground with nice kids to play with. Rui Liang, if everybody would be like you how joyful and peaceful the world would be. Dan Moon, thanks for introducing me into the American student life and the Korean food! Jens Stehle, dankeschön for being my mentor. Kazu Miura, domo arigato, great memories have been made with the one hundred dollar Ford. Changfu Wu, big buddy and my Chinese bro. Fengyan Jia, my Chinese sis. Xie xie. Yin-Chih Fu, it is our paper! Always nice to see you again at meetings. Ping-Chen, always joking and smiling. Chin-Yi Chuo, reading papers or sleeping…we will never know. Ozgur Dede, my fellow slidemaster, the endurance made us stronger. Maribeth Thomas, Eric Rainis, Suzan Moore, Jesse Fisk, Fabio Vercillo, Matt Fisher, Steve Abramowitch, Noah Papas, Sinan Karaoglu, Sabrina Noorani, Alexis Wickwire, Alejandro Almarza, Andrew Feola, Giovanni Zamarra, Carry Voycheck, Nick Drury, thanks for the happy hours at Hemmingway's, great conferences at Washington D.C., Chicago, San Diego, San Francisco, Stanford, Florence, Las Vegas, Long Beach and Arezzo, and the MSRC soccer team! Serena Saw, Diann Decenzo, Richard Debski, and Guogang Yang, many thanks for keeping the playground rolling.

Het AMC. Mijn paranimfen, Martijn van de Giessen en Mahyar Foumani. Martijn, heel veel dank! Wat begon als een vrijdagmiddagproject groeide uit tot hoofdstuk 1, 2 en 4 van dit proefschrift. Klinische vragen werden in een hand omdraai omgetoverd tot beeldschone en tegelijkertijd accurate antwoorden. Een Hollandse meester in medische beeldverwerking. Je droge humor is ook iconisch. Mahyar, multiculturelemultitalent, jij ook heel veel dank! Je wijze hulp, het brainstormen, je aandeel in het koffie apparaat, wekelijkse Kam Kee, alsmede voor het erven van je huisgenoten. Succes met de laatste loodjes van je reeds indrukwekkende proefschrift.

G-4. Mikel Reilingh, kamergenoot en mede-pinda. Typetjes en vooral Leendert nadoen kon je als de beste. Bedankt voor de gezelligheid in de pindahok. "Today was a great day for research, but now it's time to go home". Carola van Eck, zo snel promoveren en in Pittsburgh in opleiding komen doen weinigen je na. Petje af! Natuurlijk wil ik ook Inger Sierevelt, Peter de Leeuw, Jacob van Oldenrijk, Gabrielle Tuijthof, Job Doornberg, Christiaan van Bergen, Laurens Kaas, Geert Buijze, Wouter Mallee en andere collega's op de G-4 hartelijk danken. Het avondprogramma van de jaarlijkse enkelcursus was altijd weer een hoogtepunt. Rosalie van der Sandt, hartelijk dank voor je hulp en tips bij het afronden van mijn proefschrift. Simon Strackee, heel veel dank voor je adviezen! Handchirurgie is inderdaad een mooie (orthopedische) superspecialisatie.

L0. Jeroen van Wijngaarden bedankt voor je enthousiasme en weekendexcursies met El Cryo. Pepijn van Horssen, jij ook veel dank, niet alleen voor El Cryo, maar ook voor de fluorescerende experimenten in de avonduren en weekenden. Dr. ir. Geert Streekstra, hartelijk dank voor je adviezen, het gebruik van El Cryo en je hulp. Prof. dr.ir. Jos Spaan, dat El Cryo het af en toe begaf, lag niet aan de knieën, maar op toeval en botte pech. Hartelijk dank voor het gebruik. Prof.dr. Ton van Leeuwen, hartelijk dank voor je gastvrijheid, adviezen en de lessen.

Uniklinikum Münster. Prof.dr. med. Michael Räschke, Steffen Schanz, and Martin Schulze, thank you very much for your help, great lab facilities and generous hospitality during the experiments. Martin, the Eureka moment was not in the Lab but in Saigon: remembering that you wrote the hotel address on the back of your belt!

Prof.dr. Paul-Peter Tak, beste Paul-Peter, hartelijk dank voor je adviezen, warme gastvrijheid en enthousiasme. Het was fijn experimenteren in je laboratoria met behulpzame collega's en analisten. Dr. Margriet Vervoordeldonk, beste Margriet, eveneens hartelijk dank voor je warme gastvrijheid en supervisie.

Dr. Hans Bras, Rob Poeser, Iwan Nectar, Rene Sijmons, Rijn Visser, Frank Bernhard, hartelijk dank voor de gastvrijheid en faciliteiten op de afdeling pathologie. Cindy Cleypool en Rijk Gihaux, eveneens hartelijk dank voor de faciliteiten, hulp en geduld op de afdeling anatomie en embryologie.

wijlen Oma Jansen, Alda Jansen, Henk en Janine Jansen, Jan en Kitty Jansen, onze familie met een Nederlands achternaam. Zonder jullie altruïsme voor ontheemde vluchtelingen en later liefde zouden we hier niet zijn. Bedankt dat jullie er zijn!!!

Prof.dr. Vo Van Thanh, thank you very much for your warm hospitality and your teachings when we had the fortunate chance to visit you and the Hospital for Traumatology and Orthopaedics in Ho Chi Minh City. The feeling that we had after our short visit was not captured in words until I recently read an article about you and one of your philosophies: "A doctor must be both talented and virtuous. To become a doctor is not difficult, but to win the patients' respect and love is truly a challenge." I am also very grateful for your help with my thesis, without chapter 13 my thesis is like a tree without roots.

Co-auteurs/co-authors: Dan Moon, Kazutomo Miura, Yin-Chih Fu, Rui Liang, Savio L-Y. Woo, Shawn D. Burton, Changfu Wu, Michael S. Sacks, Steven Abramowitch, Ping-Cheng Liu, Alejandro Almarza, Thomas Gilbert, Ann Stewart-Akers, Jennifer Sydeski,

Stephen Badylak, Carola van Eck, Freddy H. Fu, Maarten van den Berg, Jurre Geel, Martin Schulze, Michael J. Räschke, Martijn van de Giessen, Geert J. Streekstra, Lucas J. van Vliet, Cornelis A. Grimbergen, Frans M. Vos, Jeroen P. van den Wijngaard, Pepijn van Horssen, Jos A. Spaan, C. Niek van Dijk, Leendert Blankevoort, Hans Derriks, Ton van Leeuwen, Tamara Ramwadhdoebe, Cor van der Hart, Paul Peter Tak, Sietske Dellbrügge without your teachings, advice, great lab facilities and help there would not be this thesis.

Neefjes, nichtjes, achterneefjes en achternichtjes, met elkaar opgegroeid en nog regelmatig naar ons thuisbasis Enschede. Heel fijn dat jullie er zijn!

Ba và Má yêu thương, tiếng Việt có nhiều câu nói chính xác và nhiều bài hát ý nghĩa sâu sắc. Những bài hát này cho ba và má: youtube.com + Ba ma Tan 2 juni 2015. Một người không thể mong muốn được một cha mẹ tốt hơn thế.

Anh 2 và chi Lien, hai chau Alyssa và Annaleigh, em Tien và em Evelyn, em Trang và em Thai, gia đình là tất cả, bedankt dat jullie er zijn!!!

Thu Hong, như ☯ …